Targeting Branched Chain Amino Acid Metabolism in Tumor Microenvironment

by

Ziwen Zhu

A dissertation submitted in partial fulfillment
of the requirements for the degree of
Doctor of Philosophy
(Biomedical Engineering)
in the University of Michigan
2020

Doctoral Committee:

Associate Professor Deepak Nagrath, Chair
Assistant Professor Kelly B. Arnold
Professor Theodore S. Lawrence
Associate Professor Sunitha Nagrath

Ziwen Zhu

ziwenzhu@umich.edu

ORCID iD: 0000-0002-6681-9153

DEDICATION

To my parents, Hongshun and Xue.

ACKNOWLEDGEMENTS

First, I would like to thank my parents, Hongshun and Xue. I would not go into a science career without you. I have not seen you two for more than seven years, and I really hope you are doing well in China. Your love and support set the foundation for everything I have now. Thanks to my cat, Val, for her company in the past year. She is named after this project.

I would like to thank my advisor Dr. Deepak Nagrath for his guidance throughout the completion of my degree. I would also like to thank the members of my committee: Dr. Kelly B. Arnold, Dr. Theodore S. Lawrence, and Dr. Sunitha Nagrath for their valuable feedback and guidance on my research.

Thank you to all my collaborators: Drs. Meredith A. Morgan, Jiaqi Shi, Vaibhav Sahai at the University of Michigan for providing all of the patient samples. Dr. Edna Cukierman at Fox Chase Cancer Center, Mara H. Sherman at Oregon Health & Science University, Dr. Anirban Maitra at M.D. Anderson Cancer Center for providing CAF cell lines.

I would also like to acknowledge the Research Histology and Immunohistochemistry Core, the Flow Cytometry Research Core, and the Microscopy and Image Analysis Lab (MIL) at the University of Michigan. Especially the MIL, I spent countless good days with the confocal microscopy.

Thanks for my friends, Hongyun, Ting-Wen, Anjali, Suny and Eric. I would not be able to go through all the difficulties during the past four years without you guys. Thanks to my undergraduate student, Pooja, you made many of my experiments easier.

To future readers, I would like you to know everything that comes in a full circle. It has not been the time yet to give up as long as you still feel it is not the end. Do not let others bring you down, you are never going to please everyone. There is a game always on between the people, that is "lose once you get serious." Furthermore, there is always a time in life that is full of uneasiness, we have no other choice but to face it. Giving up may not mean you are weak, it just means you are strong enough to let it go. Remember to keeping away from those consuming and depleting you. The best defense is a good offense. Time will tell the truth in the end, hope one day you can also look back, and smile on perils past.

TABLE OF CONTENTS

LIST OF TABLES

LIST OF FIGURES

LIST OF ABBREVIATIONS

ATP: Adenosine triphosphate

BCA: Bicinchoninic acid

BCAAs: Branched-chain amino acids

BCKAs: Branched-chain keto acids

BCKDH: Branched-chain ketoacid dehydrogenase

BSA: Bovine serum albumin

CAFs: Cancer-associated fibroblast cells

ChIP-PCR: Chromatin Immunoprecipitation-Polymerase chain reaction

CoA: Coenzyme A

CTCs: Circulating tumor cells

DAPI: 4’,6-Diamidino-2-Phenylindole, Dihydrochloride

DMEM: Dulbecco's Modified Eagle Medium

DMSO: Dimethyl sulfoxide

ECAR: Extracellular acidification rate

ECM: Extracellular matrix

EMT: Epithelial-mesenchymal transition

EpCAM: Epithelial Cell Adhesion Molecule

FBS: Fetal bovine serum

FCCP: Carbonyl cyanide 4-(trifluoromethoxy)phenylhydrazone

FFPE: Formalin-fixed, paraffin-embedded

GFP: Green fluorescent protein

Gln: Glutamine

H&E: Hematoxylin and eosin

HSP90: Heat shock protein 90

IF: Immunofluorescence

IgG: Immunoglobulin G

IHC: Immunohistochemistry

IL: Interleukin

ISA: Isotopomer spectral analysis

Iso: Isoleucine

KIC α-ketoisocaproate [ketoleucine]

KIV α-ketoisovalerate [ketovaline]

KMV α-keto-β-methylvalerate [ketoisoleucine]

Leu: Leucine

MID: Mass isotopologue distribution

MMP: Matrix metallopeptidase

MPE: Mole Percent Enrichment

MSCs: Mesenchymal stromal cells

OCR: Oxygen consumption rate

OXPHOS: Oxidative phosphorylation

PBS: Phosphate buffered saline

PCR: Polymerase chain reaction

PDAC: Pancreatic ductal adenocarcinoma

PFA: Paraformaldehyde

Pyr: Pyruvate

RPMI: Roswell Park Memorial Institute

SEM: Scanning Electron Microscope

TGF: Transforming growth factor

TME: Tumor microenvironment

Val: Valine

α-KG: α-ketoglutarate

ABSTRACT

Branched Chain amino acids (BCAAs) play an essential role in cell metabolism supplying both carbon and nitrogen in pancreatic cancers, and their increased levels have been associated with increased risk of pancreatic ductal adenocarcinomas (PDACs). It remains unclear how stromal cells regulate BCAA metabolism in PDAC cells and how mutualistic determinants control BCAA metabolism in the tumor milieu. In chapter 1, we present an overview of PDAC biology, tumor microenvironment (TME), altered cancer metabolism and BCAA metabolism. In chapter 2, we uncover differential gene expression of enzymes involved in BCAA metabolism accompanied by distinct catabolic, oxidative, and protein turnover fluxes between cancer-associated fibroblasts (CAFs) and cancer cells with a marked branched-chain keto acids (BCKA)-addiction in PDAC cells. In chapter 3, we showed that cancer-induced stromal reprogramming fuels this BCKA-addiction. We then show the functions of BCAT2 and DBT in the PDAC cells in chapters 3 and 4. We identify BCAT1 as the BCKA regulator in CAFs in chapter 5. In chapter 6, we dictated the internalization of the extracellular matrix from the tumor microenvironment to supply amino acid precursors for BCKA secretion by CAFs. We also showed that the TGF-β/SMAD5 axis directly targets BCAT1 in CAFs in chapter 7. In chapter 8, we validate the in vitro results in human patient-derived circulating tumor cells (CTCs) model. Furthermore, the same results were also validated in PDAC tissue slices, which recapitulate tumor heterogeneity and mimic the in vivo microenvironment in chapter 9. We conclude this manuscript with chapter 10 in which we propose future

studies and present directions towards pancreatic cancer research. In summary, our findings reveal therapeutically actionable targets in stromal and cancer cells to regulate the symbiotic BCAA coupling among the cellular constituents of the PDAC microenvironment.

Chapter 1 Introduction

1.1 Pancreatic ductal adenocarcinoma (PDAC)

Pancreatic cancer has a high propensity for spreading to nearby organs, and it is seldom detected in its early stages [1]. The aggressive biological nature of pancreatic cancer makes it the most lethal digestive cancer and the fourth leading cause of cancer-related deaths in the United States. Treatment strategies for pancreatic cancer have mainly focused on only the malignant cells in the tumor. However, in recent years, surrounding stroma in the tumor microenvironment is essential for tumorigenesis, as evidenced by several studies. The goal of my research is to understand the metabolic interaction between tumor stromal cells and cancer cells to target these interactions for therapeutic benefit.

Pancreatic cancer has an unusually high propensity to spread to nearby organs and is seldom detected in its early stages. Due to its aggressive phenotype, pancreatic cancer is the most lethal digestive cancer and the fourth leading cause of cancer-related death in the United States. The median survival rate of pancreatic cancer patients with metastatic disease is 6-9 months, for them with the locally advanced is one year. For the resected disease, it is about two years [1]. It is estimated that in 2020, 57,600 adults (30,400 men and 27,200 women) in the United States will be diagnosed with pancreatic cancer. It is also estimated that 47,050 deaths (24,640 men and 22,410 women) will occur from

pancreatic cancer this year [1]. The estimated global mortality rate of pancreatic cancer at the beginning of the twenty-first century was a dismal 98%, and a recent study predicts that by the year 2030, the annual number of deaths will reach 88,000 in the USA. It is projected to become the second leading cause of cancer-related deaths in the United States by 2030 [2]. The only potentially curative therapy that currently exists is surgical resection followed by adjuvant treatment. However, only 20% of patients have resectable disease. [2]. Therefore, there is an urgency to investigate and develop novel strategies for pancreatic cancer treatment.

1.1.1 Causes of pancreatic cancer

Pancreatic cancer can originate from pancreatic acinar, ducts, and islets. Pancreatic tumors that arise from pancreatic ductal epithelium are the most common. Pancreatic ductal adenocarcinomas occur more frequently in the pancreatic head. The tumors located in the head of the pancreas are mostly hard and have no apparent boundaries with healthy pancreatic epithelial tissues, and can be widely infiltrated in the tissues around the pancreas. Pathological sections show a marked increase in fibrotic tissue, which is similar to the pathological features of chronic pancreatitis. Pancreatic cancer is a disease caused by multiple factors, such as smoking, chronic inflammation, and large amounts of secretion of certain inflammatory factors that can cause disease [3].

Most pancreatic cancers have some gene alterations, such as amplifications, deletions, translocations, inversions, frameshifts, and substitutions. Disruptions of several genes in pancreatic cancer are almost universal and are present in 70%–98% of patients [4]. The mutation of genes can either enhance the function of the protein, sometimes making it even constitutively active or diminish the function completely. Subsequently,

the changes in protein functions can cause uncontrolled proliferation, migration, invasion, and adhesion of cells, protection from apoptosis and other types of cell death, DNA repairing, microsatellite instability, and other processes, which further lead to the development, growth, and spread of cancer. It has been proven that KRAS, TP53, and SMAD4 genes play an essential role in the development of pancreatic cancer [5].

1.1.2 Genetic mutations

1.1.2.1 KRAS

More than 90% of pancreatic cancer patients have KRAS gene mutations in their bodies, indicating that KRAS plays an essential role in the pathogenesis of pancreatic cancer [6]. The pathways involved in the KRAS gene are rough as follows: Under normal conditions, Ras binds to GDP, extracellular signals act on growth factor receptors to dissociate the two, and Ras binds to GTP encoded by KRAS. Ras-GTP active conjugate will gradually decrease with the hydrolysis of GTP. When the KRAS gene is activated and mutated, the Ras protein's GTPase activity is lost, and its signal continues to be amplified, thereby enabling several signaling pathways, including the phosphoinositide three kinase PI3K-AKT signaling pathway, Raf/MAPK, etc. [7].

1.1.2.2 SMAD4

In the later stage of pancreatic cancer lesions, SMAD4 deletion may occur, and SMAD4 protein has been shown to play a critical role in the process of transmitting extracellular signals through the TGF-β signaling pathway. TGF-β is an important tumor suppressor gene in normal cells, which can regulate cell proliferation and differentiation. The signal pathways involved are as follows: type I or III serine/threonine kinase receptor

binds to TGF-β ligand and dimerizes the receptor, and the phosphorylated Smad2/Smad3 protein binds to SMAD4 protein and transfers to the nucleus. Combined with transcription cofactors to regulate the cell cycle, differentiation, and growth [8]. The loss of SMAD4 in patients with pancreatic cancer lesions interrupts the above signaling pathways, making it lose its regulatory effect on cells.

1.1.2.3 TP53

Up to 85% of pancreatic cancer patients have inactivated TP53, and it also plays an essential role in regulating cell cycle and apoptosis [9]. The regulatory pathways involved in TP53 are as follows: DNA damage activates the TP53 gene to promote p21 transcription, which is related to cyclin-CDK complex binds and stops the cell cycle in the G1 phase. It has been reported that germline mutations are also associated with familial pancreatic cancer, including the DNA mismatch repair gene MLH1 [10], the positive trypsinogen gene PRSS1 [11], and the target genes INK4A and LKB1 of sure tumor suppressors [12]. Recent evidence shows that the interaction of epithelial, stroma and extracellular matrix proteins plays an important role in the process of pancreatic cancer. It can be seen that PDAC development is a complex process, and the molecular pathway mechanism needs to be clarified.

1.1.3 Signaling pathways

1.1.3.1 TGF-β signaling pathway

The human transforming growth factor TGF-β family includes TGF-β subtypes, kinetin, bone morphogenetic proteins (BMPs), growth, and differentiation factors (DGFs) total of 33 Members [13]. The role of TGF-β has two-phase specificity, which can inhibit

tumor growth in the stage of tumorigenesis and can promote tumor invasion and metastasis in the late stage of the tumor. The mechanism of action of TGF-β is to form heterotrimers by binding to cell membrane surface receptors, activate R-Smad protein to transmit signals into the cell, R-Smad binds to Co-Smad and transfers to the nucleus, and binds to target genes to regulate protein synthesis. The TGF-β family can regulate cell growth, survival, differentiation, and invasion, and plays an important role in embryo development and maintaining tissue homeostasis [14, 15]. TGF-β family members are involved in the occurrence and development of many diseases, including fibrosis, autoimmune diseases and cancer [16]. Epithelial-mesenchymal transition (EMT) refers to the ability of epithelial cells to transform into stromal cells and obtain migration morphologically. The tumor microenvironment, including tumor-associated macrophages, dendritic cells, and regulatory T cells, produces TGF-β1 that can effectively induce cell EMT [17]. Studies have also shown that overexpression of TGF-β1 can cause chronic pancreatitis in mice [18], and TGF-β1-induced EMT is a bridge connecting inflammation and cancer [19]. Overexpression of TGF-β1 in the inflammatory microenvironment promotes the EMT process of chronic pancreatitis to pancreatic cancer by down-regulating miR-217, and miR-217 promotes this process by inhibiting the expression of SIRT1 [20]. During the development of EMT, the Wnt signaling pathway provides EMT ability to epithelial cells, and the TGF-β/BMP family provides a suitable micro-environment for EMT, and the two synergistically induce EMT [21]. In cancer, many stem cell pathways, such as Wnt, Ras, SHH (sonic hedgehog), and Notch (Notch homolog) signaling pathways are highly activated and provide tumor cells with EMT capabilities. Immune infiltrating cells secrete TGF-β1, IL8, IL6, MMPs and

TNF-α and other EMT promoting factors to induce EMT in the tumor microenvironment [20].

SMAD4 is the main effector of the TGF-β signaling pathway, in more than 50% of pancreatic cancer patients lose their activity [21]. The inactivation of SMAD4 alone cannot lead to the cancelation of the pancreas, and it is also optional for the development of normal pancreas [22]. Inactivation of the TGF-β signaling pathway leads to the up-regulation of TGF-α expression, and SMAD4 inactivation coordinates the up-regulation of TGF-α expression to promote pancreatic fibrosis and promote pancreatic intraepithelial neoplasia, leading to the transformation of chronic pancreatitis into pancreatic cancer [23]. The hallmark of chronic pancreatitis is the fibrosis of pancreatic tissue, and the continuous activation of stellate cells is an important reason for promoting pancreatic fibrosis.

1.1.3.2 JAK/STAT pathway

The Janus kinase/signal transducers and activators of transcription (JAK/STAT) signaling pathway mediate multiple cytokine signal transduction pathways. It is widely involved in regulating cell proliferation and other biological processes such as differentiation, apoptosis and immune response. The activation of the JAK/STAT pathway is included in the occurrence and development of various diseases, including solid tumors, lymphomas, leukemias, chronic inflammation and other diseases [24]. The basic transmission process of the JAK/STAT signaling pathway is: cytokines and their receptors cause the dimerization of the receptor molecules, which makes the JAKs coupled to the receptors approach each other and are activated by interactive tyrosine phosphorylation. JAKs catalyzes the phosphorylation of the tyrosine of the receptor itself

and form the corresponding docking site of STATs, allowing STATs to bind to the receptor through the SH2 domain and achieve their phosphorylation activation under the action of JAKs. Then STATs form homo/heterodimerization, it enters the nucleus and combines with the promoter of the target gene to activate the transcription and expression of the corresponding gene.

STAT3, as an important molecule in the inflammatory signaling pathway, also plays an important role in tumor development and invasion. The activation of the JAK/STAT pathway can inhibit apoptosis and promote tumor cell proliferation and invasion. Activated STAT3 can damage the extracellular matrix to different degrees and cause the degradation and destruction of the tissue basement membrane, providing a suitable environment for early metastasis of tumor cells. Also, STAT3 can promote the EMT process and promote the transformation of chronic inflammation into cancer. A recent study found that the Regenerating Family Member 3 Alpha (REG3A) high expression and SOCS3 methylation can up-regulate the JAK/STAT3 pathway and promote the malignant proliferation of human pancreatic cancer cells [25]. IL-6 can also activate the JAK/STAT pathway to promote the malignant transformation of chronic inflammation, leading to the occurrence of various malignant tumors [26]. Further research found that the mechanism of action of REG3A is similar to IL-6. In the inflammatory environment induced by IL-6, REG3A promotes the proliferation of pancreatic cancer cell lines by up-regulating the expression of JAK2/STAT3 pathway, while highly expressed STAT3 can positively Feedback upregulates the expression of REG3A, thereby forming a positive feedback loop to continuously promote the malignant proliferation of pancreatic cancer cells [27].

1.1.3.3 MAPK pathway

The MAPK signaling pathway chain is composed of MAPK, MAPK kinase (MAPKK) and MAPKK kinase (MAPKKK), and is one of the important pathways in the signal transmission network of eukaryotes. It plays a key role in cytoplasmic functional activities and participates in the processes of cell proliferation, differentiation, migration and apoptosis. The MAPK signal transduction pathway uses a highly conserved tertiary kinase cascade to transmit signals: extracellular signals activate MAPKKK, which in turn activates MAPKK; then, MAPK is activated by phosphorylation of specific tyrosine and serine residues in the MAPK molecule. There are four subfamilies in the MAPK family, including extracellular signal-regulated kinase 1/2 (ERK1/2), c-Jun amino-terminal kinase (JNK), p38 mitogen-activated protein kinase (p38MAPK), and extracellular signals Regulate kinase 5 (ERK5).

Early studies reported that ERK1/2 is the main regulatory pathway for the activation and proliferation of pancreatic stellate cells [28, 29]. Platelet-derived growth factor (PDGF) can stimulate the activation of pancreatic stellate cells, and its stimulation depends on the activation of the ERK1/2 pathway. ERK pathway inhibitor PD98059 blocks the proliferation of pancreatic stellate cells after acting on pancreatic stellate cells and can inhibit the migration of pancreatic stellate cells by up to 50% [29]. Also, the inhibition of pancreatic stellate cells by hydrogen sulfide (H2S) donor NaHS is achieved through the ERK1/2 pathway [30]. Angiotensin II can induce the proliferation of pancreatic stellate cells, and it can activate JNK and ERK1/2 while promoting the proliferation of pancreatic stellate cells, suggesting that angiotensin II may achieve the proliferative effect on pancreatic stellate cells through JNK and ERK [31]. JNK inhibitor

SP600125 can inhibit the activation of JNK and AP-1 while inhibiting PDGF-induced pancreatic stellate cell activation, indicating that the activation of the JNK pathway can promote the activation of pancreatic stellate cells [32]. In a mouse model of chronic pancreatitis, BMP inhibits the activation of pancreatic stellate cells by inhibiting the TGF-β/Smad2 and p38MAPK pathways, and plays a role in reversing pancreatic tissue fibrosis [33]. Studies have reported that high glucose uptake can significantly activate the proliferation of rat pancreatic stellate cells, and the p38MAPK blocker SB203580 can reduce the expression of α-SMA, indicating that high glucose environment-induced pancreatic stellate cells proliferation is mediated through the p38MAPK pathway [34].

1.1.3.4 NF-κB pathway

Nuclear transcription factor kappa B (NF-κB) is an important type of transcriptional activation factor that exists in various eukaryotic cells and is widely involved in a series of biological processes, including immune response, cell proliferation and apoptosis. It is closely related to the occurrence and development of various tumors. The NF-κB family includes the five members of the oncogenes C-Rel, NF-κB1 (p50/p105), NF-κB2 (p52/p100), Re1A (p65) and RelB. Under normal circumstances, most of the NF-κB dimer in the cell is inactive in the cell by binding to one of the three NF-κB inhibitory proteins (IκBα, IκBβ, IκBε) in the cytoplasm. Recent studies have shown that chronic inflammation, NF-κB stimulation, is related to the development of cancer [35]. NF-κB shows abnormal activation in both chronic pancreas and pancreatic cancer, suggesting its important role in the development of chronic pancreatitis to pancreatic cancer [36]. The autocrine of pro-inflammatory factors such as IL-1α can induce the activation of NF-κB, and the continuously activated NF-κB promotes the

development of pancreatic cancer [37]. Activated NF-κB and downstream target genes such as pro-inflammatory factors TNF-α and IL-1 are key factors for the transformation of inflammation into tumorigenesis. Studies have reported that the mechanism of aspirin in preventing pancreatic cancer is to block the activation of NF-κB in the inflammatory response to inhibit the occurrence of pancreatic cancer [38]. IKK2 is an inhibitor of κB kinase 2, a member of the NF-κB pathway. IKK2 coordinates the Notch pathway to upregulate Notch target genes HES1 and HEY1, inhibits the expression of anti-inflammatory factors, and promotes the development of pancreatic cancer [39]. Besides, NF-κB can also promote EMT by inhibiting the expression of E-cadherin, and NF-κB is also necessary for TGF-β1-induced EMT [40, 41].

1.1.3.5 TLRs pathway

Toll-like receptors (TLRs) are a highly conserved family of receptors, including at least 12 members. TLRs can specifically recognize pathogen-associated molecular patterns (PAMPs), which can not only activate innate immunity but also play an important role in regulating acquired immunity. It is a bridge connecting innate immunity and acquired immunity. Many immune effector cells, including monocytes/macrophages, neutrophils, and dendritic cells, express TLRs. TLRs recognize and bind PAMPs to activate downstream signaling molecules, inducing chemokines, interleukins, and other costimulatory molecules. Current research indicates that TLRs mediate at least two signal cascade amplification pathways, one is the myeloid differentiation factor 88 (MyD88) dependent pathway, and the other is the MyD88 independent pathway [42].

On the one hand, TLRs play an important role in immunity, and excessive activation of TLRs is also crucial in promoting tumor formation and migration. Studies

have shown that TLR4 and TLR7 are highly expressed in human and mouse pancreatic cancer cells [43, 44]. The continuous activation of TLR in acute and chronic pancreatitis models not only aggravates inflammation of the pancreas but also accelerates tumor formation in the pancreas [44]. LPS can induce the activation of NF-κB through the TLR4/MyD88 pathway, thereby producing a series of biological effects such as promoting cell proliferation, migration and invasion [45]. TLR7 is not expressed in normal human and mouse pancreatic tissues. Still, in the KRAS mutant pancreatic cancer mouse model and human pancreatic cancer samples, whether it is in epithelial cells or macrophages, dendritic cells, T/ B cells have extremely high expression levels. In pancreatic cancer with obvious inflammation, the activation of TLR7 accelerates the formation and deterioration of pancreatic tumors [46].

1.1.3.6 The non-coding RNA pathways

The non-coding RNA pathways have also been shown to involve in the malignant transformation of chronic pancreatitis. MicroRNA (miRNA) and long-chain non-coding RNA (lncRNA) are non-coding RNAs with post-transcriptional regulatory functions in eukaryotic organisms, which play an important role in various biological pathways. It has been reported in that in pancreatic cancer, miR-1290, miR-200a and miR-200b showed high expression and predicted poor prognosis, and could be used as a diagnostic indicator for pancreatic cancer in the future [47, 48].

1.2 Tumor microenvironment (TME)

The tumor microenvironment was proposed by Ioannides in 1993 [49]. It specifically refers to the local environment in which tumors develop and develop. It mainly consists of tumor cells, stromal cells, immune cells and their secreted cytokines, and the surrounding extracellular matrix. A unique environment is conducive to tumor survival, proliferation, invasion and metastasis [49]. The characteristics of the pancreatic cancer tumor microenvironment include abundant matrix, hypoxia, insufficient blood supply, and high immunosuppression. It is difficult for traditional radiotherapy and chemotherapy to play a therapeutic role. Therefore, finding new therapeutic targets through pancreatic cancer tumor microenvironment is a promising research direction.

1.2.1 Stromal cells and extracellular matrix

The stromal cells of pancreatic cancer are mainly pancreatic stellate cells and cancer-associated fibroblasts. The extracellular matrix mainly includes collagen, fibronectin and hyaluronic acid. Stromal cells and extracellular matrix play a vital role in the proliferation, invasion and metastasis of pancreatic cancer [50]. The matrix barrier formed by their interaction is an important reason for the resistance of pancreatic cancer to radiotherapy and chemotherapy.

1.2.1.1 Pancreatic stellate cells (PSCs)

Pancreatic stellate cells are one of the primary cells in the microenvironment of pancreatic cancer. Under physiological conditions, pancreatic stellate cells are at the resting stage and are mainly involved in maintaining the normal structure of pancreatic tissues [51]. Pancreatic tumor cells can transform resting pancreatic stellate cells into activated myofibroblast-like cells [52]. Transformed pancreatic stellate cells can rapidly proliferating and secrete large amounts of extracellular matrix and cytokines, forming a

microenvironment that is conducive to tumor growth. PSCs have been shown to promote the growth and proliferation of pancreatic cancer. Pancreatic stellate cells and pancreatic tumor cells promote each other through "positive feedback." Pancreatic tumor cells secrete platelet-derived growth factor, TGF-β, fibroblast growth factor, etc. to promote the activation of pancreatic stellate cells and recruit them around the tumor cells. Activated pancreatic stellate cells rapidly proliferate and secrete TGF-β, fibroblast growth factor, connective tissue growth factor, etc. in a paracrine manner, which in turn promotes the growth and proliferation of pancreatic tumor cells [53]. PSCs can also promote the invasion and metastasis of pancreatic cancer. The results of studies on pancreatic ductal cancer organoids showed metalloproteinase two secreted by pancreatic stellate cells could induce the destruction of the basement membrane structure and promote local tumor invasion [54]. Through inhibition of metalloproteinase, two can weaken the destruction of pancreatic stellate cells to the basement membrane, retaining the organoid duct structure [54].

PSCs can also promote chemotherapy resistance. On the one hand, pancreatic stellate cells secrete a large amount of extracellular matrix and cytokines to form a microenvironment of dense fiber, hypoxia, and insufficient blood supply. Among them, occlusion of non-functional blood vessels and an impenetrable fiber barrier make it difficult for chemotherapy drugs to enter the tumor tissue through the blood [55]. On the other hand, pancreatic stellate cells downregulate the nucleoside transporter that mediates the uptake of gemcitabine in tumor tissues by secreting cysteine-rich angiogenin inducers, leading to pancreatic cancer resistance to gemcitabine [56]. In recent studies, PSCs also showed immunosuppression properties. Nuclear factor κB in pancreatic

stellate cells can increase the expression of chemokine ligand 12, thereby reducing the cytotoxic T cell infiltration killing effect [55]. Pancreatic stellate cells regulate the secretion of various cytokines in T cells and induce the apoptosis of $CD4^+$ and $CD8^+$ T cells by overexpressing galectin-1, assisting tumor immune escape [57].

1.2.1.2 Cancer associated fibroblasts (CAFs)

Cancer associated fibroblasts are fibroblasts of mesenchymal origin and an important part of tumor stromal cells. There are a large number of cancer associated fibroblasts in the pancreatic tumor microenvironment, which mainly promote the invasion, metastasis and chemotherapy resistance of pancreatic cancer by secreting growth factors, chemokines and extracellular matrix. Cancer associated fibroblasts have been shown to promote tumor stromal barrier and angiogenesis by secreting a large amount of extracellular matrix and tumor-associated angiogenesis factors, thereby accelerating tumor progression and reducing chemotherapy drug penetration [58]. Cancer associated fibroblasts promote tumor proliferation, invasion and metastasis by secreting IL-6, IL-8, chemokine two and chemokine ligand 12 etc. Results show that the use of a new vinblastine derivative, Conpholine, can inhibit the activity of cancer associated fibroblasts and reduce the synthesis of cytokines, thereby reducing pancreatic cancer tissue fibrosis, inhibiting tumor proliferation, metastasis, and increasing the permeability of chemotherapy drugs [59]. Cancer associated fibroblasts can also mediate the formation of chemotherapy resistance through a variety of signaling pathways and exosome pathways. The use of specific inhibitors can improve the efficacy of chemotherapy drugs [60].

Some research results show that inhibiting or depleting tumor-related fibroblasts in mouse model experiments can delay the progression of pancreatic cancer. Still, the same results have not been obtained in clinical trials [61]. There are also research results showing that a dense matrix barrier may delay tumor invasion and metastasis, and simply eliminating the matrix may lead to tumor progression. Application of curcumin can make cancer associated fibroblasts lose the characteristics of mesenchymal cells and transform into nearly normal fibroblasts, thereby inhibiting the tumor-promoting effect of tumor-associated fibroblasts [62]. Therefore, reversing the abnormal cell structure may be a feasible strategy for tumor targeted therapy.

1.2.1.3 Hyaluronic acid

Hyaluronic acid is highly expressed in various tumors and is closely related to tumor progression. On the one hand, hyaluronic acid is deposited in large amounts around pancreatic cancer tissue. Its high hydrophilicity leads to the collapse of blood vessels and low perfusion, forming a physical barrier that hinders the delivery of chemotherapy drugs, stimulating the migration ability of pancreatic cancer cells and cancer associated fibroblasts, and participate in the invasion and metastasis of pancreatic cancer [63]. Recent results show that the degradation of hyaluronic acid by pegylated hyaluronidase can gradually restore the interstitial pressure and microvascular abnormalities [64]. The combined use of pegylated hyaluronidase and hyaluronic acid synthesis inhibitor can improve anti-tumor drug penetration, thereby delaying tumor progression and prolonging patient survival time [65]. Another recent study showed that the use of hyaluronic acid synthesis inhibitor 4-methylumbelliferone in a mouse xenograft model could reduce the hyaluronic acid in the tumor and promote the

infiltration of the γδT cells into the tumor tissue, thereby inhibiting tumor growth [66]. This means that the hyaluronic acid synthesis inhibitor may become an effective immunosensitizer. Stromal cells and extracellular matrix play an extremely important role in the proliferation, invasion and metastasis of pancreatic cancer. Targeted therapy for stromal cells and extracellular matrix is an important direction of pancreatic cancer research. Some research results show that simple elimination of stromal cells and extracellular matrix may lead to further progress of pancreatic cancer, suggesting that stromal cells and extracellular matrix may play a role in inhibiting the progress of pancreatic cancer [67].

1.2.2 Immune cells

The immune system plays an important role in removing malignant cells. Pancreatic cancer can imbalance the number and function of immune cells with anti-tumor effects through a variety of ways, thereby creating a highly immunosuppressed microenvironment to help tumor cells escape immune surveillance.

1.2.2.1 Tumor-associated macrophages (TAMs)

Normal macrophages can differentiate into two phenotypes, M1 and M2, under different conditions. M1 type macrophages can promote local inflammation of tumors and participate in immune surveillance; M2 type macrophages can secrete IL-10, TGF-β and other cytokines to promote tumor angiogenesis, participate in tissue remodeling, suppress the immune response and induce chemotherapy resistance, thereby accelerating the proliferation, invasion and metastasis of pancreatic cancer [68]. Pancreatic cancer can actively recruit monocytes by secreting macrophage colony-stimulating factor, TGF-β, IL-6, IL-10, etc. and promote their transformation into M2 macrophages [69]. The results

of a co-injection experiment in mice showed that M2-type macrophages could induce tumor cell epithelial-mesenchymal transition, promote tumor growth and peritoneal metastasis and confer stronger chemotherapy resistance on tumor cells [70]. In pancreatic cancer, specific inhibition of macrophage colony-stimulating factor and chemokine ligand two can reduce tumor-associated macrophages, inhibit tumor growth and increase the killing ability of effector T cells and improve the efficacy of gemcitabine [71]. Furthermore, IL-27 can transform M2 type macrophages into M1 type and regain their anti-tumor potency [72].

1.2.2.2 Regulatory T cells (Tregs)

Regulatory T cells are a multifunctional subset of T cells that mainly induce immune tolerance and exert immunomodulatory effects in normal organisms. They mostly play an immunosuppressive role in tumor patients and promote tumors by suppressing the killing ability of effector T cells, immune evasion and transfer. TGF-β in the tumor microenvironment can induce the generation of regulatory T cells, and the application of TGF-β neutralizing antibodies can inhibit the maturation of regulatory T cells [73]. Pancreatic cancer cells can also recruit regulatory T cells to the tumor by secreting chemokine ligand 5, vascular endothelial growth factor (VEGF), the application of corresponding inhibitors can reduce the infiltration of regulatory T cells in the tumor [74]. Regulatory T cells can secrete TGF-β to directly inhibit the anti-tumor effect of $CD8^+$ T cells and natural killer cells. They can also induce apoptosis of $CD8^+$ T cells and natural killer cells by secreting granzyme B and perforin [75]. Regulatory T cells can also interact with antigen-presenting cells to inhibit their CD80 and CD86 expression, leading to dysfunction of cytotoxic T cells and dendritic cells [76]. Cytotoxic T-lymphocyte-

associated protein 4(CTLA4) on the surface of regulatory T cells plays an important role in the process of immunosuppressive regulation. Neutralizing antibodies can induce the apoptosis of regulatory T cells and reduce the inhibitory signal. A small dose CTLA4 monoclonal antibody can effectively reduce tumor volume, but systemic use of large doses will increase the infiltration of secondary lymph node regulatory T cells [77]. Gemcitabine can significantly reduce regulatory T cells in peripheral blood, and monoclonal antibodies, vaccines, and various combination treatments against regulatory T cells have also achieved positive results in animal experiments.

1.2.2.3 Myeloid-derived suppressor cells (MDSCs)

Myeloid-derived suppressor cells are a group of immature heterogeneous cells derived from bone marrow. Myeloid-derived suppressor cells in pancreatic cancer can mediate immunosuppression through a variety of pathways to assist immune escape. Myeloid-derived suppressor cells can produce arginase and nitric oxide synthase. Arginase can decompose arginine necessary for T cell proliferation, thereby reducing T cell production. Nitric oxide synthase can inhibit T cell signaling pathways and induce T cell apoptosis, thus inhibiting its cytotoxicity [78]. Myeloid-derived suppressor cells can also release reactive oxygen species, causing oxidative stress in surrounding cells, thereby promoting tumorigenesis and development. The use of antioxidants to treat pancreatic cancer can improve the prognosis of patients [79]. IL-10, IFN-γ, and TGF-β in the tumor microenvironment can activate myeloid-derived suppressor cells. The activated myeloid-derived suppressor cells can induce the proliferation of regulatory T cells and further mediate immunosuppression [80]. Myeloid-derived suppressor cells have high expression of Programmed death-ligand 1 (PD-L1). The myeloid-derived PD-L1 highly

expressed on cells can specifically bind to Programmed cell death protein 1(PD-1) to inhibit the activation of T cells and reduce the tumor-killing ability of T cells [81]. Targeting depletion of Myeloid-derived suppressor cells in pancreatic cancer can reshape the tumor matrix, increase the number of $CD8^+$ T cells in the tumor tissue and induce tumor cell apoptosis, which may be a way to enhance classic cytotoxicity and adoptive immunity based immunotherapy [82]. Tumor-associated macrophages, regulatory T cells, and myeloid-derived suppressor cells, etc., create a highly immunosuppressive microenvironment through multiple pathways, which is an important reason why pancreatic cancer is insensitive to radiotherapy and chemotherapy. The above immune cells can not only suppress the immune response in their own way, but also induce immunosuppression through a common pathway.

1.2.3 Summary

The interaction of various cells and non-cellular components in pancreatic cancer to create a microenvironment rich in the extracellular matrix, hypoxia, inadequate blood supply, and high immunosuppression is an important reason for pancreatic cancer to be insensitive to radiotherapy and chemotherapy. At present, many potential targets based on stromal cells or extracellular matrix in the tumor microenvironment have been found. A large number of experimental studies have obtained good results in animal models, but some research results suggest that tumor growth was not being restrained. Due to the complexity and specificity of the microenvironment of pancreatic cancer, compared with single-target therapy, immunotherapy, radiotherapy and chemotherapy combined with multi-target therapy, may be a more effective strategy. However, to design an efficient and safe joint scheme, we must further understand the mechanism of the tumor

microenvironment, and more research is needed to find the synergy and adverse reactions between different therapies and different drugs.

1.3 Circulating tumor cells (CTCs)

Circulating tumor cells (CTCs) are tumor cells that shed from the primary tumor tissue into the blood circulation [83]. After the CTCs enter the blood circulation, most of them undergo anoikis, blood flow shear stress, immune recognition and killing. The number of CTCs that can eventually survive in peripheral blood is very small, usually $1\sim10^2$/mL (the number of white blood cells is $10^5\sim10^6$/mL, and the number of red blood cells is $10^9\sim10^{10}$/mL). CTCs and the clusters formed by multiple CTCs play a key role in tumor metastasis [84]. The surface antigens, genotypes and pathological characterization of CTCs during the transmission process are the main points of the current research on the mechanism of cancer metastasis. CTCs based liquid biopsy technology is simple and minimally invasive and can better represent tumor heterogeneity. It has been regarded as a new type of tumor biomarker. CTCs counts, count changes, subgroup characteristics, etc. have been related to patient prognosis and have established more and more links with personalized treatment. Using the functional diagnosis results of CTCs to develop a personalized cancer treatment plan is an important and reliable way to achieve precise drug use for cancer.

1.3.1 Isolation of CTCs

The isolation methods of CTCs can be divided into two categories: biological method and physical method, according to the isolation principle [85]. Biological methods use surface antigens of CTCs that are different from other blood cells (white

blood cells, red blood cells, platelets), and physical methods are based on differences in density, size, and deformability of CTCs and other blood cells. After the red blood cells in the patient's blood sample are lysed, surface-fixed EpCAM antibodies are used to recognize and capture the CTCs expressing the EpCAM antigen directly, and the obtained CTCs can be subjected to downstream analysis. This isolation method belongs to positive enrichment in biological methods. The CELLSEARCH system is the representative of this isolation technology and is currently the only CTCs isolation system approved by the FDA for the prognosis of metastatic breast cancer, colon cancer, and prostate cancer [86-88]. Magnetic beads with leukocyte-specific antibodies are used to eliminate leukocytes to obtain an unlabeled CTCs suspension. This method is also known as negative enrichment in biological methods [89, 90]. In the physical method, the OncoQuick system does not rely on antigen recognition but is separated by the density of CTCs and other blood cells [91]. Therefore, both EpCAM positive and negative CTCs can be obtained. The technical principle of the MetaCell system is to use CTCs with a diameter greater than other blood cells, and the blood sample is filtered through a polycarbonate membrane with a pore size of 8um to separate CTCs [92]. Hou *et al.* designed spiral micro-pipes based on the principles of hydrodynamics and isolated CTCs and leukocytes by coupling inertial micro-flows with Dean circulation [93]. The same group also further designed a microfluidic device that can separate a single CTC base on this so that the obtained CTCs can be directly used for downstream molecular biological applications [94].

At present, there are also reports on the application of nanotechnology in the isolation of CTCs. Halo *et al.* attached single-stranded DNA complementary to specific

genes (such as TWIST1 or 2) mRNA in CTCs to the surface of gold nanoparticles [95]. When nanoparticles enter CTCs, the two-release fluorescence when they are combined, and CTCs can be detected semi-quantitatively according to the fluorescence intensity. It should be noted that the detection rate and purity of CTCs in different principles and different isolation systems will vary greatly. For example, when the antigen-based CELLSEARCH system and the size-based FMSA system were used to detect perioperative CTCs, the detection rate of the FMSA system was as high as 93.4%, and the average number of CTCs was 22.56/7.5mL The CellSEARCH system is only 26.1% and 0.87/7.5mL [96]. Biological methods based on antigen recognition have the advantage of high purity, but will miss CTCs that do not express the corresponding antigen, and may affect downstream functional detection due to the role of antigen antibodies; physical isolation methods based on density and size are not subject to CTCs surface antigens. The detection rate is high, but the purity may be lower due to the possibility of mixing with other blood cells. CTCs isolation technology has developed rapidly, and many more sophisticated systems already have faster sample processing speed, higher detection rates, and detection purity. What is urgently needed is the corresponding technical specifications and operating standards to standardize and standardize clinical application research and experimental research.

1.3.2 Molecular biological characteristics of CTCs

With the continuous improvement of CTCs isolation technology, the emergence of biological achievements such as genomics, transcriptomics, and proteomics has provided the possibility to reveal the molecular biological characteristics of CTCs and their role in the development of tumor metastasis. Epithelial-to-mesenchymal transition

(EMT) refers to the biological process of transforming epithelial cells into mesenchymal phenotype cells through a specific procedure [97]. In this process, tumor cells lose their polarity, adhesion and other epithelial phenotypes and transform into mesenchymal phenotypes with high movement and invasion ability, thereby greatly improving the ability of tumor cells to invade and metastasize [98]. Existing studies have shown that in the epithelial cell-derived tumor cells, the expression of E- cadherin protein is inhibited by the transcription factors of SNAI1, SNAI2, ZEB1, ZEB2, MMP9, TWIST1, TWIST2, EMT then occurs, tumor cells lost polarity, and cell adhesion sheds from tumor tissue and enters the circulatory system [99]. Most of the CTCs that enter the circulatory system undergo apoptosis or enter a dormant state under the effect of immune editing. Only about 0.1% of CTCs are still alive after 24 hours, of which less than 1/10 is still tumorigenic [100]. EMT is a complex process regulated by multiple factors and signaling pathways, and its specific mechanism still needs to be further clarified. IL-6 has long been considered to have the function of promoting EMT of colorectal malignancies. IL-6 regulates the EMT process through Fos-related antigen 1 (FRA1) and signal transducer and activator of transcription 3 (STAT3) [101]. After knocking down the expression of STAT 3 or IL-6 by siRNA, EMT, cell migration, invasion and other phenomena are hindered. The transcription factor, nuclear factor kappa-light-chain-enhancer of activated B cells (NF- κB), regulates a wide range of biological processes, including inflammation, cell expansion, and apoptosis. Maier *et al.* found that when NF- κB is inhibited, transforming growth factor β (TGF-β)-induced EMT cannot occur, and after activation of NF- κB, cells exhibit vimentin and ZEB1 related EMT features such as up-regulation and down-regulation of E-cadherin [102]. Gu *et al.* found that IL-17 in lung cancer cells have

to up-regulate ZEB1 via NF- κB pathway, further inducing EMT [103]. Based on the structural analysis of the regulatory signal network of EMT, Chanrion *et al.* proposed and verified that the loss of p53 and Notch activation synergistically induce EMT [104]. Yang *et al.* found that fucosyltransferase can activate P13K/Akt and NF- κB pathways to further activate SNAI1 and MMP-9 to induce EMT [105]. Salnikov *et al.* proved that a hypoxic environment would positively regulate EMT-related genes, resulting in decreased expression of E-cadherin and increased expression of vimentin [106]. Zheng *et al.* used genetically engineered mice knocked out of Snai1 or Twist, proving that the inhibition of EMT does not change the occurrence, spread and metastasis of pancreatic ductal adenocarcinoma, but enhanced expression of nucleoside transporters [107]. Suppression of EMT increases the sensitivity and overall survival rate to the chemotherapy drug gemcitabine [107].

1.3.3 Survival mechanism of CTCs

Entering the blood system, CTCs will be inactivated by blood shear stress and immune cell killing. During the transmission process, CTCs adopt multiple mechanisms to protect themselves, including using platelets as a protective barrier and avoiding immune recognition. Tumor cells polymerize with platelets in the blood and resist the shear stress of blood flow. Zheng *et al.* found that platelets and tumor cells express the main receptor of fibrinogen and β-integrin [108]. Fibrinogen can bridge the two types of cells, strengthen the combination of the two, and promote the protection of CTCs. Heparin and chemical derivatives can inhibit the binding of fibrinogen and β-integrin and have the potential to develop into anti-cancer metastasis drugs. In terms of immunorecognition, CD47 is a widely expressed transmembrane protein, which can bind

to the single regulatory protein α expressed by macrophages and dendritic cells to inhibit its phagocytosis. Willingham *et al.* systematically analyzed CD47 expression of malignant tumor cells from various parts of the human body (including ovary, breast, colon, bladder, prostate, etc.), CD47 expression of tumor cells was found to be about 3.3 times that of corresponding normal cells on average [109]. The same study found that CD47 mRNA levels were negatively correlated with the patient's progression-free survival (PFS), and anti-CD47 antibodies restored phagocytosis, further proving that high expression of CD47 can reduce the immune system's killing of CTCs.

Monocyte chemoattractant protein-1 (MCP-1) is a chemokine that can attract immune cells such as natural killer cells (NK) and memory T lymphocytes and is related to tumor growth and diffusion. Mardani *et al.* analyzed and compared the MCP-1 concentration in the serum samples of healthy volunteers and patients with benign/malignant salivary gland tumors, and found that the MCP-1 concentration in the blood samples of patients with high progression was low, and believed that low concentration MCP-1 provided favorable conditions for the tumor diffusion [110]. NK cells are a type of cells that directly kill tumor cells through perforated proteins and granzymes or indirectly eliminate tumors by regulating factors such as interferon γ (IFN-γ), tumor necrosis factor-alpha (TNF-α) and other factors, and their activation depends on a variety of protein receptors. Rocca *et al.* found that the expression of CD16. NKG2D, DNAM-1, CD161, NKp46, NKp30 and other activated receptors on the surface of NK cells in peripheral blood were negatively regulated. In contrast, inhibitory receptors such as CD85j and NKG2A were positively regulated; these regulations reduce the cytotoxicity of NK cells and the amount of IFN- γ secretion [111]. It is speculated that

during the spread of cancer, the decrease in NK cell activity leads to enhanced survival of tumor cells in the circulatory system. The overexpression of protease-activated receptors-1 (PAR-1) on the surface of breast cancer, prostate cancer, melanoma cells is also related to its enhanced metastatic ability. Villares *et al.* found that PAR-1 negatively regulates the level of Maspin, and the latter can increase the apoptosis of tumor cells and reduce tumor angiogenesis [112]. After fully understanding the molecular-level mechanism of CTCs to avoid immune system attacks, it is possible to use human autoimmunity to intervene in the occurrence and development of tumor metastasis.

1.3.4 Heterogeneity

Tumor tissue has heterogeneity (such as different mutation sites and different cell phenotypes). CTCs not only have the same heterogeneity but also may become an effective tool for studying tumor heterogeneity. Li *et al.* stained CTCs of gastric cancer patients with keratin 8, 18, 19, and EpCAM as epithelial (E) markers, and vimentin and TWIST as mesenchymal (M) markers. Then categorize patients into five categories (E, E>M, E=M, E<M, M), it was found that most (31/35) samples contained two or more CTC states, that is, between epithelial cells and mesenchymal cells [113]. Another study compared the nucleus size of 304 prostate cancer CTCs and their host cancer metastasis and found that CTCs can be divided into large nuclei (>14.99 pm), small nuclei (8.54~14.99um), and extremely small according to the size of the nuclei. Nuclei (<8.54 um), the number of small and very small CTCs is significantly related to cancer metastasis, and the number of very small CTCs is significantly related to visceral metastasis [114]. Due to factors such as EMT and environmental induction, CTCs may acquire mutations that are different from tumors in situ, making them different from

tumors in situ and richer in heterogeneity. CD24 is a ubiquitous marker on the surface of breast epithelial cells. Rostoker *et al.* isolated $CD24^+$ and $CD24^-$ cells from breast cancer cell lines proving that $CD24^+$ cells are easier to aggregate into microspheres, and $CD24^+$ tumors grow faster and are easier to metastasize [115]. They also found that about 70% of the tumors that grew from $CD24^+$ cells were CD24. Pavese *et al*. used CTCs cell lines produced by orthotopically transplanted prostate cancer mice to conduct cell invasion, migration, colony formation, xenotransplantation and other experiments, and compared the doubling time, cell morphology, and migration of CTCs compared with orthotopic tumor cells. There was no obvious change in the ability and the size of the induced tumor, while the invasion ability increased by 50%, and the number of metastatic tumor cells increased [116]. Further studies have shown that the MMP-2 and EMT-related proteins of CTCs have increased in quality and show a slightly different drug sensitivity (increased resistance to mitoxantrone) from tumor cells in situ. Pailler *et al.* detected Proto-Oncogene 1 (ROS1) rearranged CTCs in patients with non-small cell lung cancer and found that the average and standard deviation of ROS1 copy number was significantly higher than that of tumor tissue cells, proves CTC has higher heterogeneity [117]. On the one hand, CTCs usually exhibit richer heterogeneity than clinically acquired local tumor tissues, and can provide strong support and guidance when formulating medication regimens based on the patient's genotype and phenotype; on the other hand, CTCs may be more Tumor tissue cells accumulate additional gene mutations, and they need to be cautious when using their molecular biological properties as a window to observe tumor tissue.

1.3.5 Application of CTCs in diagnosis and staging

Difficulties in early diagnosis and lack of effective individualized treatment are important reasons for the poor prognosis of pancreatic cancer. About 80% of pancreatic cancer patients have had peripheral tumor invasion or distant metastasis at the time of diagnosis and cannot be treated with surgery [118]. CA19-9 is the most important clinical serum biomarker for pancreatic cancer. Still, the sensitivity and specificity are only 80% and 82%. In contrast, some patients with pancreatic cancer do not have elevated CA19-9 levels, and some patients with benign diseases (such as pancreatitis, biliary obstruction) will have false positives elevated CA19-9 levels [119]. Therefore, it is necessary to find new and effective biomarkers, which can be used not only for the early diagnosis of pancreatic cancer but also to monitor the efficacy and guide clinical treatment. As an important part of liquid biopsy, CTCs are the hot spots of clinical research. The venous blood of the pancreas first flows back to the liver through the portal vein system and then reaches the systemic circulation. The peripheral blood CTCs are significantly less than those of breast cancer, prostate cancer and other tumors. Pancreatic cancer is rich in the stroma, and the proportion of tumor cells is limited, so the CTCs in peripheral blood are also less than those of colorectal cancer and gastric cancer that also return through the portal vein [120]. Some studies failed to draw meaningful conclusions due to the low detection rate of pancreatic cancer CTCs and the low CTCs count per unit of blood sample [121].

Kulemann *et al.* found that 75.0% of early pancreatic cancer patients (AJCC stage ≤ IIB) were positive for CTCs, and 71.4% of advanced patients (AJCC stage ≥ III) were positive for CTCs [122]. Therefore, CTCs not only appear in patients with metastasis or

advanced stage but can appear in different stages of pancreatic cancer. Zhang *et al.* used Pan-CK, CD45, DAPI, and CEP8 (chromosome centromere probe 8) as markers to detect CTCs from 22 cases of pancreatic cancer, 3 cases of solid pseudopapillary tumors, and 6 cases of benign pancreatic tumors and 30 healthy volunteers [123]. They found when Pan-CK$^+$, CD45$^+$, DAPI$^+$ and CEP ≥ 2 were used as the criteria for pancreatic cancer CTCs, and the CTCs count ≥ 2/3.75mL had a sensitivity and specificity of 68.18% and 94.87% for the diagnosis of pancreatic cancer, respectively [123]. Zhou *et al.* detected the expression of C-MET, h-TERT, CK20 and CEA genes in pancreatic cancer CTCs at 80%, 100%, 84% and 80%, respectively, and 0, 0, 6.7% and 0 in normal somatic cells [124]. If the above four gene expressions are used as the standard for pancreatic cancer CTCs at the same time, the sensitivity and specificity of diagnosis can reach 100%. Ankeny *et al.* detected the CTCs from 72 patients with pancreatic cancer and 28 patients with other pancreatic diseases. They showed that the positive rate of CTCs in stage I to II patients was 54.84% (17/31), and the positive rate of stage III was 78.57% (11/14), the positive rate of stage IV was 96.30% (26/27), while only 1 of 28 patients with other pancreatic diseases detected one CTCs [125]. They show that CTCs ≥3/4mL can be used as the criterion for stage IV pancreatic cancer diagnosis. CTCs are expected to become biological markers for the diagnosis and staging of pancreatic cancer.

1.4 Cancer metabolism

1.4.1 The glycolysis and TCA cycle

In the 1920s, Warburg *et al.* observed that tumor tissue consumes glucose faster than surrounding healthy tissue, and cancer cells can rely on rapid glycolysis and mitochondrial respiration at the same time [126, 127]. Since this discovery, glycolysis

and other metabolic pathways related to tumor metabolism have been extensively explored. The glycolytic metabolic pathway begins with the uptake of extracellular glucose from the environment surrounding the cell and subsequent intracellular processing of glucose in the cytosol to yield pyruvate along with numerous other products eventually. Glycolytic metabolism is a relatively inefficient pathway for the generation of cellular ATP, netting only two molecules of ATP per unit of glucose. Energy metabolism is the process of energy generation, release, conversion and utilization of energy in the process of organism metabolism. Normal cells are mainly powered by aerobic oxidative phosphorylation of glucose, and glycolysis is the main method in an anoxic environment. The energy metabolism characteristics of tumor cells are different. Even in the case of sufficient oxygen supply, tumor cells still actively take up glucose and perform glycolysis, while producing a large amount of lactate. This is the pioneer theory of the tumor energy metabolism-Warburg Effect [126]. Although glycolysis has low productivity, it is necessary for rapidly proliferating tumor cells. It not only provides ATP for tumor cells quickly but also provides a variety of biological macromolecules for the construction of new cells, thereby giving them growth advantage. The special energy metabolism pattern of tumor cells has become a new tumor sign phenomenon [128]. In recent years, research on tumor energy metabolism has become a hot research direction of scientists and even pharmaceutical companies. With the deepening of its research, targeted energy therapy of tumors will also usher in new opportunities. Since the tumor is a heterogeneous disease, the heterogeneity of cells and structure gives it a complex energy metabolism phenotype.

Although tumor cells have different energy metabolism methods, in general, the glycolysis phenotype is still dominant and dependent on glutamine consumption. The study found that even if the tumor tissue is rich in oxygen, its glycolysis is still at a productivity advantage, but oxidative phosphorylation is relatively inhibited [129]. This reprogramming of energy metabolism may be related to the following factors.

1.4.1.1 Hypoxia

With the increase in the number and volume of tumor cells, the original blood vessels have been difficult to meet the supply of nutrients and oxygen, and the number of new blood vessels is insufficient, the framework is disturbed, the self-regulation ability is poor, and there is a lack of vasomotor structure and physiological drug receptor. This also further affects the transportation of oxygen and nutrients. Besides, there are blood rheology changes in tumors. These factors will lead to the formation of a hypoxic environment with chronic diffusion disorders in tumors [130].

There are two reasons for hypoxia to cause the glycolysis energy metabolism phenotype of tumor cells. First, hypoxia stimulates the expression of hypoxia inducible factor-1 (HIF-1), which can upregulate the expression of glucose transporter 1/3 (GLUT1/3) to ensure a large amount of glucose uptake [131]. Meanwhile, HIF-1 up-regulates the expression of most glycolysis related enzymes, such as hexokinase-1/2 (HK1/2), phosphoglycerate kinase 1(PGK1), lactate dehydrogenase A (LDHA), 6-phosphofructo-2 -kinase/fructose-2,6-bisphosphatase-3/4 (PFKFB3/4), pyruvate kinase M2 (PKM2), etc., and this makes the glycolysis pathway more prereferral [132, 133]. Second, hypoxia and HIF-1 inhibit mitochondrial biosynthesis and cause mitochondrial autophagy, thereby reducing the copy number of mitochondria. They can also reduce the

expression of pyruvate dehydrogenase kinase 1 (PDK1) and acetyl-CoA production, or inhibit mitochondrial electron transport chain components iron-sulfur cluster assembly enzyme (ISCU) and cytochrome c oxidase assembly factor heme A:farnesyltransferase (COX10) expression, which in turn inhibits the mitochondrial oxidative phosphorylation function [134, 135]. Therefore, tumor cells need to supply energy by glycolysis.

1.4.1.2 Activation of oncogenes and inactivation of tumor suppressor genes

HIF-1 can bind to the promoter region of the Myc gene and stimulate Myc gene expression [136]. Also, the c-Myc gene can be activated by gene amplification and chromosomal translocation. High Myc expression is very common in tumors. Myc is a transcription factor with a wide range of biological functions, including cellular energy metabolism. Myc can stimulate the expression of many genes, including GLUT and glycolysis related genes, so that the metabolism of tumor cells moves towards the Warburg effect. Abnormal activation of the Myc gene also leads to abnormally increased synthesis of LDHA [137]. LDHA catalyzes the formation of pyruvate to form lactate, and the resulting lactate is discharged out of the cell, which is closely related to the acidification of the tumor microenvironment. This acidified environment is not good for normal tissues, but it is good for tumor tissues, which can stimulate the growth of tumor cells [138]. Recently, it has been suggested that lactate excreted by hypoxic tumor cells can be taken up by adjacent subpopulation tumor cells as an energy source, thereby forming a metabolic symbiont of lactate excretion and lactate utilization cells. This phenomenon is not unique to tumors, and it reflects that tumors use other physiological mechanisms for their rapid growth [139]. Therefore, blocking the activity of LDHA may

effectively cut off the energy source of cancer cells, thereby causing them to die without affecting normal cells with aerobic metabolism.

1.4.1.3 PKM2

Recently, researchers have discovered that pyruvate kinase M2 (PKM2) is a very important metabolic molecule behind the glycolysis process [140]. There are two isomers of M-type pyruvate kinase, PKM1 and PKM2. PKM2 is usually expressed in embryonic tissue, while PKM1 is expressed in adult tissue. When the cells become cancerous, PKM2 resumes expression, while PKM1 expression is suppressed. Analysis of various tumor cell lines confirmed that PKM2 is the only form of pyruvate kinase found in cancerous tissues. When PKM1 is used to replace PKM2 in tumor cells, it leads to a decrease in lactate production and an increase in oxygen consumption, which is exactly the opposite of the Warburg effect. Only cells expressing PKM2 can form tumors in mice, indicating that PMK2 can promote unique metabolic phenotypes in tumor cells [140]. The expression of PKM2 in tumor cells is also related to Myc protein. Myc protein can induce the expression of PKM2, which is consistent with Myc's energy metabolism of tumor cells towards the Warburg effect [141]. Recent studies have shown that PKM2 can be used as a partner factor for HIF1 transcription and enhance HIF1 transcription, from which we can see that the Warburg effect of tumor cells is the result of the synergistic effect of different factors. PKM catalyzes the conversion of phosphoenolpyruvate to pyruvate and simultaneously produces an ATP molecule. This reaction is the penultimate reaction of glycolysis. The current view is that PKM2 does not promote glycolysis, but inhibits glycolysis. As a result, the intermediate product of

glycolysis turns to biomacromolecule synthesis and maintains the redox balance of tumor cells to support the growth of tumor cells [142].

1.4.1.4 PI3K-Akt signal activation stimulates glycolysis

The PI3K-Akt signaling pathway widely exists in cells and exerts a wide range of biological functions by regulating the cell cycle, protein synthesis, and cell energy metabolism. PI3K-Akt signal is positively regulated by the oncogene KRAS and negatively regulated by the tumor suppressor gene PTEN, and mutations or inactivation of the KRAS gene and PTEN gene are common in tumors, so many tumors have PI3K-Akt signaling activation [143]. Akt enhances the Warburg effect of tumor cells by increasing the activity of GLUT, HK, PGK and PFK1 and other factors [142]. HK is the first rate-limiting enzyme for glycolysis, catalyzing the phosphorylation of glucose to glucose 6-phosphate. After isomerization of 6-phosphate glucose, fructose 6-phosphate is formed, and then fructose 6-phosphate is catalyzed by PFK1 to 1,6-phosphate fructose, and then enters glycolysis. Both HK and PFK1 are key enzymes for glucose to enter glycolysis. Akt can also enhance protein and lipid synthesis by activating the mammalian target of rapamycin (mTOR) signal [144]. At the molecular level, the above metabolic changes also activate HIF, tilting cellular energy metabolism towards glycolysis.

1.4.1.5 TP53 regulates cellular energy metabolism

Although about 56% to 63% of the ATP energy of most tumor cells comes from anaerobic glycolysis, the remaining about 44% to 37% of the ATP energy still needs to be provided by aerobic oxidation. The tumor suppressor gene TP53 plays an important role in regulating the balance between mitochondrial aerobic oxidation and glycolysis [145]. TP53 is a transcription factor with a wide range of biological functions, including

cellular energy metabolism. Recent studies showed that TP53-induced genes, such as TP53 Induced Glycolysis Regulatory Phosphatase (TIGAR) and Synthesis Of Cytochrome C Oxidase 2 (SCO2) are involved in cell energy metabolism [146]. TIGAR reduces the level of fructose-2,6-bisphosphate in cells, thereby inhibiting glycolysis levels, and SCO2's role is to participate in the assembly of cytochrome c oxidase (located in Electron transport chain complex IV), which is related to the mitochondrial electron transport chain [146]. Abnormal expression of SCO2 can increase the mitochondrial reactive oxygen species (ROS) and affect the mitochondrial oxidative phosphorylation function. Therefore, the inactivation of TP53 in tumor cells is the main force for tumor cells to obtain glycolysis phenotype.

1.4.1.6 Impaired mitochondrial oxidative phosphorylation

Warburg believed that tumor cells mainly adopt aerobic glycolysis for energy supply because mitochondria are irreversibly damaged. Studies have also found that tumor cell mitochondrial oxidative phosphorylation function may be damaged, which is related to hypoxia, mitochondrial DNA mutations, and electron transport chain dysfunction [147]. Abnormal expression of energy metabolism enzymes, such as mitochondrial Tu Translation Elongation Factor (TUFM) is involved in the malignant biological behavior of colon cancer [148], cytochrome B (Cytb) mutation is associated with bladder cancer [149], mutations of isocitrate dehydrogenase IDH1 and IDH2 are associated with glioma and acute myeloid leukemia [150], and mutations in fumarate hydratase (FH), succinate dehydrogenase (SDH) and other genes are involved in the formation of kidney cancer and paraganglioma [151]. The abnormality of these key molecules involved in the process of mitochondrial oxidative phosphorylation not only

inhibits the production of mitochondrial energy but at the same time, the functional mutations obtained by themselves increase the heterogeneity of tumor cells. Besides, some cancer cells produce a "truncated tricarboxylic acid cycle" due to damage to the respiratory chain [152]. Because the damaged mitochondria are attacked by reactive oxygen species (ROS), ROS inhibits the activity of aconitase and increases the concentration of citrate in the mitochondria. After the citrate enters the cytoplasm, it cooperates with acetyl-CoA to complete the TCA cycle. The NADH produced by this process inhibits the complete tricarboxylic acid cycle. It does not produce energy but provides raw materials for biological macromolecules for rapidly growing tumor cells. Therefore, under the above circumstances, assuming that the total cellular ATP is unchanged if the oxidative phosphorylation function is weakened, the role of glycolysis must be enhanced to maintain the cell energy balance.

1.4.1.7 Other aspects

In addition to the above reasons, other factors can also cause tumor cell glycolysis phenotype. Chronic inflammation is a major cause of tumorigenesis. Some inflammatory factors can promote glycolysis of breast cancer cells, and miR-155 can be involved as a transit molecule between inflammation and glycolysis [153]. In addition to inflammatory pathways, microRNAs lin28/let-7 regulatory axis post-transcriptionally regulates the metabolic enzyme PDK1, thereby reprogramming tumor metabolism to promote glycolysis [154]. There are also lncRNAs, such as UCA1 promotes the glycolysis ability of bladder cancer cells by increasing HK-2 expression [155]. The researchers also found that defects in fatty acid metabolism can aggravate the aerobic glycolysis process of colorectal cancer and promote malignant features of the tumor, which is related to the

deletion of the Abhydrolase Domain Containing 5 (ABHD5) associated with lipid droplets [156]. Activation of certain signaling pathways such as Wnt signaling can drive the glycolytic phenotype of colon cancer cells and promote their proliferation, which depends on the activation of PDK1, a downstream target of Wnt [157].

1.4.1.8 ATP supply for growth and proliferation

Tumor cells can overcome the constant uptake of nutrients caused by the stimulation of normal cell growth signals, and by ingesting glucose and glutamine in large amounts, they can obtain the ability to continue to grow, divide and multiply. Fast-growing tumor cells can still produce a high proportion of ATP/ADP using glycolysis because lack of ATP is not conducive to cell survival, and it has a complete energy-sensing signal pathway [158]. AMP-activated protein kinase (AMPK) acts as an energy sensor. When AMP/ATP increases, AMPK activates, which can increase ATP by increasing glucose transport and fatty acid oxidation and appropriately inhibit the consumption of ATP by anabolic metabolism [159]. In addition to providing sufficient ATP for cell growth and proliferation, enhanced glycolysis metabolism can also inhibit cell death, because, on the one hand, it reduces the production of reactive oxygen species, thereby weakening the damage of oxygen free radicals to the cell; on the other hand, it reduces caspase-dependent and non-dependent apoptosis, such as overexpression of glyceraldehyde 3-phosphate dehydrogenase (GAPDH) can increase glycolysis and ATP levels, blocking non-caspase-dependent apoptosis [160]. After inhibiting cancer cell PDK1 with small molecules of sodium dichloroacetate (DCA), forcibly increasing oxidative phosphorylation and inhibiting glycolysis, it can make cancer cell membrane

hyperpolarization and potassium ion voltage-gated channels open, triggered mitochondrial activation-induced caspase-dependent apoptosis [161].

1.4.1.9 Provide macromolecular materials to form new cells

In addition to the need for ATP, rapidly proliferating tumor cells also need biological macromolecular materials to form new cells. The unique energy metabolism of tumor cells can provide a large number of metabolic intermediates to facilitate the synthesis of fatty acids, membrane phospholipids, nucleic acids, and proteins [162]. For example, tumor cells increase the production of acetyl-CoA through reductive glutamine metabolism and up-regulate the expression of fatty acid synthases (FASN) by HIF-1, which is conducive to the large-scale synthesis of fatty acids. On the one hand, fatty acids synthesize phospholipids to facilitate cell membrane construction. On the one hand, the synthesis of triglycerides facilitates energy storage and signal transmission, which are closely related to tumor formation and progression [163, 164]. Many tumor cells specifically express pyruvate kinase PKM2, which can promote the conversion of sugar to membrane phospholipids, giving cancer cells a selective growth advantage [140]. A large number of pyruvate products produced by glycolysis can stimulate the synthesis of lipids, while glucose 6-phosphate can synthesize ribose and NADPH through the pentose phosphate pathway; glutamine metabolite glutamate can also be metabolized by the TCA cycle [164]. Converted to lactic acid, together with lactic acid produced by glycolysis, NADPH is produced for phospholipid biosynthesis, and oxaloacetate is used as an intermediate product of the TCA cycle [165].

Based on previous knowledge, it can be seen that the metabolic phenotype of tumor cells provides potential theoretical value for the diagnosis and treatment of clinical

tumors, such as the application of metabolic imaging technology. An in-depth interpretation of the internal molecular mechanism of different energy metabolism phenotypes of tumor cells will help to reveal the causal relationship between tumor cell metabolism changes and biological behaviors and provide new opportunities for targeted energy therapy of tumors, such as "starved" tumor cells. After the glycolysis phenotype of tumor cells is promoted, they will be completely wiped out.

1.4.2 Amino acid metabolism

The proliferation of cancer cells needs to obtain the corresponding energy and material basis to meet the biosynthesis needs of replication while maintaining the redox steady state. A large number of studies have shown that the metabolism of tumor cells is abnormally active, and the nutrients and energy necessary to maintain their rapid proliferation can be obtained in various ways [162]. The metabolism of cancer cells is also different from that of normal cells, and its metabolic changes are also considered to be the hallmarks of cancer [142, 166]. In recent years, several studies have shown that the metabolic level of various amino acids in tumor cells has changed to adapt to the increase in energy requirements and changes in the environment [128]. Multiple signaling pathways and transcription factors often drive the changes in tumor amino acid metabolism. A large number of basic and clinical trials have shown that targeting tumor-dependent amino acid metabolism and developing new drugs can effectively inhibit tumor growth [167].

1.4.2.1 Arginine metabolism

Arginine (Arg) is synthesized from citrulline through a two-step catalytic synthesis of Argininosuccinate Synthase 1 (ASS1) and Argininosuccinate lyase (ASL),

and then Arginase 1 (Arg1) breaks down arginine into ornithine and urea. Arg and Ornithine carbamoyltransferase (OTC) are used to convert ornithine to citrulline for recycling in mitochondria. The abnormality of ASS1, ASL or OTC will affect the storage of arginine in the cell. ASS1 deficiency is common in tumors, causing tumor cells to have to obtain arginine in serum [168]. Therefore, the rapid depletion of arginine in serum can be used as a new strategy for cancer treatment [169]. Arginine deiminase (ADI) and Arg1 can deplete arginine in serum by converting arginine to citrulline and ornithine, then inducing of cell cycle arrest, apoptosis, autophagy and causing inhibition of angiogenesis [170, 171].

1.4.2.2 Asparagine and aspartate metabolism

Mammalian cells produce asparagine from aspartate and glutamine via asparagine synthetase (ASNS). However, some cancer cells lack ASNS expression and need to rely on asparagine in serum to meet their needs. ASNS catalyzes the synthesis of the non-essential amino acid asparagine from aspartate and glutamine. ASNS expression is highly regulated at the transcriptional level and is also subject to the amino acid response. Lacking ASNS protein expression is a hallmark of acute lymphoblastic leukemia (ALL), so this is auxotrophic for asparagine. Using bacterial L-asparaginase (L-ASPase) for ALL treatment is the first example of anti-cancer treatment for tumor metabolism. L-ASPase is widely present in the serum of microorganisms, plants and some serrated animals. It is an enzyme inhibitor produced by microbial fermentation. L-ASPase catalyzes the deamidation of asparagine, which rapidly consumes asparagine in serum, leading to the inhibition of tumor cell protein synthesis and growth inhibition [172]. Many clinical trials

are currently evaluating the efficacy of L-ASPase in treating a series of malignant hematological tumors.

Other hematological and solid cancers also have elevated ASNS levels, so they should also respond to asparagine deprivation. In the past few years, some reports have shown that in certain cancer types, ASNS is overexpressed, thereby promoting cell proliferation, chemoresistance, and metastatic behavior [173, 174]. Limiting asparagine by knocking out asparagine synthase, treating it with L-asparaginase, or restricting asparagine in the diet can reduce metastasis without affecting the growth of the primary tumor. Moreover, asparagine availability also promotes the epithelial-to-mesenchymal transition [174]. Activated transcription factor 4 (ATF4) is the main transcriptional regulator of the integrated stress response (ISR), which transforms cells to survive the nutrient transformation. Zinc Finger and BTB domain-containing protein 1 (ZBTB1) has been shown to regulate ASNS directly through binding [175]. The loss of ZBTB1 sensitizes T-cell leukemia cells that are resistant to treatment to L-asparaginase, which is a chemotherapy that reduces the serum asparagine content [175].

1.4.2.3 Glutamine metabolism

Normal cells can produce glutamine by self-synthesis, but tumor cells rely on self-synthesized glutamine to not meet their rapid proliferation needs and need to ingest glutamine from extracellular or enhance glutamine metabolism pathways through the membrane transporter. Tumor cells rely on SLC (solute carrier) superfamily transporters on the cell membrane to take up glutamine from the extracellular environment. As a key transporter for the transfer of glutamine into cells, SLC1A5, SLC7A5, SLC7A11 and SLC6A14 play an important role in tumor cells [176]. It has been reported that the

expression of the transporter SLC6A4 is upregulated in colon cancer, cervical cancer, breast cancer and pancreatic cancer, and it is expressed at low levels in normal cells. Blocking the SLC6A14 protein will affect the intracellular biosynthesis of tumor cells, but has little effect on normal cells [177]. Nicklin *et al.* found that inhibition or deletion of SLC1A5 would lead to a decrease in glutamine content in tumor cells, mTOR signaling pathway could not be activated, and eventually, tumor growth was inhibited [178].

In mitochondria, glutamine is catalyzed by glutaminase (GLS) to glutamate. There are two subtypes of glutaminase in the human body: renal glutaminase (GLS1) and liver glutaminase (GLS2). In the tumor cells of lymphoma, glioma, breast cancer, pancreatic cancer, non-small cell lung cancer and kidney cancer, the use of small-molecule inhibitors or genetic knockdown suppresses the widely expressed GLS1 and produces antitumor activity [179]. In B lymphoma cells and prostate cancer cells, the highly expressed oncogenic transcription factor c-Myc can inhibit miRNA-23a/b, up-regulate the expression of GLS1, enhance glutamine metabolism, and promote the proliferation of tumor cells [180]. Wang *et al.* found that the up-regulation of GLS1 in breast cancer depends on the role of Rho family proteins and the NF-κB signaling pathway and proved that the reduction of GLS1 expression could effectively inhibit the proliferation of tumor cells [181]. c-Myc can induce GLS1 without inducing GLS2 expression, while the tumor suppressor p53 induces GLS2 without inducing GLS1 expression. GLS2 expression is reduced or even deleted in hepatocellular carcinoma. GLS2 overexpression can significantly reduce the formation of tumor cell colonies, indicating the potential role of GLS2 in inhibiting the growth of tumor cells [182]. After

Glutamine is catalyzed into glutamate by GLS, glutamate is oxidized and deaminated by glutamate dehydrogenase (GLUD1, GLUD2) and transaminase (GOT1, GOT2) into α-KG and ammonia in the mitochondria, and enters the TCA cycle. GLUD can regulate the production of α-KG in tumor cells, and its expression is up-regulated in lung cancer and breast cancer cells. The knockdown of GLUD1 can inhibit tumorigenesis in lung cancer xenograft models [183].

Whereas most cells use glutamate dehydrogenase (GLUD1) to convert glutamine-derived glutamate into α-KG in the mitochondria to fuel the TCA cycle, KRAS derived PDAC relies on a distinct pathway in which glutamine derived aspartate is transported into the cytoplasm where it can be converted into oxaloacetate (OAA) by aspartate transaminase (GOT1) [165]. Furthermore, OAA is converted into malate and then pyruvate, then increases the $NADPH/NADP^+$ ratio, which is used to maintain the cellular redox state [165]. Tumor vascular tissue usually leads to areas of nutritional deficiencies and hypoxia. Even we understand the response of solid tumors to hypoxia, but little is known about how nutritional deficiency locally affects tumor growth and treatment response. Due to decreased levels of low glutamine in the core region of the tumor, histone hypermethylation is caused, which is a key cofactor containing the Jumonji domain-containing (JmjC) histone demethylases (JHDMs) [184]. Low glutamine-induced histone hypermethylation leads to de-differentiation and drug resistance, which is mainly mediated by methylation on H3K27[184]. Increased consumption of glutamine will lead to the consumption of nutrients in the tumor, which may cause metabolic stress, thereby affecting tumor progression. Glutamine deficiency regulates EMT by upregulating the main EMT regulator, Zinc finger protein SNAI2 (SNAI2) [185]. This

process depends on the MEK/ERK signaling pathway and ATF4 [185]. SNAI2 in PDAC cells are necessary for glutamine deprivation-induced EMT, cell movement, and nutritional stress survival.

At present, many inhibitors against GLS have anti-tumor activity. Glutamine analogs, 6-Diazo-5-oxo-L-norleucine (DON), can successfully inhibit glutamine metabolic enzymes by combining with the enzyme active site, which has antitumor activity. Still, its clinical application is limited due to non-selectivity and toxicity [167]. Bis-2-(5-phenylacetamido-1,3,4-thiadiazol-2-yl)ethyl sulfide (BPTES) is a selective allosteric modulator of GLS1, inhibits the proliferation of glutamine-dependent cancer cells *in vitro*, and slows the growth of transplanted animal tumors and the oncogenic factor c-Myc Growth of mouse tumors [181, 186]. CB-839, which is currently undergoing clinical trials, has a similar allosteric binding mechanism and particular characteristics to BPTES, but exhibits stronger inhibitory activity and unique kinetic properties. CB-839 has shown antiproliferative activity in triple-negative breast cancer (TNBC) cell lines and shows significant antitumor activity in two xenograft tumors [179]. The main component of green tea catechins, epigallocatechin gallate (EGCG), is an inhibitor of GDH, which can inhibit the growth of glutamine-dependent cancer cells [187]. Pan-transaminase inhibitor, Aminooxyacetate (AOA), mainly inhibits glutamylation in breast cancer cell lines that highly express c-Myc by activating the endoplasmic reticulum stress pathway, leading to cancer cell death [188].

1.4.2.4 Serine and glycine metabolism

Changes in the de novo serine synthesis pathway (SSP) are common in cancer cells. Start with 3-phosphoglycerate (3-PG), the intermediate metabolite of glycolysis,

produce serine after involving 3- Phosphoglycerate dehydrogenase (PHGDH), Phosphoserine aminotransferase 1 (PSAT1) and three enzymatic reactions regulated by Phosphoserine phosphatase (PSPH). The increased expression of enzymes in SSP is one of the factors that cancer cells can survive in a serine starvation environment. Increased PHGDH expression can promote melanoma and breast cancer growth in mice [189]. The expression of PHGDH in triple-negative breast cancer and melanoma cells is significantly increased, and inhibition of PHGDH expression can lead to a significant decrease in the proliferation rate of tumor cells [190]. PHGDH and PSAT1 are activated in non-small cell lung cancer and participate in tumorigenesis and development [191]. Besides, PSAT1 and PSPH are also highly expressed in highly metastatic breast cancer cell lines [192]. Inhibition of PHGDH can attenuate brain metastasis and improved survival in mice with multiple cancer types [193].

Serine is a non-essential amino acid that inhibits the de novo synthesis of serine and may cause tumor cell tolerance [194]. Exogenous serine is converted into glycine by serine hydroxymethyltransferase (SHMT1 or SHMT2), providing a carbon unit to participate in the one-carbon cycle for nucleotide biosynthesis. Increased levels of SHMT1 and SHMT2 have been observed in transgenic mice susceptible to the oncogenic factor Myc-driven B-cell lymphoma [195]. SHMT2 is one of the most commonly expressed "metabolic genes" in human tumors [196]. Knocking out of SHMT2 seriously damages the proliferation of cancer cells. Moreover, glycine decarboxylase (GLDC) in the glycine cleavage system (GCS) is one of the most up-regulated genes in tumor-initiating cells isolated from non-small cell tumors, inhibition of GLDC can improve the survival rate of patients with non-small cell lung cancer [197].

1.4.2.5 Tryptophan metabolism

In mammalian cells, L-tryptophan (Trp) catabolizes mainly through the kynurenine pathway and converts to L-kynurenine (Kyn). Three different dioxygenases control the catabolism of Trp by the kynurenine pathway: tryptophan 2,3-dioxygenase (TDO), indoleamine 2, 3-dioxygenase 1 (IDO1) and indoleamine 2, 3-dioxygenase 2 (IDO2). The cleaved product N-formyl kynurenine is enzymatically reacted or spontaneously hydrolyzed to Kyn. IDO is the rate-limiting enzymes in the kynurenine pathway and is highly expressed in a variety of human tumors [198]. IDO can suppress innate and adaptive immune cell responses by depleting tryptophan, which is essential for T cell proliferation in the tumor microenvironment, and causing the accumulation of tryptophan metabolite kyn and its derivatives, resulting in the rapid proliferation of tumor cells [199]. IDO (IDO1 and IDO2) are overexpressed in a variety of cancers, and most studies have been focused on the research of IDO1. Preclinical studies have shown that targeting IDO1 in rodent models can trigger an anti-tumor immune response and inhibit tumor growth [198]. IDO2 is a paralog of IDO1, and they have similar structures. However, IDO1 and IDO2 exhibit different substrate specificities and tissue distribution. The expression of IDO2 in various cancers has been confirmed [200]. Also, IDO2 is necessary to induce several key inflammatory cytokines, and targeting IDO1 and IDO2 can enhance immune effects [201]. TDO, a homotetrameric protein, together with IDO1 and IDO2 catalyze the first rate-limiting reaction of the kynurenine pathway, but TDO has a higher affinity for L-tryptophan than IDO1. TDO is usually expressed in the liver, and most of it is highly expressed in human tumors [202]. Preclinical studies have shown

that TDO inhibitors can promote the immune rejection of host cells against tumor cells and can be used as a safe and effective cancer treatment [203].

1.5 BCAA metabolism

BCAAs are essential amino acids include leucine, isoleucine, and valine, which not only act as building blocks for tissue proteins (accounting for 35% of the essential amino acids in muscle) but also contribute carbon and nitrogen through catabolism. Unlike other amino acids, BCAA levels are not regulated by the liver. BCAA is relatively high in dietary protein, accounting for 15-20% of protein intake [204]. Under physiological conditions, BCAA is in a steady-state, and it plays a variety of important physiological functions in the body, which are important nutritional signals that affect metabolism.

1.5.1 The biological role of BCAA

1.5.1.1 Influencing the structure and function of the protein

BCAA plays an important role in protein structure (especially globular proteins) and functions, especially the interaction between membrane protein transmembrane regions and phospholipid bilayer. Mutation of BCAA sites in proteins caused by gene mutations will cause certain diseases. For example, the replacement of isoleucine with valine in thyroxine carrier protein will lead to cardiomyopathy characterized by amyloid deposition [205]. In Peroxisome proliferator-activated receptor alpha (PPAR-α) protein, leucine replacing valine will cause changes in blood lipids [206]. BCAA can also promote protein synthesis through the mammalian target of rapamycin (mTOR) signaling pathway, and leptin can enhance this effect [207].

1.5.1.2 Regulate the energy metabolism of the body and tissue cells

About 20% of the ingested BCAA is oxidized and decomposed by the TCA cycle and the biological oxidation system to produce adenosine triphosphate (ATP) for energy supply [208]. BCAA can also perform gluconeogenesis through the alanine-glucose cycle and the glutamine pathway to maintain blood glucose levels. Besides, BCAA catabolism plays an important role in regulating cardiac glucose metabolism. BCAA can directly inhibit pyruvate dehydrogenase complex (PDH) activity leads to a significant decrease in glucose uptake, oxidation, glycogen content, and protein glycosylation in hearts [209].

1.5.1.3 Regulating cell growth and metabolism as a signaling molecule

A large number of studies have shown that BCAA, especially leucine, can activate protein synthesis, glucose utilization, lipid metabolism, cell growth of the liver, skeletal muscle and other tissues by activating a series of signaling molecules such as mTOR activation, insulin sensitivity, autophagy, and neurotransmitter synthesis are regulated [207, 210, 211]. Recent studies have shown that BCAA metabolic derivative 3-hydroxyisobutyric acid can also promote skeletal muscle vasculature signal transduction or directly promote the synthesis of branched-chain fatty acids in adipocytes [212, 213]. Extensive biological functions BCAA can be converted into neurotransmitters, hormones and other important physiologically active substances in addition to the above functions. Besides, recent studies have found that an unbalanced intake of BCAA in food will promote the decomposition of lipids. BCAA can promote glucose utilization by up-regulating glucose transporters in the intestinal and muscle tissues [214]. BCAA can promote intestinal development, intestinal amino acid transport and mucin production, which are beneficial to breast health, breast milk quality and embryo growth, respectively

[215-217]. BCAA can also participate in the upregulation of innate and adaptive immune responses [218].

1.5.2 Regulation of body BCAA level

Increased plasma BCAA levels depend not only on their intake but also on their balance between catabolism and protein synthesis and degradation in the body.

1.5.2.1 BCAA catabolic regulation

BCAA mainly depends on food intake, so its content mainly depends on catabolic regulation [219]. BCAA is the only amino acid that can be metabolized outside the liver. Catabolic metabolism is mainly carried out in the liver, skeletal muscle, heart muscle and other tissues. The first step in the catabolism of BCAA is the reversible production of the corresponding branched-chain α-keto acid, α-ketoisovalerate (KIV), α-keto-β-methylbutyrate (KMV), and α-ketoisocaproate (KIC) (Figure 1.1), by the catalysis of branched-chain aminotransferase (BCAT) and the synergy of α-ketoglutarate and glutamine. The second step of BCAA catabolism is a rate-limiting step: BCKA was catalyzed by the mitochondrial branched-chain alpha ketoacid dehydrogenase (BCKDH) complex to produce branched-chain acyl-CoA intermediates. The liver is the main oxidative decarboxylation site of BCKA, and 80% of the body's BCKA is decomposed in the liver [220]. The above two steps are the basic steps of BCAA metabolism. After oxidative decarboxylation, BCKA is transformed into the corresponding branched acyl-CoA through its respective metabolic pathway and finally enters the TCA cycle for complete oxidation and energy supply.

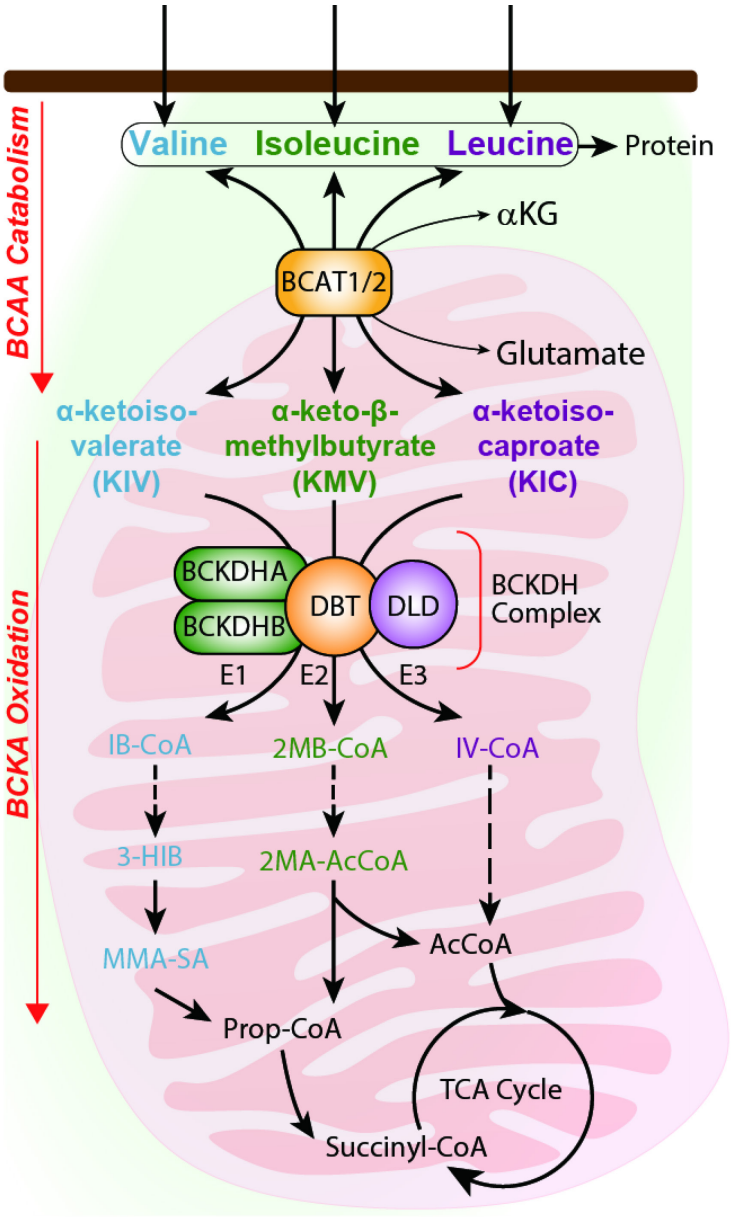

Figure 1.1 Schematic of BCAA metabolism.

The catabolism regulation of BCAA in the body mainly depends on the activity of the rate-limiting enzyme BCKDH complex. BCKDH kinase (BCKDK) and BCKDH phosphatase (PPM1K, PP2Cm) can regulate the activity of BCKDH complex and affect BCAA metabolism. The BCKDH complex is located on the mitochondrial inner membrane matrix side and contains three subunits: alpha-ketoacid dehydrogenase (E1

component), dihydrolipoyltransacylase (E2 component), and dihydrolipoamide dehydrogenase (E3 component). The activity of the BCKDH complex is mainly regulated by the phosphorylation level of the E1α subunit serine at position 293. Under the action of BCKDK, the phosphorylation of the E1α subunit of the BCKDH complex is inactivated, while under the action of PP2Cm, its dephosphorylation is activated (Table 1.1). Studies have shown that when the activity of the BCKDH complex in the liver decreases, it not only causes BCKA to accumulate in the body but also causes an increase in the content of BCAA in the circulating blood [221].

Table 1.1 BCAA metabolism related enzymes

Enzyme Name	**Full name**	**Location**
BCAT1	Branched-chain amino acid transaminase 1	cytosolic
BCAT2	Branched-chain amino acid transaminase 2	mitochondrial
BCKDHA	Branched-chain keto acid dehydrogenase E1, alpha polypeptide	mitochondrial
BCKDHB	Branched-chain keto acid dehydrogenase E1 subunit beta	mitochondrial

DBT	dihydrolipoamide branched chain transacylase E2	mitochondrial
DLD	dihydrolipoamide dehydrogenase	mitochondrial
BCKDK	Branched-chain keto acid dehydrogenase kinase	mitochondrial
PP2Cm	protein phosphatase 2cm	mitochondrial

Nutritional status and hormone signals can also change the gene expression of BCAA-related regulatory enzymes: in the rat liver, a low-protein diet can increase BDK mRNA expression, while removing BCAA in the culture medium can increase the BCKDK expression level of cultured hepatocytes and make BCKDH complex activity reduced [222]. BCKDK activity is also regulated by allosteric modulation of BCKA, thiamine pyrophosphate and other factors. BCKA can allosterically inhibit BCKDK and weaken the interaction between BCKDK and BCKDH complex [223]. Mitochondrial matrix resident type 2C phosphatase (PP2Cm) is the only endogenous BCKDH phosphatase found so far. PP2Cm is a soluble protein located in the mitochondrial matrix. Its distribution is tissue-specific. It is highly expressed in the brain, heart, liver, kidney, and diaphragm, but low in skeletal muscle [223]. Studies have shown that starvation or low BCAA status can inhibit PP2Cm transcription, and PP2Cm can compete with BCKDK to bind and interact with the BCKDH complex E2 subunit. This competitive effect is regulated by BCKA levels, which cause low levels of BCKA to make BDK

dominant and high levels of BCKA dominate the role of PP2Cm [223]. The study found that PP2Cm knockout mice had BCAA catabolism disorders, which showed a significant increase in plasma BCAA concentration [222].

1.5.2.2 Protein synthesis and degradation balance

Protein synthesis and degradation rate can also affect plasma BCAA levels. Studies have confirmed that insulin, insulin-like growth factor and BCAA can damage the autophagy process and the ubiquitin-proteasome pathway mediated by mTORC1 and PI3K/AKT pathways, thereby inhibiting the rate of protein degradation in muscle and liver [224]. Amino acids can stimulate protein synthesis in human leg muscles, while insulin can reduce protein synthesis in human leg muscles [225].

1.5.3 BCAA and diseases

BCAA maintains a steady-state under physiological conditions and exerts a variety of important physiological functions. When its catabolism is abnormal, resulting in the accumulation of BCAA and decomposition products, it may produce a series of harmful effects. Genetic defects of BCAA catabolism-related genes can cause a series of inborn metabolic diseases, such as Maple syrup urine disease (MSUD) [226]. In recent years, a large number of studies have shown that abnormal catabolism of BCAA is associated with many diseases such as Huntington's disease, pancreatic cancer, cardiovascular disease, diabetes, obesity.

1.5.3.1 BCAA and MSUD

MSUD is a rare autosomal recessive genetic disease with an incidence rate of about 1/85,000 [227]. It was first reported by Menkes *et al.* in 1954 that it got its name

because of the peculiar smell of caramel (maple sugar) in the urine of children [228]. The disease is due to the congenital disability of branched-chain alpha ketoacid dehydrogenase (BCKDH) complex, which causes the catabolism of branched-chain amino acids (leucine, isoleucine, valine) to be blocked, and the corresponding keto acids cannot be oxidatively decarboxylated and retained. In the body, it produces nervous system damage and maple odor urine. According to the different activity of BCKD complex, MSUD is divided into 5 types: classic type (< 2%), intermediate type (3% ~ 8%), intermittent type (8% ~ 15%), effective type of vitamin B1 and E3 subunit-deficient type [229]. The key to the treatment of MSUD during the acute phase is to promote protein synthesis, inhibit protein breakdown, and avoid damage to the nervous system caused by the accumulation of branched-chain amino acids. The branched-chain amino acid with a large degree of damage to the nervous system is leucine, and the blood leucine concentration is usually higher than isoleucine and valine. Therefore, the rapid reduction of leucine with neurotoxicity in plasma is the focus of treatment.

1.5.3.2 BCAA and diabetes

As early as 1942, studies reported that plasma BCAA levels in diabetic patients increased significantly, and plasma BCAA levels in obese patients also increased significantly. However, this phenomenon has not received due attention. Until 2009, Newgard et al. [25] reported that BCAA is involved in the development of insulin resistance in obese patients. McCormack et al. [26] found that serum BCAA levels (not BCAA dietary intake) are associated with obesity and insulin resistance. A large number of studies have shown that plasma BCAA levels in patients with diabetes are significantly increased, and BCAA can increase the risk of type 2 diabetes (T2DM) by five times. The

Framingham Heart Study evenly matched 378 respondents based on body mass, lipid metabolism indicators, and other clinical variables. The results showed that the high BCAA group was more prone to diabetes, and subsequent Malmo studies also confirmed this conclusion [27]. Recently, a large human genome-wide association study showed that the mechanism of impaired BCAA metabolism is involved in the pathophysiological process of T2DM. These results suggest that there may be a causal relationship between BCAA and insulin resistance.

Studies have confirmed that the activity of the BCKD complex in diabetic patients and animal liver is reduced, and it leads to the accumulation of plasma BCAA and BCKA. BCAA accumulation can inhibit the transport and utilization of pyruvate and fatty acids [16], inhibit the use of insulin-stimulated sugars [28], promote glycogen synthesis and lead to hyperglycemia [29]. BCAA inhibits phosphatidylinositol-3-kinase and insulin signaling by activating mTOR/p70S6 kinase (which phosphorylates insulin receptor substrate 1), which may be one of the mechanisms that promote T2DM after elevated BCAA levels [30]. However, some studies have shown that BCAA activation of mTORC1 is not enough to cause insulin resistance; while long-term supplementation of BCAA activates mTOR, insulin resistance has not been found. Most research results support the positive correlation between the accumulation of BCAA and its metabolites and the increased risk of insulin resistance. Therefore, the content of BCAA in circulating blood has potential clinical application value as a biomarker to predict the level of insulin resistance in diabetes.

1.5.3.3 BCAA and heart disease

BCAA and its metabolites play an important role in the regulation of cardiac substrate metabolism. Elevated BCAA levels can affect the development of cardiovascular and metabolic diseases. Li *et al.* found that chronic accumulation of BCAA can inhibit glucose metabolism and sensitize the heart to ischemic injury [209]. This further indicates that high BCAA levels can increase ischemia-reperfusion injury (I/RI) caused by myocardial infarction. High levels of BCAA can selectively inhibit PDH activity, thereby interfering with the usage of pyruvate by mitochondria. This is because the chronic accumulation of BCAA causes the downregulation of the hexosamine biosynthesis pathway (HBP), which decreases protein O-linked N-acetylglucosamine (O-GlcNAc) modification and inactivates PDH, resulting in a marked reduction in myocardial glucose oxidation and an increase in fatty acid oxidation.

The heart has high energy consumption and is sensitive to the nutritional environment. Therefore, abnormal metabolism of nutrients will seriously affect the heart function and the progress of related diseases. Sun *et al.* showed that BCAA metabolism changes the most significant in the cardiac metabolism of mice with heart failure induced by stress overload [230]. They found that the expression of a variety of important BCAA catabolism related genes (BCAT2, BCKDHA, BCKDHB, DBT, PP2Cm) was reduced, and the expression of BCKDK did not change significantly, which made the role of BCKDK dominant, leading to a significant increase in BCAA catabolism in the heart. Abnormal catabolism of BCAA can promote myocardial contractile disorders independently of other pathological factors, and impaired catabolism of BCAA and its increased BCKA will impair mitochondrial function and induce myocardial oxidative

stress, significantly promoting the progression of heart failure [230]. Kruppel Like Factor 15(KLF15) is an important transcriptional regulator of nutrient metabolism, and its various target genes are involved in the regulation of glucose and lipid metabolism. The same study also found that KLF15 plays an important role in regulating BCAA catabolism. The decrease in KLF15 expression in pathologically stressed myocardium may be one of the mechanisms of BCAA catabolism abnormalities induced by pressure overload in heart disease [230]. Another study showed that BCKA could down-regulate the mTORC2-Akt signaling pathway and increase myocardial apoptosis induced by pressure overload in a concentration-dependent manner [231].

Furthermore, myocardial BCAA metabolism is significantly impaired after MI in mice, resulting in a significant increase in myocardial BCAA levels. Activating the myocardial mTOR signaling pathway aggravates cardiac dysfunction and myocardial remodeling, and promotes the progression of heart failure after MI [231]. These all indicate that the reduction of BCAA metabolism related gene expression and the accumulation of BCAA and BCKA metabolites caused by BCAA catabolism disorder are one of the signs of heart disease.

Chapter 2 Characterization of BCAA Metabolism in CAFs and Cancer Cells

2.1 Introduction

Pancreatic tumors have a rich stromal diversity containing fibroblasts, stellate cells and infiltrating immune cells, which cumulatively account for up to 90% of the total tumor volume. Fibroblasts are the most common cells in the normal pancreatic stroma. Fibroblasts were first defined as cells in the connective tissue that synthesized collagen 150 years ago [232]. Fibroblasts in normal tissues are generally present as single cells in the interstitial space or occasionally near a capillary, without any association with a basement membrane, but are embedded within fibrillar ECM of the interstitium [232]. These cells exhibit classic spindle-shaped morphology with a potential for planar polarity. Fibroblasts in normal tissue are generally considered indolent with negligible metabolic and transcriptional activity. Resting fibroblasts may share many features with mesenchymal stem cells. In response to the presence of tumor cells, quiescent fibroblasts and stellate cells become activated cancer-associated fibroblasts (CAFs) that express alpha-smooth muscle actin (αSMA). CAFs develop from bone marrow-derived mesenchymal stem cells, pancreatic stellate cells (PSCs), and quiescent resident fibroblasts through distinct pathways of activation. However, a recent study showed that tumors form their CAFs predominantly from precursors present in the local tumor microenvironment, and the contribution from bone marrow is rare [233]. It is known that CAFs contribute to tumor proliferation, invasion, and metastasis, and they are a physical

barrier for drugs that help enable chemoresistance [232]. However, there is a lack of knowledge regarding the metabolic interactions between CAFs and cancer cells.

2.2 Expression of BCAA metabolism related enzymes in cell lines

Metabolic activity of the BCAAs, leucine, valine, and isoleucine, is both cell- and tissue-dependent and takes place in several steps beginning with BCAA deamination. BCAA transaminase (BCAT), the enzyme that initiates this process, has two isoforms (BCAT1 in the cytosol and BCAT2 in the mitochondria), which result in corresponding branched-chain ketoacids (BCKAs), α-ketoisovalerate (KIV), α-keto-β-methylbutyrate (KMV), and α-ketoisocaproate (KIC). The second step in BCAA metabolism involves irreversible BCKA oxidation catalyzed by the mitochondrial inner membrane complex, branch-chain α-ketoacid dehydrogenase (BCKDH) complex. The BCKDH complex consists of three catalytic components, alpha-ketoacid dehydrogenase (E1 component), dihydrolipoyltransacylase (E2 component), and dihydrolipoamide dehydrogenase (E3 component). E1 has two isoforms encoded by BCKDHA and BCKDHB, the DBT gene encodes E2, and the DLD gene encodes E3. BCKDH complex E1 and E3 units are linked via E2. Oxidation of BCKAs results in IB-CoA, 2MB-CoA and IV-CoA, which are further converted into succinyl-CoA and acetyl-CoA that act as anaplerotic or ketogenic sources for the TCA cycle.

To determine the differences in BCAT catabolism between stromal and PDAC cells, we analyzed protein and gene expression of BCAT1 and BCAT2 (Figure 2.1a-b). Interestingly, we found that CAFs had significantly higher BCAT1 expression when compared to PDAC cell lines. In contrast, BCAT2 expression was higher in PDAC cells

relative to CAFs. Besides, PDAC cells displayed a higher expression of the BCKDH complex enzymes BCKDHA, BCKDHB, and DBT than CAFs (Figure 2.1c). Differential DBT expression was also corroborated by immunoblotting (Figure 2.1a). These results suggest differential BCAA deamination and oxidation potential in stromal and cancer cell lines.

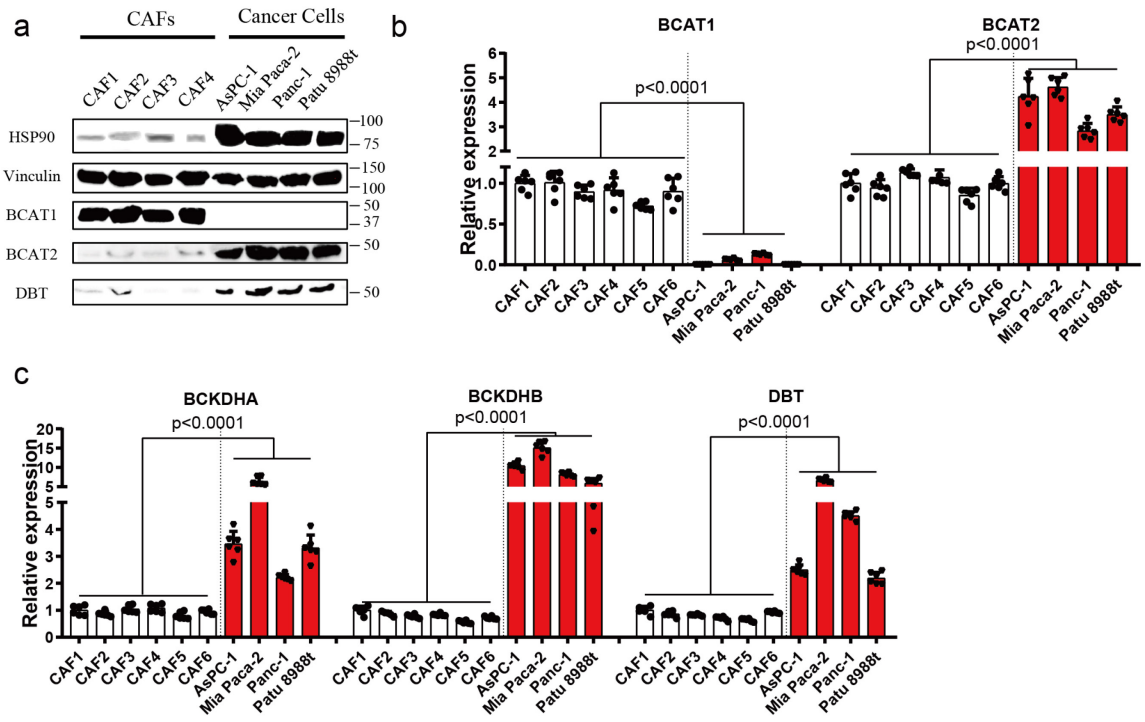

Figure 2.1 Expression of BCAA metabolism related enzymes in CAFs and cancer cell lines. **a**. Immunoblots of BCAT1, BCAT2 and DBT expression in CAFs and pancreatic cancer cell lines. HSP90 and Vinculin used as loading control. n = 4 biologically independent samples. Experiments were repeated independently three times with similar results. **b**. Relative BCAT1 and BCAT2 mRNA expression in CAFs and pancreatic cancer cell lines. Expression normalized to gene expression in CAF1. n = 4 biologically independent samples. **c**. Relative BCKDHA, BCKDHB, and DBT mRNA expression were determined by qRT–PCR in CAFs and pancreatic cancer cell lines. Expression normalized to gene expression in CAF1. n = 4 biologically independent samples.

2.3 Expression of BCAA metabolism related enzymes in PDAC tissues

To corroborate our observations regarding BCAT1/2 expression in cancer and CAF cell-lines, we analyzed human PDAC tissue through staining. IHC staining of PDAC tumor similarly revealed that the stromal component had significantly higher expression of BCAT1 compared to its epithelial counterpart (Figure 2.2). We further compared BCAT1 and α-SMA expression in PDAC patient paired tumor and adjacent normal regions (Figure 2.3) and found that both BCAT1 and α-SMA were highly expressed in CAFs compared to fibroblasts in the normal stroma, thereby suggesting that enhanced BCAT1 expression in tumor stroma is associated with distinct desmoplasia differing from normal tissue (Figure 2.3).

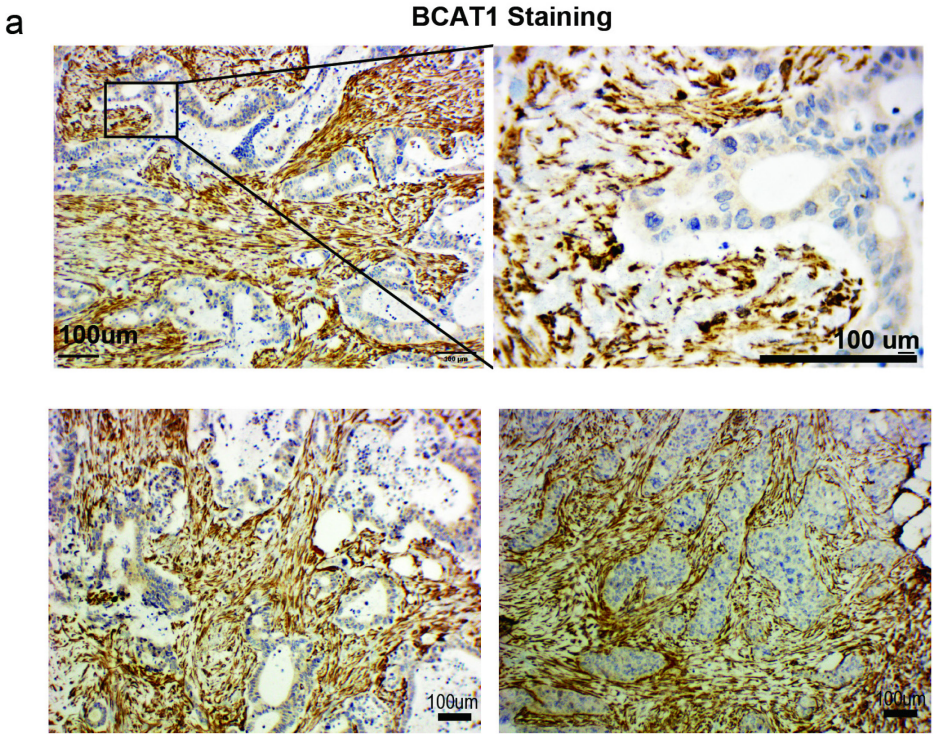

Figure 2.2 BCAT1 expression in human PDAC tissues Representative IHC staining image comparing BCAT1 expression between stromal and tumor compartments. Experiments were repeated independently three times with similar results.

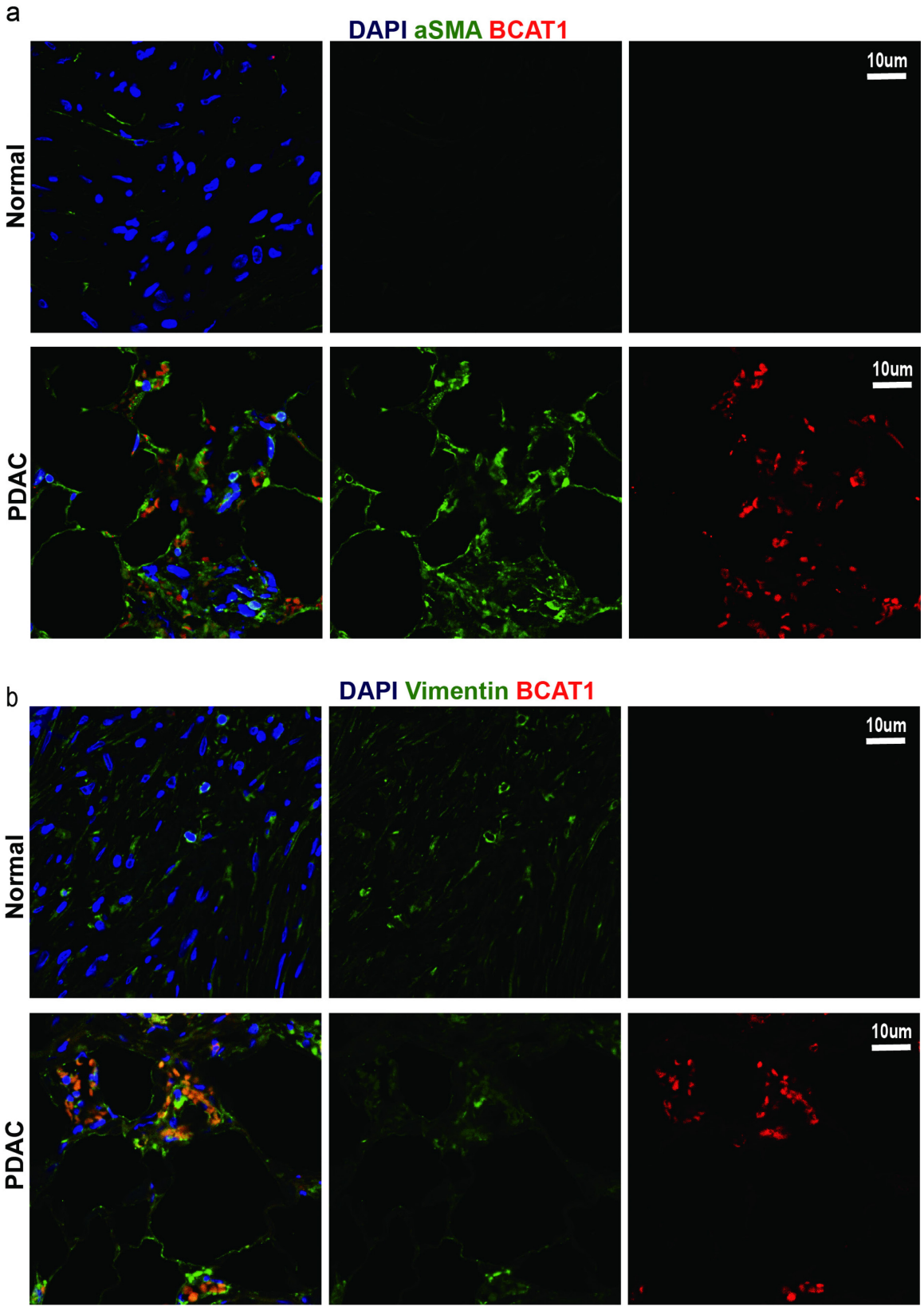
a
DAPI aSMA BCAT1
Normal
PDAC
10um
10um
b
DAPI Vimentin BCAT1
Normal
PDAC
10um
10um

Figure 2.3 BCAT1 expression in paired healthy and PDAC tissue. Representative IF images were showing protein expression of stromal αSMA, BCAT1 and Vimentin from paired healthy and PDAC tissue. Experiments were repeated independently two times with similar results.

2.4 PDAC cells are more BCAA dependent

Since differential gene and protein expression does not always translate to metabolic phenotype, we measured BCAA catabolic flux using ^{13}C-labeled BCAAs in PDAC cells and CAFs (Figure 2.4a). We observed that CAFs had three-fold higher BCAA catabolic flux compared to PDAC cell-lines. To evaluate the essentiality of BCAAs for CAFs' and cancer cells' growth, we cultured them under BCAA deprived conditions. Expectedly, CAFs were observably resilient to BCAA deprivation *vis a vis* proliferation, whereas cancer cells were BCAA-dependent (Figure 2.4b-c). The finding that cancer cells not only have reduced BCAA catabolic flux compared to CAFs but are BCAA-addicted for growth suggests that BCAA intermediates like BCKAs play a significant role in maintaining metabolic activity in the nutrient-starved pancreatic milieu.

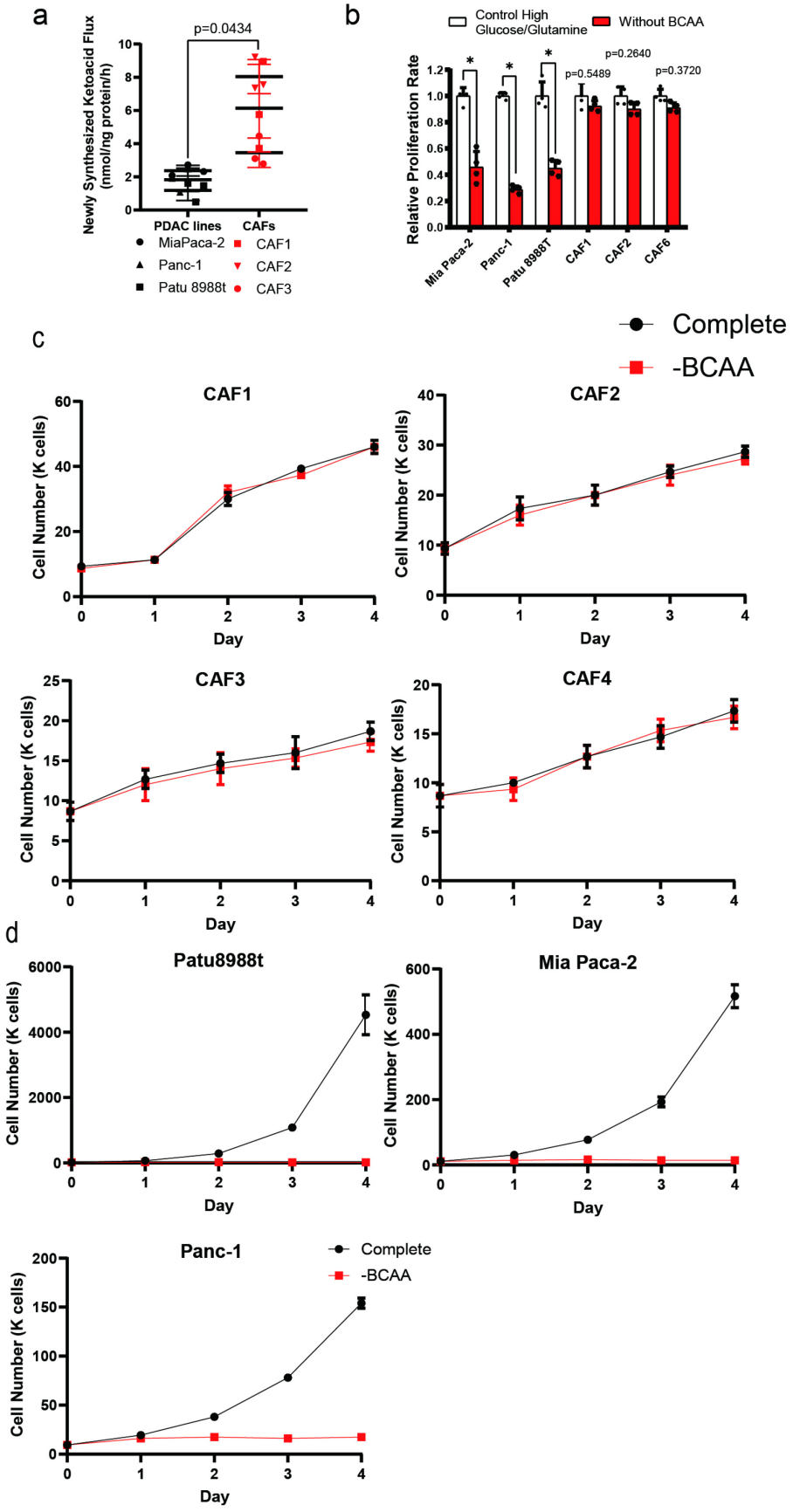
a
Newly Synthesized Ketoacid Flux (nmol/ng protein/h)
p=0.0434
PDAC lines
CAFs
MiaPaca-2
Panc-1
Patu 8988t
CAF1
CAF2
CAF3
b
Control High Glucose/Glutamine
Without BCAA
Relative Proliferation Rate
p=0.5489
p=0.2640
p=0.3720
Mia Paca-2
Panc-1
Patu 8988T
CAF1
CAF2
CAF6
c
Complete
-BCAA
CAF1
CAF2
CAF3
CAF4
Cell Number (K cells)
Day
d
Patu8988t
Mia Paca-2
Panc-1
Complete
-BCAA

Figure 2.4 Growth rates of pancreatic cancer cells or CAFs under BCAA deprivation. **a**. The stable-isotope tracing experiment reveals that CAFs deaminate BCAAs into BCKAs at a rate three-fold faster than PDAC cells. n = 3 biologically independent samples. **b**. Relative proliferation rates of Mia Paca-2, Panc-1 and Patu 8988t pancreatic cancer cells or CAFs under BCAA deprivation. n = 4 biologically independent samples. **c**. Absolute cell numbers of PDAC CAFs were determined in the presence or absence of BCAA. n = 3 biologically independent samples. **d**. Absolute cell numbers of PDAC cells were determined in the presence or absence of BCAA. n = 3 biologically independent samples.

2.5 Discussion

Previously, most BCAA catabolism studies were focused only on the cancer cells in diseases like glioma, lung cancer or pancreatic cancer, and they completely ignored the role of the stroma. In this chapter, we examined the BCAA related enzyme expression in the PDAC tumor microenvironment. We also analyzed the difference of BCAA catabolism flux that is distributed within the PDAC tumor microenvironment. First, CAFs had high BCAT1 expression, while PDAC cell lines lack expression of BCAT1. In contrast, BCAT2 expression was higher in PDAC cells relative to CAFs. IHC staining of human PDAC tissue found that the stromal component had significantly higher expression of BCAT1 compared to its epithelial counterpart. Similar expressions were also confirmed in normal pancreas tissue.

Moreover, the BCAA catabolic flux using 13C-labeled BCAAs revealed that CAFs had three-fold higher BCAA catabolic flux compared to PDAC cell-lines. Moreover, compared to PDAC cells, CAFs were observably resilient to BCAA deprivation. These findings suggest that PDAC cells have reduced BCAA catabolic flux compared to CAFs, and stromal BCAT1 may also play an important role in the PDAC tumor environment.

Chapter 3 BCAT2 Regulates BCKA-Mediated De Novo Protein Synthesis in PDAC cells

3.1 Introduction

Our previous work that genetic mutations can also influence how BCAA metabolism impacts PDAC progression [234]. Malic enzyme 2(ME2) is near the SMAD4, which is commonly deleted PDAC, in the human genome, so ME2 is usually a passenger deletion in PDAC. When ME2 is deleted, malic enzyme 2(ME3) became essential. Moreover, ME3 regulates BCAT2 through AMP-activated protein kinase (AMPK)-sterol regulatory element-binding protein 1 (SREBP1) pathways [234]. Knockdown of BCAT2 in ME2-deficient PDAC cell lines inhibited colony formation, which could be rescued by nucleotide supplementation, suggesting BCAAs to play an important role in PDAC. Li *et al.* showed that BCAT2 is elevated during PDAC progression. Pancreatic tissue-specific knockout of BCAT2 impedes the progression of pancreatic intraepithelial neoplasia (PanIN) in mice. Functionally, BCAT2 enhances BCAA uptake to sustain BCAA catabolism and mitochondrial respiration. Mechanistically, KRAS stabilizes BCAT2 through spleen tyrosine kinase (SYK) and E3 ligase tripartite-motif-containing protein 21 (TRIM21), so BCAT2-mediated BCAA catabolism is critical for the development of PDAC harboring KRAS mutations [235]. Lei *et al.* show that BCAT2 is acetylated, which is acetylated at lysine 44 (K44) [236]. BCAT2 acetylation leads to its degradation through the ubiquitin-proteasome pathway,

and they also identified cAMP-responsive element-binding (CREB)-binding protein (CBP) and SIRT4 as the acetyltransferase and deacetylase for BCAT2, respectively [236]. All these data suggest that BCAT2 has an important role in PDAC.

MicroRNAs have also been shown to regulate BCAT2. MiR-182 can reduce the expression of Bcat2, Foxo3 and Adcy6 to regulate the hypertrophic response in placental growth factor-induced mice [237]. The knocking down of BCAT2 promotes Akt (Ser473)/p70-S6K (Thr389) phosphorylation and cardiomyocyte hypertrophy [237, 238]. In muscle cells, Dhanani *et al.* showed that leucine is required for myotube formation, which can also be replaced by KIC and BCAT2 is induced in the differentiation [239]. The inhibition of BCAT2 also abolished myoblast differentiation [239]. Moreover, both of KLF15 and PGC-1α can regulate BCAA metabolism by targeting BCAT2 skeletal muscle [240, 241].

3.2 CAF support PDAC cell growth under BCAA deprivation

To address whether upregulated BCAA deamination in pancreatic CAFs fuels the BCAA addiction of cancer cells, we measured the proliferation rate of GFP-labeled PDAC cell lines, Mia PaCa-2, Panc-1 and PaTu 8988t, directly coculture with patient-derived CAFs or normal fibroblasts (NOFs). Notably, we observed that CAFs completely rescued the loss of proliferation of cancer cells under BCAA-deprivation, while NOFs did not affect (Figure 3.1a-c). Similar results were also seen by AsPC-1 and BxPC3

PDAC cell lines (Figure 3.1d). These data suggest that CAFs may either be secreting BCAAs or their catabolic product, BCKAs.

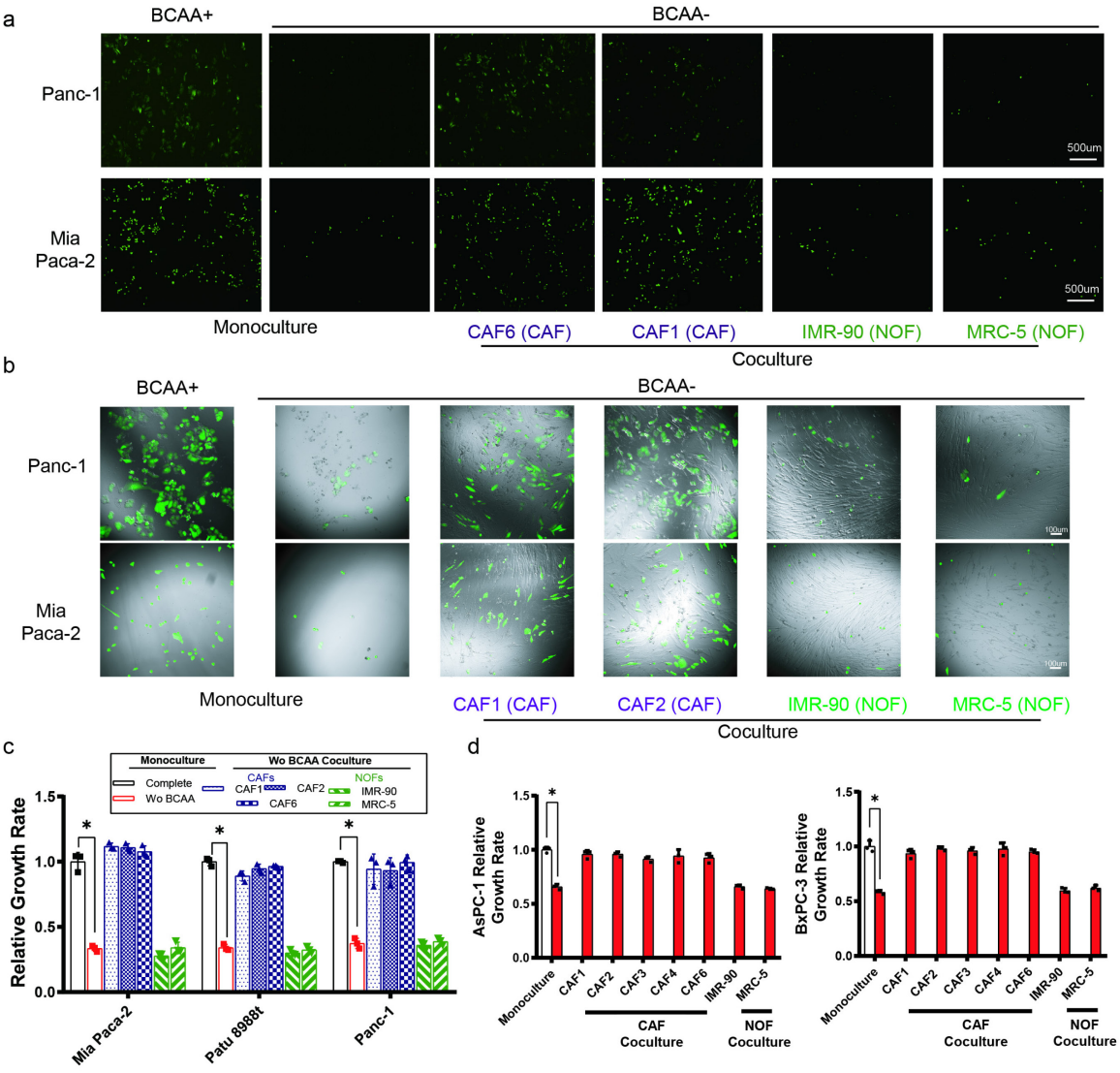

Figure 3.1 CAFs support PDAC growth under BCAA deprivation. **a**. Fluorescence microscopy images comparing the growth of GFP-labeled Mia Paca-2 and Panc-1 cells in contact co-cultures with CAFs or NOFs under BCAA deprivation. Experiments were repeated independently three times with similar results. **b**. Fluorescence microscopy images merged with brightfield images comparing the growth of GFP-labeled Mia Paca-2 and Panc-1 cells in contact co-cultures with CAFs or NOFs under BCAA deprivation. **c**. Relative proliferation rates of Mia Paca-2, Patu 8988t and Panc-1 pancreatic cancer cells

under BCAA deprivation. n = 3 biologically independent samples. **d**. Relative growth rates of AsPc1 and BxPC-3 cells co-cultured with CAFs or NOFs under BCAA deprivation. n = 3 biologically independent samples.

3.3 CAF secrete BCKA to support PDAC cells

First, we check the CAF's rescue effect at different co-culture ratio, since the ratio influences the effect, it supposes to come from soluble factor secreted by CAFs (Figure 3.2a). We measured BCKA secretion by CAFs to be around 200 pmol/μg protein, which increased under BCAA-deprivation to around 300 pmol/μg protein (Figure 3.2b). Interestingly, we found that under BCAA-deprivation, BCKAs rescued the proliferation at concentrations as low as 5-50uM, whereas 100μM BCAA was needed to obtain a similar effect (Figure 3.2d). This suggests that BCKA is a more effective nutrient at lower concentrations compared to BCAAs (Figure 3.2c).

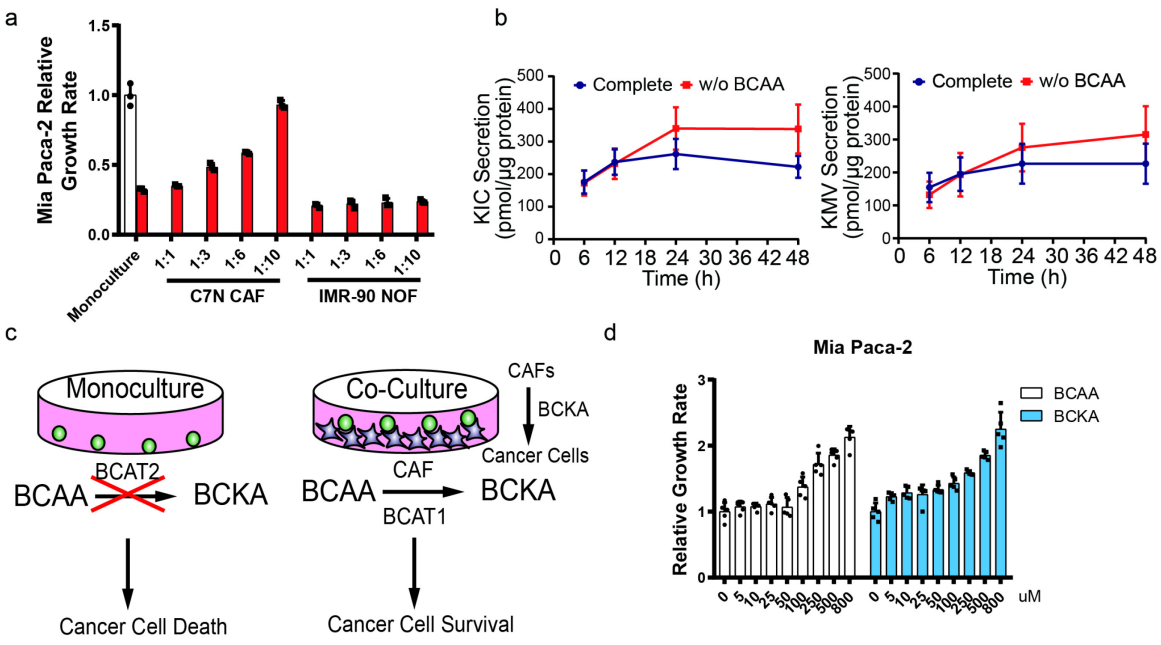

Figure 3.2 CAFs support PDAC growth through BCKA. **a**. Relative growth rates of Mia Paca-2 cells co-cultured with CAFs or NOFs at different seeding ratios under BCAA deprivation. n = 3 biologically independent samples. **b**. BCKA secretion by CAFs estimated by measuring the extracellular concentration of BCKAs, KIC and KMV, at 6, 12, 24, and 48 hours by LC-MS. n = 3 biologically independent samples. **c**. Model for the rescue of proliferation in BCAT2 KD cancer cells by BCKAs released from CAFs under BCAA deprivation. **d**. Relative growth rates of Mia Paca-2 cells in various concentrations of BCAAs or BCKAs. n = 6 biologically independent samples.

3.4 BCKA contribute to TCA cycle and protein synthesis

Once the CAF-secreted BCKAs are consumed by cancer cells, they may be used directly for BCKA oxidation through the BCKDH complex to maintain oxidative TCA cycle metabolite levels. BCKAs can also act as substrates for de novo synthesis of BCAAs through reanimation by the reversible enzyme BCAT2 (Figure 3.3). Although not explicitly shown before, this newly synthesized BCAAs could maintain *de novo* protein synthesis in cancer. To confirm the fate of BCKAs, we cultured cancer cells with

^{13}C labeled BCKAs. They estimated their contribution towards the TCA cycle as an anaplerotic substrate and for *de novo* BCAA and subsequent *de novo* protein synthesis (Figure 3.3). We observed that BCKAs are indeed oxidized and incorporated into the TCA cycle via acetyl-CoA and succinyl-CoA, as evident from the ^{13}C labeled TCA intermediates citrate, malate, and aspartate (Figure 3.3).

Interestingly, BCKAs were also utilized for *de novo* protein synthesis and were found to contribute more than 60% of the intracellular BCAA pools under BCAA-deprived conditions (Figure 3.3). Further, ^{15}N labeled glutamine and serine were found to contribute the required nitrogen for BCAA synthesis commensurately. The amino acid composition of intracellular protein was determined using acid hydrolysis and GC-MS analysis. The constituent BCAAs in the protein achieved 40% enrichment from ^{13}C labeled BCKAs and 50% enrichment from ^{15}N labeled glutamine and serine, definitively proving that BCKA-derived BCAAs contributed significantly to *de novo* protein synthesis (Figure 3.3).

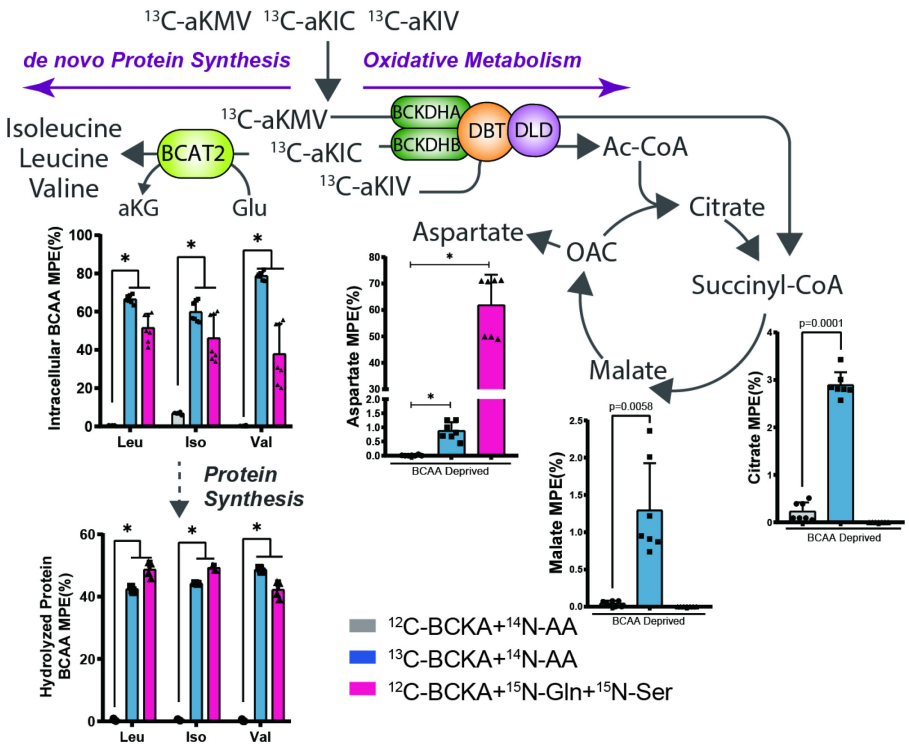

Figure 3.3 BCKA metabolism in PDAC cells. The fate of 13C-BCKAs in PDAC cells elucidated by measuring mole percent enrichment (MPE) of TCA cycle intermediates that represent BCKA oxidation and of intracellular BCAAs and BCAAs from acid-hydrolyzed proteins that represent de novo protein synthesis. n = 7 biologically independent samples for intracellular metabolites and n = 4 biologically independent samples for protein hydrolyzed metabolites.

3.5 BCKA contribute to protein synthesis through BCAT2

To substantiate the functional role of BCAT2 in the BCAA metabolism of PDAC cells, we silenced BCAT2 using both CRISPR and short hairpin (sh) RNA in PDAC cells (Mia Paca-2, Panc-1 and Patu 8988t). We found that BCAT2 knockdown (KD) significantly reduced the growth rate of PDAC cells implying that BCAT2 plays an important role in these cells (Figure 3.4ab). The knockdown of BCAT2 resulted in a decrease of the ^{13}C enrichment of BCAAs obtained after protein hydrolysis, thereby confirming the BCKA-mediated, anabolic, regulatory role of BCAT2 in PDAC (Figure

3.4c). Having delineated that BCKAs can contribute towards *de novo* protein synthesis, we next assessed whether CAFs could promote protein synthesis in cancer cells. We used the SUnSET assay to measure *de novo* protein synthesis and found that CAFs, indeed increased protein synthesis in cancer cells (Figure 3.4d). Consistent with significant enrichment of labeled BCKA-derived BCAAs in hydrolyzed protein, BCKA supplementation restored the loss of newly synthesized protein levels under BCAA deprivation (Figure 3.4e). To establish the essentiality of BCAT2 in PDAC, we cocultured BCAT2 knockdown PDAC cells with patient-derived CAFs (Figure 3.4f). Intriguingly, knocking down BCAT2 in cancer cells had no effect on CAF-mediated rescue of cancer cell growth under BCAA deprivation conditions.

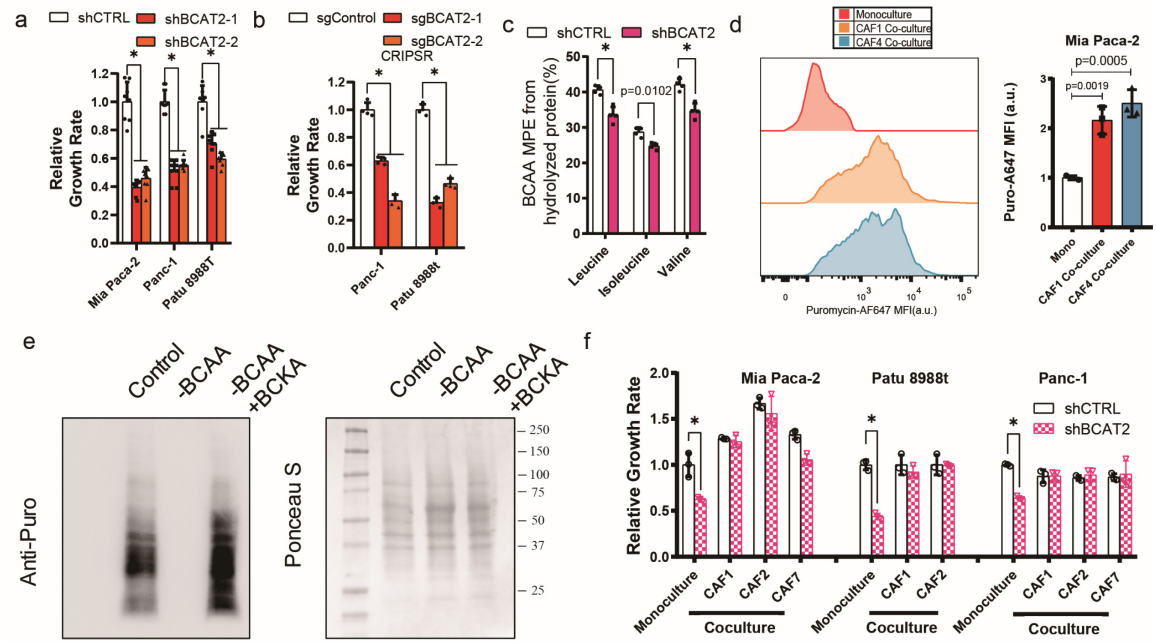

Figure 3.4 BCAT2 regulates protein synthesis in PDAC cells. **a**. Relative proliferation rates of Mia Paca-2, Panc-1 and Patu 8988t pancreatic cancer cells with BCAT2 knockdown by shRNA. n = 4 biologically independent samples. **b**. Relative proliferation rates of Panc-1 and Patu 8988t pancreatic cancer cells with BCAT2 knockdown by CRISPR. n = 4 biologically independent samples. **c**. Mole percent enrichment (MPE) of BCAAs in hydrolyzed protein obtained from BCAT2 knockdown

Mia Paca-2 cells cultured with 13C-BCKA. n = 4 biologically independent samples. **d**. FACS analysis of GFP-labeled Mia Paca-2 cells detected with Alexa 647–labeled antibodies to puromycin (puro-A647). n = 3 biologically independent samples. **e**. Representative images of SUnSET assay of Mia Paca-2 cells cultured in the indicated medium for 48 hr. Whole-cell lysates were subjected to western blotting with puromycin antibody. Experiments were repeated independently three times with similar results. **f**. CAF cocultures rescue the loss of growth in BCAT2-knockdown PDAC cells. n = 6 biologically independent samples.

3.6 CAF support PDAC cells through BCKA independent of autophagy

We further excluded the possibility that BCAAs are directly catabolized from autophagy-induced protein degradation[242] by knocking down autophagy-related 5/7 (ATG5/7) in CAFs and coculturing them with PDAC cells under BCAA deprivation. We found that ATG5/7 knockdown did not suppress CAF-mediated rescue of cancer cell-growth under BCAA-deprivation (Figure 3.5a). Moreover, autophagy inhibitors, chloroquine, Bafilomycin A1 and LY294002 did not inhibit the rescue effect of CAFs on cancer cell growth under BCAA-deprivation conditions (Figure 3.5b). These results provide strong evidence of the regulation of BCAA metabolism by BCAT2 in PDAC cells.

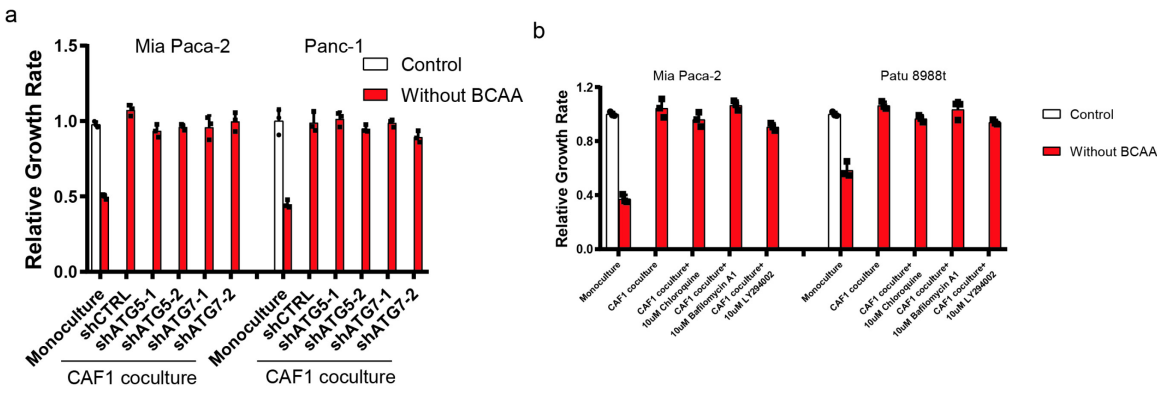

Figure 3.5 CAF support PDAC cells under BCAA deprivation independent of autophagy. **a**. Relative growth rates of Mia Paca-2 and Panc-1 cells co-cultured with

ATG-5/7 knockdown CAFs. n = 3 biologically independent samples. **b**. Relative growth rates of Mia Paca-2 and Patu 8988t cells cocultured with CAFs treated with autophagy inhibitors (chloroquine, Bafilomycin A1 and LY294002) under BCAA deprivation. n = 3 biologically independent samples.

3.7 Discussion

The role of BCAA catabolism in cancer was largely overlooked until 2013 when Tonjes *et al.* reported overexpression of BCAT1 in gliomas, which excrete glutamate and promote glioma cell proliferation [243]. BCAT1 expression in glioma is specific to those gliomas with wild-type isocitrate dehydrogenase 1 and 2 (IDH1 and IDH2). Also, BCAT1 is required for chronic myeloid leukemia (CML) growth. It was shown that BCAT1 is upregulated during the progression of CML and promotes BCAA production in leukemia cells by the amination of branched-chain keto acids [244]. BCAAs are also important nitrogen sources since the transamination of BCAAs leads to the regeneration of glutamate, which can be used for biosynthesis of other nonessential amino acids. Previous studies have demonstrated that elevated plasma levels of BCAAs are associated with a greater than 2–fold increased risk of pancreatic cancer [245]. Previously we demonstrated that knockdown of BCAT2 in Malic Enzyme 2 (ME2)-deficient pancreatic cell lines inhibited cell proliferation, which could be rescued by nucleotide supplementation, suggesting that BCAA is an important nitrogen source in pancreatic cancer [234]. Pancreatic tissue-specific knockout of BCAT2 impedes the progression of PanIN in mice, and BCAT2 enhances BCAA uptake to sustain BCAA catabolism and mitochondrial respiration [235]. Also, BCAT2 can be acetylated, which is acetylated at

lysine 44 (K44), and its acetylation leads to degradation through the ubiquitin-proteasome pathway [236].

In this chapter, we showed that CAFs are secreting BCAA catabolic products, BCKAs. Moreover, CAF-secreted BCKAs are consumed by PDAC cells. They can be used directly for BCKA oxidation through the BCKDH complex to maintain oxidative TCA cycle metabolite levels. BCKAs can also act as substrates for de novo synthesis of BCAAs through reanimation by the reversible enzyme BCAT2. We also found that BCAT2 knockdown significantly reduced the growth rate of PDAC cells implying that BCAT2 plays an important role in these cells. We also showed that CAFs increased protein synthesis in cancer cells. However, when we cocultured BCAT2 knockdown PDAC cells with CAFs, knocking down BCAT2 in cancer cells had no effect on CAF-mediated rescue of cancer cell growth under BCAA deprivation conditions. This would suggest that BCAT2 is not only an important enzyme in BCAA metabolism for PDAC cells.

Chapter 4 BCKDH Complex Is Essential for PDAC Cells Growth and Biosynthesis

4.1 Introduction

Since the catabolism of BCAA starts with branched-chain aminotransferases giving rise to corresponding BCKA. The second step is catalyzed by the mitochondrial inner membrane complex called branch-chain α-ketoacid dehydrogenase (BCKDH) complex. The BCKDH complex consists of three catalytic components, alpha-ketoacid dehydrogenase (also referred to as the E1 component), dihydrolipoyl transacylase (E2 component), and dihydrolipoamide dehydrogenase (E3 component). The branched-chain keto acid dehydrogenase E1 has two isoforms, alpha polypeptide and subunit beta, which are encoded by BCKDHA and BCKDHB, respectively. Dihydrolipoamide dehydrogenase (E3 component) is encoded by the DLD gene, which also acts as the common part for pyruvate dehydrogenase and alpha-ketoglutarate dehydrogenase. Compared to BCAT1/2, BCKDH was not well studied yet. Most of the research related to BCKDH is coming from MUSD; these studies identified different mutations of BCKDHA, BCKDHB, and DBT can cause MUSD [246]. Lee *et al.* found knocking down of BCKDHA inhibited PDAC cell proliferation but not pancreatic duct epithelial cell proliferation [247]. Similar to adipocyte, BCKDHA knockdown also inhibited fatty-acid synthesis in PDAC cells, indicating that PDAC cells also utilize BCAAs for fatty acid biosynthesis [247, 248]. Xue *et al.* found that BCKDK is widely expressed in

colorectal cancer patients and related to survival times [249]. Nevertheless, BCKDK promotes colorectal cancer by enhancing the MAPK signaling pathway through direct MEK phosphorylation rather than by branched-chain amino acid catabolism [249]. White *et al.* found inhibition of BCKDK or overexpression of the PPM1K can regulate BCKDH complex activity, lower circulating BCAA, reduce hepatic steatosis, and identified ATP-citrate lyase (ACL) as an alternate substrate of BCKDK and PPM1K [250]. Hepatic overexpression of BCKDK increased ACL phosphorylation and activated de novo lipogenesis. Furthermore, mechanically ChREBP-β regulates BCKDK and PPM1K transcription levels to control lipid metabolism [250].

The DBT gene encodes Dihydrolipoyl transacylase (E2), it is also the center of the BCKDH complex E1 and E3 are all linked to it [251]. Targeting the DBT gene will directly target the whole BCKDH complex instead of the target of genes, BCKDHA and BCKDHB. Furthermore, its encoded component is the core of the BCKDH complex, which all makes DBT a good target in BCAA catabolism.

4.2 PDAC cells are DBT dependent

Because BCAT2 knockdown did not result in a loss of cancer cell growth in cocultures with CAFs under BCAA-deprivation, we hypothesized that irreversible BCKA oxidative decarboxylation by the BCKDH complex might be facilitating biosynthesis. To regulate BCKDH complex activity, we targeted the core, the E2 component encoded by DBT. Knocking down DBT using shRNA-DBT profoundly reduced proliferation and colony formation (Figure 4.1a-c). In agreement with the essentiality of the BCKDH complex, the addition of BCKAs under BCAA deprivation rescued the loss of

proliferation in PDAC cells (Figure 4.1d), but not in CAFs (Figure 4.1e).To confirm that BCKA-mediated growth-rate rescue is conferred via the BCKDH complex and not due to BCAT2, we cultured DBT knockdown cells under BCAA deprivation. As expected, BCKA-mediated rescue of cancer cell growth was attenuated (Figure 4.1f).

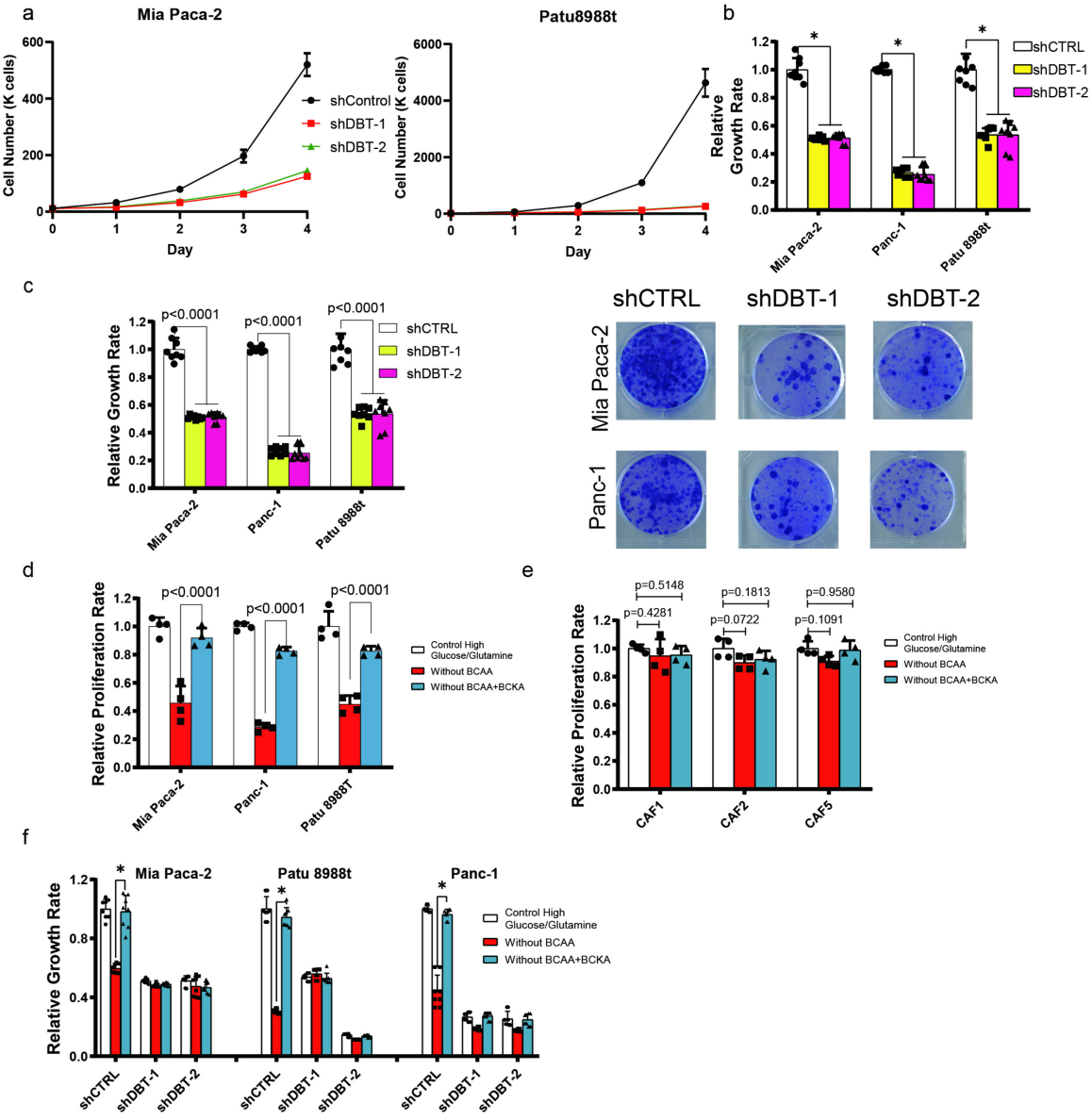

Figure 4.1 PDAC cells are DBT dependent. **a**. Absolute cell numbers of PDAC cells expressing control shRNA or two independent shRNAs to DBT. n = 3 biologically independent samples. **b**. Relative proliferation rates of Mia Paca-2, Panc-1 and Patu 8988t cells expressing control shRNA or two independent shRNAs to DBT. n = 8 biologically independent samples. **c**. Colony-formation assay of DBT knockdown PDAC

cell lines. n = 3 biologically independent samples. **d**. BCKAs can rescue BCAA deprivation in the cancer monoculture. n = 4 biologically independent samples. **e**. BCKA does not influence CAF proliferation. n = 4 biologically independent samples. **f**. Relative proliferation rates of DBT knockdown cells in BCAA depleted media under BCKA replete conditions. n = 8 biologically independent samples.

Next, we cocultured DBT-knockdown PDAC cells with CAFs under BCAA deprivation to substantiate the BCKDH-dependent role of CAF-secreted BCKA in maintaining PDAC cells' growth (Figure 4.2a-b). Notably, knockdown of DBT in PDAC cells abrogated the rescue effect from CAFs, thereby validating the role of the BCKDH complex.

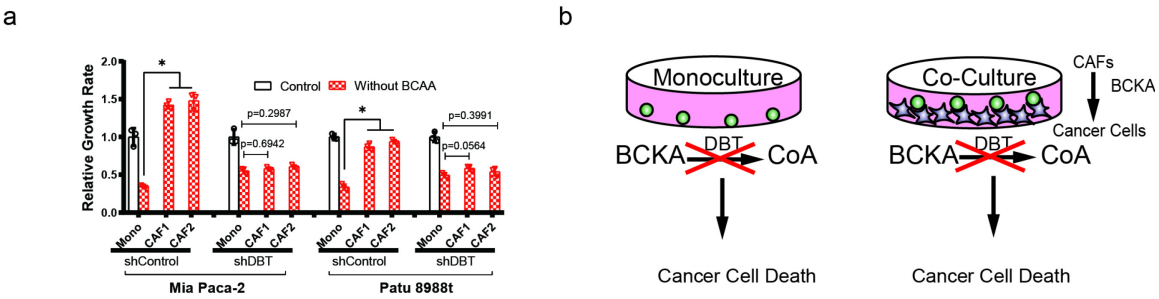

Figure 4.2 CAF's rescue effect is regulated by DBT. a. Relative proliferation rates of DBT knockdown cells co-cultured with CAFs. n = 3 biologically independent samples. **b**. Schematic for the loss of rescue in DBT knockdown cancer cells by BCKA released from CAFs under BCAA deprivation.

4.3 BCKA support NADH through DBT

Given that complete oxidation of one molecule of KIV, KMV, or KIC can provide 6, 5, or 10 NADH molecules, respectively, BCKA-driven NADH could provide a substantial measure of BCKA oxidative capacity in cells. To further validate the effect of BCKA oxidation on mitochondrial activity, we used a fluorescent, genetically encoded NADH sensor to measure mitochondrial NADH/NAD^+ in MiAPaCa-2 cells cultured in the absence or presence of either BCAA or BCKA (Figure 4.3). Interestingly, BCKAs

increased the mitochondrial NADH/NAD$^+$ ratio and corroborated our findings that BCKA oxidation enhances energy metabolism. BCKAs have two fates in the cells; they can either be reanimated into BCAAs via BCAT2 or be oxidized through the BCKDH complex. To investigate both possible fates, we measured NADH in DBT, BCAT2 knockdown PDAC cells and PDAC cells under varying α-KG/Glutamate ratios.

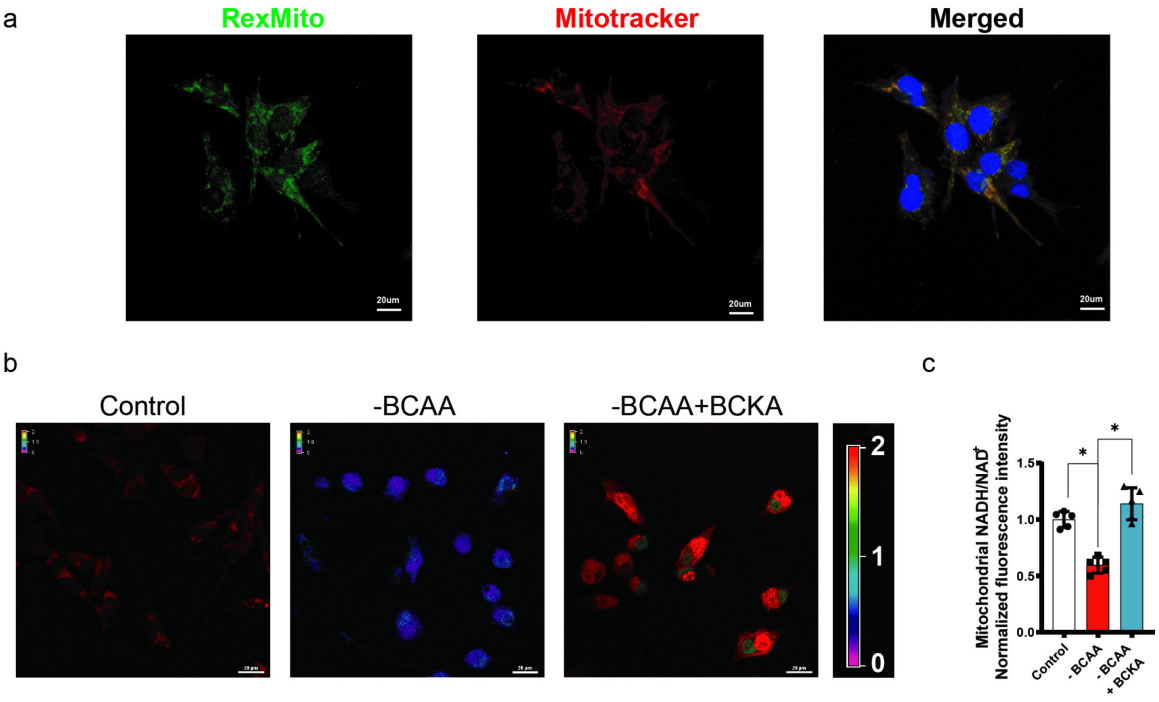

Figure 4.3 BCKA rescue NADH supply under BCAA deprivation. a. Colocalization of Mitotracker and RexMito fluorescence in Mia Paca-2 cells. Mitotracker (red), RexMito (green), and DAPI (blue). Experiments were repeated independently three times with similar results. **b**. NADH/NAD$^+$ ratio measured using confocal fluorescence imaging of Mia Paca-2 cells in BCAA depleted media under BCKA replete conditions. Experiments were repeated independently three times with similar results. **c**. NADH/NAD$^+$ ratio measured using confocal fluorescence imaging of Mia Paca-2 cells in BCAA depleted media under BCKA replete conditions. n = 5 biologically independent samples.

The knockdown of DBT reduced the NADH/NAD$^+$ ratio in PDAC cells, confirming the involvement of DBT and BCKA oxidation in increasing this ratio (Figure 4.4). We further increased the ratio of α-KG/glutamate by supplementing αKG in the

media to regulate the flux of the BCAT2 pathway to reduce the reanimation of BCKAs and favor oxidation. The increased α-KG/glutamate ratio nudges BCKAs towards oxidation, which is confirmed with the observation of an increased NADH/NAD ratio and increased growth of PDAC cells (Figure 4.5). Since the effect of modulating NADH should directly affect mitochondrial oxygen consumption rate (OCR), we measured OCR under different substrates and varying α-KG/glutamate ratios. As seen in Figure 4.5e, increasing the α-KG/glutamate ratio (by supplementing α-KG) increased the OCR significantly, whereas the converse was true when this ratio was decreased (by supplementing glutamate).

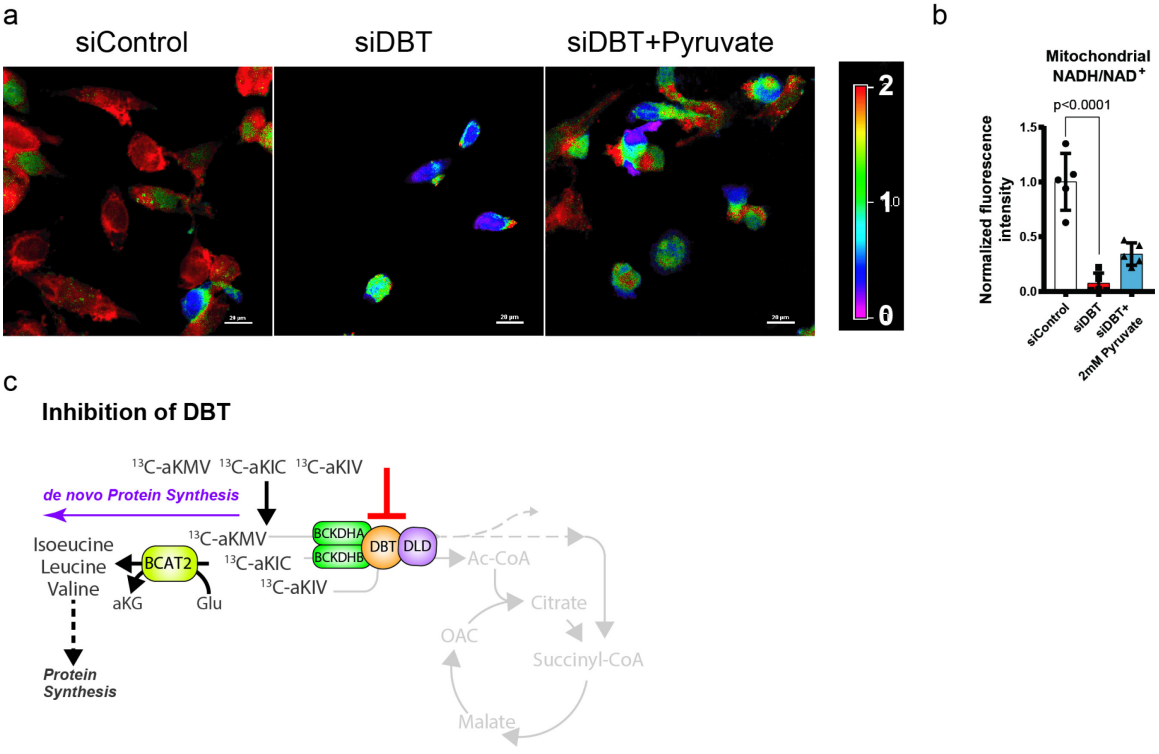

Figure 4.4 Inhibition of DBT reduces NADH. a. NADH/NAD$^+$ ratio measured using confocal fluorescence imaging of Mia Paca-2 transfected with siControl or siDBT. **b**. NADH/NAD$^+$ ratio measured using confocal fluorescence imaging of Mia Paca-2 cells transfected with siControl or siDBT. n = 5 biologically independent samples. **c**. DBT inhibition impedes oxidation of BCKAs via BCKDH complex, and thus pushes the accumulated BCKAs to be reanimated to BCAAs.

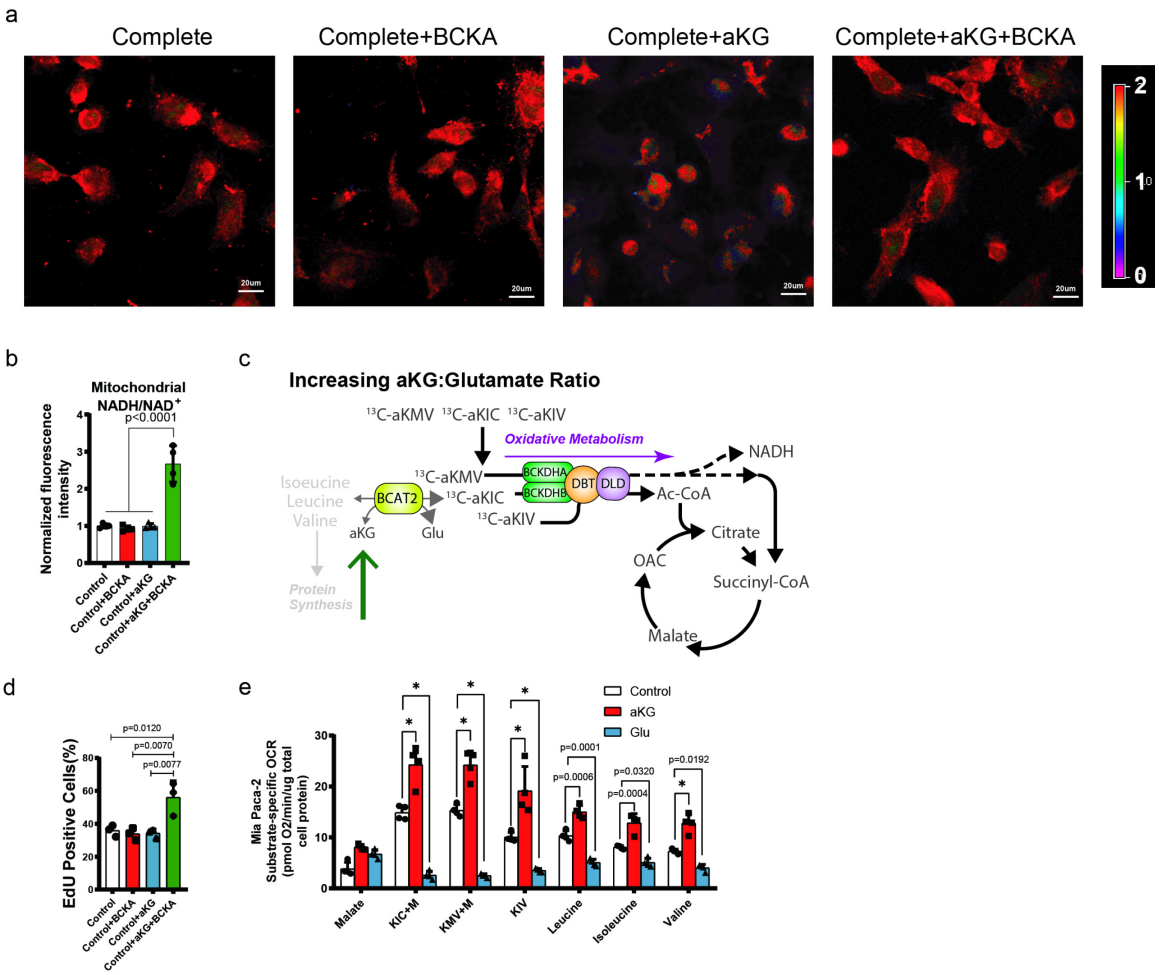

Figure 4.5 α-KG/Glutamate ratio regulates BCKA oxidation. a. NADH/NAD$^+$ ratio measured using confocal fluorescence imaging of Mia Paca-2 cells in complete media with 4mM α-KG added BCKAs. **b**. NADH/NAD$^+$ ratio measured using confocal fluorescence imaging of Mia Paca-2 cells in complete media with 4mM a-KG added BCKAs n = 4 biologically independent samples. **c**. BCKAs have two fates, but the reanimation of BCKAs is dependent on nitrogen availability via glutamate. We regulate the α-KG/glutamate ratio by supplementing α-KG to impede the reanimation of BCKAs via BCAT2, thereby pushing BCKAs towards oxidation via BCKDH. **d**. EdU uptake was measured in Mia Paca-2 cells in the presence of a-KG or/and BCKA after one day. n = 3 biologically independent samples. **e**. Substrate-specific oxygen consumption rate (OCR) in permeabilized pancreatic cancer cells measured using Seahorse Analyzer. n = 6 biologically independent samples.

Finally, we used BCAT2 knockdown cells and found that adding BCKAs in BCAT2 knockdown cells (Fig. 3M, Extended Fig. 3J-K) increased NADH, thus

substantiating that two outcomes, delamination and oxidation of BCKA, control its fate. Cumulatively, these experiments show that both fates of BCKAs are relevant in the context of PDAC cells. Thus BCKAs contribute to both the proliferation and bioenergetic metabolism of PDAC cells.

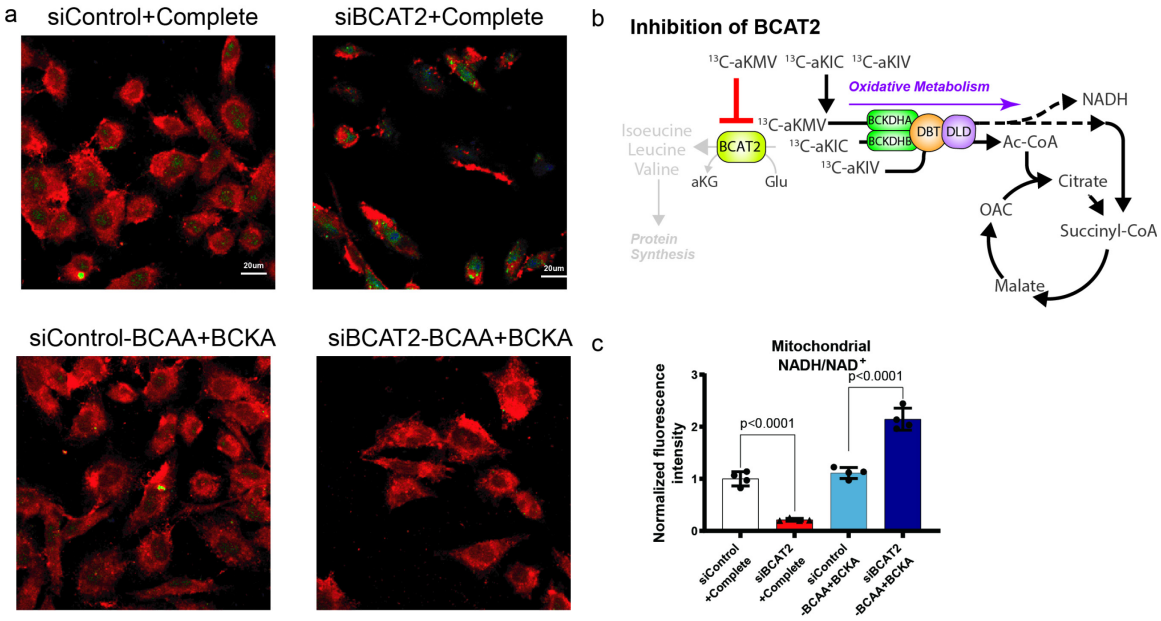

Figure 4.6 BCAT2 regulates downstream BCKA oxidation. a. NADH/NAD$^+$ ratio measured using confocal fluorescence imaging of Mia Paca-2 cells transfected with siControl or siBCAT2 in complete media or BCAA depleted media under BCKA replete conditions. **b**. BCAT2 inhibition has the same effect as α-KG supplementation and pushes the accumulated BCKAs towards oxidation via BCKDH. **c**. NADH/NAD$^+$ ratio measured using confocal fluorescence imaging of Mia Paca-2 cells transfected with siControl or siBCAT2 in complete media or BCAA depleted media under BCKA replete conditions. n = 6 biologically independent samples.

4.4 DBT regulate BCKA specific OCR

To identify the dominant substrates contributing to cellular oxidative capacity, we measured OCR. Remarkably, BCKA-driven OCR in PDAC cells is significantly higher than that of alternative substrates (Figure 4.7a). To dissect the role of BCAT2 and DBT

in the oxidative capacity of PDAC cells, we measured the OCR of DBT- and BCAT2-knockdown PDAC cells and found that their OCR was significantly reduced (Figure 4.7b-c).

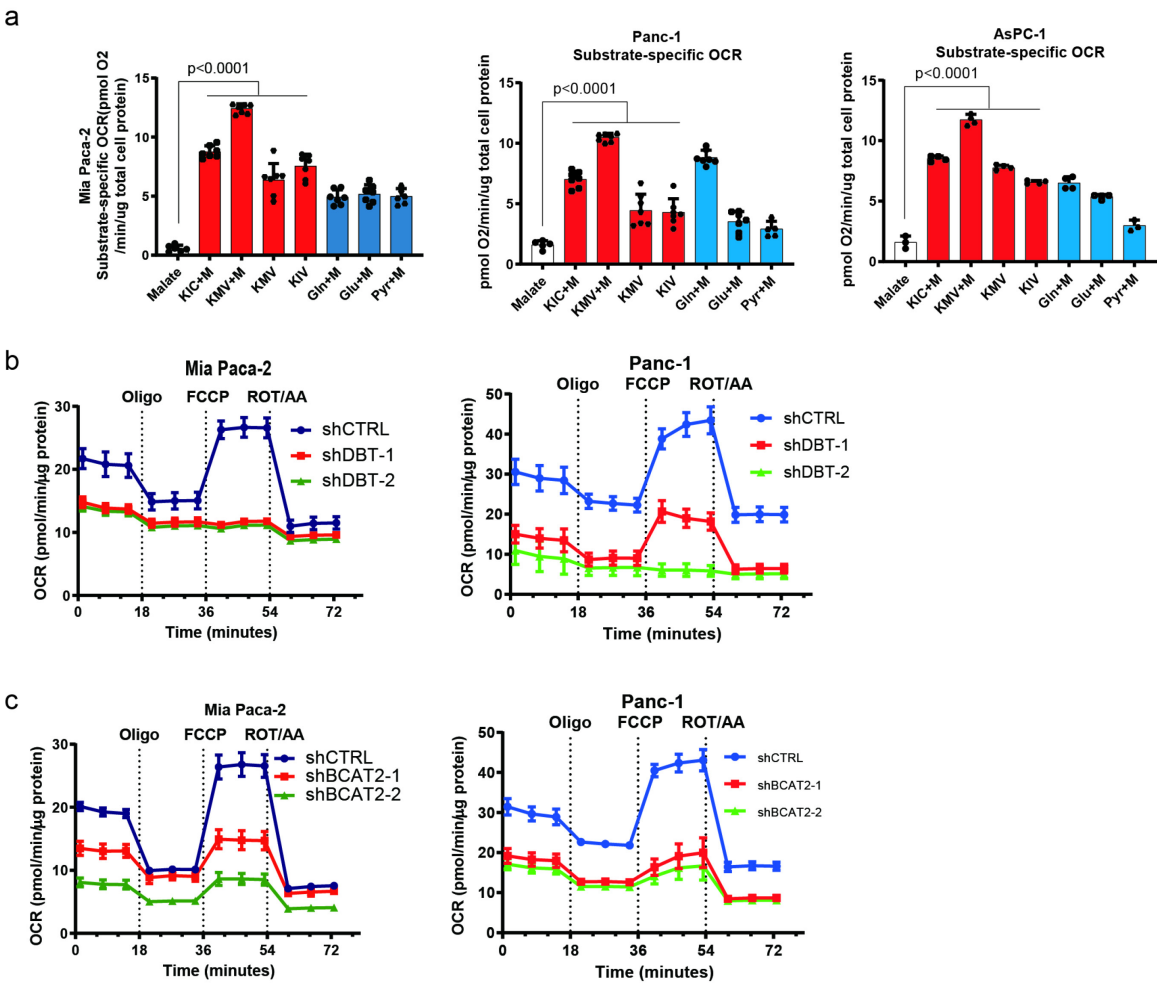

Figure 4.7 BCKA OCR is higher than BCAA in PDAC cells. a. Substrate-specific OCR in permeabilized cells. n = 4 biologically independent samples. **b**. OCR measurements in DBT knockdown cells. n = 6 biologically independent samples. **c**. OCR measurements in BCAT2 knockdown cells. n = 6 biologically independent samples.

To associate substrate specificity with BCAT2 and the BCKDH complex, we performed substrate-specific OCR in BCAT2- and DBT-knockdown cells. Interestingly, in BCAT2-knockdown cells, there was no change in BCKA-driven OCR, whereas BCAA-driven OCR was significantly reduced (Figure 4.8ab). Strikingly, in DBT-

knockdown cells, both BCAA- and BCKA-driven OCR are significantly reduced (Figure 4.8cd). Further, BCKA-driven OCR is higher than BCAA-driven OCR, thereby suggesting that BCKAs are a better fuel source for PDAC cells (Figure 4.8cd). These results strongly suggest that PDAC cells are heavily dependent on BCKAs, and DBT is a potential target for exploiting this dependency.

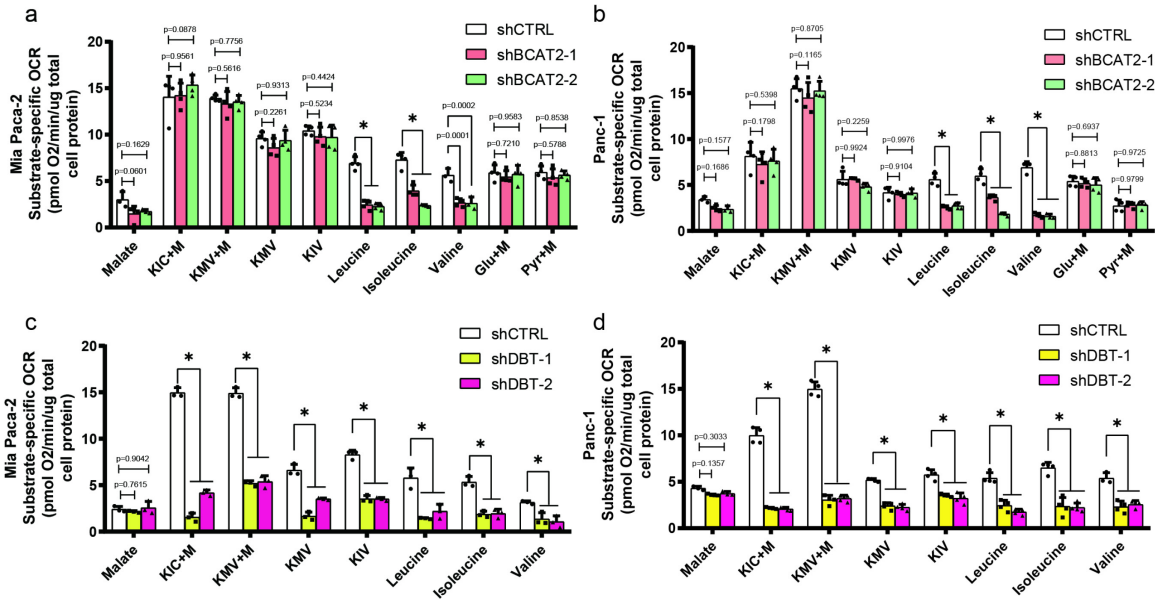

Figure 4.8 BCKA specific OCR is regulated by DBT. a. Substrate-specific OCR measurements of BCAT2 knockdown Mia Paca-2 cells. n = 4 biologically independent samples. **b**. Substrate-specific OCR measurements of BCAT2 knockdown Panc-1 cells. n = 4 biologically independent samples. **c**. Substrate-specific OCR measurement of DBT knockdown Mia Paca-2 cells. n = 4 biologically independent samples. **d**. Substrate-specific OCR measurement of DBT knockdown Panc-1 cells. n = 4 biologically independent samples.

4.5 Discussion

The second step of BCAA metabolism is catalyzed by the mitochondrial inner membrane complex called branch-chain α-ketoacid dehydrogenase complex (BCKDH complex). The BCKDH complex consists of three catalytic components, alpha-ketoacid

dehydrogenase (also referred to as the E1 component), dihydrolipoyl transacylase (E2 component), and dihydrolipoamide dehydrogenase (E3 component). The branched-chain keto acid dehydrogenase E1 has two isoforms, alpha polypeptide and subunit beta, which are encoded by BCKDHA and BCKDHB, respectively. Dihydrolipoamide dehydrogenase (E3 component) is encoded by the DLD gene, which is also a subunit of pyruvate dehydrogenase and alpha-ketoglutarate dehydrogenase complexes. The DBT gene encodes Dihydrolipoyl transacylase (E2), BCKDC E1 and E3 are linked via E2. After the second step, BCKAs are catalyzed into IB-CoA, 2MB-CoA and IV-CoA, which are then converted into succinyl-CoA and Acetyl-CoA to contribute to the TCA cycle.

Since BCAT2 knockdown did not result in a loss of cancer cell growth in cocultures with CAFs under BCAA-deprivation, we use DBT knockdown PDAC cells to characterize the functions of the BCKDH complex in this chapter. Knocking down DBT reduced proliferation and colony formation. In agreement with the essentiality of the BCKDH complex, the addition of BCKAs under BCAA deprivation rescued the loss of proliferation in PDAC cells is conferred via the BCKDH complex. Furthermore, DBT-knockdown PDAC cells with CAFs under BCAA deprivation proved the BCKDH-dependent role of CAF-secreted BCKA in maintaining PDAC cells' growth.

Also, we showed that BCKAs increased the mitochondrial NADH/NAD^+ ratio and corroborated our findings that BCKA oxidation enhances energy metabolism. BCKA's contribution to oxidization through the BCKDH complex is regulated by DBT, BCAT2 and α-KG/Glutamate ratios in PDAC cells. To identify the dominant substrates contributing to cellular oxidative capacity, we measured OCR differences in BCAT2 and

DBT knockdown cells. We showed that that PDAC cells are heavily dependent on BCKAs, and DBT is a potential target for exploiting this dependency.

Chapter 5 BCAT1 Regulates Stromal Cells' Synthesis of Ketoacids

5.1 Introduction

The BCAT1 gene, also known as the ECA39 or PNAS121, is located in the 12p12-11 segment. The mRNA is 8191 bp in length, contains 11 exons, and encodes 641 amino acids. It was first found in teratocarcinoma cell lines in 1990 [252]. In normal organisms, BCAT1 is located in the cytoplasm, which is mainly expressed in brain tissue, spinal cord, peripheral neurons and other tissues [253]. The corresponding isozyme BCAT2 is often found in mitochondria and is expressed in all tissues of the body [254]. The first step of BCAA catabolism is to transfer the α-amino group to α-ketoglutarate through BCAT1 in the cytoplasm or BCAT2 isozyme in mitochondria, the product is glutamate, and corresponding branched-chain keto acids. The resulting branched-chain keto acids can be further metabolized into acetyl-CoA and succinyl-CoA, enter the tricarboxylic acid cycle, generate precursors needed for the synthesis of other biological macromolecules and provide energy for the synthesis of mitochondrial ATP [204]. In 1996, BCAT1 was first identified as the direct target of c-MYC regulation, which is highly conservative during evolution and involved in the regulation of the yeast cell cycle [255, 256].

5.1.1 Glioma

Glioma is derived from the glial cells and neuronal cells of the nervous system, also known as neuroepithelial tumors. It is the most common malignant tumor in the brain, accounting for 35.26%-60.96% of the primary intracranial tumors [257]. The transamination of BCAA via BCAT1 provides an important nitrogen source for the body to synthesize non-essential amino acids, and down-regulation of BCAA catabolism often leads to neurological dysfunction [243]. This shows that BCAA plays an important role in maintaining normal neurological function. Tönjes *et al.* found that BCAT1 is highly expressed in gliomas carrying wild-type IDH (IDH^{wt}), but not significantly increased in mutant IDH (IDH^{mut}) gliomas and normal brain tissues [243]. It found that compared to IDH^{mut} glioma, an important difference between IDH^{wt} glioma is the overexpression of BCAT1. Therefore, it is different from the commonly used IDH1-R132H staining is similar, and BCAT1 staining can also be used for differential diagnosis of related brain gliomas; in glioma cell lines, the expression level of BCAT1 depends not only on the concentration of its substrate α-ketoglutarate, but also overexpression of IDH^{mut} can inhibit the expression of BCAT1; at the same time, in vitro experiments found that inhibiting the expression of BCAT1 in glioma cells directly leads to a reduction in glutamate production, and the cell proliferation and invasion ability also decreases; not only that, It is also found in the mouse model of glioma transplantation that the growth of the transplanted tumor is also significantly restricted under the condition of inhibiting the expression of BCAT1 [243]. Zhang *et al.* show that hypoxia upregulates the BCAA transporter LAT1 and BCAT1, but not BCAT2 in glioblastoma [258]. HIF-1α regulates BCAT1 expression by directly binding to the hypoxia response element at the first intron

of the BCAT1 in glioblastoma [258]. Knockout of HIF-1α reduces flux labeling from BCAAs in glioblastoma under hypoxia, and inhibition of BCAT1 inhibits glioblastoma cell growth under hypoxia [258]. BCAT1 expression can be used as a new diagnosis and treatment target for glioma.

5.1.2 Liver cancer

Hepatocellular carcinoma (HCC) has gradually increased in incidence in recent years and is the third leading cause of tumor death in the world [259]. Wang *et al.* discussed the expression of BCAT1 protein in hepatocellular carcinoma and its correlation with the prognosis of hepatocellular carcinoma [260]. Moreover, a later study found that BCAT1 was highly expressed in liver cancer [261]. They found that BCAT1 expression in liver cancer cell lines and c -Myc expression is positively correlated, and knocking down c-Myc can also down-regulate the expression of BCAT1 [261]. Combined with *in vivo* experiments, after interfering with the expression of BCAT1, the ability of hepatocellular carcinoma cell migration and invasion also decreases.

Conversely, loss of BCAA deamination enhances mTORC1 activity and promotes tumor development in the liver[262]. Another study also found that BCAT1 expression enhances the resistance of hepatocellular carcinoma to cisplatin drugs by inducing autophagy [263]. These findings suggest that BCAT1 is a potential biomarker for the diagnosis and treatment of hepatocellular carcinoma.

5.1.3 Ovarian cancer

Ovarian malignant tumors are one of the three most common malignant tumors in female genitals [264]. Wang *et al.* pointed out that the BCAT1 gene is overexpressed in

low-grade malignant tumors and high-grade serous epithelial ovarian tumors, and suggested that BCAT1 expression is closely related to BCAT1 due to significant hypomethylation [265]. It was found that the knocking down of BCAT1 in epithelial ovarian cancer cells attenuates cell proliferation, metastasis and invasion, and inhibits the cell cycle and inhibiting BCAT1 leads to a decrease in lipid synthesis and protein synthesis [265]. Further metabolomics analysis shows that more amino acids and sheath substances are consumed, suggesting that BCAT1 plays an important role in the metabolism of ovarian cancer [265].

5.1.4 Leukemia

Acute myeloid leukemia (AML) is the most common adult acute leukemia, and its morbidity and mortality are both high. Raffel *et al.* find the BCAA enriched and BCAT1 overexpressed in leukemia stem cells. BCAT1 is also necessary for α-ketoglutarate (α-KG) homeostasis and links BCAA deamination to epigenomic regulation via α-KG dependent dioxygenases in AML stem cells[266]. Knockdown of BCAT1 in AML cells caused accumulation of α-KG, which leads to Egl-9 family hypoxia-inducible factor 1 (EGLN1) -mediated HIF1α protein degradation. By contrast, overexpression of BCAT1 in AML cells decreased intracellular αKG levels and caused DNA hypermethylation through altered ten-eleven translocation (TET)activity. Gu *et al.* show that EZH2 and NRASG12D mutations cooperatively induce the progression of myeloid leukemias in mice [267]. BCAT1 is repressed by EZH2 in normal cells and aberrantly activated in EZH2-deficient myeloid leukemias. BCAT1 reactivation sustains intracellular BCAA pools, resulting in enhanced mTOR signaling in EZH2-deficient leukemia cells, and inhibition of BCAT1 selectively inhibits EZH2-deficient leukemia-initiating cells [267].

Hattori *et al.* showed that BCAT1 is upregulated in chronic myeloid leukemia (CML) and promotes BCAA production in CML cells by aminating the branched-chain keto acids. The inhibition of BCAT1 induces cellular differentiation and impairs the propagation of blast crisis CML [244]. They also identified Musashi2 (MSI2), an RNA binding protein that is required for CML, as a regulator of BCAT1. These studies also suggest that BCAT1 has an important role in leukemia.

5.1.5 Colorectal cancer

Colorectal cancer is a common malignant tumor of the digestive system; the overall morbidity and mortality of colorectal cancer are stable. Still, its proportion of global malignant tumor morbidity and mortality has increased [268]. BCAT1 is significantly higher expressed in colorectal cancer with distant metastasis compared to colorectal cancer without distant metastasis, and BCAT1 expression can reliably predict whether colorectal cancer is distant metastasis [269]. Mitchell *et al.* found that when screening biomarkers diagnosed by colorectal cancer, BCAT1 Methylation is more common in colorectal tissue [270]. Other studies also pointed out that methylated BCAT1 and IKZF1 are significantly increased in colorectal cancer, which is circulating in the blood [271, 272]. So BCAT1 can also be used as a potential biomarker for the diagnosis of colorectal cancer [271, 272].

5.2 CAF secreting BCKAs medicated by BCAT1

The mechanistic underpinnings of stromal BCKA secretion are necessary to elucidate its dynamics and targetable vulnerabilities. Because the synthesis of stromal BCKA is dependent on the transamination by BCAT1 or BCAT2. We first check the PDAC cell growth in shBCAT1/2 CAFs, knockdown of BCAT1 by shRNA-BCAT1 in CAFs and consequent reduced BCKA secretion significantly reduced the growth rate of PDAC cells (Figure 5.1ab). Importantly, knockdown of BCAT2 by shRNA-BCAT2 in CAFs did not affect the growth rate of PDAC cells (Figure 5.1a).

We then inhibited BCAT1 activity using Gabapentin, a BCAT1 inhibitor and measured BCKA secretion in CAFs[273]. Gabapentin concentration was selected after assessing its inhibition efficacy on BCAT1 activity (Figure 5.1c). Indeed, Gabapentin significantly reduced BCKA production and subsequent secretion by 40-50%, as observed by the extracellular BCKA concentrations using LC-MS analysis (Figure 5.1d).To conclusively associate BCAT1 with CAF-mediated rescue of cancer cells under BCAA-deprived conditions, we added Gabapentin to cocultures (Figure 5.1e). Notably, inhibition of stromal BCAT1 abrogated the CAFs' ability to rescue PDAC cell growth, whereas the addition of BCKA markedly restored the PDAC cell growth. These results suggest that BCKA synthesis in CAFs can be severely impacted upon loss of BCAT1 expression or activity.

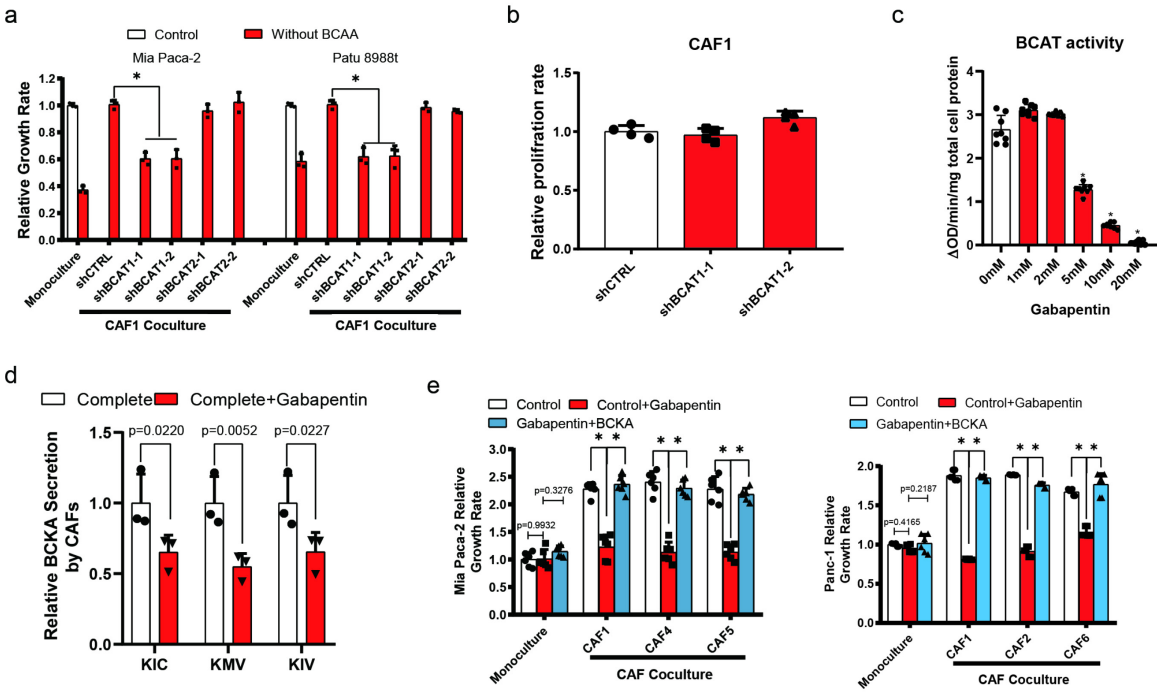

Figure 5.1 CAF secreting BCKAs medicated by BCAT1. **a**. Effect of BCAT1 knockdown in CAFs on the CAF-mediated rescue of cell growth rate under BCAA deprivation. n = 3 biologically independent samples. **b**. The effect of knockdown of BCAT1 in CAFs on CAF growth rates. n = 4 biologically independent samples. **c**. BCAT activity is CAFs treated with Gabapentin measured by spectrophotometric assay. n = 6 biologically independent samples. **d**. BCKA secretion by CAFs treated with 10mM Gabapentin. n = 3 biologically independent samples. **e**. Effect of 10mM Gabapentin on CAF-mediated rescue of MiaPaca-2 growth rate under BCAA deprived conditions. n = 6 biologically independent samples.

5.3 Inhibition of stromal BCAT1 down-regulate cancer protein synthesis and NADH

We further investigated if Gabapentin-mediated BCAT1 inhibition in CAFs could influence *de novo* protein synthesis in PDAC cells in coculture. We found that BCAT1 suppression in CAFs not only markedly reduced *de novo* protein synthesis (Figure 5.2a), but also the mitochondrial NADH/NAD^+ ratio in PDAC cells (Figure 5.2b).

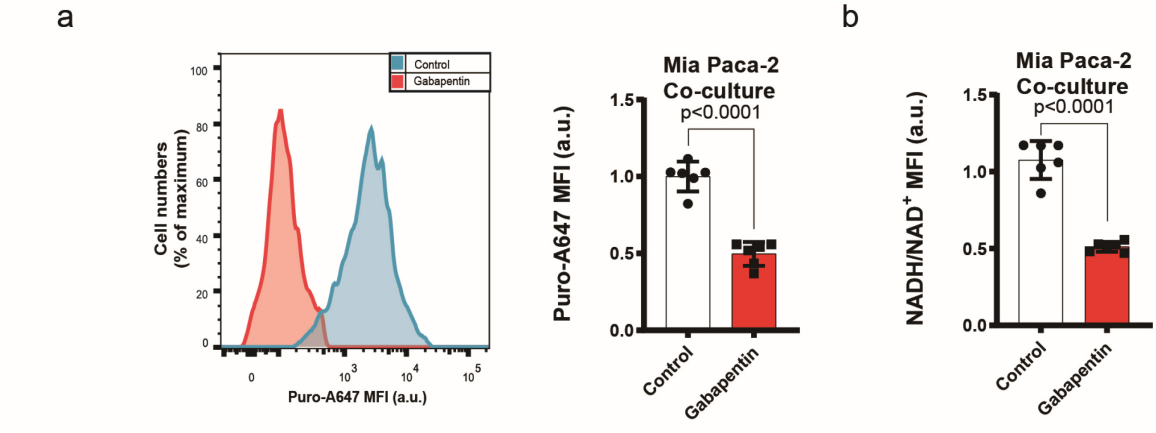

Figure 5.2 Inhibition of stromal BCAT1 down-regulate cancer protein synthesis and NADH. **a**. FACS analysis of GFP-labeled Mia Paca-2 cells detected with puromycin antibodies in the co-culture system with 10mM gabapentin. n = 6 biologically independent samples. **b**. Effect of 10mM gabapentin on the NADH/NAD^+ ratio of cancer cells cocultured with CAFs. n = 6 biologically independent samples.

5.4 Discussion

In recent studies, the high catabolic activity of BCAT1 was shown to promote cell proliferation in wild type isocitrate dehydrogenase 1 (IDH1) gliomas [243]. BCAT1 is also necessary for α-ketoglutarate (α-KG) homeostasis and links BCAA deamination to epigenetic regulation via α-KG dependent dioxygenases in acute myeloid leukemia stem cells [266]. Conversely, loss of BCAA deamination enhances mTORC1 activity and promotes tumor development in the liver [262, 274]. BCAT1 is upregulated during the progression of chronic myeloid leukemia and promotes BCAA production by aminating the BCKAs [244]. Finally, high glucose uptake suppresses BCAA deamination in cardiomyocytes [275].

In this chapter, we identified BCAT1 as the regulator of BCKA secretion in CAFs. We first performed the PDAC cell growth assay in shBCAT1/2 CAFs. After confirmation of BCAT1 in CAFs, we then used BCAT1 inhibitor, Gabapentin. Indeed, Gabapentin significantly reduced BCKA production. Furthermore, we also used Gabapentin to CAF cocultures; it showed that Gabapentin inhibits the CAFs' ability to rescue PDAC cell growth. These results suggest that BCAT1 regulates BCKA synthesis in CAFs in CAFs. Gabapentin could inhibit de novo protein synthesis and the mitochondrial NADH/NAD^+ ratio in PDAC cells in coculture. With the continuous development of BCAT1 related research, more and more are found that malignant tumors, BCAT1 is highly expressed, and it is suggested that it plays an important role in promoting tumor cell proliferation, invasion and metastasis. It may be a potential clinical aid for related tumors to diagnostic biomarkers or therapeutic targets.

Chapter 6 Internalization of The Extracellular Matrix to Supply Amino Acid Precursors for BCKA Secretion by CAFs

6.1 Introduction

One of the hallmarks of PDAC histology is desmoplasia, where the fibrosis reaction is caused by excessive fibroblasts and ECM deposition of most tumor masses [52, 276, 277]. ECM is made of structural protein, an adaptor protein, dense network structure of proteins and enzymes found in all tissues, providing biochemical and structural support for tissue homeostasis [278]. In PDAC, the deposition of ECM has increased significantly with progression. Collagen is the main structural protein in the ECM. Type I and IV collagens are the main structural proteins constituting PDAC ECM [279].

6.1.1 Collagen Type I (Col I)

Col I is a heterogeneous triplet that constitutes the extracellular matrix. The main component is fibrous collagen, and Col I has a wide range of biological activities. In addition to regulating cell protein synthesis and secretion, it can also regulate the production of some proteolytic enzymes [280]. Moreover, through the induction of tumor cells, a variety of hydrolytic enzymes are produced. Moreover, under the regulation of various cytokines, it affects the growth, differentiation, migration or gene expression of cells through the interaction with the cells, thus in the tumor and It plays an extremely

important role in the process of inflammation occurrence, development and wound healing.

The role of Col I in the process of tumor evolution has been gradually understood and increasingly valued in recent years. It is related to a variety of tumors. Kiefer *et al.* [1] found that α2β1 and α3β1 integrins can mediate the adhesion of Col I to cells, and then stimulates the proliferation and growth of cells through the transduction of signaling pathways [281]. Furthermore, incubating bladder cancer cells on Col I coating, the expression of genes related to metabolism, transcription and translation has been changed, which has increased the proliferation of cells and contributed to the bone metastasis of bladder cancer [282]. In normal tissues, Col I is mainly produced by fibroblasts in the interstitium. The content of Col I in the main depends on two aspects: one is the synthesis and deposition of collagen, and the other is the role of collagen dissolution factors. The two together determine the content of Col I in tumor tissues. In tumor tissues, tumor cells and fibroblasts are involved in the process of Col I synthesis and deposition, and there is an interaction between the two. Dahlman *et al.* found that tumor cells can stimulate the transcription of Col I mRNA of fibroblasts through direct interactions between cancer cells and fibroblasts or stimulation of cytokines such as PDGF and TGFGβ [283]. Sengupta *et al.* found that when the methylation level of α2(I) transcription initiation site increased, the steady-state level of Col I mRNA decreased, and the production of collagen decreased [284]. This shows that the collagen synthesis process is extremely complicated. It is regulated by various factors and needs further discussion.

Similarly, the dissolution factor of Col I is a factor that cannot be ignored and is closely related to tumor invasion and metastasis. In tumor tissues, the dissolution of Col I is mainly related to hydrolytic enzymes that are mainly related to MMP1, MT-MMP1, and other enzymes [285]. Although tumor cells can secrete these enzymes to degrade Col I, Col I has a certain regulatory effect on the production of these enzymes. Studies have found that Col I can regulate the production and secretion of MMP-2 and can also regulate the secretion ability of fibroblast MMP-2 and cathepsin B precursors [286]. Therefore, Col I can reduce the barrier effect on tumor invasion through the action of lytic factors, and can also induce tumor cells to produce multiple hydrolases.

The abnormal expression of Col I is related to the occurrence and evolution of multiple types of tumors. The degradation and synthesis of Col I in tumor tissue is a dynamic process, and the enhancement of collagen synthesis and deposition may be involved in preventing the growth of tumors. In contrast, the dissolution of collagen may cause tumor invasion and expansion. At the same time, in highly malignant tumors, the abnormality of collagen may promote the evolution of the tumor. It can be seen that the role of Col I in the process of malignant transformation of cancer cells cannot be ignored.

6.1.2 Collagen Type IV (Col IV)

Col IV is the main component of the dense layer of the basement membrane and also belongs to the fibrous collagen. The basement membrane has a three-dimensional network structure, which is maintained by covalent bonds and is connected with other components, such as laminin, fibronectin, etc. [287]. The extracellular matrix structure constitutes the cell's microenvironment. Current research has found that Col IV can provide sites for cell adhesion. These sites are specifically recognized by receptors on the

cell surface and participate in the regulation of cell function. Therefore, they are involved in tumors and inflammation. The development process also has important significance.

During the invasion and metastasis of many tumors, the expression of Col IV is generally reduced or absent. Col IV expression was negatively correlated with cervical lymph node metastasis in larynx cancer [288]. Erkan *et al.* found that as the degree of tumor invasion increased, the rate of expression loss of Col IV is also gradually worsened, and is closely related to the lymph node metastasis of the tumor [289]. Ozer *et al.* reported that the expression of Col IV and laminin in urinary tract tumors is closely related to the survival time of patients [290]. In recent years, studies have also found that Col IV expression is related to tumor differentiation, invasion and metastatic ability. At the same time, it has a certain value for judging tumor invasion, metastasis and prognosis.

6.2 Uptake of collagen under BCAA deprivation

Activated CAFs in PDAC is known to secrete a vast array of ECM proteins, such as collagen, enzymes, and glycoproteins [291-293]. Therefore, we surmised that under the nutrient-scarce conditions of the pancreatic TME, the ECM proteins in the milieu could be a source of amino acids for CAFs. However, there continues to be sparse data regarding the role, if any, of ECM protein uptake by stromal fibroblasts in cancer. To illustrate that CAFs utilize ECM proteins, which in turn influence CAF-mediated rescue of PDAC cells under BCAA deprivation conditions, we added collagen I or collagen IV to coculture. As seen in Figure 6.1a, both collagen I and IV enhanced PDAC cell growth

rate in coculture under BCAA-deprivation but did not affect monoculture. Further, Gabapentin attenuated ECM protein-mediated rescue of cancer cell growth by CAFs.

To characterize internalization, confirm uptake and cleavage of ECM proteins by CAFs, we used fluorogenic DQ collagen (self-quenched collagen that emits fluorescence upon degradation). We found that collagen uptake in CAFs under BCAA-deprivation increased significantly compared to the BCAA-replete condition, and this increase was pronounced in the presence of TGF-β (Figure 6.1b). To further substantiate this, we studied the uptake of collagen by both PDAC cells and CAFs and found significantly

higher collagen uptake in CAFs (Figure 6.1c) compared to PDAC cells.

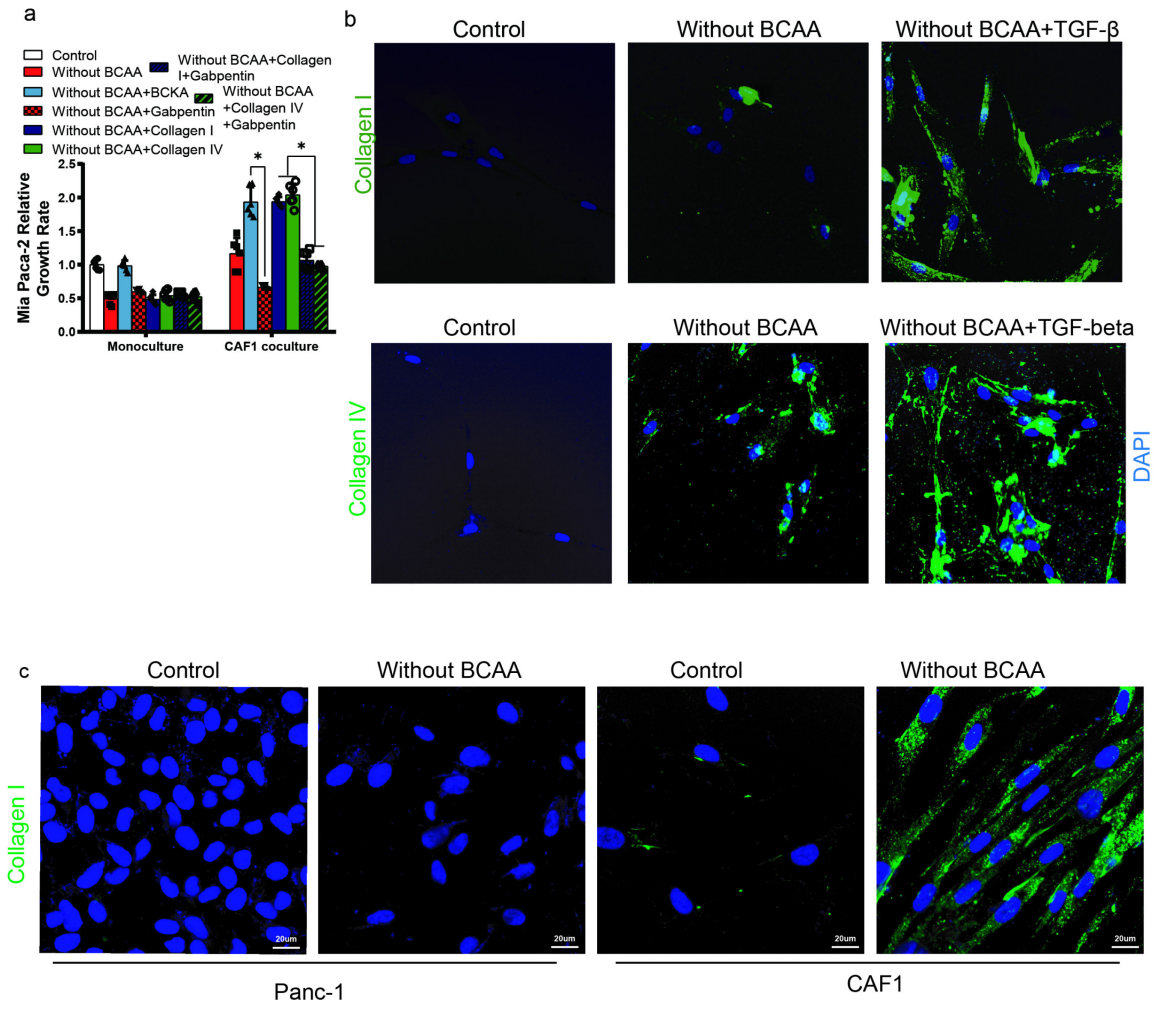

Figure 6.1 Uptake of collagen under BCAA deprivation. **a**. Relative proliferation rates of Mia Paca-2 cells co-cultured with CAFs and Collagen or 10mM Gabapentin under BCAA deprivation. n = 6 biologically independent samples. **b**. Uptake of DQ-Collagen by CAFs assessed using confocal imaging after 24 h. Experiments were repeated independently three times with similar results. **c**. Uptake of DQ-Collagen by PDAC cell lines and CAFs measured using confocal imaging after 24 h. Experiments were repeated independently three times with similar results.

6.3 Collagen uptake regulated by uPARP in CAFs

Since fibroblasts internalize ECM proteins through (uPARAP/Endo 180, which is encoded by the MRC2 gene), we measured the expression of uPARAP/Endo180 in

PDAC and CAFs. In concurrence with our previous results, uPARAP/Endo180 expression is much higher in CAFs compared to cancer cells (Figure 6.2ab). Moreover, inhibiting the expression of uPARP in CAFs significantly impacted the uptake of collagen (Figure 6.2c). These results cumulatively indicate that ECM internalization is indeed high in CAFs, and undetectable in PDAC cells. These ECM internalization results were confirmed by measuring intracellular BCAA levels and ^{13}C enrichment in CAFs cultured with ^{13}C-BCAAs for 12 hours before deprivation (Figure 6.3a). Notably, intracellular BCAA levels increased gradually over 6, 12, 24, and 48 hours post-deprivation (Figure 6.3b). Whereas, ^{13}C enrichment of BCAAs gradually decreased in the same timeframe (Figure 6.3b), indicating the introduction of unlabeled BCAAs in BCAA-deprived CAFs from ECM proteins.

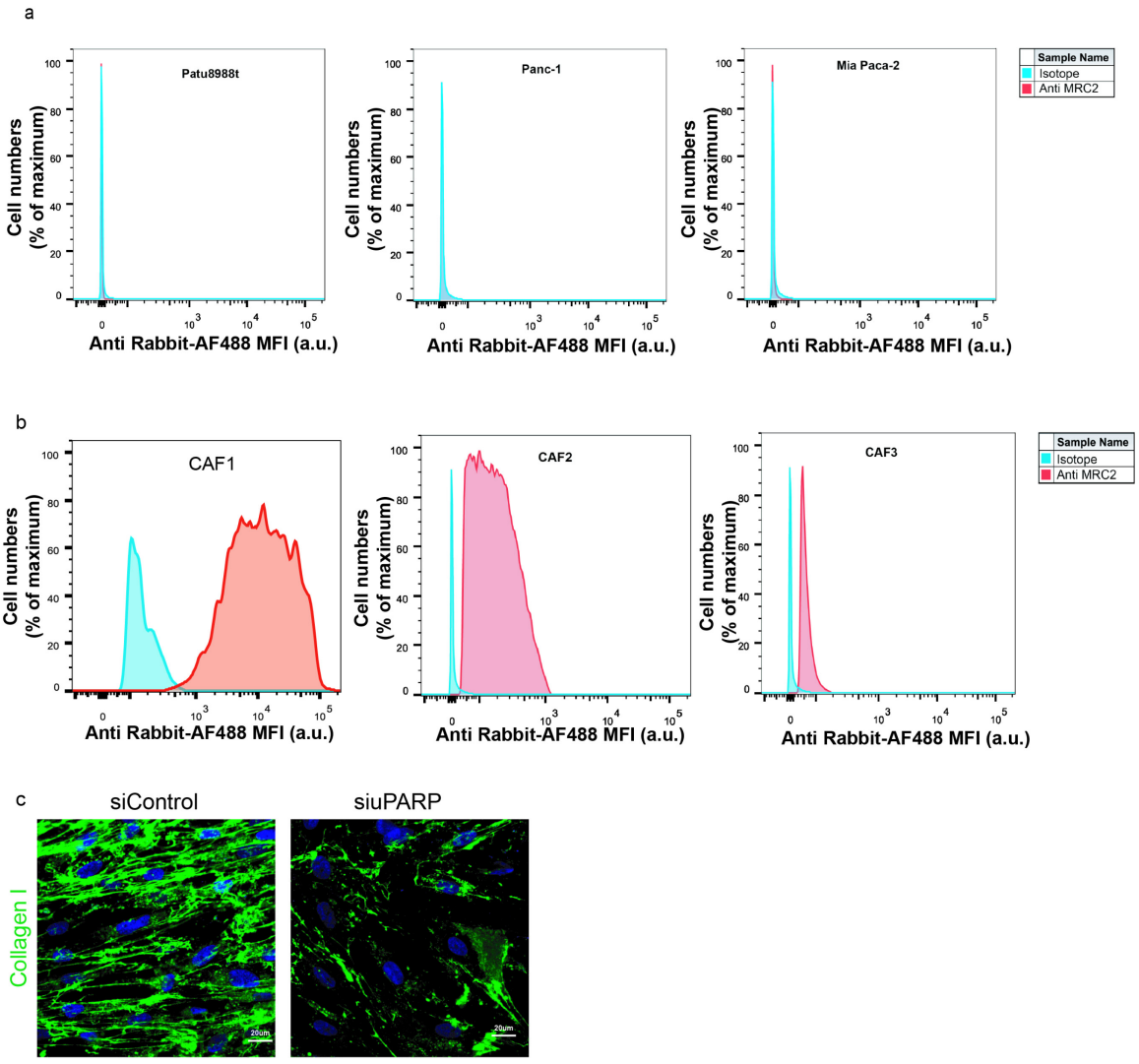

Figure 6.2 Collagen uptake regulated by uPARP in CAFs. a. Flow cytometry assay indicated the expression of MRC2 in PDAC cell lines. Experiments were repeated independently three times with similar results. **b**. Flow cytometry assay indicated the expression of MRC2 in CAFs. Experiments were repeated independently three times with similar results. **c**. Uptake of DQ-Collagen by CAFs transfected with siControl or siuPARP measured using confocal imaging after 24 h. Experiments were repeated independently three times with similar results.

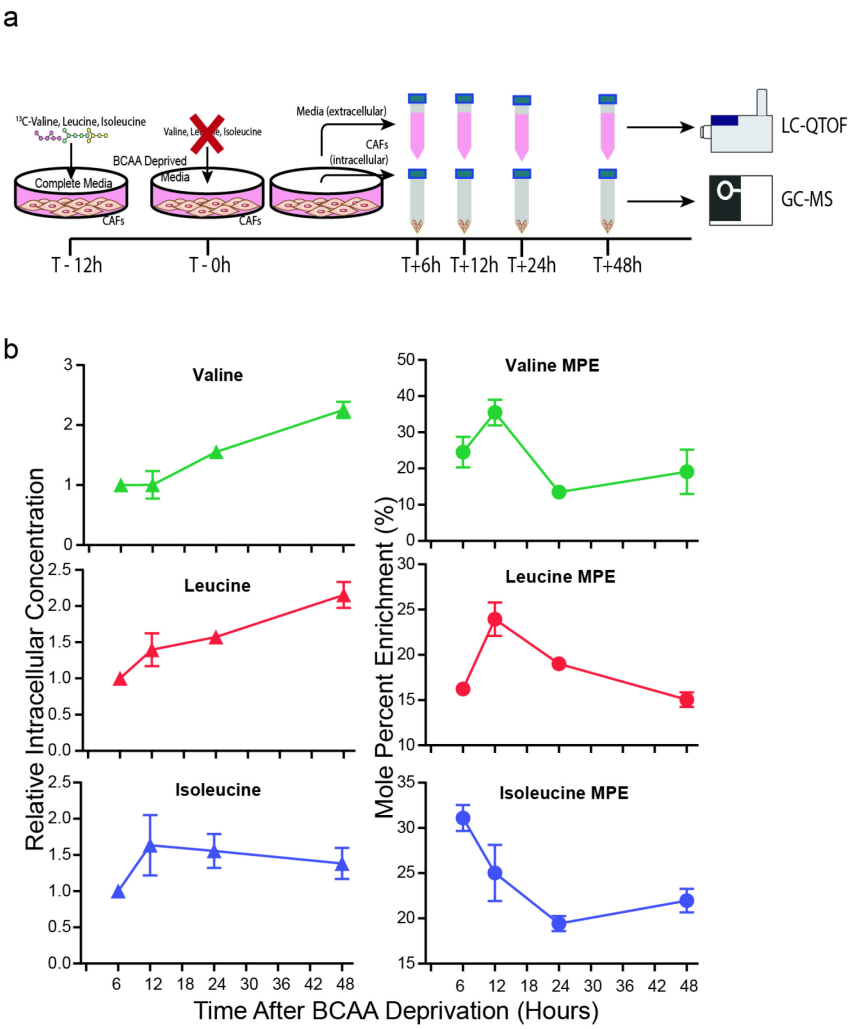

Figure 6.3 Intracellular BCAA levels in CAFs under BCAA deprivation. **a**. CAFs are cultured with labeled with 13C-BCAAs for 12 hours before inducing BCAA deprivation. Spent media and cells are collected after 6, 12, 24 and 48 hours under deprivation. Media samples are analyzed for secreted BCKAs using LC-QTOF, and intracellular samples are analyzed for BCAAs using GC-MS. **b**. Intracellular BCAA levels were measured after 6, 12, 24 and 48 hours under BCAA deprivation. Mole percent enrichment of intracellular BCAAs was measured after 6, 12, 24, and 48 hours under BCAA deprivation. n = 3 biologically independent samples.

6.4 CAFs utilize collagen through the proteasome

To understand the underlying mechanism behind the degradation of ECM proteins in CAFs, we hypothesized that proteasomal proteolysis plays a major role in the

degradation of these internalized ECM proteins under nutrient-deprived conditions. Consistent with this notion, both BCAA-deprivation and TGF-β increased the chymotrypsin-like proteasome activity in CAFs, but not trypsin-like and caspase-like protease activities (Figure 6.4a). To further investigate the role of the proteasome in collagen degradation, cells were incubated with FITC-collagen I for 48h and then stained with an antibody for the proteasome α and β subunits (Figure 6.4b). It was evident that collagen is localized with proteasomes in the CAFs, thereby suggesting that proteasomes indeed degrade ECM proteins. We further tested our hypothesis by measuring BCKA secretion from CAFs and PDAC cell growth rates in coculture under BCAA-deprived conditions. We found that Delanzomib, the chymotrypsin-like proteasome activity inhibitor, attenuated ECM protein-mediated rescue of cancer cell growth by CAFs (Figure 6.4c). These results confirm that collagen is indeed degraded by proteasomal proteolytic activity in CAFs. Further, MG-132, a potent proteasomal inhibitor, also suppressed the rescue of cancer cell growth by CAFs (Figure 6.4d). To further expand our findings, we measured CAF-secreted BCKAs in the presence of Delanzomib and found that Delanzomib impeded their ability to secrete BCKA by 40% (Figure 6.4e).

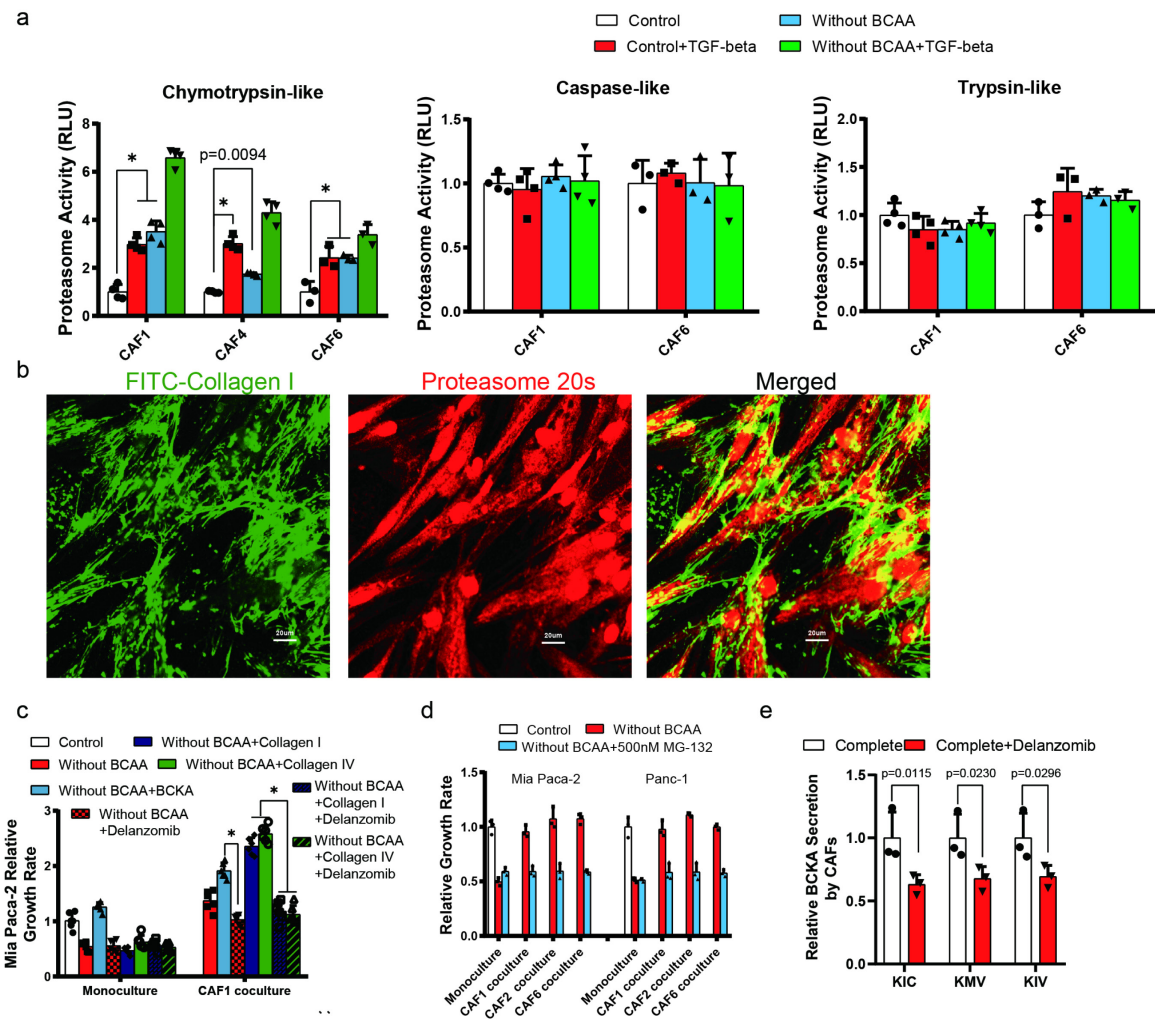

Figure 6.4 CAFs utilize collagen through the proteasome. **a**. Proteasome activity in CAFs treated with TGF-beta and under BCAA deprivation. n = 6 biologically independent samples. **b**. Colocalization of collagen and proteasome analyzed by immunofluorescence against proteasome 20s and FITC-collagen. Experiments were repeated independently three times with similar results. **c**. Relative proliferation rates of Mia Paca-2 pancreatic cancer cells cocultured with CAFs in combination with Collagen or Delanzomib under BCAA deprivation. n = 6 biologically independent samples. **d**. Relative growth rates of Mia Paca-2 and Panc-1 cells cocultured with CAFs treated with MG-132 under BCAA deprivation conditions. n = 8 biologically independent samples. **e**. BCKA secretion by CAFs treated with Delanzomib. n = 3 biologically independent samples.

6.5 CAF derived ECM labeling and tracing

To establish whether internalized ECM proteins are a carbon source for CAF-secreted BCKAs, we cultured CAFs on decellularized ^{13}C-BCAA-labeled ECM proteins (Figure 6.5a). Decellularized ^{13}C-BCAA-labeled ECM was obtained by culturing CAFs with ^{13}C-labeled leucine, isoleucine, and valine for eight days so that CAFs could incorporate labeled BCAAs into ECM protein. To confirm the ECM structure, we used scanning electron microscopy to observe the matrix and found that the CAF-derived 3-D matrix is free of cellular debris and remained attached to the culture surface (Figure 6.5b). Secreted ECM proteins were acid hydrolyzed, and their constituent BCAAs were found to be enriched by 40-50% ^{13}C-labeled BCAAs (Figure 6.5c-e). We then cultured CAFs with ^{13}C-BCAA labeled ECM under BCAA-deprived conditions and analyzed the spent media obtained after 48 hours of culture. BCKAs secreted by the CAFs were analyzed using LC-MS and found to be enriched with ^{13}C derived from the proteolyzed ECM (Figure 6.5f). This indicated that when CAFs were cultured with this labeled ECM, they internalized and proteolyzed it to maintain intracellular BCAA pools and produce and secrete BCKAs. Collectively, these results provide evidence that the ECM in the pancreatic milieu could serve as a storage pool of BCAAs for the CAFs under nutrient-stressed conditions.

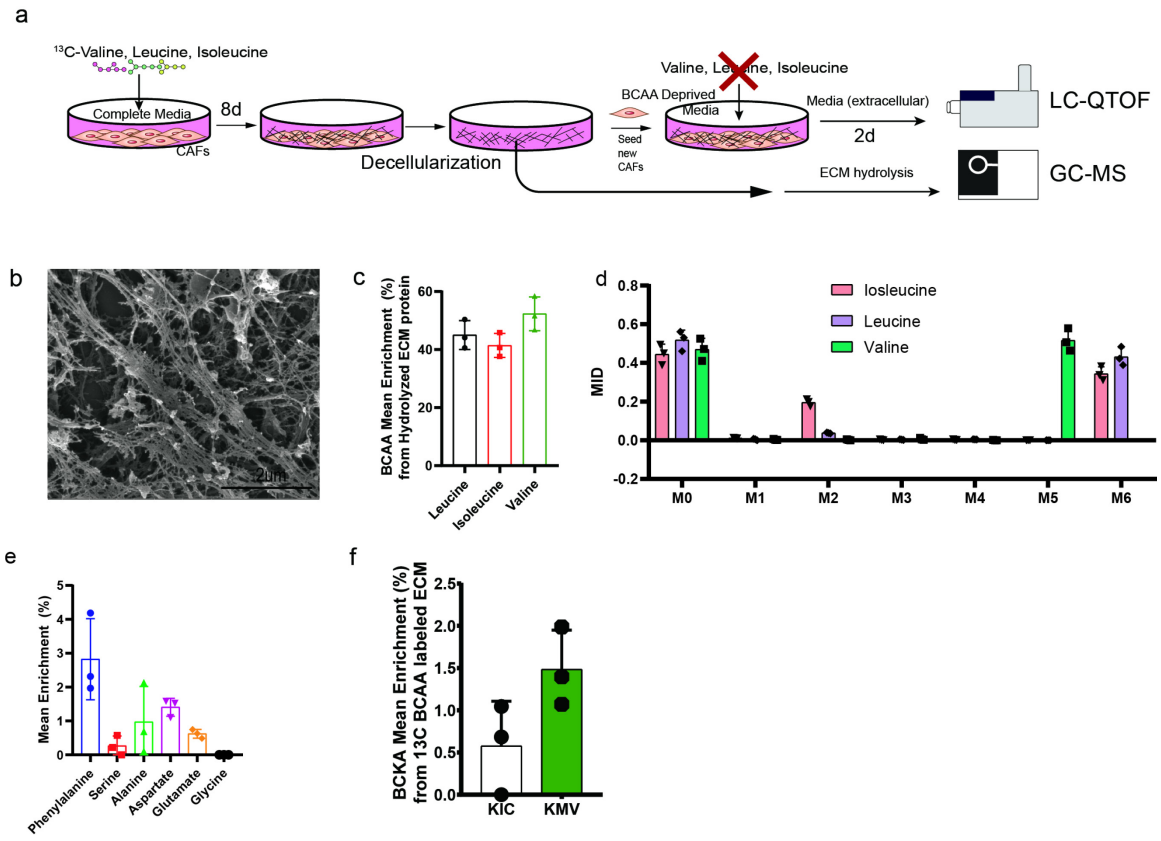

Figure 6.5 CAF derived ECM labeling and tracing. **a**. Schematic of the protocol used to synthesize ECM labeled with 13C-BCAAs and secretion of 13C-BCKAs after culturing BCAA-deprived CAFs in ECM labeled with 13C-BCAAs. **b**. Scanning electron microscopy image of CAF-derived 3-D matrices. Experiments were repeated independently two times with similar results. **c**. Fractional enrichment of BCAAs after acid hydrolysis of decellularized ECM proteins produced by CAFs cultured with 13C-BCAAs. n = 3 biologically independent samples. **d**. Mass isotopomer distribution of BCAAs after acid hydrolysis of decellularized ECM proteins produced by CAFs cultured with 13C-BCAAs. n = 3 biologically independent samples. **e**. Fractional enrichment of amino acids after acid hydrolysis of decellularized ECM proteins produced by CAFs cultured with 13C-BCAAs. n = 3 biologically independent samples. **f**. Fractional enrichment of BCKAs secreted by CAFs at the end of 48h of being cultured under BCAA deprivation on ECM labeled with 13C-BCAAs. n = 3 biologically independent samples.

6.6 Discussion

In this chapter, we characterized the BCAA source for CAFs under BCAA deprivation. CAFs have been shown to secrete a vast array of ECM proteins, such as collagen, enzymes, and glycoproteins [277]. Therefore, we surmised that under the nutrient-scarce conditions of the pancreatic TME, the ECM proteins in the milieu could be a source of amino acids for CAFs. To illustrate that CAFs utilize ECM proteins, which in turn influence CAF-mediated rescue of PDAC cells under BCAA deprivation conditions, we showed collagen I or collagen IV could further support PDAC cells in cocultures. To characterize internalization, confirm uptake and cleavage of ECM proteins by CAFs using DQ collagen. We showed that collagen uptake in CAFs under BCAA-deprivation increased significantly compared to the BCAA-replete condition or in the presence of TGF-β.

It is well-established that stromal cells, including fibroblasts, internalize ECM proteins through (uPARAP/Endo 180, which is encoded by the MRC2 gene) [294, 295], and the expression of uPARAP/Endo180 is maximal in fibroblasts. We first showed that uPARAP/Endo180 expression is much higher in CAFs compared to cancer cells. Furthermore, inhibition of uPARP in CAFs significantly reduced the uptake of collagen. We also tested the proteasomal proteolysis role in the degradation of these internalized ECM proteins under nutrient-deprived conditions. WE also proved that proteasomes indeed degrade ECM proteins since the collagen is co-localized with proteasomes in the CAFs. We found that proteasome inhibitor Delanzomib reduced ECM protein-mediated rescue of cancer cell growth by CAFs. To establish whether internalized ECM proteins

are a carbon source for CAF-secreted BCKAs, we cultured CAFs on decellularized 13C-BCAA-labeled ECM proteins. BCKAs secreted by the CAFs were found to be enriched with 13C derived from the proteolyzed ECM. This indicated that when CAFs were cultured with this labeled ECM, they internalized and proteolyzed it to maintain intracellular BCAA pools and produce and secrete BCKAs. Collectively, we showed that the ECM in the pancreatic milieu could serve as a storage pool of BCAAs for the CAFs under nutrient-stressed conditions, and proteasome can also be a potential target in PDAC tumors.

Chapter 7 Cancer Cells Regulate BCAT1 In Stromal Cells Through TGF-β

7.1 Introduction

Transforming growth factor β (TGF-β) is a newly discovered group of TGF-β superfamily that can regulate cell growth and differentiation. In recent years, it has been found that TGF-β has important adjustment effects on cell growth, differentiation and immune function, such as inhibiting the growth of epithelial cells and endothelial cells, suppressing the differentiation of lymphocytes and suppressing the proliferation of immune cells. These biological functions have an inhibitory effect on the occurrence and development of tumor cells. However, studies have shown that TGF-β1 can promote the infiltration and migration of tumor cells when regulating the immune system of cells and the microenvironment of tumors [296, 297].

7.1.1 Molecular biological feature of TGF-β

The TGF-β superfamily consists of more than 40 proteins, including TGF-β, activin (A, AB, B, C, E), inhibin (A, B), bone morphogenetic proteins (BMPs) and growth and differentiation factors (GDFs). The human TGF-β cDNA sequence shows that the monomeric TGF-β is a polypeptide containing 112 amino acid residues, and the gene is located in the chromosome 19q13, human TGF-β has three subtypes of TGF-β1, TGF-β2, and TGF-β3. There are also two subtypes of TGF-β4 and TGF-β5 in birds and amphibians. The role of TGF-β1 is multi-directional, and almost all types of tissues in the

human body can synthesize and secrete. It plays an important role in regulating the growth of cells, the formation of the extracellular matrix, immune regulation, neovascularization, cell death and tumor development [298].

TGF-β1 needs to be activated with its receptor before it can exert its biological effects. Common receptors are TβRI (53 kDa), TβRIII (75 kDa) and TβRIII (280 kDa). TβR TβRII and I belong to transmembrane proteins, and they also have serine protein kinase activity in cells. TβRII is first activated by binding to a ligand, and then recruited and combined with TβRI. They jointly determine the identification characteristics of TGF-β. Activated TβRII can make the sequence of TβRII amino acid fragments phosphorylated by TTSGSGSG, which further activates the receptor's serine protein kinase activity, which triggers a cascade of cell signal transduction reactions. TβRI can promote the phosphorylation of Smad2 and Smad3 proteins and connect with the “pocket” structure of the SMD4 protein Mh2 region to form R-Smad-SMAD4 oligomers into the nucleus and further regulate target gene transcription [299]. The Smads protein is the central nucleus of the TGF-β1 signal that enters the nucleus from the cytoplasm. The Smad pathway is the classic pathway for the transduction of TGF-β signals. Besides, the activity of TGF-β signal transduction is also regulated by the negative feedback loop of I-Smads (suppressive Smads: Smad6, Smad7) [300]. Moreover, TGF-β can also conduct signal transduction through non-classical SMAD-independent pathways. So far, SMAD-independent pathways mainly include RhoA-Rock1, RAS, ShcA, ERK1/2, and p38 MAPK pathways [301].

7.1.2 The role of TGF-β1 in the development of tumors

Under physiological conditions, TGF-β1 can effectively inhibit the growth of many types of cells, including tumor cells. The mechanism by which TGF-β1 suppresses normal cell growth is to regulate the genes so that the cell proliferation period is at rest. In the early stage of the tumor, it inhibits the proliferation of cancer cells by resisting mitosis. TGF-β1 controls cell proliferation mainly by blocking cell cycle progression and inducing or activating cyclin-dependent kinase (CDK) inhibitors such as p27Kip1 [302]. However, when the tumor develops to an uncontrollable stage, TGF-β1 loses this inhibitory effect on most tumor cells. At this time, the tumor cells began to secrete TGF-β1. TGF-β1 can promote vascularization by up-regulating the expression of microRNA, increasing the ability of cancer cells to bind to adherent molecules of cells, thereby enhancing the invasion of cancer cells and promoting the growth of micro-circulation and metastasis of tumors [303]. At this time, TGF-β1 can induce normal cell death around the cancer cells, thereby eliminating their inhibitory effect on tumor growth.

In the later stage of the tumor, TGF-β1 becomes a tumor-promoting factor, which plays an important role in the transition of the tumor. In PDAC, TGF-β1 can convert human acinar cells to duct-like cells in a SMAD-dependent pathway [304]. Furthermore, TGF-β1 regulates miR-100 and miR-125b through SMAD2/3 to promote PDAC progression [305].

7.1.3 TGF-β1 and EMT

EMT is the transformation of epithelial cells into cells with an interstitial phenotype. The biological process is not only a basic process of body development but also a feature of tumor occurrence. Through EMT, epithelial cells have lost cell polarity,

epithelial phenotypes, such as connection to the basement membrane. At the same time, they have obtained higher migration and invasion, resistance to decay, and the ability to decompose the extracellular matrix [98]. TGF-β1 is an important regulatory factor in the process of EMT. Extracorporeal studies have shown that TGF-β recognition is the main inducer of EMT. The regulators of EMT can be adjusted through the Smad pathways, mainly including Snail, Slug, Twist, Cripto-1, FoxC2 and Six1 [306]. Activating the Smd2/3 in the epithelial cells can induce the expression of the nuclear HMGA2, and it can stimulate Snail1, Snail2, Slug, Twist by transcription [307]. TGF-β1-mediated formation of the Snail Smad3/4 complex can inhibit the expression of E-cadherin in epithelial cells, and E-cadherin will be lost during the EMT process and in the post-tumor period [308]. TGF-β1 inhibitors are being used reversal epithelial-mesenchymal transition as metastasis inhibitors in clinical trials [309].

7.2 PDAC cell condition media activate BCAT1

To unravel the mechanism underlying the regulation of BCAT1 expression in CAFs, we postulated that cancer cells reprogram fibroblasts to upregulate their BCAT1 expression to meet the cancer cells' demand for BCKAs under BCAA deprivation. It is well-established that resident quiescent fibroblasts and bone marrow-derived mesenchymal stem cells (MSCs) serve as precursors of activated CAFs, and factors secreted by cancer cells modulate this transformation [310]. We first transformed NOFs and MSCs into CAFs by culturing them in PDAC cell-conditioned medium (CM) for four weeks and measured the expression of genes involved in BCAA metabolism. This revealed that the basal expression of BCAT1 in NOFs and primary MSCs is low,

however, increased activation of NOFs and primary MSCs using cancer cell CM progressively increased BCAT1 expression and expression of activated CAF markers α-smooth muscle actin, (αSMA), podoplanin (PDPN), and fibroblast specific protein (FSP1) (Figure 7.1). Consistent with previous results, there was no change in BCAT2 gene expression in MSCs and NOFs cultured in PDAC cell CM (Figure 7.2). These results were further corroborated when CAFs were exposed to PDAC CM for three weeks, and similar upregulation of BCAT1 was found with no significant changes in BCAT2, BCKDHA, and BCKDHB (Figure 7.3). Next, we asked if these activated NOFs could acquire PDAC-supporting characteristics of CAFs. Notably, we found that, like CAFs, activated NOFs completely rescue PDAC cell growth under BCAA-deprivation conditions (Figure 7.4).

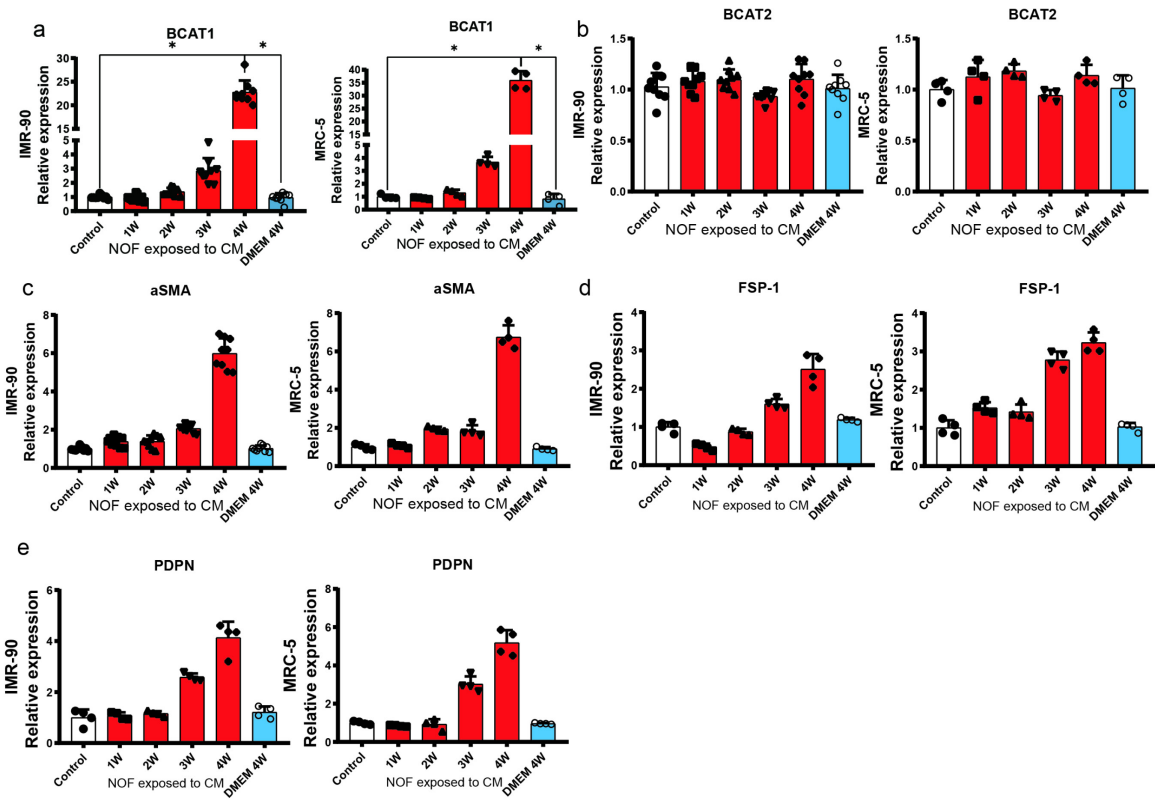

Figure 7.1 Panc-1 CM activates BCAT1 in NOFs. a. Effect of pancreatic cancer cell-conditioned media (CM) on BCAT1 expression in NOFs over four weeks. n = 8 biologically independent samples. **b**. BCAT2 expression in NOFs treated with pancreatic cancer cell-conditioned media (CM). n = 8 biologically independent samples. **c**. α-smooth muscle actin, (α-SMA) expression in NOFs cultured with pancreatic cancer cell-CM over four weeks. n = 8 biologically independent samples. **d**. fibroblast specific protein (FSP1) expression in NOFs cultured with pancreatic cancer cell-CM over four weeks. n = 8 biologically independent samples. **e**. podoplanin (PDPN) expression in NOFs cultured with pancreatic cancer cell-CM over four weeks. n = 8 biologically independent samples.

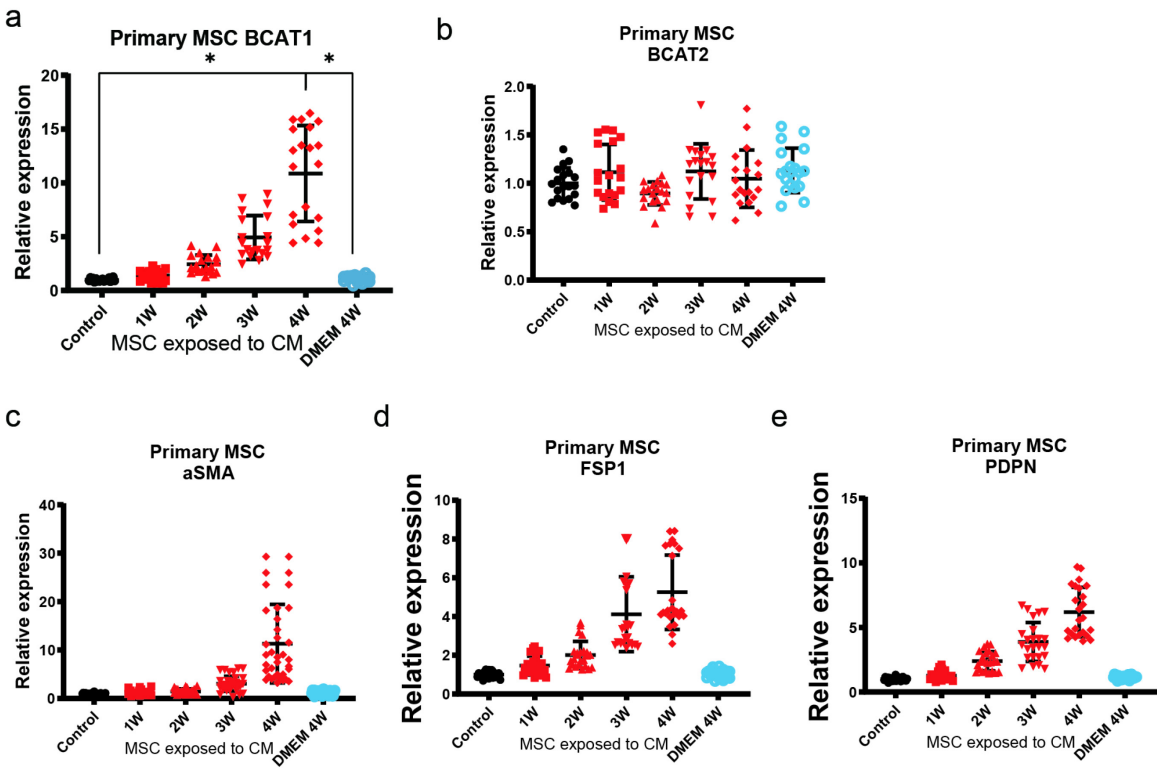

Figure 7.2 Panc-1 CM activate BCAT1 in MSCs. a. Effect of pancreatic cancer cell CM on BCAT1 expression in primary MSCs over four weeks. n = 6 biologically independent samples. **b**. Effect of pancreatic cancer cell CM on BCAT2expression in primary MSCs over four weeks. n = 6 biologically independent samples. **c**. Effect of pancreatic cancer cell CM on αSMA expression in primary MSCs over four weeks. n = 6 biologically independent samples. **d**. Effect of pancreatic cancer cell CM on FSP-1 expression in primary MSCs over four weeks. n = 6 biologically independent samples. **e**. Effect of pancreatic cancer cell CM on PDPN expression in primary MSCs over four weeks. n = 6 biologically independent samples.

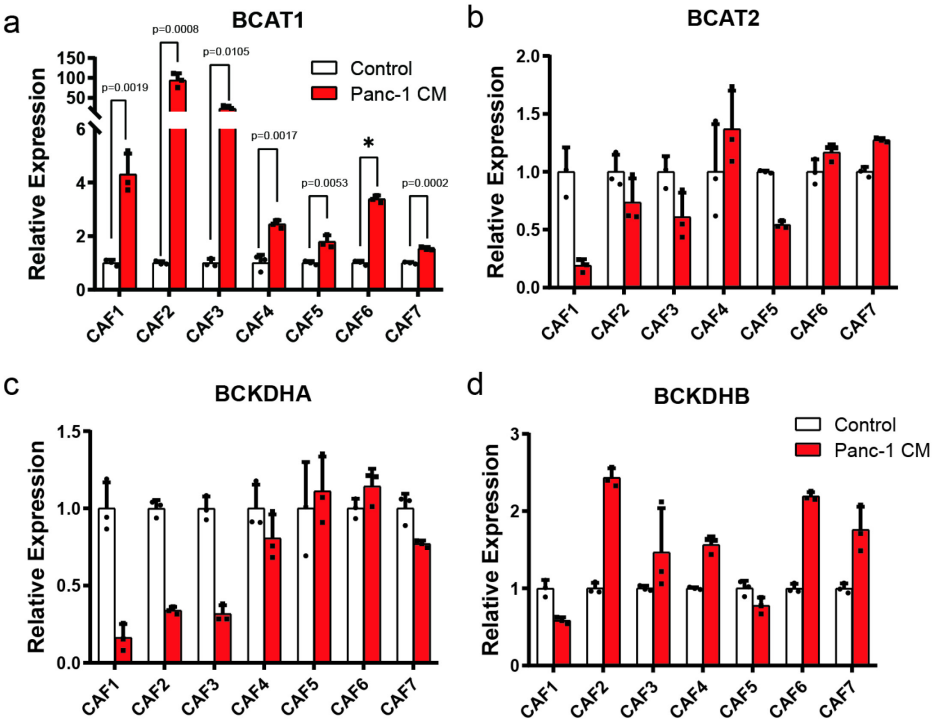

Figure 7.3 Panc-1 CM activates BCAT1 in CAFs. a. Effect of pancreatic cancer cell CM on BCAT1 expression in various CAFs. n = 6 biologically independent samples. **b**. Effect of pancreatic cancer cell CM on BCAT2 expression in various CAFs. n = 6 biologically independent samples. **c**. Effect of pancreatic cancer cell CM on BCKDHA expression in various CAFs. n = 6 biologically independent samples. **d**. Effect of pancreatic cancer cell CM on BCKDHB expression in various CAFs. n = 6 biologically independent samples.

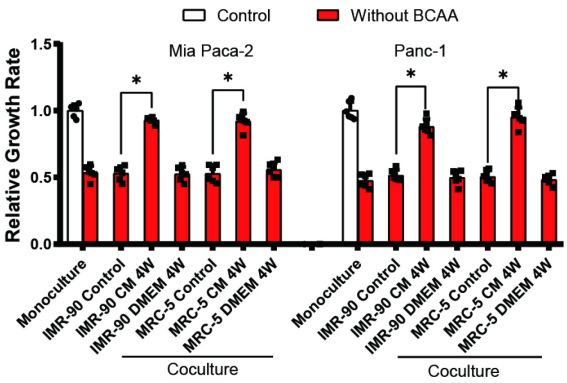

Figure 7.4 Activated CAF rescue cancer cell growth under BCAA deprivation. The growth rate of pancreatic cancer cells cultured with activated NOFs under BCAA deprivation. n = 6 biologically independent samples.

7.3 TGF-β regulated stromal BCAT1

Having established that fibroblast activation specifically upregulates BCAT1 expression in CAFs, we sought to elucidate the congruence between NOF activation pathways and BCAT1 expression. Although the signaling pathways that activate fibroblasts are still being studied, many pathways converge towards TGF-β-based activation [311]. We assessed if TGF-β could regulate BCAT1 expression in CAFs and surprisingly found that induction of BCAT1 expression by TGF-β is pronounced in CAFs (Figure 7.5a). By contrast, TGF-β could neither influence BCAT2 expression in CAFs nor induce changes in BCAT1 expression in PDAC cells (Figure 7.5ab). Importantly, depletion of TGF-β with a neutralizing antibody abrogated upregulation of stromal BCAT1 and αSMA expression mediated by cancer cell-secreted TGF-β. In contrast, there was no change in BCAT2 gene expression (Figure 7.5c-e). These results were further confirmed using immunofluorescence (Figure 7.6a). We also employed a genetic approach using αvβ5-integrin KO CAFs, which becomes activated upon pre-activated (as opposed to immature/latent) TGF-β in a non-cell-autonomous way. The BCAT1 expression of αvβ5-integrin KO CAFs failed to be activated by conditioned media obtained from cancer cells (Figure 7.6b). Additionally, we measured the secretion rate of TGF-β by cancer cells and CAFs (Figure 7.6c). We found that cancer cells secreted TGF-β at several folds higher concentrations compared to CAFs, thereby corroborating our claim that cancer-cell secreted TGF-β regulates BCAT1 expression.

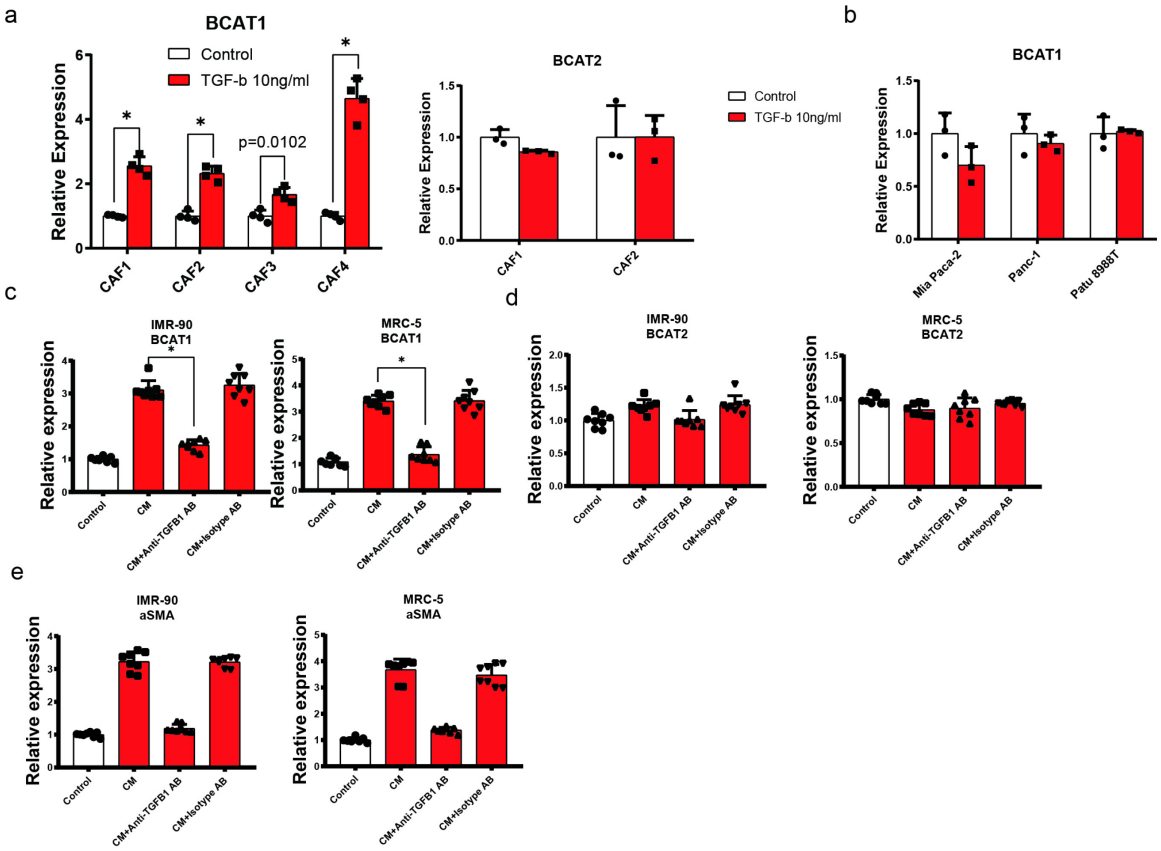

Figure 7.5 TGF-β regulated stromal BCAT1. a. BCAT1 and BCAT2 mRNA expression measured in CAFs after two days of treatment with TGF-β. n = 6 biologically independent samples. **b**. BCAT1 expression in cancer cells treated with TGF-β. n = 8 biologically independent samples. **c**. BCAT1 expression in NOFs cultured with pancreatic cancer cell-CM in the presence of Anti-TGFB1 antibodies or isotype antibodies for three weeks. n = 8 biologically independent samples. **d**. BCAT2 expression in NOFs cultured with pancreatic cancer cell-CM in the presence of Anti-TGFB1 antibodies or isotype antibodies for three weeks. n = 8 biologically independent samples. **e**. αSMA expression in NOFs cultured with pancreatic cancer cell-CM in the presence of Anti-TGFB1 antibodies or isotype antibodies for three weeks. n = 8 biologically independent samples.

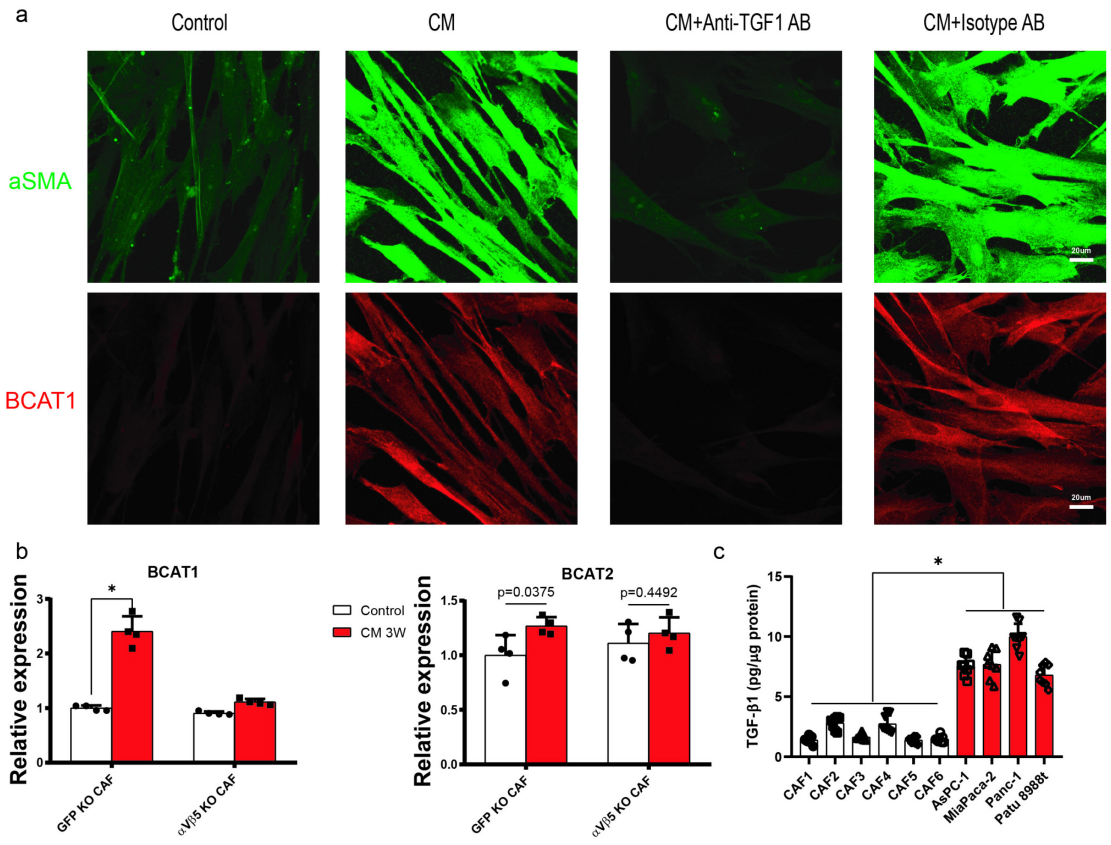

Figure 7.6 Cancer cell-derived TGF-β regulated stromal BCAT1. **a**. Representative images from IF analysis of BCAT1 and αSMA expression in NOFs cultured with pancreatic cancer cell-CM in the presence of Anti-TGFB1 antibodies or isotype antibodies for three weeks. Experiments were repeated independently twice with similar results. **b**. BCAT1 and BCAT2 expression in control and Integrin αvβ5 KO CAFs cultured with pancreatic cancer cell-CM for three weeks. n = 4 biologically independent samples. **c**. ELISA shows TGF-β secretion levels from CAFs and PDAC cell lines. n = 8 biologically independent samples.

7.4 TGF-β regulated stromal BCAT1 through SMAD5

Previous studies have provided evidence that SMAD proteins are the effectors of TGF-β activation, and once activated, they regulate gene expression by translocating to the nucleus. NOF activation significantly upregulated SMAD2, SMAD4 and SMAD5

(Figure 7.7).

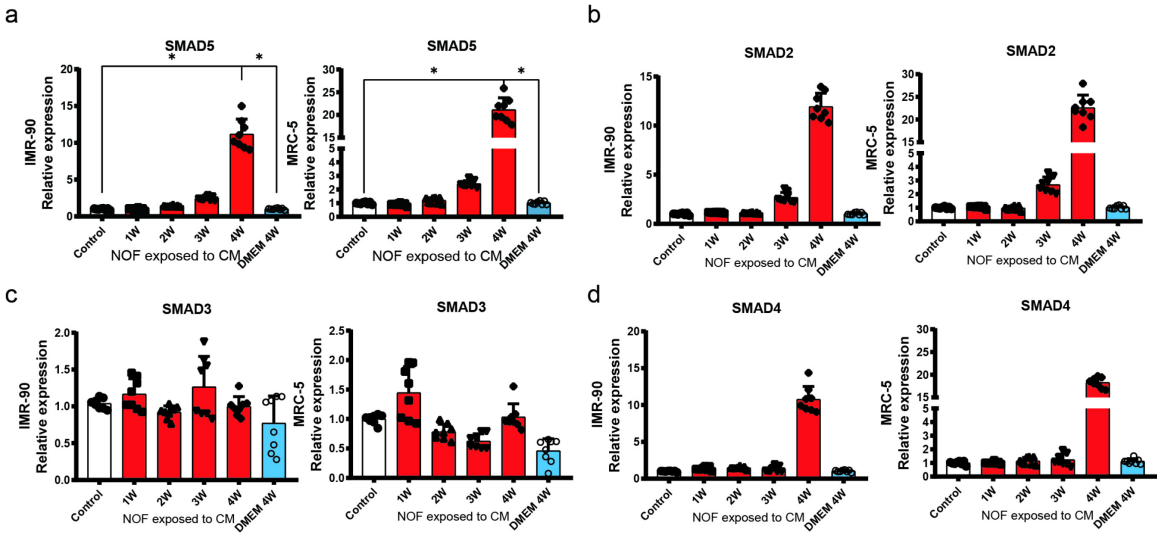

Figure 7.7 Panc-1 CM regulates SMADs in NOFs. **a**. Effect of pancreatic cancer cell CM on SMAD5 expression in NOFs over four weeks. n = 6 biologically independent samples. d. SMAD2 expression in NOFs treated with pancreatic cancer cell-CM. n = 8 biologically independent samples. e. SMAD3 expression in NOFs treated with pancreatic cancer cell-CM. n = 8 biologically independent samples. f. SMAD4 expression in NOFs treated with pancreatic cancer cell-CM. n = 8 biologically independent samples.

To establish which SMAD directly regulated BCAT1 expression, we performed quantitative ChIP-PCR to elucidate the targets for the BCAT1 binding regions. Our analysis revealed the enrichment of SMAD5 for BCAT1 promoter binding regions compared to the control regions (Figure 7.8a). Furthermore, only SMAD5 binding to the BCAT1 promoter regions is increased upon TGF-β activation, while SMAD4 binding was not affected. To further decipher if TGF-β and SMAD5 activation increased the BCAT1 promoter activity, we performed a dual-luciferase reporter assay. We found that incubation with TGF-β strongly increased BCAT1 promoter activity in CAFs (Figure 7.8b). Expectedly, the increase of TGF-β-mediated BCAT1 promoter activity is suppressed on treatments with either TGF-β pathway inhibitor, RepSox or via silencing

of SMAD5 expression (Figure 7.8b). Further, IHC staining confirmed that the stromal component had increased expression of SMAD5 compared to the epithelial compartment (Figure 7.8c). To conclusively elucidate the transcriptional regulation of BCAT1 by SMAD5, we measured mRNA levels of BCAT1 in CAFs when transfected with siRNAs targeting SMAD4 or SMAD5 (Figure 7.8d). SMAD5 inhibition significantly impacted the BCAT1 expression at mRNA and protein levels (Figure 7.8e). In contrast, SMAD4 silencing did not induce any changes in BCAT1 expression. These results provide strong evidence that cancer cell-secreted TGF-β upregulates stromal BCAT1 activity through SMAD5 activation in stromal cells (Figure 7.8f).

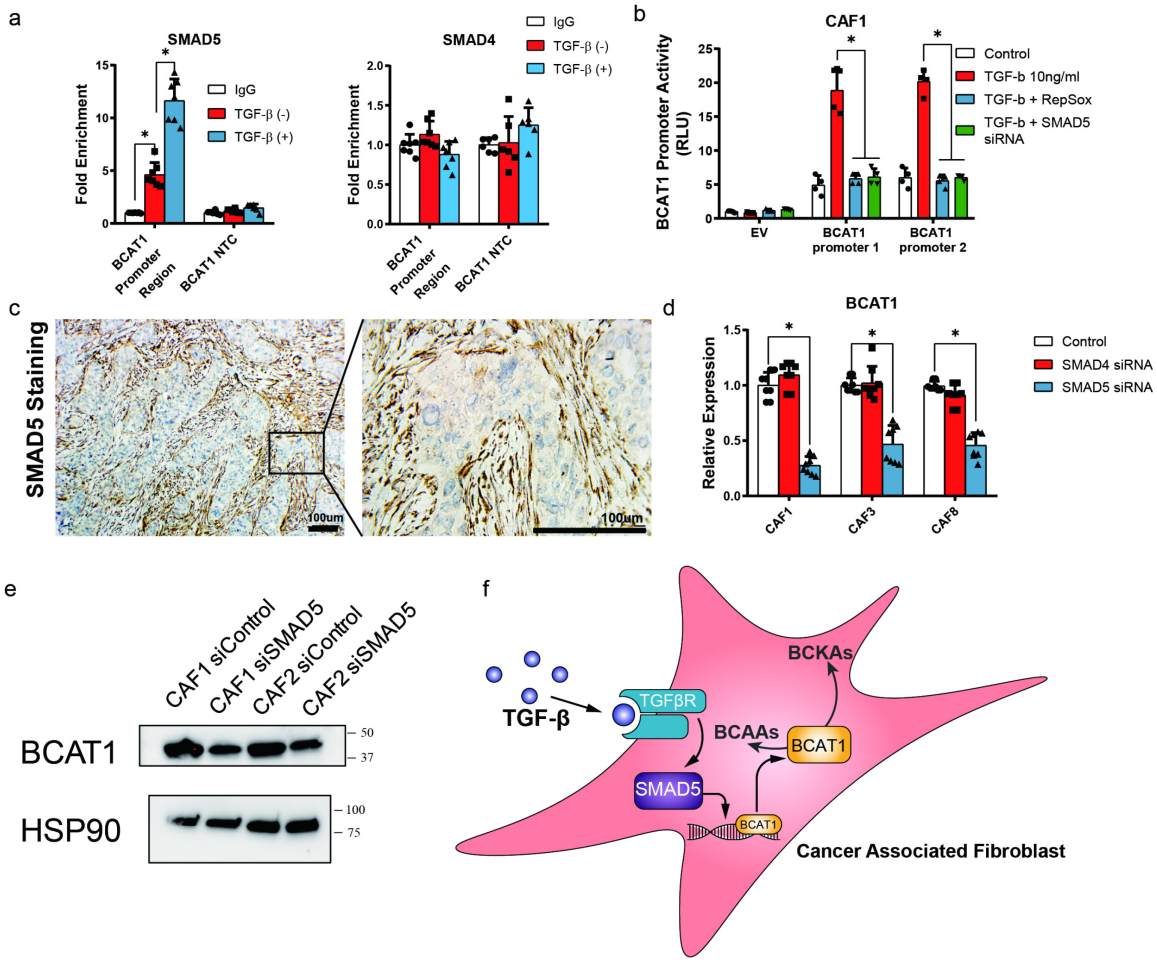

Figure 7.8 TGF-β regulated stromal BCAT1 through SMAD5. **a**. ChIP assays performed with control IgG and anti-SMAD5 or anti-SMAD4 antibodies in CAFs treated with PBS control or TGF-β. n = 4 biologically independent samples. **b**. Transient transfection assays in CAFs with the reporter plasmid containing BCAT1 promoter. n = 8 biologically independent samples. **c**. Representative IHC staining image comparing SMAD5 expression between stromal and tumor compartments. Experiments were repeated independently three times with similar results. **d**. mRNA expression of BCAT1 in CAFs treated with siRNAs targeting SMAD4 or SMAD5. n = 6 biologically independent samples. **e**. Immunoblots showing BCAT1 protein expression in CAFs treated with control siRNA and SMAD5 siRNA. Experiments were repeated independently three times with similar results. **f**. TGF-β secreted by cancer cells regulates BCAT1 expression in CAFs by activating SMAD5, which binds to the BCAT1 promoter.

7.5 Discussion

TGF-β1 in the tumor microenvironment has a significant effect on the antitumor activity of T cells. In the presence of exogenous IL-2 and IL-4, TGF-β1 can regulate the growth of T cells and usually promotes proliferation [312]. TGF-β1 can cause the resident macrophage to become an inhibitor of $CD4^+$ T cell proliferation [313]. TGF-β1 can inhibit the differentiation of cytotoxic T cells and the lysis of cancer cells mediated by cytotoxic T cells. Also, TGF-β1 can block the expression of granzyme A, granzyme B and perforin, while the expression of granzyme B is directly linked to the Smad transcription factor [314]. TGF-β1 also has the function of suppressing the effect of NK cells and neutrophils, which leads to the deterioration of tumors [315]. The enhancement of TGF-β1 and IL-6 levels has the effect of promoting the progress of inflammation and gastric cancer. TGF-β1 also showed suppression of the expression of the cell populations MHC I and MHC II. The decrease of tumor cell MHC I expression will reduce the dissolution effect of tumor cells of NK cells, thereby accelerating the growth and migration of tumors.

In this chapter, we showed that TGF-β could regulate BCAT1 expression in CAFs and induction of BCAT1 expression by TGF-β is pronounced in CAFs. Furthermore, depletion of TGF-β with a neutralizing antibody abrogated upregulation of stromal BCAT1 and αSMA expression mediated by cancer cell-secreted TGF-β. Moreover, we identified SMAD5 as the regulator of BCAT1 through quantitative ChIP-PCR and dual-luciferase reporter assay. In summary, we showed that cancer cell-secreted TGF-β upregulates stromal BCAT1 activity through SMAD5 activation in stromal cells.

Chapter 8 Patient-derived Circulating Tumor Cells Have Upregulated BCKDH Metabolism and Modulate Stromal Cells

8.1 Introduction

The number of CTCs that can be collected in clinical blood samples is very limited, except for cell counting and gene sequencing, it is usually not sufficient for routine drug sensitivity testing or cell phenotype analysis. Therefore, stable culture expansion of CTCs is a downstream function of CTCs. At the same time, in the case of a small number of cells, the lack of paracrine signals between cells will increase the difficulty of cell culture expansion. Yu *et al.* collected CTCs from estrogen receptor-positive breast cancer patients using CTC-ichip, and cultured in RPMI-1640 medium with epidermal growth factor (EGF), basic fibroblast growth factor (bFGF), B27 Supplement, with ultra-low attachment plates and hypoxia (4% O_2) conditions [316]. Then 17.14% (6/35) sample CTCs proliferated successfully with doubling times of 3 days to 3 weeks. At the same time, it was also reported that adhesion would induce CTCs to age. Cayrefourcq *et al.* used the CELLSEARCH system to collect the CTCs suspension culture of patients with metastatic colorectal malignant adenocarcinoma, and the culture was first placed in DMEM/F12 medium with FBS, insulin, L-glutamine, EGF, FGF-2, N2 Supplement, and cultured under hypoxic (2% O_2) condition [317]. After a few weeks, the cultures then transferred to RPMI-1640 medium with EGF, FGF-2, Insulin-Transferrin-Selenium (ITS) under normal oxygen conditions to obtain a cell line capable of long-term survival [317].

Gao *et al.* centrifuged the CTCs from patients with metastatic prostate cancer using the Ficoll Paque system, dispersed in Matrigel as organoids, and soaked in DMEM/F12 medium with A83-01, B27 Supplement, Dihydrotestosterone (DHT), EGF, FGF2, FGF10, Glutamax Supplement, HEPES, N-Acetyl-L-cysteine (NAC), Nicotinamide, Noggin, R-spondin 1, SB202190 and Y-27632. Then, 5.88% (1/17) of the samples were successfully amplified with a doubling time of 1 week [318]. The mutation and pathology were similar to those of tumor cells and tissues in situ. Zhang *et al.* used CTC-chip to collect CTCs in the peripheral blood from patients with early-stage lung cancer [319]. First, fibroblasts, collagen and Matrigel were added to the chip, soaked in RPMI-1640 medium supplemented with FBS. After 3D co-culture for one week, the number of tumor cells increased to an average of 8 times; after the cells were released from the chip and transferred to a multi-well plate for one week, the number of tumor cells increased to an average of 54 times, with a total culture success rate of 73.68% (14/19) [319]. In a recent study, Rivera-Báez *et al.* used high-throughput, label-free Labyrinth isolated CTCs based on cell sizes, CTCs were isolated from 10 locally advanced, then cultured in a simple, 2D monoculture approach with RPMI1640, CTCs from 3 individual patients successfully grew into cell lines [320]. The generally low success rate of CTCs cultivation is the academic problem facing us. At present, there is no "gold standard" applicable to the cultivation of tumor cells from all different sources, but the successful cultivation of CTCs for each type of tumor will greatly advance the research and clinical treatment of tumor metastasis.

8.2 BCAA related enzymes expression in CTCs

To replicate tumor-stroma interactions in humans in the context of PDAC cell BCAA metabolism, and overcome inconsistencies observed in animal models, we have relied on human CTCs derived models. CTCs shed by the primary tumor are the seeds of metastasis[321] and established as a potential biomarker of disease progression[322]. CTCs mediate metastasis of many solid tumors, including PDACs, even after the resection of the primary tumor[323]. These cells can extravasate from the primary tumor site into the bloodstream and invade distant sites, resulting in the formation of metastases. CTCs freshly obtained from PDAC patient blood using the Labyrinth, a label-free size based inertial microfluidic CTC isolation device [324], allowed us to compare their transcriptional profile with the cells obtained from a healthy subject and CAF cell lines (Figure 8.1ab). Healthy control samples are the PBMCs that were not depleted during our Labyrinth processing. Therefore, the data represents the background signal for gene expression in PBMCs and deviations from that are due to the presence of the CTCs in the patient samples. It showed that the gene expression of BCKDHA and DBT are higher in Day 0 CTCs compared to healthy controls and CAFs (Figure 8.1c). In contrast, BCAT1 expression is much higher in CAFs compared to CTCs (Figure 8.1c). These data indicate the clinical relevance and corroborative evidence of our observations in the *in vitro* model. We then used patient-derived expanded CTC lines for downstream experiments [320]. Similar to PDAC cell lines, CTC lines showed lower expression of BCAT1 compared to CAFs, and higher expression of DBT compared to CAFs at the mRNA level (Figure 8.1d). Consistent with our findings in PDAC cell lines, CTC lines also had higher expression of BCAT2 and lowered BCAT1 at the protein level (Figure 8.1e).

Further, BCKAs could rescue the impeded proliferation of CTC lines under BCAA deprivation, thereby demonstrating that similar to their cancer cell line counterparts, CTC lines are also BCKA-dependent in stromal rich conditions (Figure 8.1f).

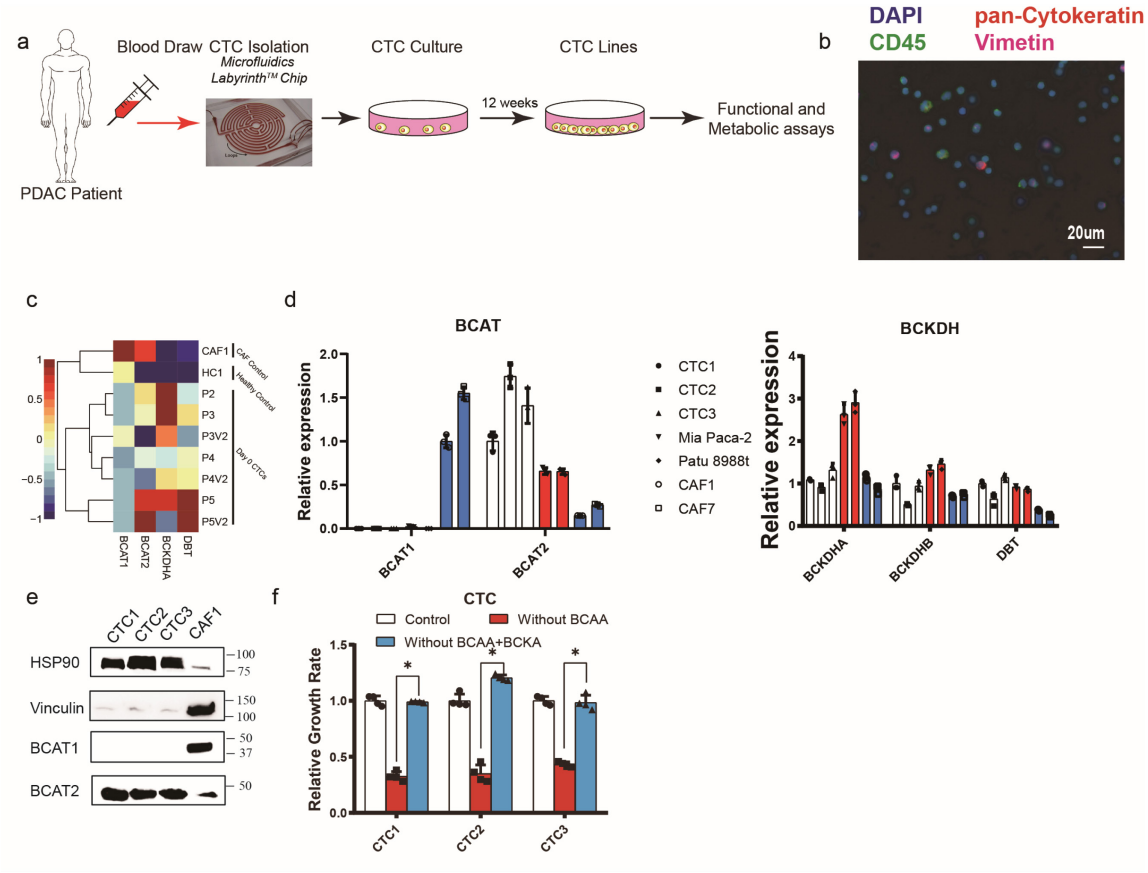

Figure 8.1 BCAA related enzyme expression in CTCs. **a**. CTCs are isolated from the blood of PDAC patients using the microfluidics-based Labyrinth^{TM} Chip. Isolated CTCs are purified to generate CTC cell-lines used for downstream analyses. **b**. Representative images of CTCs separated by Labyrinth. Cells are stained with DAPI (blue), cytokeratin (red), CD45 (green) and Vimentin (pink). Experiments were repeated independently three times with similar results. **c**. Heatmap of gene expression of BCAT1, BCAT2, BCKDHA and DBT measured by qRT-PCR from Day 0 CTCs isolated from PDAC patients, CAF1 cells, and cells isolated from a healthy subject. n = 7 biologically independent samples. **d**. Relative BCAT1, BCAT2, BCKDHA, BCKDHB and DBT mRNA expression determined by qRT–PCR in CAFs and Patient-derived CTCs. n = 4 biologically independent samples. **e**. Immunoblots of BCAT1 and BCAT2 expression in CAFs and Patient-derived CTCs. HSP90 is used as loading control. Experiments were repeated independently three times with similar results. **f**. The influence of BCAAs and BCKAs on the growth of CTCs. n = 8 biologically independent samples.

8.3 BCAA metabolism in CTCs

Most interestingly, there is a marked increase in the secretion of BCKAs by CAFs when they are cocultured with CTC lines as measured from the extracellular BCKA concentrations after 6, 12, 24, 36 and 48 hours of coculture (Figure 8.2ab). We did not find any secretion of ketoacids from cancer cells alone (Figure 8.2c). We next assessed if TCA cycle substrates other than BCKA could also rescue the loss of growth rate of PDAC cells- and CTC lines under BCAA deprivation. This could also reveal the role of BCKAs as opposed to other TCA cycle substrates in the oxidative TCA cycle. Anaplerotic TCA substrates only partially rescued the reduction in growth rate; however, BCKAs could completely rescue the growth of PDAC cells and CTC lines under BCAA deprivation (Figure 8.2d).

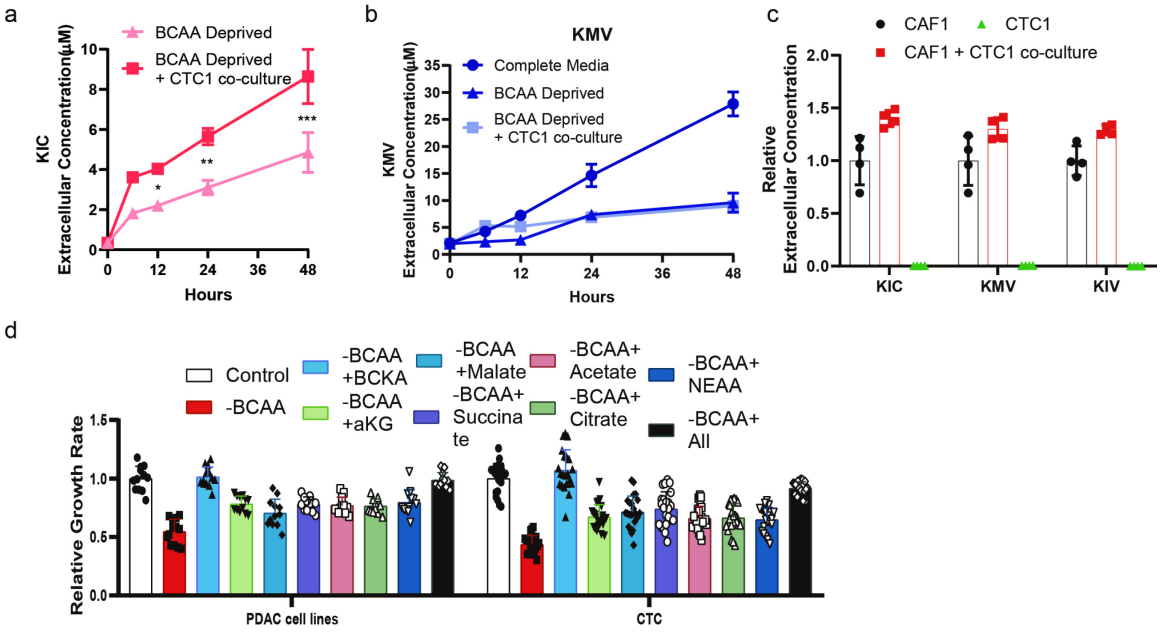

Figure 8.2 BCAA metabolism in CTCs. **a**. KIC concentration in spent media from CAFs in monoculture or cocultured with CTC line. n = 3 biologically independent samples. *,p=0.0001,**,p=0.0008,***,p=0.0093. **b**. Extracellular concentration of BCKAs secreted by CAFs in monoculture and cocultured with CTCs over 6,12, 24 and

48 hours. n = 3 biologically independent samples. **c**. Extracellular concentration of BCKAs secreted by CAFs in monoculture or cocultured with CTCs, and CTCs in monoculture for 48 hours. n = 4 biologically independent samples. **d**. The relative growth rate of PDAC cell lines and CTC lines under BCAA deprivation but supplemented with α-KG, malate, succinate, acetate, citrate, NEAA mixture or the combination in the BCAA-deprived media. n = 8 biologically independent samples.

8.4 BCAA metabolism in CTC organoid model

We further corroborated our main hypothesis that stromal BCAT1 maintains the BCAA metabolism in a CTC-organoid model (Figure 8.3a-c). To generate the CTC derived organoid, CAF was first seeded on CAF-derived 3D ECMs one day before. Then the fresh isolated CTC was seeded on the cultures. CTC derived Organoid was cultured as previously described without TGF-β modulators (360). Importantly, the targeting of stromal BCAT1 reduced proliferation and *de novo* protein synthesis in cytokeratin+ cancer cells of CTC-organoids (Figure 8.3d). Our results substantiate that CAFs maintain their ability to fuel high BCKA demand observed in CTCs, a system that can capture the tumor heterogeneity more closely.

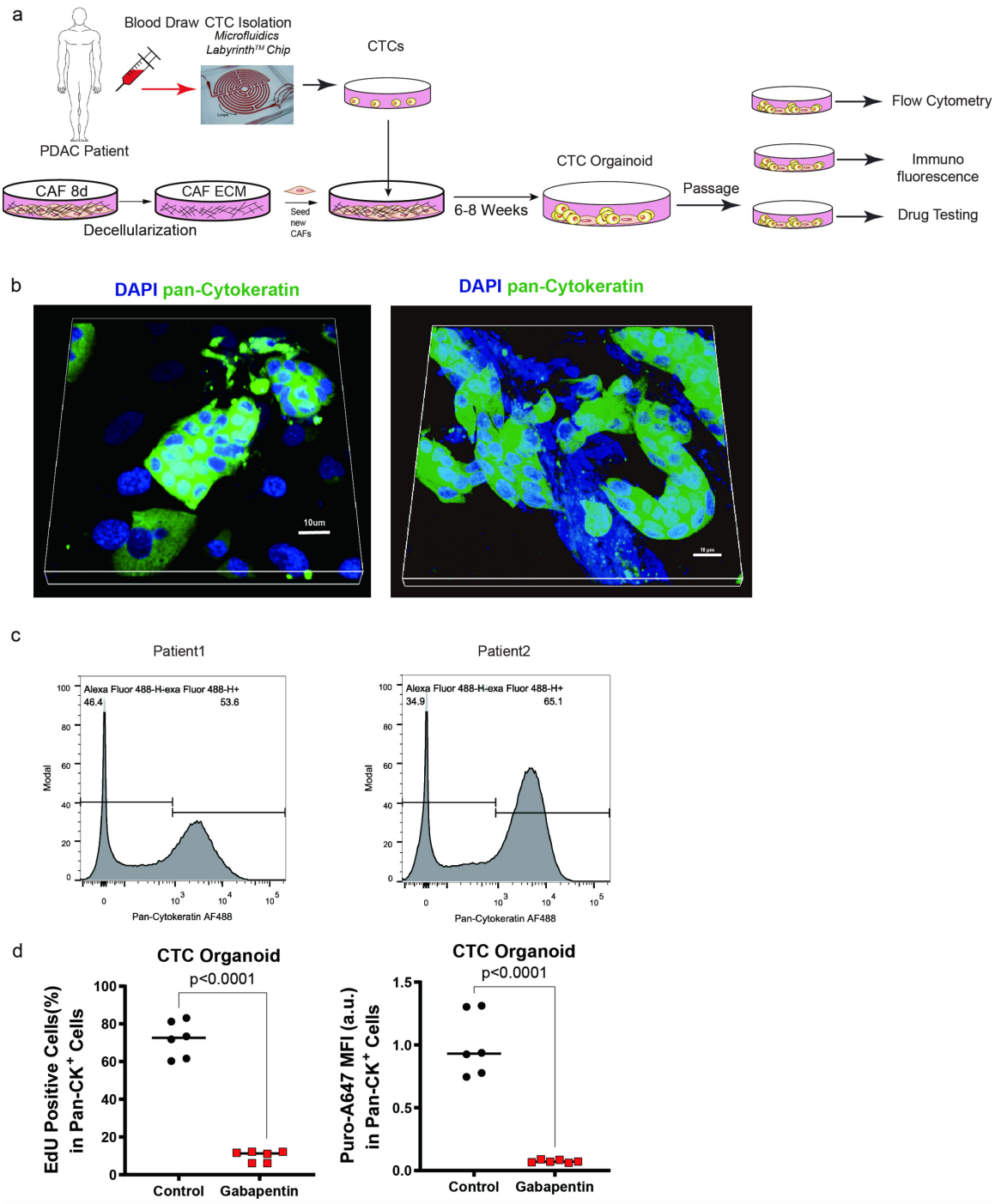

Figure 8.3 BCAA metabolism in the CTC organoid model. **a**. Schematic of the protocol used to generate CTC derived organoid with CAF secreted ECM. **b**. Representative images from CTC derived organoids. Cytokeratin is shown in green, and the nuclei stained with DAPI are shown in blue. Experiments were repeated independently three times with similar results. **c**. Representative FACS data of Pan-Cytokeratin positive tumor cells in CTC derived organoid. Experiments were repeated independently three times with similar results. **d**. EdU staining and SUnSET assay on Pan

Cytokeratin+ tumor cells in the CTC derived organoid cultured with Cancer associated fibroblasts treated with vehicle or 10mM Gabapentin. n = 6 biologically independent samples.

8.5 Discussion

To replicate tumor-stroma interactions in humans PDAC, we used human CTCs derived models to confirm the BCAA metabolism. We isolated CTCs freshly obtained from PDAC patient blood using the Labyrinth. We found that the expression of BCKDHA and DBT is higher in Day 0 CTCs compared to healthy controls and CAFs. In contrast, BCAT1 expression is much higher in CAFs compared to CTCs. We then used patient-derived expanded CTC lines for downstream experiments. Similar to PDAC cell lines, CTC lines showed lower expression of BCAT1 compared to CAFs, and higher expression of DBT compared to CAFs. Moreover, the same with our findings in PDAC cell lines, CTC lines also had higher expression of BCAT2 and lowered BCAT1 at the protein level.

Organoids are miniature models of tissues grown in a 3D semi-solid extracellular matrix supplemented with specific growth factors. A single epithelial cell can form organoids within 7-10 days. These can dissociate into individual cells to restart organoid formation. In 2015, it was first reported the utility of organoid models to better understand the development of pancreatic ductal adenocarcinoma [325]. After transplantation, organoids derived from murine and human PDAC produced lesions reminiscent of pancreatic intraepithelial neoplasia and then developed into invasive PDAC [325]. Organoids derived from CTC may be very useful for simulating metastatic processes and drug-induced screening [326].

We further corroborated our main hypothesis that stromal BCAT1 maintains the BCAA metabolism in a CTC-organoid model. To generate the CTC derived organoid, CAF was first seeded on CAF-derived 3D ECMs one day before. Then the fresh isolated CTC was seeded on the cultures. CTC derived Organoid was cultured as previously described without TGF-β modulators. Importantly, the targeting of stromal BCAT1 reduced proliferation and de novo protein synthesis in cytokeratin+ cancer cells of CTC-organoids.

Chapter 9 Validation of Stromal BCAT1 and PDAC DBT in Tissue Slices

9.1 Introduction

Ex vivo cultures of tumor tissue slices derived from different organs have been previously established [327]. Tissue slice culture has recently been shown to resemble the architecture of the original organ or tumor closely. It has been used in drug toxicity studies, drug testing mechanisms of resistance and gene therapy assays in pancreatic cancer [328, 329]. Because tissue slices in *ex vivo* culture retain most components of the tumor microenvironment, they are believed to more likely mirror *in vivo* tumor models then monoculture [327]. Cultured slices maintain their baseline morphology, surface area, and microenvironment for at least six days in culture, which provides enough time to test drugs or perform gene therapy assays. The tissue slices can also be tested using stable isotope tracer methods, which allows for metabolic analysis [330]. By using the tumor and the tissue surrounding the tumor, you more accurately model the effect of cancer treatments by avoiding genetic, physiologic and environmental complications that could be produced in a monoculture. Also, the tissue slice culture provides the ability to determine treatment effects on tumor and surrounding tumor tissue from an individual patient.

Studies have demonstrated that tissue slice culture resembles the architecture of the original organ or tumor and can be utilized to study better drug toxicity, resistance mechanisms and gene therapy testing in pancreatic cancer [328, 329]. Since tissue slices in *ex vivo* culture retain most components of the tumor microenvironment, they are believed to recapitulate *in vivo* tumor models [327]. To test our hypothesis, we will address the contribution of BCAA catabolism from the tumor microenvironment using tissue slice cultures.

9.2 PDAC Tissue slice model

We then illustrated that CAF-derived BCKAs support BCKA-dependence in CTC cell lines we wanted to validate these findings in a setting that mimics the *in vivo* TME. Previous studies have demonstrated that tissue slice culture resembles the architecture of the original organ or tumor and can be utilized to study better drug toxicity, resistance mechanisms, and gene therapy in pancreatic cancer [329]. Since tissue slices in *ex vivo* culture retain most of the components of the TME, they are believed to recapitulate better stromal-rich tumors than other *in vivo* tumor models [327]. We obtained fresh PDAC patient tissue slices, as shown here and validated their viability for fourteen days in culture (Figure 9.1).

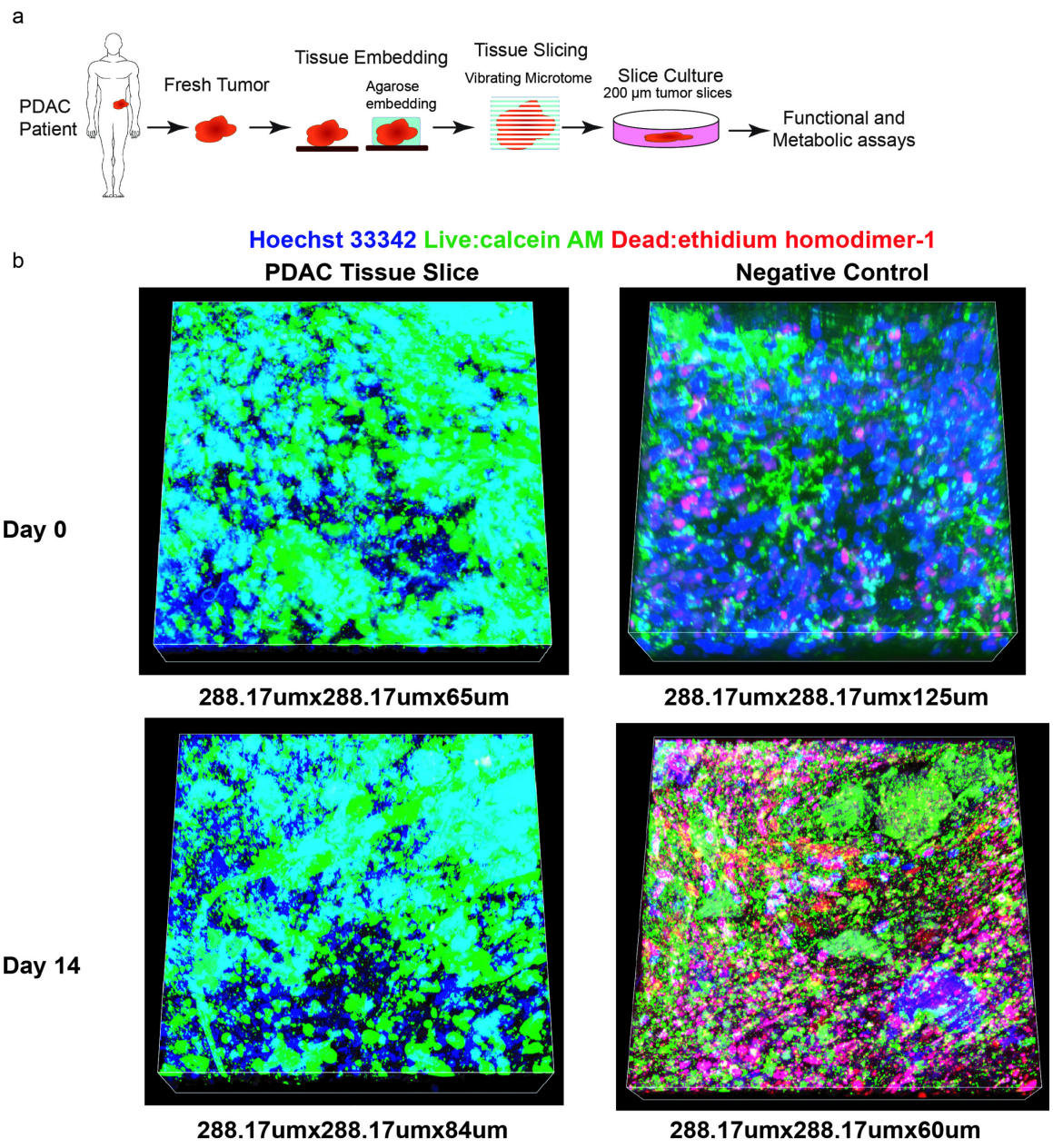

Figure 9.1 PDAC Tissue slice model. **a**. Schematic of human PDAC tissue slice culture. The freshly biopsied tumor is embedded in agarose and sliced into 200 µm thick slices using a vibrating microtome. Slices are cultured for downstream metabolic and functional analyses. **b**. Representative Live Dead assay of tissue slice at Day 0 and Day 14. Live cells fluoresce bright green, whereas dead cells fluoresce red. Positive controls were fixed by methanol. Experiments were repeated independently three times with similar results.

9.3 Targeting BCAA metabolism in tissue slice by siRNAs

Based on our extensively developed mechanistic crosstalk, we examined whether simultaneously targeting the stromal-BCAT1 and cancer cell-DBT could result in an enhanced therapeutic effect. We used BCAT1 and DBT siRNAs to inhibit BCAA metabolism. Remarkably, knocking down either BCAT1 or DBT significantly reduced PDAC cell viability (Figure 9.2). Both PCNA and Ki67 positive cell populations significantly reduced in cytokeratin positive cells when either knocking down DBT or BCAT1 alone or combinations. Further, a reduction in expression of both DBT and BCAT1 validated our siRNA-DBT and siRNA-BCAT1 silencing (Figure 9.3a).

Moreover, there were no changes in other BCAA-related genes. Next, we asked if BCKAs were indeed consumed by PDAC cells in our tissue slice model. Tissue slices were cultured in media containing ^{13}C labeled BCKAs, and after 48 hours, the slices were homogenized in a cryo-cooled homogenizer to extract intracellular metabolites as well as intercellular protein. Intracellular BCKAs were found to be enriched between 10% and 40%. Subsequently, ^{13}C-BCKA-derived BCAAs were utilized for *de novo* protein synthesis. This is corroborated by the BCAAs obtained by hydrolyzing the intercellular tumor-slice protein, which was enriched by 2-15% (Figure 9.3b).

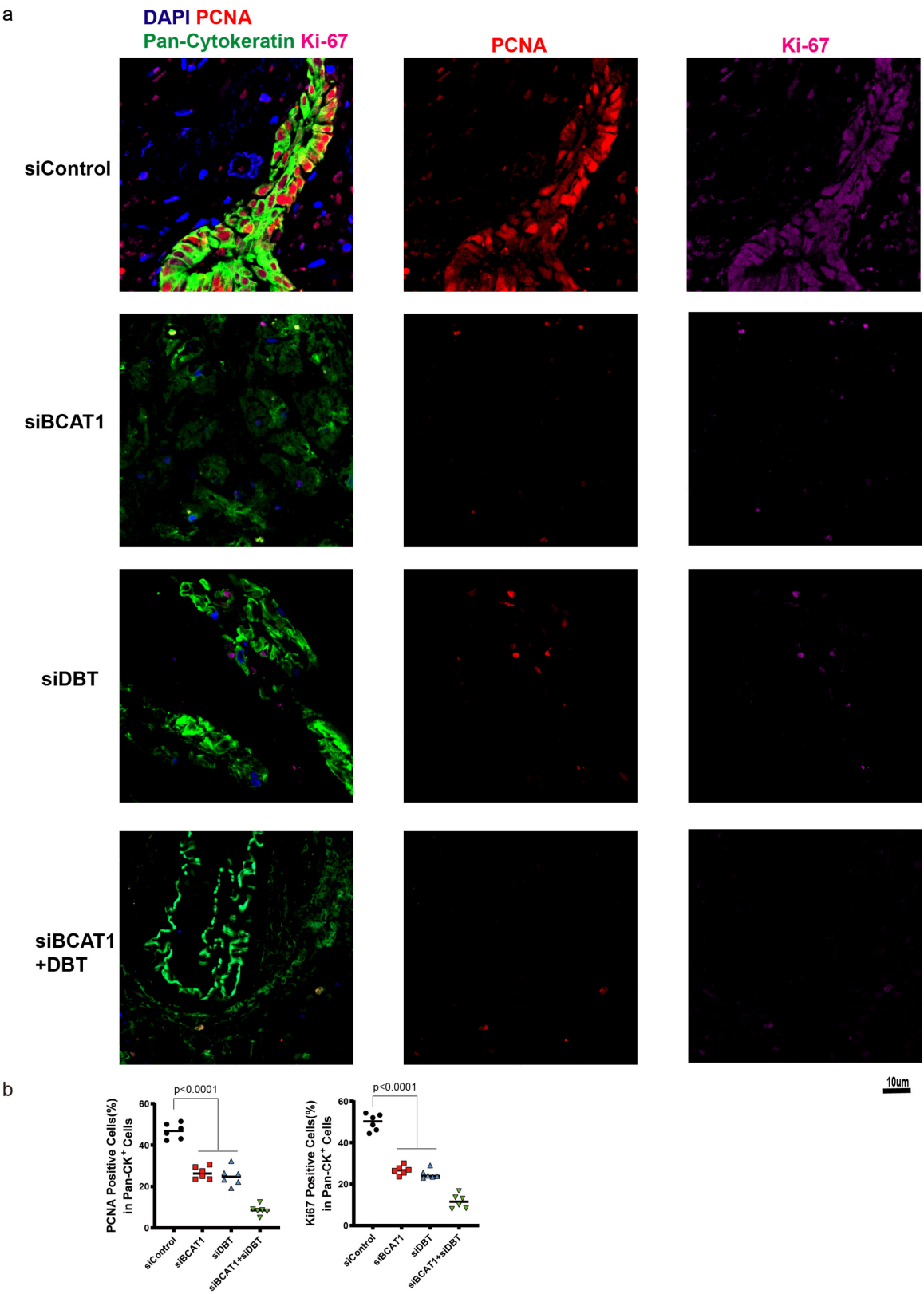
a
DAPI PCNA
Pan-Cytokeratin Ki-67
PCNA
Ki-67
siControl
siBCAT1
siDBT
siBCAT1
+DBT
10um
b
p<0.0001
PCNA Positive Cells(%)
in Pan-CK+ Cells
60
40
20
0
siControl
siBCAT1
siDBT
siBCAT1+siDBT
p<0.0001
Ki67 Positive Cells(%)
in Pan-CK+ Cells
60
40
20
0
siControl
siBCAT1
siDBT
siBCAT1+siDBT

Figure 9.2 Targeting BCAA metabolism in tissue slice by siRNAs. **a**. Representative images from IF analysis of PDAC tissue treated with BCAT1 and DBT siRNAs. Cytokeratin is shown in green, PCNA staining is shown in red, Ki-67 staining in pink, and the nuclei stained with DAPI are shown in blue. Experiments were repeated independently twice with similar results. **b**. Percentage of PCNA-positive and Ki67-positive in Pan Cytokeratin+ tumor cells identified using IF. n = 6 biologically independent samples.

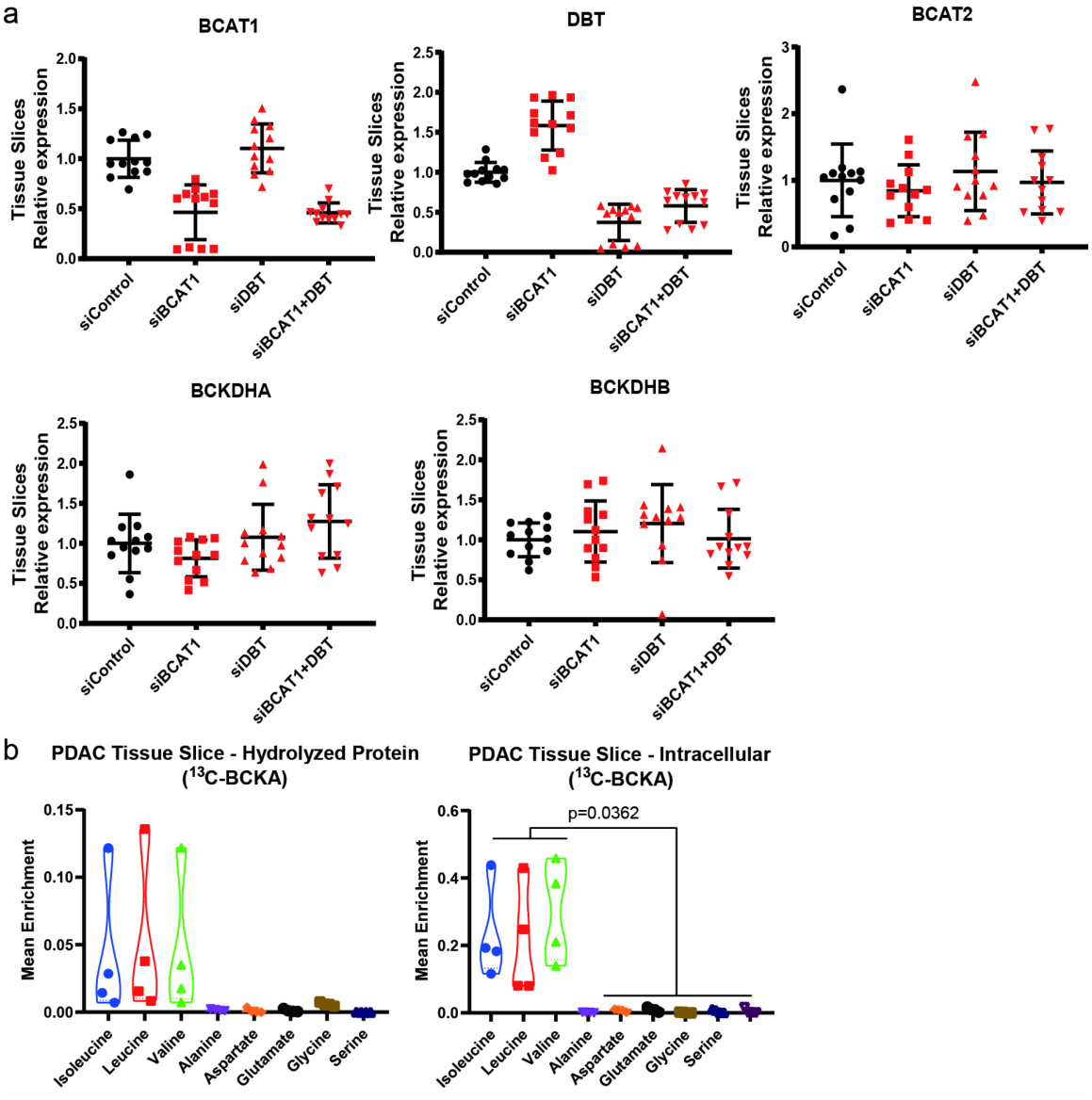

Figure 9.3 Validation of BCAA metabolism in tissue slice. **a**. The efficiency of BCAT1 and DBT siRNAs in the human PDAC tissue slices. Expression of BCAT1, BCAT2, DBT, BCKDHA and BCKDHB in the human PDAC tissue slices treated with BCAT1 and DBT siRNAs. n = 6 biologically independent samples. **b**. Fractional

enrichment of BCAAs of human PDAC tissue slices cultured with 13C-BCKAs. n = 5 individual tissue samples from distinct patients. Violin plot represents the entire range of values, lines at the median, 10-90 percentiles.

9.4 Gabapentin inhibits protein synthesis in the tissue slice

We next tested if suppressing stromal BCAT1 could reduce BCKA-mediated *de novo* protein synthesis in cancer cells inside tissue slices using SUnSET IF. To specifically analyze cancer cells, we used areas of colocalization of puromycin with cytokeratin, a cancer cell-specific marker. Notably, cancer cell-specific *de novo* protein synthesis was pronouncedly reduced in slices cultured with Gabapentin (Figure 9.4). Overall, our results highlight that stromal-BCAT1 not only supports PDAC cell BCKA demand but also exposes the synthetic lethal vulnerabilities in stromal-rich PDAC by co-targeting stromal BCAT1 and the cancer BCKDH complex (specifically DBT) as a clinically relevant therapy.

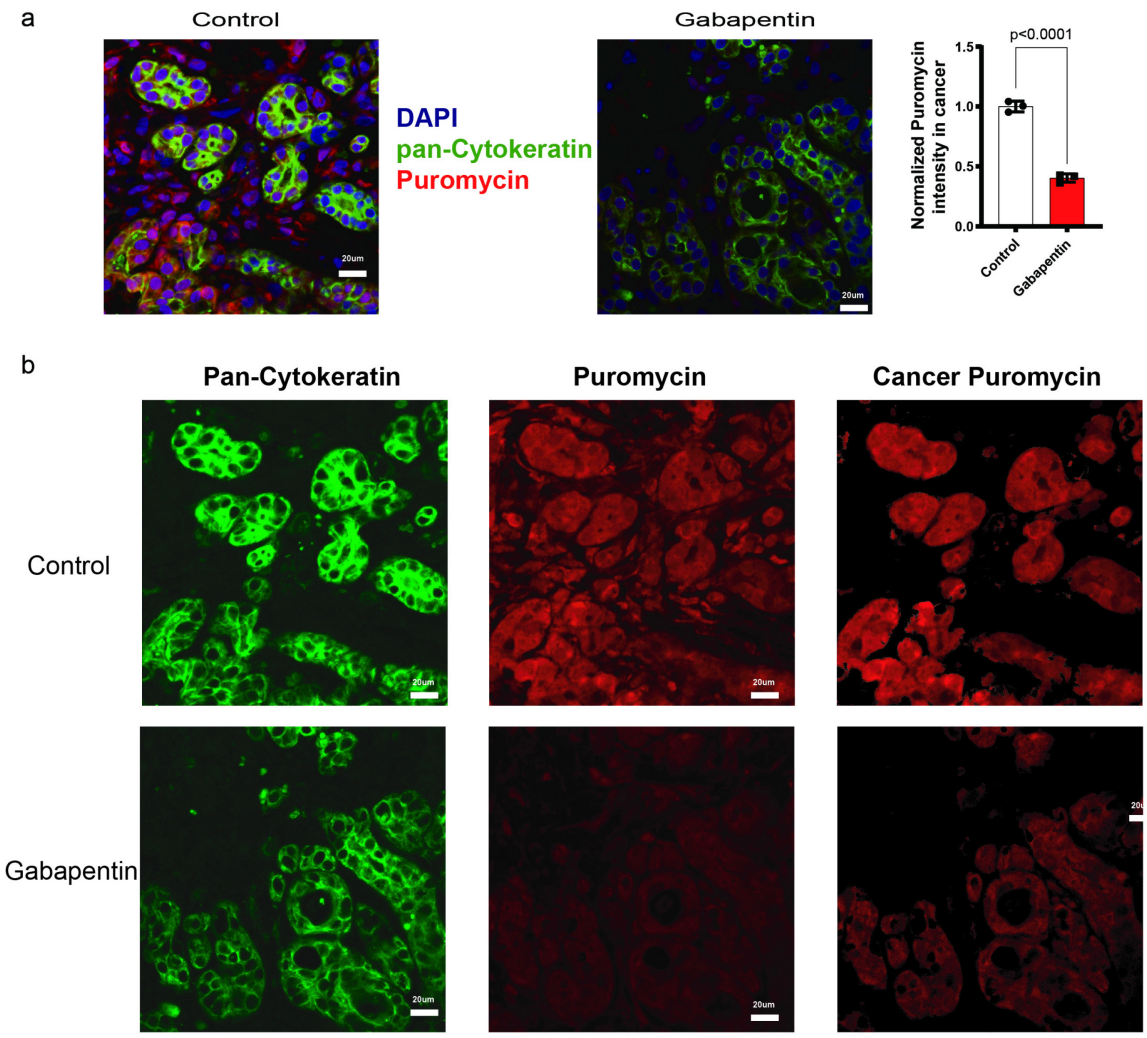

Figure 9.4 Gabapentin inhibits protein synthesis in tissue slice. **a**. Representative images from SUnSET IF analysis of PDAC tissue treated with vehicle or 10mM Gabapentin. n = 3 biologically independent samples. **b**. Representative images from SUnSET IF analysis of PDAC tissue treated with vehicle or 10mM Gabapentin. Cytokeratin is shown in green, and Puromycin staining is shown in red. Experiments were repeated independently three times with similar results.

9.5 Discussion

In the development of effective targeting therapy for pancreatic cancer, it is essential to have a powerful platform to accurately and reproducibly study the interaction of CAFs with PDAC cells in the tumor microenvironment. In this chapter, we have shown that the tissue slice culture of fresh human PDAC can survive for at least two weeks. There is much evidence to support our view that slice culture can accurately short-term model the tumor microenvironment. The literature is scarce, but it is growing recently, describing the precise section culture of different normal and tumor tissues. In this chapter, we using PDAC tissue slices to study tumor microenvironment metabolism demonstrated for the first time, and we also studied cancer cells and CAFs crosstalk in tissue slice. In order to further enhance our ability to understand the interactions between cells in tissue slices, we used multiple fluorescent antibodies to stain cancer cells and CAFs in tissue slices.

In this chapter, we inhibited BCAA metabolism using BCAT1 and DBT siRNAs. Remarkably, knocking down either BCAT1 or DBT significantly reduced PDAC cell viability. Next, we checked BCKAs consumption in the tissue slice model. Intracellular BCKAs were found to be enriched between 10% and 40%, and 13C-BCKA-derived BCAAs were utilized for de novo protein synthesis, which was enriched by 2-15%. Furthermore, inhibiting stromal BCAT1 could reduce BCKA-mediated de novo protein synthesis in cancer cells inside tissue slices using SUnSET IF.

Since the main goal of our work is to develop biopsy culture as a platform for evaluating the effects of immunotherapy, with particular emphasis on the development of

personalized cancer care, we have developed a technology to inspect biopsy culture directly. Using fluorescent-conjugated antibodies to stain viable sections of cancer cells allows us to obtain three-dimensional images through confocal microscopes. We hope to study further the endogenous 3D or subcellular interactions of cancer cells and CAFs in patient samples.

Chapter 10 Conclusions and Future Directions

10.1 Summary of research

Several recent reports conclude that the stromal cells'-secretory pathways play a major role in mitigating avid nutrient deficiency and increasing prototypic pro-survival pathways in PDAC cells. Pancreatic CAFs have been shown to secrete alanine and lysophosphatidylcholines, supporting the metabolic needs of PDAC cells in the nutrient-deprived tumor milieu [242, 331]. Like macrophages, CAFs also secrete pyrimidines that induce gemcitabine resistance [332, 333]. Furthermore, while our study was in progress, it was recently shown that BCAAs contribute around 20% of the carbon in the TCA cycle of the pancreas [334]. However, the stromal role in PDAC BCAA metabolism, if any, is still unclear.

In contrast to the current studies in BCAA metabolism, we investigated how stromal CAFs regulate BCAA metabolism in PDAC cells and whether there exists a mutualistic relationship *vis a vis* BCAA metabolism between CAFs and PDAC cells. We found an increase of BCAA catabolic fluxes and the associated BCAA catabolic enzyme, BCAT1, gene and protein expression in stromal CAFs compared to PDAC cells. Conversely, the BCAA oxidative enzyme complex, BCKDH, along with mitochondrially expressed BCAT2, was increased in cancer cells. We found that BCKAs play a significant role in maintaining metabolic activity in the nutrient-starved pancreatic

milieu. Unconventionally, BCKAs was used as a substrate for *de novo* synthesis of BCAAs by the reversible action of BCAT2, and these newly synthesized BCAAs maintained *de novo* protein synthesis in cancer cells in BCAA deprived conditions. Our results provide strong evidence for dependency on the BCKDH complex and suggest its synergistic involvement with BCAT2 in regulating BCAA metabolism in PDAC cells. To our knowledge, this is the first report that uncovers heavy reliance on BCKAs in stromal-rich tumors and reveals DBT as a vulnerable target to exploit this dependency. Recent studies investigated BCAT2's role in PDAC development and found BCAT2 is elevated in both mouse and human PDAC models [235, 247], which was responsible for enhancing BCAA uptake to sustain BCAA catabolism, mitochondrial respiration, and fatty-acid biosynthesis [247]. Our work develops a systematic understanding of BCAA metabolism in the PDAC tumor microenvironment, especially in the context of the pancreatic cancer-cell centric observations of previous studies.

In contrast, we found that BCAT2 regulates BCKA-mediated *de novo* protein synthesis in PDAC cells and elucidate the central role of the BCKDH complex in regulating PDAC bioenergetics. On the other hand, DBT knockdown, which reduces BCKDH complex levels, is detrimental to both BCAA-driven and BCKA-driven knockdown. Together, this shows that BCKA-driven oxidation is only dependent on BCKDH expression and not on BCAT2 expression. Our results are also in line with Neinast et al. [334], where they show that BCKDK inhibitors do not affect BCKDH-mediated oxidation in the pancreas, alluding to a high basal BCKDH activity in the pancreas. Several CAF subpopulations have been identified recently, which may explain the heterogeneity or plasticity seen in CAFs.

Further, the effect of varying concentrations of the BCAT1 inhibitor, Gabapentin on LAT transporters, is poorly studied in CAFs and must be assessed in future studies. Within the scope of this study, we have worked extensively to develop clinically relevant human PDAC-derived *ex vivo* models to corroborate and highlight the impact of the metabolic crosstalk discovered *in vitro*. Due to the dynamic interplay of metabolism in distinct compartments of the tumor, this study was focused on *in vitro* and clinical *ex vivo* studies, where these metabolic mechanisms can be observed, characterized and quantified readily. Unfortunately, validating these observations in popular *in vivo* models such as KPC and KP mouse models becomes extremely challenging. One major divergence of mouse models from human PDAC tumors is the limitation of studying the interaction between human PDAC cancer cells with mouse CAFs. The second major challenge is the technological limitations of assessing compartmentalized metabolism in vivo. In the future, improvement in mass spectrometry imaging and increasing sensitivity of chromatography-coupled MS will allow spatial resolution of not only static metabolite abundances but also the flux of metabolites across cell-types and tissue compartments.

We discovered that ECM proteins could be a source of amino acids for BCKA synthesis in CAFS under certain nutrient-starved conditions. Interestingly, TGF-β upregulated ECM-protein internalization and BCAT1 expression in CAFs are essential for BCKA synthesis in CAFs. Recently, PDAC cells were shown to use ECM proteins for maintaining amino acid levels [335]. However, our findings that CAFs uptake ECM under nutrient limiting conditions are in congruence with previous studies underscoring that ECM uptake through the uPARAP receptor is upregulated in fibroblasts [336]. Before our results, CAFs were shown to secrete ECM and induce a fibrotic environment

in tumors. By contrast, our results stress that this process is reversed under nutrient-deprived conditions.

Moreover, we showed that internalized ECM is degraded through proteasomal proteolysis, specifically through the chymotrypsin-like proteasome activity. Using decellularized ^{13}C-BCAA-labeled ECM proteins, we observed that BCKAs secreted by CAFs were enriched with ^{13}C derived from the proteolyzed ECM, thereby confirming that ECM in the pancreatic milieu could serve as a source for CAF-secreted BCKAs under nutrient-stressed conditions. We reveal a mechanistic basis behind TGF-β mediated BCAT1 regulation in CAFs, showing that the TGF-β/SMAD5 axis directly targets BCAT1 in CAFs. Thus, cancer-secreted TGF-β regulates the internalization of ECM from the TME to supply amino acid precursors for BCKA secretion by CAFs. Our *in vitro* findings were further corroborated in two different patient-derived models: CTCs and PDAC tumor slices. These lines of evidence expand our findings to systems that recapitulate tumor heterogeneity and mimic the *in vivo* cancer microenvironment. Our results indicate that BCAT1 in CAFs supports the high BCKA demand in PDAC cells. We reveal the synthetically lethal BCAA metabolism vulnerabilities in PDAC. Our efforts in co-targeting stromal BCAT1 and the cancer BCKDH complex -specifically DBT- bridge the gap between knowledge of BCAA metabolism in the stroma and BCAA utilization in cancer cells.

10.2 Future directions

10.2.1 CAF heterogeneity in BCAA metabolism

There are also several CAF subpopulations identified recently, and this may prove the heterogeneity or plasticity of CAF. Moreover, different CAFs may have different metabolic profiles and coupling with cancer cells. The first population was also identified as the population we used. It is a population that expressed markers of myofibroblasts, such as αSMA, and was therefore named myofibroblastic CAFs, which is known to bed regulated by TGF-β/SMAD pathways [337]. Furthermore, there is a population that expressed inflammatory markers such as IL6 and leukemia inhibitory factor (LIF) and was therefore named inflammatory CAFs, which is regulated by IL-1/JAK pathways [337, 338]. IL1 induces LIF expression and downstream JAK/STAT activation to generate inflammatory CAFs and demonstrate that TGFβ antagonizes this process by downregulating IL1R1 expression and promoting differentiation into myofibroblasts. Our initial result showed that IL-1 does not influence BCAT1 or SMAD5 (Figure 10.1). Nevertheless, there are still other CAF populations.

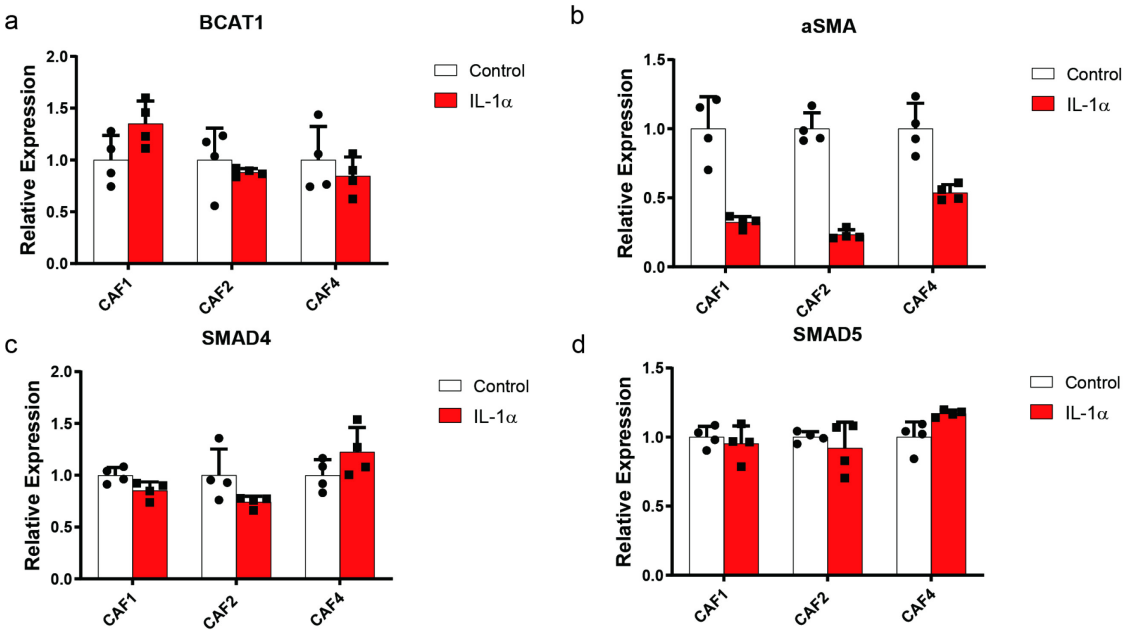

Figure 10.1 IL-1 does not influence BCAA related genes. **a**. BCAT1 mRNA expression measured in CAFs after two days of treatment with IL-1α. n = 4 biologically independent samples. **b**. αSMA mRNA expression measured in CAFs after two days of treatment with IL-1α. n = 4 biologically independent samples. **c**. SMAD4 mRNA expression measured in CAFs after two days of treatment with IL-1α. n = 4 biologically independent samples. **d**. SMAD5 mRNA expression measured in CAFs after two days of treatment with IL-1α. n = 4 biologically independent samples.

Recently, there is a new CAF subtype that expresses MHC class II (MHCII)–related genes and induces T-cell receptor (TCR) ligation in $CD4^+$ T cells in an antigen-dependent manner named these cells antigen-presenting CAFs[339]. Antigen-presenting CAFs can convert into myofibroblasts upon suitable culture conditions, suggesting that pancreatic CAF subpopulations represent dynamic and interconvertible. Moreover, the MHCII expressed by antigen-presenting CAFs acts as a decoy receptor to deactivate $CD4^+$ T cells by inducing either anergy or differentiation into Tregs. In this case, antigen-presenting CAFs are expected to decrease the $CD8^+$ to the Treg ratio and contribute to

immune suppression in the PDAC microenvironment. Future studies are warranted to assess the role of the heterogeneous population of CAFs in BCAA metabolism.

10.2.2 Deactivation of pancreatic CAFs through sodium butyrate and GW3965

Previously, we showed that sodium butyrate (NaB) and GW3965 (GW) could deactivate CAFs [340]. NaB is a 4-carbon short-chain fatty acid, which is naturally derived from the fermentation of dietary fiber through the gut microbiota [341]. NaB has been shown as an HDAC inhibitor and a regulator of cell proliferation, apoptosis and differentiation [342]. In cancer, overexpression of HDAC usually inhibits tumor suppressor genes, cell cycle inhibitors, epithelial differentiation factors and apoptosis-inducing factors. HDAC inhibitor can induce cell differentiation, apoptosis and inhibit HIF1-α and VEGF [343].

Liver X receptor (LXR) agonists have also been used to inhibit tumor cell growth. LXR is a member of the nuclear receptor superfamily of ligand-dependent transcription factors. They perform important cellular functions, including regulating cholesterol homeostasis, lipid and glucose metabolism, and regulating inflammation [344]. LXR agonist has been shown to disrupt proliferation, the cell-cycle progression of PDAC cells [345]. At the molecular level, LXR is the controlling factor of several cell cycle genes. LXR can also inhibit inflammation-related genes such as IL-6 [346]. LXRs are also effective regulators of adipogenesis through SREBP1c and its down-regulated genes FAS, ACC and SCD-1 [347]. LXR-induced SREBP stimulates the transcription of many genes involved in the synthesis and uptake of cholesterol and fatty acids. GW3965 is a synthetic LXR agonist that has been shown to alter the distribution of adipose tissue in mice and inhibit the production of inflammatory cytokines [348].

We examined that treatment of PDAC tissue slices with NaB and GW would restore CAFs' quiescent state. We show that the treated tissue slices show reduced expression of CAF activation markers (Figure 10.2) and up-regulated expression of quiescent markers (Figure 10.3).

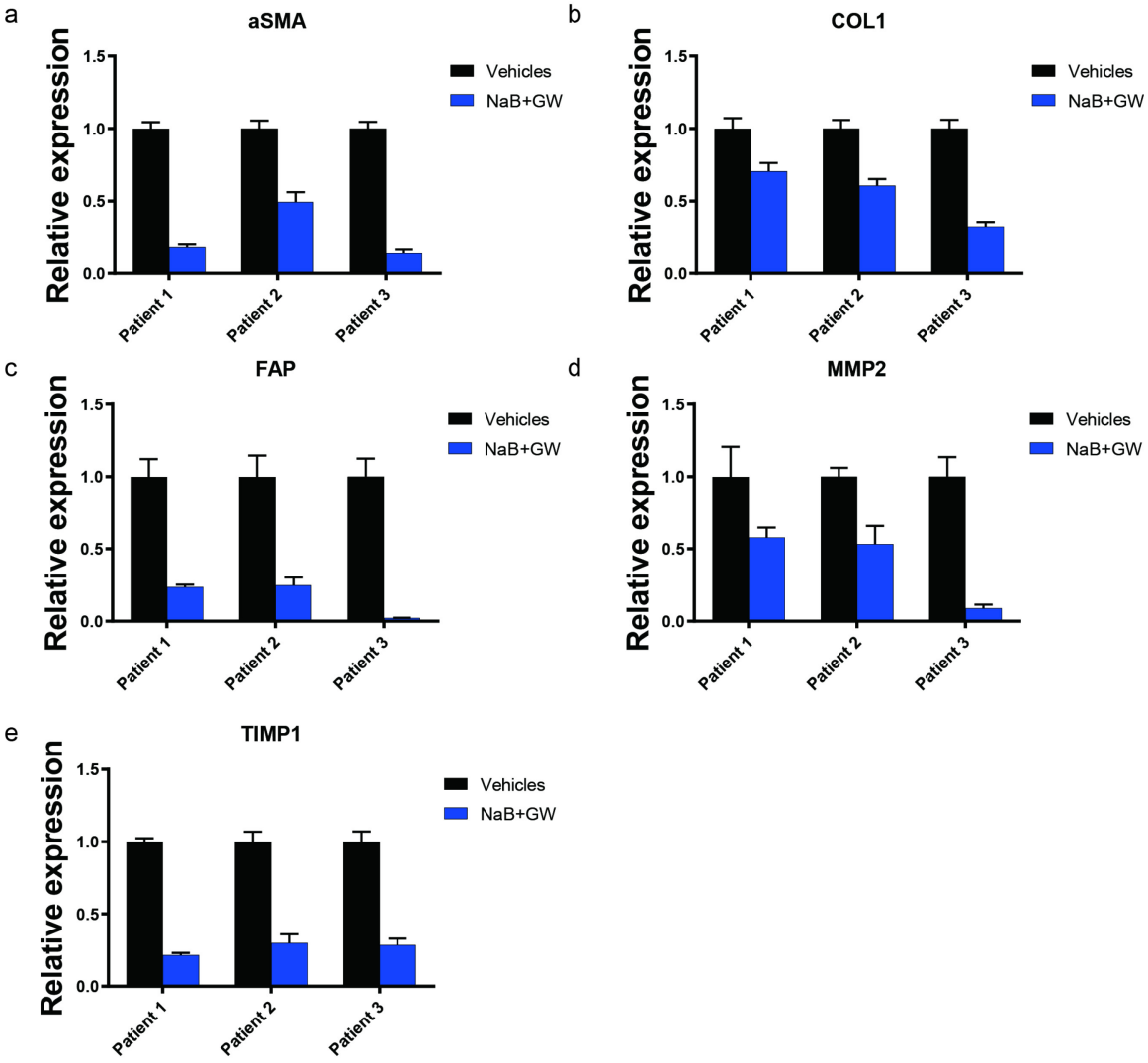

Figure 10.2 Expression of CAF activation markers in PDAC tissue slices. **a**. Relative αSMA mRNA expression in PDAC tissue slices. n = 4 biologically independent samples. **b**. Relative COL1 mRNA expression in PDAC tissue slices. n = 4 biologically independent samples. **c.** Relative FAP mRNA expression in PDAC tissue slices. n = 4 biologically independent samples. **d.** Relative MMP2 mRNA expression in PDAC tissue slices. n = 4 biologically independent samples. **e.** Relative TIMP1 mRNA expression in PDAC tissue slices. n = 4 biologically independent samples.

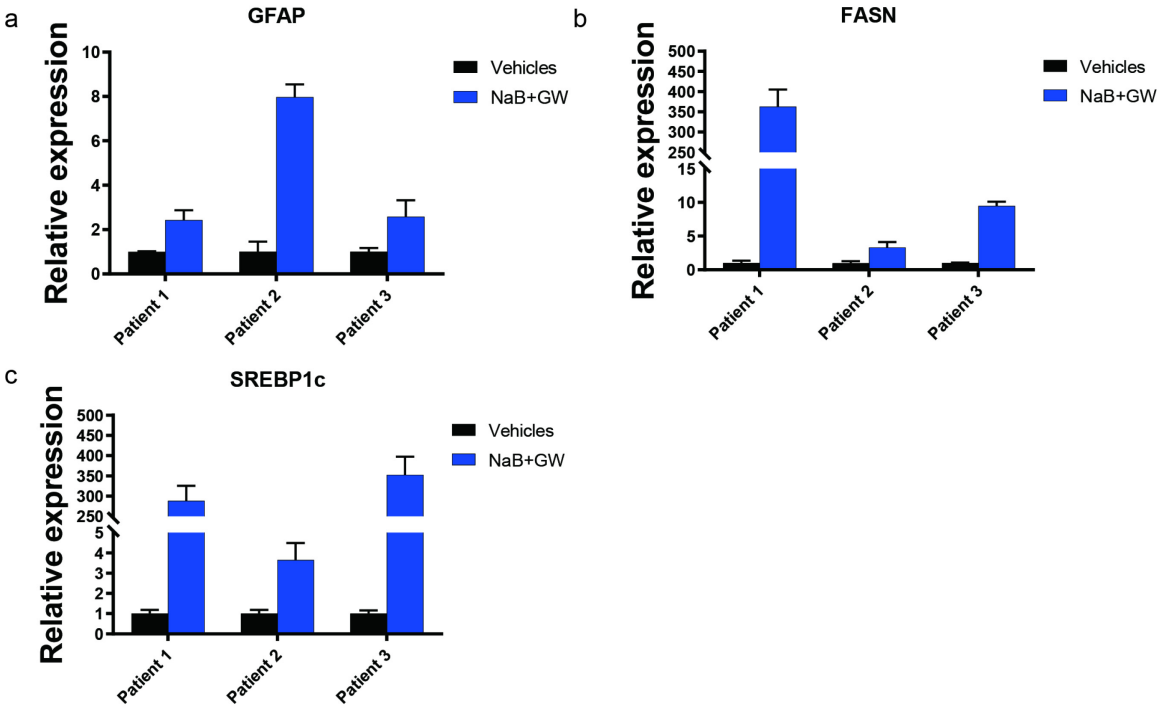

Figure 10.3 Expression of quiescent markers in PDAC tissue slices. **a**. Relative GFAP mRNA expression in PDAC tissue slices. n = 4 biologically independent samples. **b**. Relative FASN mRNA expression in PDAC tissue slices. n = 4 biologically independent samples. **c.** Relative SREBP1c mRNA expression in PDAC tissue slices. n = 4 biologically independent samples.

Besides, we show that NaB and GW treatment can also influence the properties of ECM. As shown in the figure, if we treated the CAFs from the beginning, the CAFs stopped to produce ECM; if treated in the middle, the CAF ECM would be deactivated to normal ECM (Figure 10.4a-c). For the adhesion assay, we further showed that the deactivated ECM is harder for PDAC cells to attach (Figure 10.4d-e). The properties of this ECM still need to be further examined. We could further examine whether the stromal cell-induced quiescence caused by NaB and GW treatment would lead to a decrease in tumor growth and metastasis.

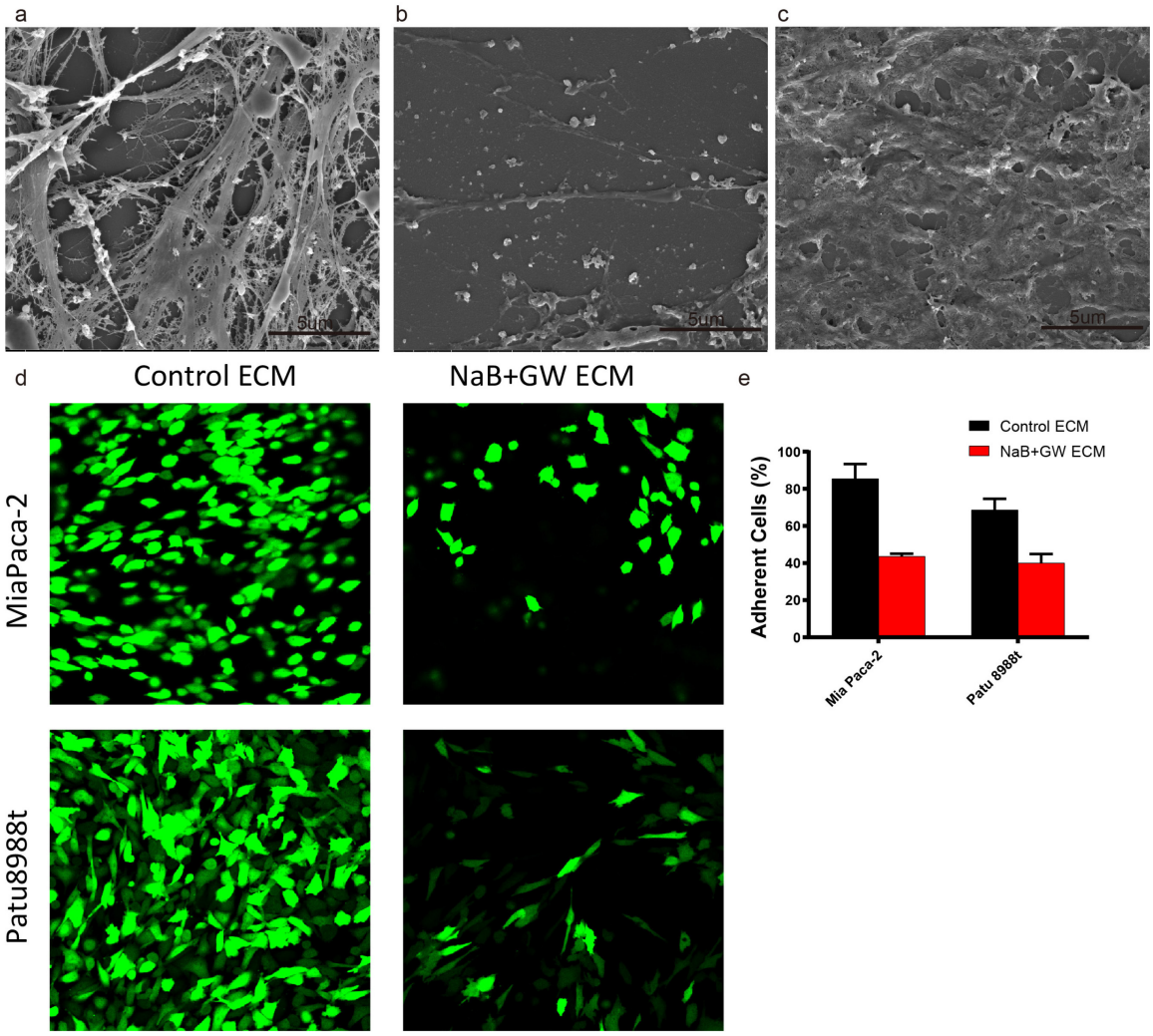

Figure 10.4 Deactivation of ECM by NaB + GW. **a-c**. Scanning electron microscopy image of CAF-derived 3-D matrices treated by vehicles (**a**), NaB + GW for eight days (**b**) or four days (**c**). Experiments were repeated independently two times with similar results. **d**. Fluorescence microscopy images comparing the adhesion of GFP-labeled Mia Paca-2 and Patu 8988t cells with ECM treated by vehicles and NaB + GW. Experiments were repeated independently two times with similar results. **e.** Relative adhesion percentage of Mia Paca-2 and Patu 8988t pancreatic cancer cells with ECM treated by vehicles and NaB + GW. n = 3 biologically independent samples.

10.2.3 CAFs secrete NAD^+ precursors to support PDAC cells.

The Nicotinamide adenine dinucleotide (NAD) and its phosphorylated form (NADP) contained in nicotinamide play an important role in the metabolism of all

organisms. Like many phosphorylation products, NAD is synthesized de novo by some smaller units, such as tryptophan (Trp), nicotinamide (Nam), nicotinic acid (NA), nicotinamide riboside (NR) and nicotinamide mononucleotide (NMN). Trp becomes NAD^+ through the de novo biosynthetic pathway in the liver [349]. Once converted to other molecules, it merges with the Preiss-Handler pathway, which is the same pathway used by NA to reach NAD^+. Although tryptophan does produce NAD+, its efficiency is 60 times lower than other precursors [350].

Nam is a common form of vitamin B3, sometimes called niacinamide. Nam will go through the same remedial approach as NR, but it must be stopped by bypassing the rate-limiting step before NR becomes NAD^+. Nam also participated in the salvage part of the approach. When enzymes that consume NAD^+ (such as sirtuins (a family of proteins that regulate cell health)) use NAD^+, they divide it into the necessary parts and then send them back as needed to create more NAD^+ [351]. NA is another form of vitamin B3, also known as niacin, and is sometimes used as a general term for all vitamin B3. Nicotinic acid was discovered by chemists who study nicotine, and its name was changed to niacin to distinguish it from tobacco. As we all know, NA causes flushing. Since the 1940s, NA has been used to fortify flour and rice all over the world due to its advantages. NA enters NAD^+ through the Preiss-Handler pathway, which also integrates chemically converted tryptophan (amino acid NAD^+ precursor) into NAD^+ [352].

Nicotinamide Mononucleotide (NMN) is an intermediate compound between NR and NAD^+, which means that NR must first become NMM before it can become NAD^+ [353]. NMN is a new member of NAD^+ precursor products. We know it is a beneficial precursor, but only recent studies have begun to clarify its ability to enter cells intact.

NMN and NR have never been intensively studied in clinical studies to see if one NAD^+ produces less NAD^+ energy than the other. NR is a form of vitamin B3 and is generally considered to be a highly effective precursor, which means that it consumes the least energy when taken orally and becomes NAD^+. This is because NR bypasses a step in the NAD^+ biosynthetic pathway, which is also the niacinamide pathway [354]. NR is increasingly used for NAD^+ supplementation because it is well known that NR can increase the level of NAD^+. In animal studies, this increase leads to specific benefits such as mitochondrial health, but so far, there is no evidence that these animal studies can be inferred to humans. NaR (nicotinic acid riboside) is a newly discovered eukaryotic NAD^+ precursor. NaR is converted to NAD^+ in three steps, first by nicotinamide riboside kinase (NMRK)-dependent [355].

In the initial siRNA screening, we identified the CAF-mediated rescue of PDAC cell growth rate under NAD^+ precursors deprivation. Furthermore, this effect is further enhanced when NAPRT is knockdown. This suggested that CAF is secreting NaR (Figure 10.5ab). Colony formation assay suggested NaR is an effective NAD^+ precursor (Figure 10.5c). Further, gemcitabine is a pyrimidine anti-nucleoside, has long served as a core component of chemotherapy treatments for PDAC. Gemcitabine resistance has been shown to be easily developed in PDAC, although the mechanism behind this link remains unclear. Since NaR is also a nucleoside analog, it probably completes the transporters with gemcitabine, and this could cause gemcitabine resistance. Our results indicated that NaR could cause gemcitabine resistance at low concentrations (Figure 10.6). Thus, NaR released by CAFs may directly confer gemcitabine resistance to PDAC cells.

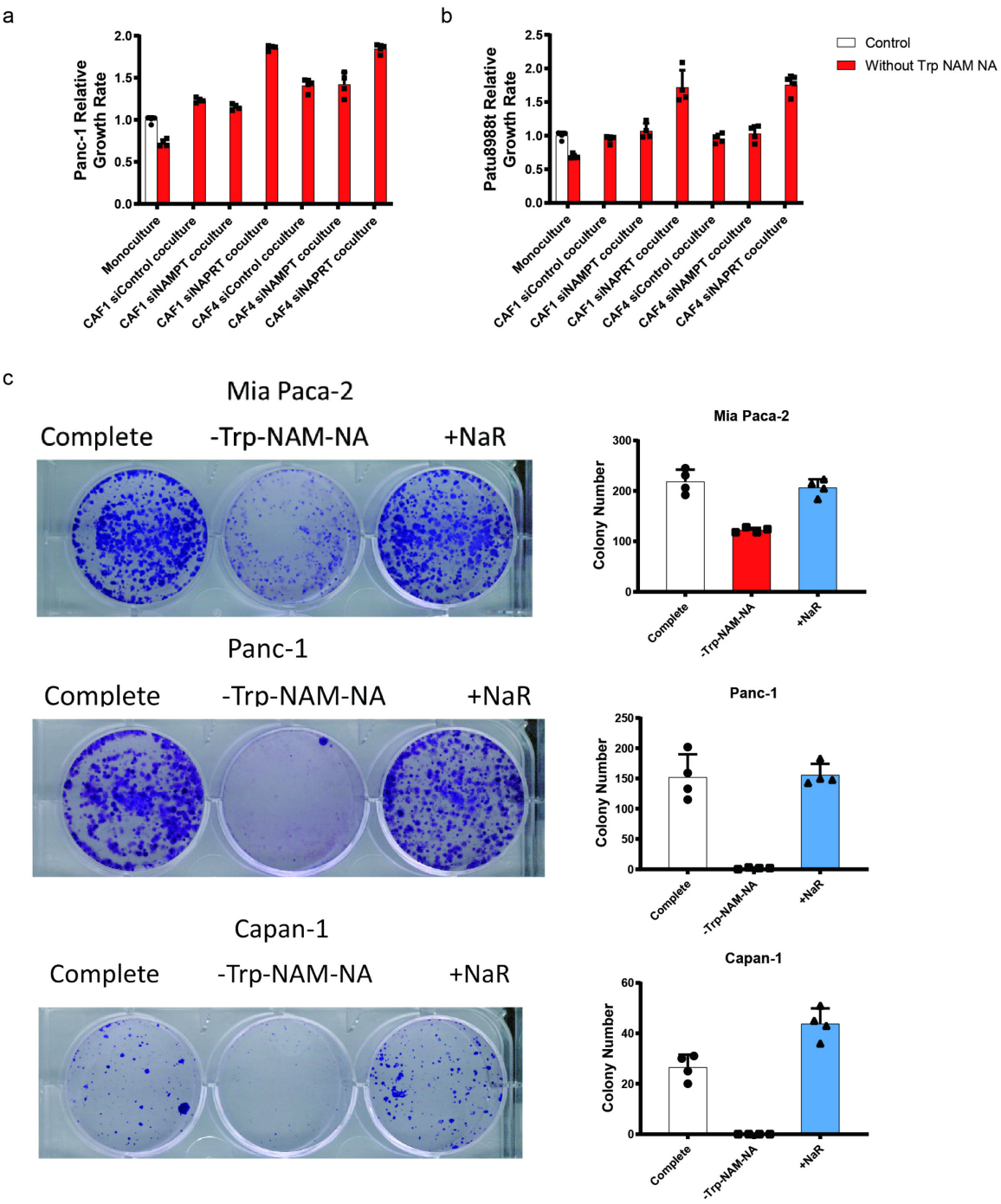

Figure 10.5 CAFs secrete NaR to support PDAC cells. **a**. Effect of NAMPT or NAPRT knockdown in CAFs on the CAF-mediated rescue of the Panc-1 cell growth rate under NAD^+ precursors deprivation. n = 4 biologically independent samples. **b**. Effect of NAMPT or NAPRT knockdown in CAFs on the CAF-mediated rescue of Patu8988t cell growth rate under NAD^+ precursors deprivation. n = 4 biologically independent samples. **c.** Colony-formation assay of PDAC cell lines with NaR. n = 4 biologically independent samples.

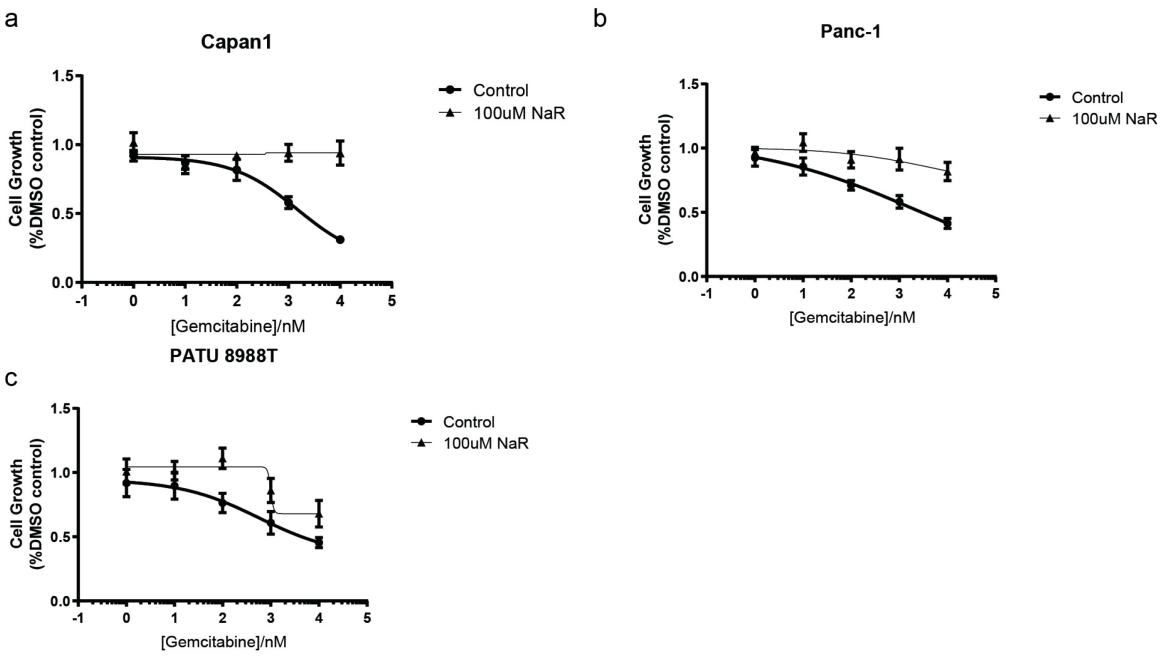

Figure 10.6 NaR Confer Gemcitabine Resistance to PDAC Cells. **a**. Relative viability and IC50 of Capan1 cells treated with Gem in the presence of NaR. n = 4 biologically independent samples. **b**. Relative viability and IC50 of Panc-1 cells treated with Gem in the presence of NaR. n = 4 biologically independent samples. **c.** Relative viability and IC50 of Patu8988t cells treated with Gem in the presence of NaR. n = 4 biologically independent samples.

Previous studies showed that members of the SLC29 family (ENT, equilibrative nucleoside transporters) and/or SLC28 family (CNT, concentrative nucleoside transporters) family could mediate the transport of NaR and NR. We performed RT-PCR to identify which CNT or ENT isoform mRNA is most abundant in CAFs (Figure 10.7ab). We found that SLC28A2 and SLC28A3 are highly expressed in CAFs, while cancer cells have high expression of ENTs. Also, the CAF-mediated rescue of PDAC cell growth rate under NAD^+ precursors deprivation is reduced when SLC28A2 is knockdown (Figure 10.7c). Furthermore, this effect is further enhanced when NAPRT is knockdown. To check the effect of CAF on PDAC cell NAD^+ metabolism, we treated

PDAC cells with CAF CM or NaR. CAF CM and NaR have a similar effect in PDAC cells, up-regulated NMRK1 and down-regulate NAMPT or NAPRT (Figure 10.8a). This suggests that CAF shifts PDAC cells to more NaR dependent, and reduced dependence of NAM and NA. Also, NaR can support OCR and fatty acid oxidation in PDAC cells (Figure 10.8bc).

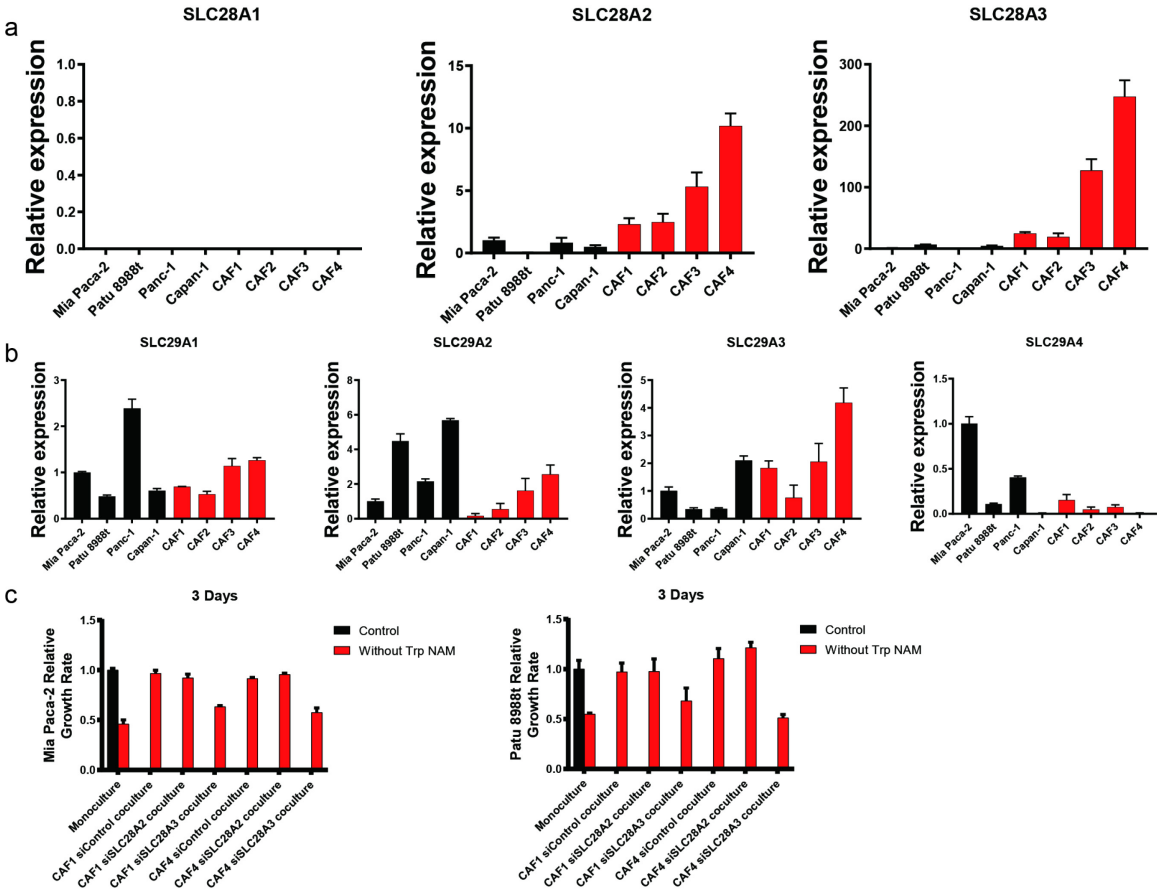

Figure 10.7 CAF secrete NaR through SLC28A2. **a**. Expression of SLC28 family (CNT) in CAFs and pancreatic cancer cell lines. n = 4 biologically independent samples. **b**. Expression of SLC29 family (ENT) in CAFs and pancreatic cancer cell lines. n = 4 biologically independent samples. **c.** Effect of SLC28A2 or SLC28A3 knockdown in CAFs on the CAF-mediated rescue of Patu8988t cell growth rate under NAD^+ precursors deprivation.

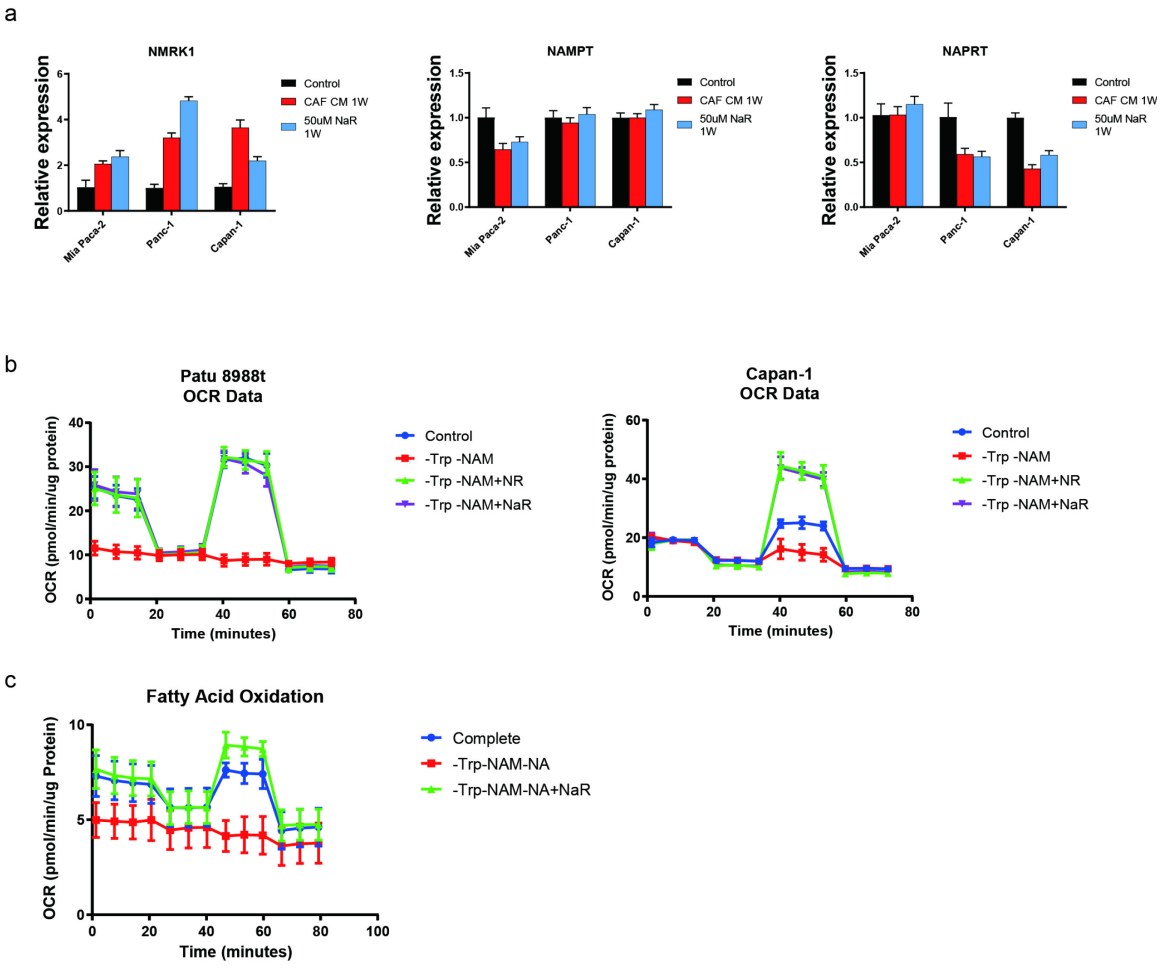

Figure 10.8 CAF secreted NaR up-regulated NMRK1 and down-regulate NAMPT or NAPRT. **a**. Expression of NMRK1, NAMPT and NAPRT in PDAC cells treated with CAF CM or NaR. n = 4 biologically independent samples. **b**. OCR measurements in PDAC cells with NaR. n = 6 biologically independent samples. **c.** Fatty acid oxidation OCR measurements in PDAC cells with NaR. n = 6 biologically independent samples.

10.2.4 Identifying BCKA Transporters

Unlike BCAAs, BCKA transport is not governed by a single amino acid transporter. However, it is instead mediated by monocarboxylate transporters (MCTs), which also control the transport of lactate, pyruvate, and ketone bodies through the plasma membrane. There are at least 7 MCTs that are active in different tissue types. In

order to identify the MCT in the pancreatic tumor stroma, we performed RT-PCR to identify which MCT isoform mRNA is most abundant in CAFs (Figure 10.9). We found that MCT1 is highly expressed in PDAC cells, while MCT2 is highly expressed in CAFs. Nevertheless, because MCTs are shared with lactate, pyruvate and other α-keto acids, we cannot identify the specific transporters based on the expression.

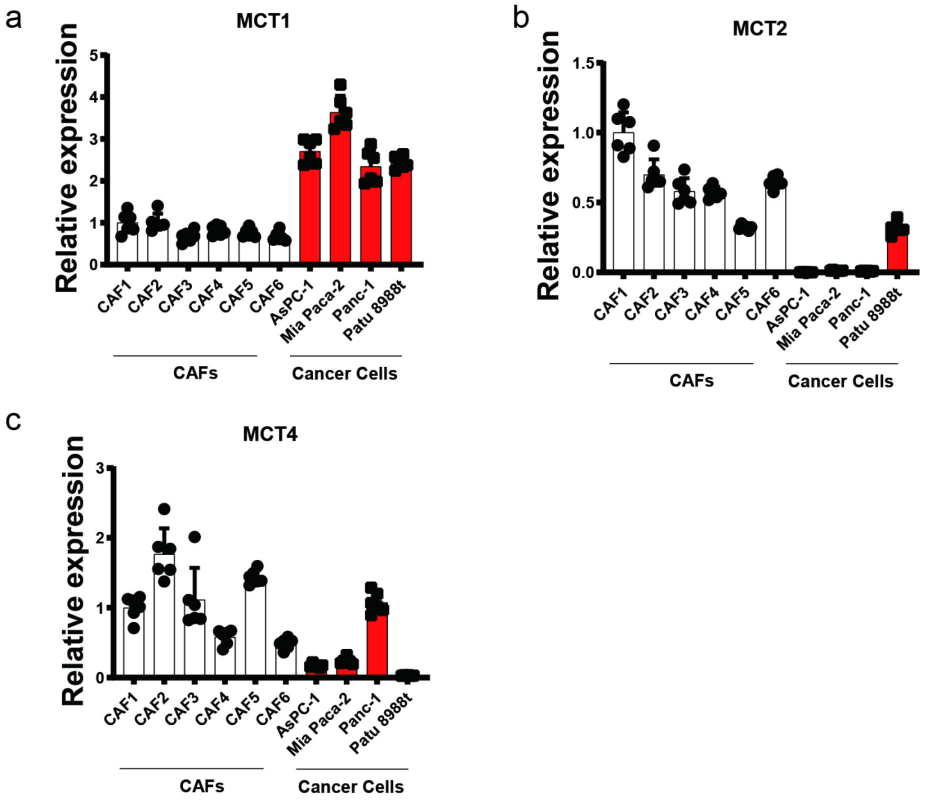

Figure 10.9 Expression of monocarboxylate transporters in CAF and PDAC cell lines. **a**. Relative MCT1 mRNA expression in CAFs and pancreatic cancer cell lines. Expression normalized to gene expression in CAF1. n = 6 biologically independent samples. **b**. Relative MCT2 mRNA expression in CAFs and pancreatic cancer cell lines. Expression normalized to gene expression in CAF1. n = 6 biologically independent samples. **c**. Relative MCT4 mRNA expression in CAFs and pancreatic cancer cell lines. Expression normalized to gene expression in CAF1. n = 6 biologically independent samples.

For the future study, we will perform CRISPR screening to identify the BCKA related transporters. A previous study indicated BCAT2 is a bifunctional protein

catalyzing branched chain amino acid transamination and branched chain alpha-keto acid transport [356]. The transport properties of BCAT2 suggest that this protein may be the branched-chain alpha-keto acid transporter [356]. So, in order to implement such a screening strategy, we will use the BCAT2 knockout cell lines we generated. We will transduce the BCAT2 knockout cells with a lentiviral single guide RNA (sgRNA) library that targets ~3000 metabolic enzymes, small-molecule transporters, and metabolism-related transcription factors (~10 sgRNAs per gene) and also contains 499 control sgRNAs [357]. The transduced cells were cultured in DMEM media with or without BCKAs. For each gene, we generated a gene score by calculating the mean log2 fold-change in abundance from the beginning to the end of the culture period of all the sgRNAs targeting the gene (Figure 10.10).

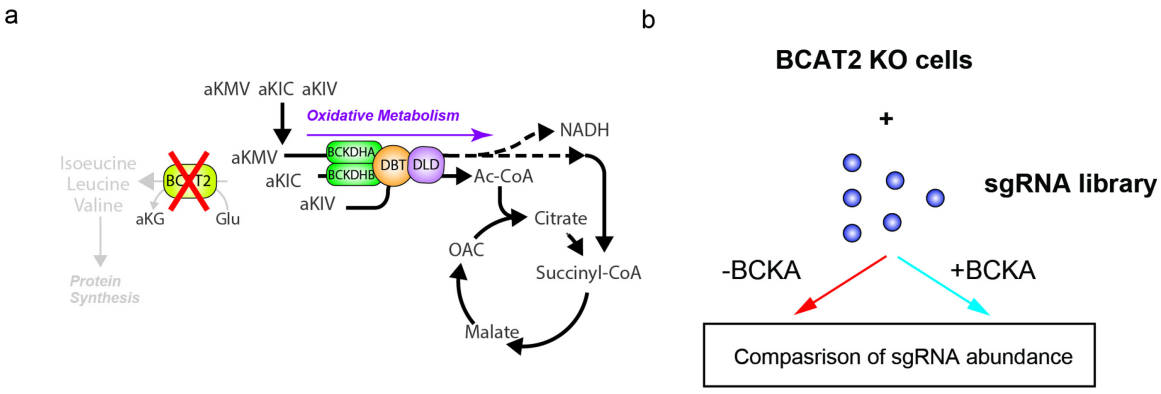

Figure 10.10 Screening strategy of BCKA transporters. **a**. Schematic of BCAT2 knockout cells. **b**. Screening strategy of BCKA transporters.

10.2.5 Nuclear BCAT2 regulate lipid metabolism

PPARs are members of the superfamily of transcription factors expressed by the target gene [358]. PPARs include three subtypes: PPARα, PPARβ, and PPARγ, and PPARs of different subtypes that regulate different target genes. PPARs are known as

fatty acid receptors, mainly involved in fatty acid metabolism [359]. PPARα is mainly expressed in liver tissues, by regulating the expression of genes related to fatty acid oxidation in the liver, it can differentiate liver fat cells, fat storage, transportation and fatty acid oxidation. The PPARα gene mainly regulates the mitochondrial and peroxisomal β oxidation system and microsomal ω oxidation system [359]; PPARα can also regulate the peroxisomal β oxidation pathway through the expression of some key enzymes (such as acetyl coenzyme A oxidase, ACSL1 and dehydrogenase multifunctional enzyme, ketone acetyl coenzyme A thiolase, etc.) [360]. Also, some studies have shown that activated PPARα can also mediate the expression of apolipoprotein apoA I; promote lipoprotein lipase synthesis, catalyze lipolysis of triglycerides (TG) in lipoproteins into free fatty acids (FFA) [358].

PPARγ can be divided into four subtypes: γ1, γ2, γ3, and γ4 [361]. PPARγ is mainly involved in the fat tissue differentiation and lipid metabolism process, including regulating lipid metabolism, fat cell terminal differentiation, and glycometabolism; besides, PPARγ is used in the development of liver fibrosis development process. Previous studies have shown that PPARγ is highly expressed in adipocytes and can induce liver cells to express apolipoproteins, fatty acid oxidase systems and lipoprotein lipases, etc., thereby promoting the oxidative metabolism of lipids, which can also enhance fatty acid transport proteins and fatty acid transfer enzymes Gene expression of fatty acid storage such as FAT/CD36, aP2, phosphoenolpyruvate carboxykinase (PEPKK), ACSL1, etc., and inhibits β3-adrenergic receptors, leptin and tumor necrosis factor-alpha (TNFα) expression and fatty acid release [360]. Also, PPARγ plays an important role in the transformation of HSC from static phenotype to active phenotype.

PPARγ regulates liver fibrosis signal channels such as TGFβ/Smad signal channel, Ras-MAPK signal channel, NF-κB signal channel, etc., to slow down the process of fibrosis [361].

When we were first staining the BCAT2 in human PDAC tissue, we found BCAT2 is also located in the nucleus. Since BCAT2 is a transaminase, BCAT2 can also transport lipid to the nucleus to bind with PPARs as other transaminases. The co-localization is also confirmed in the PDAC cell lines (Figure 10.11).

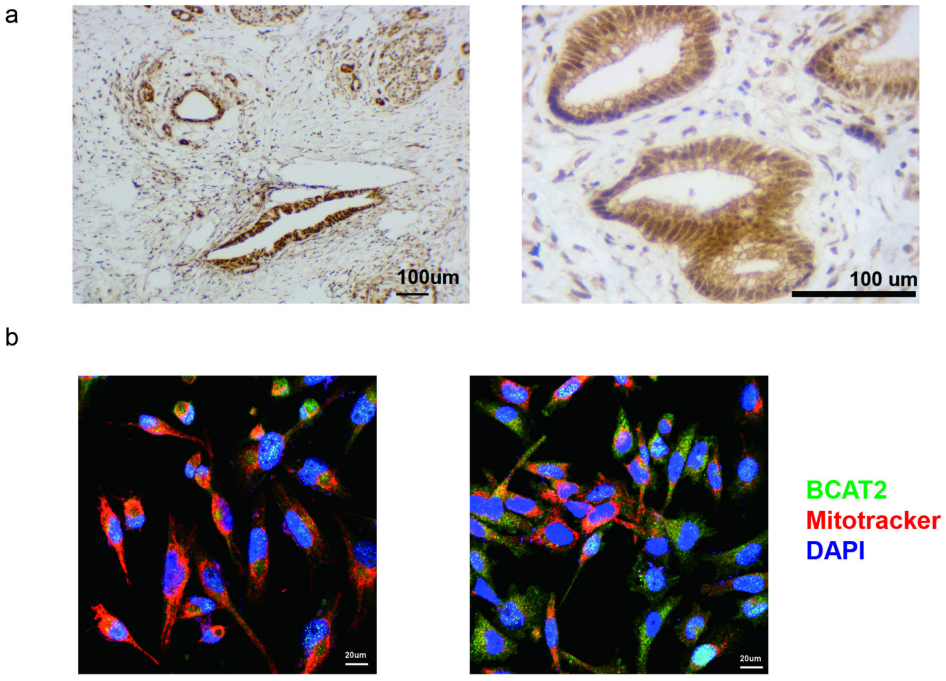

Figure 10.11 Expression of BCAT2 in PDAC tissue and cell lines. **a**. Representative IHC staining image of BCAT2 expression in human PDAC tissue. Experiments were repeated independently three times with similar results. **b**. Colocalization of BCAT2, mitochondria and nucleus analyzed by immunofluorescence against BCAT2, Mitotracker and DAPI. Experiments were repeated independently three times with similar results.

To further check the interference between BCAT2 and PPARs. We used the BCAT2 knockdown cells treated with PPAR inhibitors, and we found that GW9662,

which inhibits PPARα/γ, is more effective in BCAT2 knockdown cells (Figure 10.12). Moreover, we also checked the expression of PPAR in the BCAT2 knockdown cells, similar to the GW99662 result, and we found that BCAT2 knockdown cells have a high expression of PPARA and lower expression of PPARG. These data indicate that BCAT2 may be linked to PPARα/γ functions.

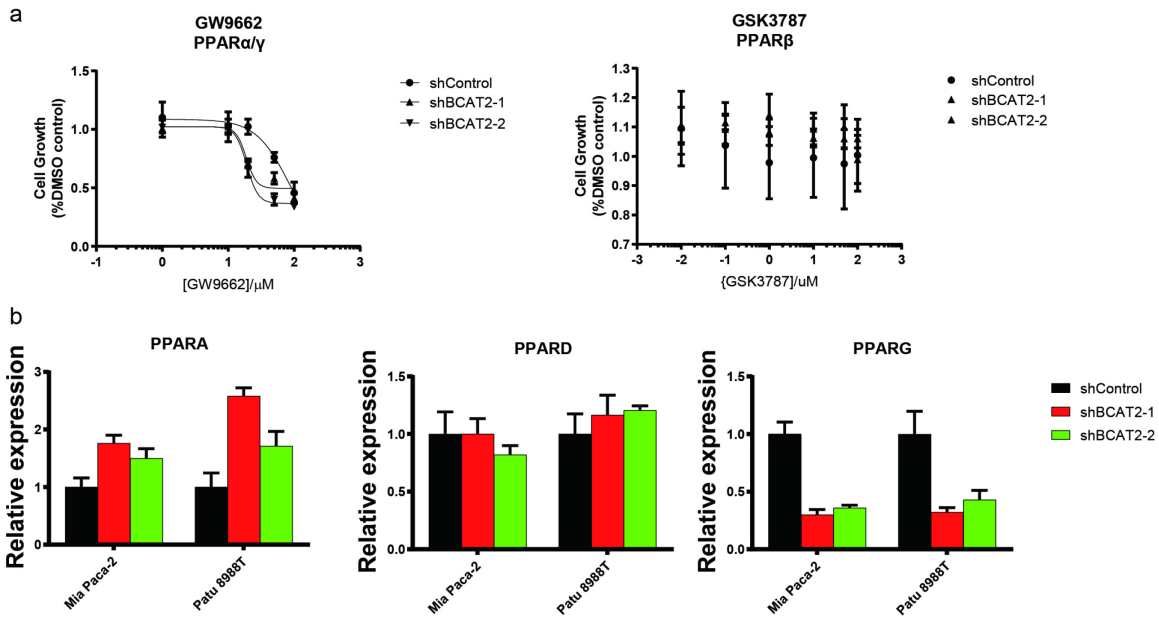

Figure 10.12 BCAT2 and PPAR. **a**. Representative IHC staining image of BCAT2 expression in human PDAC tissue. Experiments were repeated independently three times with similar results. **b**. Colocalization of BCAT2, mitochondria and nucleus analyzed by immunofluorescence against BCAT2, Mitotracker and DAPI. Experiments were repeated independently three times with similar results.

Since PPAR regulates lipid metabolism, we check the lipid oxidation in BCAT2 knockdown cells. We found the lipid oxidation is up-regulated in the BCAT2 knockdown cells (Figure 10.13a). Furthermore, a recent study has shown that ferroptosis is linked to lipid oxidation [362]. So we check the use of Erastin, which is a small molecule capable of initiating ferroptotic cell death in the BCAT2 knockdown cells (Figure 10.13b). We

found that Erastin is more effective when BCAT2 is knocking down. This further proves the BCAT2 may be linked to lipid metabolism.

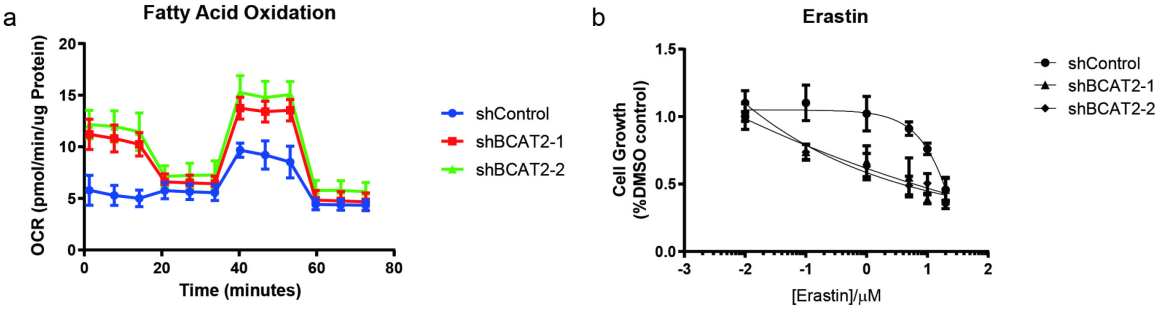

Figure 10.13 BCAT2 and lipid oxidation. **a**. Representative IHC staining image of BCAT2 expression in human PDAC tissue. Experiments were repeated independently three times with similar results. **b**. Colocalization of BCAT2, mitochondria and nucleus analyzed by immunofluorescence against BCAT2, Mitotracker and DAPI. Experiments were repeated independently three times with similar results.

Chapter 11 Materials and Methods

11.1 Cell Culture

11.1.1 *PDAC Cell lines*

All the cell lines used in this study were purchased from ATCC, used below passage 25 and continuously cultured in 100 U/ml penicillin and 100 U/ml streptomycin. The Mia Paca-2, Panc-1 and Patu 8988t cell lines were routinely cultured in Dulbecco's modified Eagle's medium (DMEM) with 10% fetal bovine serum (FBS) (Atlanta Biologicals, S11150). AsPc1 and BxPC3 cell lines were routinely cultured in Roswell Park Memorial Institute (RPMI) 1640 (Invitrogen) with 10% FBS. All cell lines were mycoplasma free based on PCR-based assays run every month in the lab.

For metabolic and metabolomics assays, 10% dialyzed FBS (Sigma-Aldrich, F0392) was used. For the rescue experiments, the DMEM medium without BCAAs was used (United States Biological).

11.1.2 *Fibroblast Cell Culture*

Patient-derived fibroblast cells were kindly provided by Drs. Edna Cukierman, Anirban Maitra and Mara Sherman and internal STR profiling were maintained and checked annually. CAFs were cultured at 37˚C under 5% CO2 using DMEM supplemented with 10% FBS and 100 u/ml-mg/ml penicillin-streptomycin. Normal fibroblast cell lines IMR-90 and MRC-5 were purchased from ATCC and cultured at

37˚C under 5% CO2 using DMEM supplemented with 10% FBS and 100 u/ml-mg/ml penicillin-streptomycin. MSCs were provided by Dr. Michael Andreeff and cultured in α-MEM containing 10% FBS, 4% pooled human platelet lysate and 1% penicillin-streptomycin. Only third or fourth passage cells were used for experiments.

11.1.3 CTC Cell Culture

Cells were maintained at 37°C, 5% CO_2 under normoxic conditions. PDAC CTC-derived cell lines were grown in RPMI-1640 supplemented with 10% FBS and 1% antibiotic-antimycotic (Gibco).

11.1.4 Tissue slice culture

Fresh pancreatic cancer tissue samples were procured immediately after surgical resection from the University of Michigan Hospital. Informed consent was obtained from all patients. The remaining connective, fibrotic or adipose tissue was removed with razor blades. Tumor specimens were embedded in 3% low melting point agarose/PBS before cutting in the Leica VT1200 tissue slicer. The slice thickness ranged between 100–200 μm. Slices were then cultured in DMEM with penicillin (100 U/mL), streptomycin (100 U/mL) and amphotericin (Fungizone 2.5 μg/mL). All experiments were performed in triplicate and were repeated at least three times.

11.2 CTC isolation from patient blood and healthy controls

The experimental protocol was approved by the University of Michigan Medicine Institutional Review Board, and all patients gave their informed consent to participate in the study. Patients were diagnosed with metastatic PDAC and were treatment naïve at the time of the first sample collection. Blood was collected in EDTA tubes and processed

within two hours of sample collection. Red blood cells (RBCs) were depleted from the sample using RBC aggregation via HetaSep™ (STEMCELL Technologies) following the manufacturer's protocol. Briefly, blood was divided into 3 mL aliquots and mixed with 600µL HetaSep™, and centrifuged at 90xg for 1 minute, at room temperature, with the centrifuge brake off. The sample was then further incubated for an additional 10 minutes at room temperature to improve RBC depletion. The nucleated cell fraction was collected and diluted to 3x the original blood volume with phosphate-buffered saline (PBS) (Gibco). The resultant sample was processed through the Labyrinth at a flowrate of 2500 µL/min. The flow was stabilized for 1 mL of flow volume, before the CTC outlet, outlet 2, was collected, termed the CTC-enriched labyrinth product. This sample was divided into CTC enumeration (800 µL) and RNA analysis (≈3-4 mL).

11.3 Immunofluorescent staining and CTC enumeration

The CTC-enriched labyrinth product was divided across 4 Polysine microscope slides (Thermo Scientific), 200µL each, using Thermo Scientific™ Cytospin 4 (Thermo Scientific). The slides were placed into an EZ Cytofunnel (Thermo scientific) and spun at 800rpm for 10 minutes. To fix the cells, 200µL of 4% paraformaldehyde (PFA) was added to the Cytofunnel and spun a second time under the same conditions. Slides were stored at 4°C coated in PBS until used for immunofluorescent staining.

Slides were permeabilized with 0.2% Triton X-100 for 3 minutes, washed 3x with PBS, and blocked using 10% goat serum (Life Technologies) for 30 minutes at room temperature. The slides were then incubated overnight at 4°C with primary antibodies diluted in 10% goat serum - mouse anti-human Pan-Cytokeratin (CK) (Bio-Rad, MCA1907), mouse anti-human CD45 (Bio-Rad, MCA87GA), and rabbit anti-human

Vimentin (Vim) (CST, 5741). The next day the slides were washed 3x with 5 minutes incubation PBS washes. Slides were then incubated in the dark for 45 minutes at room temperature with secondary antibodies - (Alexa Fluor 488, 546, and 647). The slides were washed 3x with 5minute incubation PBS washes and mounted using Prolong Gold Antifade Mountant with DAPI (Invitrogen). The slides were scanned using a Nikon TI microscope at 20x magnification. The tiled images were individually analyzed, and CTC was identified based on their fluorescent signature in each channel.

Cells were considered CTCs when they were $DAPI^{+}$/CD45 $(AF488)^{-}$/CK $(AF546)^{+}$. CTC phenotype was determined based on vimentin expression. Cells were considered epithelial if $DAPI^{+}$/CD45$(AF488)^{-}$/CK(AF546) $^{+}$/Vim $(AF647)^{-}$, and epithelial to mesenchymal transition (EMT) if $DAPI^{+}$/CD45$(AF488)^{-}$/CK$(AF546)^{+}$/Vim $(AF647)^{+}$.

11.4 Proliferation assay

Cells were cultured on 96-well plates in the indicated conditions. For cancer cells, cell growth was measured after that as fluorescence intensity using a plate reader (SpectraMax M5, Molecular Devices). For CAFs, the CyQUANT® direct cell proliferation assay was performed according to the manufacturer's instructions.

11.5 Coculture assay with fibroblasts

Direct coculture in which two cell types were grown in physical contact was performed. In brief, CAFs or NOFs were seeded first, and after the attachment, GFP labeled pancreatic cancer cells were seeded overnight. The medium was changed to BCAA deprivation or with different drugs after 24 hours. Fluorescence value as proliferation rates was measured at 485/515 nm, or flow cytometry assay was performed.

11.6 Conditioned media (CM) preparation

PANC-1 cells were grown in DMEM + 10% FBS medium, and conditioned medium was harvested after 16 h and centrifuged at 3,000 rpm for 5 min, and the supernatant was passed through the 0.45-μm filter. NOFs or MSCs were exposed to fresh CM repeatedly for four weeks.

11.7 Colony formation assay

Cell growth of shRNA-treated cell lines was assayed through crystal violet staining. 500 cells were seeded in 6-well plates. At the indicated time point (usually two weeks), cells were fixed with 80% methanol and stained with crystal violet solution overnight. All experiments were performed in triplicate.

11.8 Protein assay

Protein assays are used to do normalization in our experiment and are done according to Bicinchoninic Acid (BCA) Protein Assay protocol (Thermo Fisher). In brief, 200 μl reagent mixture was added to a 96-well assay plate and mixed with samples or standard, and then incubated at 37°C for 30 min. The absorbance was read on a spectrophotometer at 562 nm, and a standard curve was generated to determine sample protein concentration.

11.9 SiRNA, shRNA and CRISPR knockdown

Cells were transfected with siBCAT1 (Sigma, EHU072291), siDBT (Sigma, EHU035851), siSMAD4 (Sigma, EHU149321), siSMAD5 (Sigma, EHU104241), siMRC2(Sigma, EHU003351) and respective negative controls (Sigma, SIC001) using Lipofectamine RNAiMAX Reagent (Thermo Fisher Scientific) and Opti-MEM

accordingly to manufacturer's instructions and analysis was performed three days after transfection.

shRNA vectors were purchased from Sigma-Aldrich (St. Louis, USA). The clone IDs for each shRNA are as follows: shBCAT1-1: TRCN0000005907; shBCAT1-2: TRCN0000010976; shBCAT2-1: TRCN0000035115; shBCAT2-2: TRCN0000286266; shDBT-1: TRCN0000025837; shDBT-2: TRCN0000025838; A non-targeting shRNA (shCTRL) was used as a control. Knockdown was confirmed by qRT–PCR or immunoblotting.

For CRISPR knockdown of BCAT2, sgRNA oligonucleotide pairs (Pair1, CACCGCACGGATCATATGCTGACGG, AAACCCGTCAGCATATGATCCGTGC, Pair2, CACCGGTTCACGGATCATATGCTGA, AAACTCAGCATATGATCCGTGAACC were phosphorylated, annealed, and cloned as previously described into the BbsI-linearized pSpCas9(BB)-2A-Puro (PX459) V2.0 (PX459) plasmid (Addgene, #62988).

11.10 Quantitative RT-PCR

Total RNA was isolated using Trizol (Life Technologies) according to the manufacturer's instructions. RNA concentration was determined using a purified RNA by NanoDrop Lite Spectrophotometer (Thermo Fisher Scientific) and 1µg of cDNA synthesized using the iScript cDNA synthesis kit (BioRad). Quantitative-RT PCR was performed using a QuantStudio 3 Real-Time PCR System (Applied Biosystems, Foster City, CA) with the Power SYBR™ Green PCR Master Mix (Invitrogen, Carlsbad, CA) as

per the manufacturer's instructions. The primer sequences used for qRT–PCR are shown in Table 11.1.

Table 11.1 Primer sequences for qRT-PCR.

Gene	Forward	Reverse
BCAT1	GCCTTGGTGTGTGACAATGG	CCATCACCCCCTGATGTCTG
BCAT2	AAATGGGCCTGAGCTGATCC	GAGTCATTGGTAGGGAGGCG
BCKDHA	GGAACGCCACTTCGTCACTA	GTGTGGCAGCGAAGTTGAAG
BCKDHB	TGGAGTCTTTAGATGCACTGTTG	CGCAATTCCGATTCCAAATCCAA
DBT	TTGCCTCCTTCACCCAAAGTT	TGCCTGTGAATACCGGAGGT
SMAD2	AACCTGCATTTTGGTGTTCGAT	CCATCTACAGTGAGTGAGGGC
SMAD3	AGCTGACACGGAGACACATC	GTTGCATCCTGGTGGGATCT
SMAD4	GAGACATACAGCACCCCAGC	TGTGGAAGCCACAGGAATGT
SMAD5	ACAACACAGCCTTCTGGTTCA	CGTGGCATTTTGTGGCATGT

For the CTCs, the remainder of the CTC-enriched labyrinth product was centrifuged at 300xg for 10 minutes to pellet the cells. The cell pellet was resuspended in 700µL TRIzol to lyse the cells and incubated at room temperature for 5 minutes and frozen at -20°C until

ready for RNA purification. RNA was purified using a modified lysis protocol and the Total RNA Purification kit (Norgen Biotek Corp.). Once thawed, 140µL of chloroform was added to the TRIzol sample and centrifuged at 12,000xg for 15 minutes. The RNA layer was collected and mixed with an equal volume 70% ethanol and loaded onto the spin column and washed 3x using the provided wash solution and eluted into 30µL volume. cDNA was prepared using SuperScript IV VILO with ezDNase™ Enzyme (Invitrogen) following the manufacturer's protocol. Real-time PCR was performed using TaqMan™ Fast Advanced Master Mix (Applied Biosystems) with following probes 18s: Hs99999901_s1, BCAT1:Hs00398962_m1, BCAT2:Hs01553550_m1, BCKDHA: Hs00958109_m1, BCKDHB: Hs00609053_m1, DBT: Hs01066445_m1 following the manufacturer's protocol and run on the QuantStuido 3. Detection thresholds were determined using the QuantStuido™ Design & Analysis Software.

11.11 Immunoblotting

Cells were washed twice in ice-cold phosphate-buffered saline (PBS), scraped and collected as pellets after centrifugation at 4,000 r.p.m. for 5 min. The pelleted cells were incubated in RIPA buffer with proteinase and phosphatase inhibitors for 15 min. Lysates were then collected and centrifuged at 14,000 r.p.m. for 15 min at 4 °C. Protein concentrations were measured using the BCA Assay. SDS–PAGE and immunoblotting were performed in pre-cast Bis-Tris 4–20% gradient gels (Bio-Rad). Blots were imaged using a ChemiDoc (Bio-Rad ChemiDoc™ MP System). The following antibodies were used: BCAT1 (Novus Biologicals, NBP2-01826), BCAT2 (Cell Signaling Technologies (CST), 9432S), DBT (Abcam, ab151991), HSP90 (CST, 4877) and Vinculin (Santa Cruz Biotechnology, sc-25336).

11.12 ChIP-PCR

CAFs were treated with vehicle or 5 ng/ml TGF-β1, then cross-linked, fixed and processed with Simple ChIP Enzymatic Chromatin IP Kit (Magnetic Beads) (CST, 9003) according to the manufacturer's instructions. Cell lysates were Immuno-precipitated with anti-SMAD4 antibody (CST. 38454), SMAD5 antibody (CST, 12534) and rabbit IgG ChIP grade (CST, 2729). Region of BCAT1 promoter or non-promoter region were amplified by Power SYBR™ Green PCR Master Mix (Invitrogen, Carlsbad, CA) as per the manufacturer's instructions.

11.13 Dual-luciferase reporter assay

BCAT1 promoter regions were conjugated to the translation start site of the NanoLuc gene in the pNL2.1 vector (Promega). CAFs were plated in 96-well plates 12 h before transfection. The NanoLuc reporter vectors were co-transfected with promoter firefly luciferase reporter vector using Lipofectamine 3000 Reagent (Thermo) according to the manufacturer's protocol. After 48 h of the transfection, the luminescence was quantified and normalized using Nano-Glo Dual-Luciferase Reporter Assay (Promega).

11.14 Puromycin incorporation assay

Surface sensing of translation (SUnSET) assay was performed as previously described[363]. Briefly, cells were incubated with 10μg/mL puromycin (Thermo Fisher) for 10 min, followed by washing with ice-cold PBS and lysing with RIPA buffer. Cell lysates were loaded onto SDS–PAGE, and western blotting was performed with a mouse anti-puromycin monoclonal antibody (Millipore), and normalized against Ponceau S staining (Sigma).

11.15 Mitochondrial NADH/NAD$^+$ measurement

Mitochondrial NADH/NAD$^+$ sensor, RexMito, was prepared as previously described[364]. Mia Paca-2 cells were transfected using Lipofectamine 2000 Reagent (Thermo) according to the manufacturer's protocol. Then the cell medium was replaced by a complete medium, BCAA deprived medium, or BCAA deprived medium with BCKA. We used a Nikon A1Si Laser Scanning Confocal Microscope to visualize the fluorescence of transfected cells 24–48 h after transfection. Fluorescence detection was carried out using the 488 laser line for RexYFP and 561 laser line for HyPerRed-C199S. Imaging intensity was measured, and Ratio imaging was generated by Nikon NIS-Elements AR.

11.16 Flow cytometry

In the mixed coculture, cancer-associated fibroblasts were seeded in a 6-well plate for 24 hours. For the SUnSET assay, then GFP labeled cells were added and cocultured for three days in the indicated medium. Puromycin intensity was analyzed by FACS in tumor cells with GFP gating. For the NADH/NAD+ measurement, PKH26 labeled cells were added and cocultured for three days in the indicated medium. NADH/NAD$^+$ ratio was analyzed by FACS in tumor cells with PKH26 gating. All data were acquired with the Bio-Rad ZE5 flow cytometry analyzer, and analysis was performed using FlowJo.

11.17 Measurements of OCR

Mitochondrial OCR was measured by XF96 Analyzer (Seahorse Biosciences). Cells were seeded in 96-well seahorse plates and incubated at 37 °C with 5% CO2 overnight. The medium was replaced with 100 μL medium free of serum and sodium bicarbonate. Plates were then incubated in a CO2-free incubator for one h before placing

them in the analyzer. The OCRs were measured with the procedure of 3-min mixing, 2-min waiting, and 3-min measuring. Oligomycin, FCCP and Rotenone/Antimycin A were injected through port A, B and C, respectively, to calculate mitochondrial function under different stress. All data were normalized to total cell protein as measured by the BCA assay.

11.18 Substrate specific OCR

OCR was measured in MAS medium supplemented with 0.2% (w/v) BSA, four mM ADP, 1 nM XF Plasma Membrane Permeabilizer (Seahorse Bioscience), 500 nM Coenzyme B12 and biotin and sequentially offered Oligomycin, FCCP and antimycin. Permeabilized pancreatic cancer cells were offered 5 mM branched-chain ketoacids. Substrate specific respiration was calculated as the maximum respiration, and the data were normalized to total cell protein.

11.19 Immunohistochemistry (IHC) and immunofluorescence (IF) staining

Tissues were fixed in 10% formalin overnight and embedded in paraffin. PDAC sections were deparaffinized in xylene, rehydrated through sequential ethanol, and rinsed in PBS. Non-specific signals were blocked using 10% goat serum in 0.1% Triton X-100. Tumor samples were stained with the following primary antibodies: αSMA(Sigma, A5228, 1:500), BCAT1 (Sigma, HPA048592, 1:200), SMAD5 (Sigma, HPA058931, 1:200), Ki-67(Santa Cruz Biotechnology,sc-23900,1:500), PCNA(Santa Cruz Biotechnology, sc-56,1:500). After overnight incubation, the slides were washed and incubated with biotinylated secondary antibody (Vector Laboratories) for 30min at room temperature. All slides were then incubated with avidin-biotin-peroxidase complex for 30 min, and the signals were visualized by using DAB Substrate Kit (Vector Laboratories).

The tissue sections were counterstained with VECTOR Hematoxylin QS and mounted with VectaMount after dehydration. IF staining was performed on tissue slices or chamber slide cultures (Thermo Fisher Scientific). The primary antibody was Anti-Proteasome 20S alpha + beta (Abcam, ab22673). Samples were mounted on microscope slides with Prolong Antifade with DAPI and imaged using a Nikon A1Si Laser Scanning Confocal Microscope.

11.20 BCAT activity assay

The enzymatic activity assay is performed as previously described[365]. CAFs were homogenized in the buffer consisting of 20 mM EDTA, 20 mM EGTA, 0.4% (w/v) CHAPSO, 5 mM DTT, protease inhibitor cocktail, and 25 mM Hepes. The tissue homogenates were then frozen in a -80 °C freezer for one h and then thawed at room temperature. The cellular debris was removed by centrifugation at 15,000g for 10 min at 4 °C. The supernatant is then mixed with reaction buffer containing 10 mM L-leucine, 2 mM NAD^+, and 100 mM sodium carbonate/bicarbonate buffer. The disappearance of absorbance at 340 nm due to NADH oxidation is measured continuously. BCAT activity is quantified by comparing the rate of loss of absorbance at 340 nm in the spectrophotometric assay mixture with or without bacterial leucine dehydrogenase or lacking bacterial leucine dehydrogenase.

11.21 Collagen Uptake

For the collagen uptake assays, cells were cultured with 25 μg/ml Collagen for indicated periods in different media. Subsequently, cells were washed three times with ice-cold PBS and fixed with 4% formaldehyde in PBS for 15 min. After fixation, cells were washed in PBS and mounted using Prolong Antifade + DAPI.

11.22 Proteasome activity assay

Proteasome activity was assessed by using the Cell-Based Proteasome-Glo Assay (Promega, G1180). Cells were trypsinized and plated according to the manufacturer's recommended instructions. Then cell medium was replaced by complete medium, BCAA-deprived medium or medium with 5 ng/ml TGF-β. Luminescence was detected using SpectraMax M5 Microplate Reader (Molecular Devices) after two days.

11.23 Preparation of CAF-derived 3D ECMs

The cell-derived ECMs were generated as previously described[277]. Briefly, confluent CAF cultures were maintained for eight days in the presence of daily added and freshly prepared ascorbic acid and ^{13}C-labeled leucine, isoleucine and valine. Matrices were fixed or decellularized seven days after plating. Cells were extracted from the matrices using 0.5% Triton X-100 (Sigma-Aldrich) and 20 mM NH_4OH. The matrices were washed in PBS three times and then treated with 10 U/ml DNAse (Sigma-Aldrich) in DPBS for 30 minutes at 37°C. Labeled ECM was washed with PBS before plating CAFs; after 48 hours, the media was extracted for LC-MS.

11.24 CTC derived organoid culture

To generate the CTC derived organoid, CAF was first seeded on CAF-derived 3D ECMs one day before. Then the fresh isolated CTC was seeded on the cultures. CTC derived Organoid was cultured as previously described without TGF-β modulators[325], it uses Advanced DMEM/F12 (Gibco) containing 1X antibiotic-antimycotic (Gibco) as the base. Supplements include the following: N-acetyl-L-cysteine (NAC; Sigma-Aldrich),

Gastrin I(Sigma-Aldrich), Nicotinamide (Sigma-Aldrich), R-spondin 1 (Peprotech), EGF(Peprotech) and FGF-10(Peprotech).

11.25 Scanning electron microscopy (SEM)

ECM was fixed in 2.5% glutaraldehyde in PBS at room temperature for one hour and then rinsed with PBS, followed by sequential dehydration with ethanol at concentrations of 50%, 70%, 90%, 95%, and 100% for 10 min each. The specimen was then immersed for 10 min in a solution of 1:1 ethanol: hexamethyldisilazane (HMDS) and then transferred to 100% HMDS, followed by overnight air dry in the hood. The dehydrated specimen attached to double-sided carbon tape is mounted on a SEM stub and coated with gold by sputtering. The ECM was examined by FEI Nova 200 Nanolab Dual-beam FIB scanning electron microscope under low beam energies (2.0-5.0 kV) at the Michigan Center for Materials Characterization (MC2) at the University of Michigan.

11.26 Metabolic flux analysis

11.26.1 Metabolite extraction for in vitro studies

Cells cultured in 6-well plates were quenched with 800 µL of ice-cold methanol/water (1:1) solution containing 1 µg of Norvaline. Cells were scraped while keeping the plate on ice, followed by the addition of 800 µL of chloroform. The cell extracts were transferred to microcentrifuge tubes and vortexed for 30 minutes at 4 °C.

11.26.2 Metabolite extraction from tissue slices

Frozen tissue slices were transferred to Preceyllys CKMix Lysing tubes (Bertin Corp., 03961-1-009) and kept on dry ice. 200 µL of ice-cold methanol/water (1:1) solution containing 1 µg of Norvaline was added to the tubes to submerge the beads and

tissue barely. The samples were homogenized using a Precellys Evolution Homogenizer with the Cryolys attachment to maintain the temperature below 4 °C in the homogenization chamber. Homogenization was achieved using two 30 second cycles at 6000 rpm with a pause of 60 seconds. Additional homogenization cycles were performed only when samples were not homogenized. Following homogenization, an additional 600 µL of ice-cold methanol/water (1:1) solution was added to the tubes, as well as 800 µL of chloroform. The homogenized extracts were transferred to microcentrifuge tubes and vortexed for 30 minutes at 4 °C.

11.26.3 Sample processing for polar metabolites, the amino acid composition of proteins, and lipids

Metabolite extracts were centrifuged at 14,000g for 10 mins to separate the polar phase, protein interphase and chloroform phase. The water/methanol phase containing polar metabolites were transferred to fresh microcentrifuge tubes and dried in a SpeedVac and stored at -80 °C until GC-MS analysis. The chloroform phase containing lipids were transferred to microcentrifuge tubes and dried under nitrogen and stored at -80 °C. The protein layer was rinsed gently with chloroform, then PBS, and the liquid was discarded. The rinsed protein fractions were transferred to glass tubes with sealable caps and subjected to acid hydrolysis with 6M hydrochloric acid at 100 °C for 18-24 hours to obtain constituent amino acids. Hydrolyzed samples were dried under nitrogen and stored at -80 °C until GC-MS analysis.

11.26.4 GC-MS analysis for intracellular polar metabolites and amino acids from hydrolyzed protein

30 µL of methoxyamine hydrochloride (MOX, Thermo Scientific) was added to dried samples and incubated at 30 °C for 2 hours with intermittent vortexing. 45 µL of MBTSTFA+1% TBDMCS was added to the samples and incubated at 55 °C for 1 hour. Derivatized samples were transferred to GC vials with glass inserts and added to the GC-MS autosampler queue. GC-MS analysis was performed using an Agilent 7890 GC equipped with a 30-m HP-5MSUI capillary column connected to an Agilent 5977B MS. For polar metabolites, the following heating cycle was used for the GC oven: 100 °C for three minutes, followed by a ramp of 5 °C/min to 300 °C and held at 300 °C for a total run time of 48 min. Data were acquired in scan mode. The relative abundance of metabolites was calculated from the integrated signal of all potentially labeled ions for each metabolite fragment. Mass Isotopologue Distributions (MID) were corrected for natural abundance using IsoCor before analysis with the model. Metabolite levels were normalized to internal standard Norvaline's signal and quantified using 6-point calibration with external standards for 19 polar metabolites.

11.26.5 LC-MS analysis to quantify BCKA secretion in media samples

Spent culture media samples were collected from culture plates, and 200 µL was transferred to fresh microcentrifuge tubes for metabolic analysis. 800 µL of pre-chilled methanol was added to media samples and kept at -20 °C for 2 hours to deproteinize the samples. The samples were centrifuged at 14,000g for 10 minutes at 4 °C, following which the supernatant was transferred to fresh tubes and dried in the SpeedVac. Media samples were derivatized with 500 µL of 12.5 mM OPD (o-phenylenediamine) solution

in 2M hydrochloric acid. Samples were incubated at 80 °C for 20 minutes and transferred to an ice-bath to terminate the derivatization reaction. The derivatized solution was transferred to microcentrifuge tubes containing 0.08g of sodium sulfate. 500 µL of ethyl acetate was added to the samples, followed by vigorous vortexing and centrifuging at 1000g for 10 minutes. The ethyl acetate phase containing the derivatized ketoacids was transferred to fresh tubes and dried under nitrogen. The dried samples were reconstituted in 200 µL of 200 mM ammonium acetate solution and transferred to LC vials with glass inserts. The samples were analyzed with an Agilent Infinity LC stack using an Agilent Eclipse Plus C18 column (2.1 mm x 100 mm x 1.8 µm) connected to an Agilent 6520 QTOF. The following parameters were used for analysis, 5 mM ammonium acetate as Solvent A, methanol as solvent B, 380 µL/min flow rate, 5-10 µL injection volume, 55% B for 4.2 minutes, ramp B to 95% for 0.9 minutes, retain 95% B for 1.5 minutes, return to initial conditions and equilibrate for 2.5 minutes. The analysis was performed in full-scan mode with the MS in positive ion mode.

11.26.6 Mole Percent Enrichment (MPE)

MPE represents the fractional contribution of ^{13}C from a substrate to intermediate metabolite. It is calculated as follows, where N_C is the number of carbons that can be labeled as ^{13}C, and x_i is the fraction of $(M+i)^{th}$ isotopologue:

$$\mathrm{MPE} = \left(\sum_{i=0}^{N_C} i * x_i \right) / N_C$$

11.26.7 Newly synthesized BCKA flux

To estimate *de novo* synthesized branched-chain ketoacid flux from 13-carbon labeled BCAA, we measure 13-carbon enrichment in respective branched-chain ketoacid much before cells reach isotopic steady-state:

$$\text{BCAA catabolic flux} = \frac{[(\text{13C mean enrichment})_{t=T} - (\text{13C mean enrichment})_{t=0}] * (\text{Intracellular abundance of BCKA})}{(\text{Total cell protein}) * (\text{Time to achieve 13C enrichment, T})}$$

11.27 Statistics and Reproducibility

Data are presented as mean ± s.d. All experiments were repeated twice with similar results unless otherwise stated. Graphpad Prism software V8.4 was used to conduct the statistical analysis of all data. A comparison of the data sets obtained from the different experimental conditions was performed with the two-tailed Student t-test. Comparisons between multiple groups were made using one-way analysis of variance (ANOVA) with Tukey's post hoc comparison, and two-way ANOVA with Dunnett's post-testing for comparisons between multiple groups with independent variables. *$P < 0.0001$ unless otherwise stated.

Bibliography

[1] R.L. Siegel, K.D. Miller, A. Jemal, Cancer statistics, 2020, CA: a cancer journal for clinicians, 70 (2020) 7-30.

[2] L. Rahib, B.D. Smith, R. Aizenberg, A.B. Rosenzweig, J.M. Fleshman, L.M. Matrisian, Projecting cancer incidence and deaths to 2030: the unexpected burden of thyroid, liver, and pancreas cancers in the United States, Cancer research, 74 (2014) 2913-2921.

[3] D. Li, K. Xie, R. Wolff, J.L. Abbruzzese, Pancreatic cancer, Lancet, 363 (2004) 1049-1057.

[4] J. Cicenas, K. Kvederaviciute, I. Meskinyte, E. Meskinyte-Kausiliene, A. Skeberdyte, J. Cicenas, KRAS, TP53, CDKN2A, SMAD4, BRCA1, and BRCA2 Mutations in Pancreatic Cancer, Cancers (Basel), 9 (2017) 42.

[5] S. Yachida, E. Vakiani, C.M. White, Y. Zhong, T. Saunders, R. Morgan, R.F. de Wilde, A. Maitra, J. Hicks, A.M. Demarzo, C. Shi, R. Sharma, D. Laheru, B.H. Edil, C.L. Wolfgang, R.D. Schulick, R.H. Hruban, L.H. Tang, D.S. Klimstra, C.A. Iacobuzio-Donahue, Small cell and large cell neuroendocrine carcinomas of the pancreas are genetically similar and distinct from well-differentiated pancreatic neuroendocrine tumors, Am J Surg Pathol, 36 (2012) 173-184.

[6] J.P.t. Morris, S.C. Wang, M. Hebrok, KRAS, Hedgehog, Wnt and the twisted developmental biology of pancreatic ductal adenocarcinoma, Nature reviews. Cancer, 10 (2010) 683-695.

[7] H. Huang, J. Daniluk, Y. Liu, J. Chu, Z. Li, B. Ji, C.D. Logsdon, Oncogenic K-Ras requires activation for enhanced activity, Oncogene, 33 (2014) 532-535.

[8] X. Xia, W. Wu, C. Huang, G. Cen, T. Jiang, J. Cao, K. Huang, Z. Qiu, SMAD4 and its role in pancreatic cancer, Tumour Biol, 36 (2015) 111-119.

[9] Y. Saiki, A. Horii, Molecular pathology of pancreatic cancer, Pathol Int, 64 (2014) 10-19.

[10] A.K. Win, J.P. Young, N.M. Lindor, K.M. Tucker, D.J. Ahnen, G.P. Young, D.D. Buchanan, M. Clendenning, G.G. Giles, I. Winship, F.A. Macrae, J. Goldblatt, M.C. Southey, J. Arnold, S.N. Thibodeau, S.R. Gunawardena, B. Bapat, J.A. Baron, G. Casey, S. Gallinger, L. Le Marchand, P.A. Newcomb, R.W. Haile, J.L. Hopper, M.A. Jenkins, Colorectal and other cancer risks for carriers and noncarriers from families with a DNA

mismatch repair gene mutation: a prospective cohort study, J Clin Oncol, 30 (2012) 958-964.

[11] N. Howes, M.M. Lerch, W. Greenhalf, D.D. Stocken, I. Ellis, P. Simon, K. Truninger, R. Ammann, G. Cavallini, R.M. Charnley, G. Uomo, M. Delhaye, J. Spicak, B. Drumm, J. Jansen, R. Mountford, D.C. Whitcomb, J.P. Neoptolemos, P. European Registry of Hereditary, C. Pancreatic, Clinical and genetic characteristics of hereditary pancreatitis in Europe, Clin Gastroenterol Hepatol, 2 (2004) 252-261.

[12] A.F. Hezel, A.C. Kimmelman, B.Z. Stanger, N. Bardeesy, R.A. Depinho, Genetics and biology of pancreatic ductal adenocarcinoma, Genes Dev, 20 (2006) 1218-1249.

[13] C.H. Heldin, M. Vanlandewijck, A. Moustakas, Regulation of EMT by TGFbeta in cancer, FEBS Lett, 586 (2012) 1959-1970.

[14] A. Moustakas, C.H. Heldin, The regulation of TGFbeta signal transduction, Development, 136 (2009) 3699-3714.

[15] J. Massague, TGFbeta in Cancer, Cell, 134 (2008) 215-230.

[16] K.J. Gordon, G.C. Blobe, Role of transforming growth factor-beta superfamily signaling pathways in human disease, Biochimica et biophysica acta, 1782 (2008) 197-228.

[17] I.E. Dumitriu, D.R. Dunbar, S.E. Howie, T. Sethi, C.D. Gregory, Human dendritic cells produce TGF-β1 under the influence of lung carcinoma cells and prime the differentiation of CD4+ CD25+ Foxp3+ regulatory T cells, The Journal of Immunology, 182 (2009) 2795-2807.

[18] M.J. Truty, R. Urrutia, Basics of TGF-beta and pancreatic cancer, Pancreatology, 7 (2007) 423-435.

[19] J. Fuxe, M.C. Karlsson, TGF-β-induced epithelial-mesenchymal transition: a link between cancer and inflammation, Seminars in cancer biology, Elsevier, 2012, pp. 455-461.

[20] S. Deng, S. Zhu, B. Wang, X. Li, Y. Liu, Q. Qin, Q. Gong, Y. Niu, C. Xiang, J. Chen, J. Yan, S. Deng, T. Yin, M. Yang, H. Wu, C. Wang, G. Zhao, Chronic pancreatitis and pancreatic cancer demonstrate active epithelial-mesenchymal transition profile, regulated by miR-217-SIRT1 pathway, Cancer letters, 355 (2014) 184-191.

[21] G. Yang, X. Yang, Smad4-mediated TGF-beta signaling in tumorigenesis, Int J Biol Sci, 6 (2010) 1-8.

[22] K. Izeradjene, C. Combs, M. Best, A. Gopinathan, A. Wagner, W.M. Grady, C.-X. Deng, R.H. Hruban, N.V. Adsay, D.A. Tuveson, KrasG12D and Smad4/Dpc4 haploinsufficiency cooperate to induce mucinous cystic neoplasms and invasive adenocarcinoma of the pancreas, Cancer cell, 11 (2007) 229-243.

[23] D. Garcia-Carracedo, C.C. Yu, N. Akhavan, S.A. Fine, F. Schonleben, N. Maehara, D.C. Karg, C. Xie, W. Qiu, R.L. Fine, H.E. Remotti, G.H. Su, Smad4 loss synergizes with TGFalpha overexpression in promoting pancreatic metaplasia, PanIN development, and fibrosis, PLoS One, 10 (2015) e0120851.

[24] C. Recio, A. Oguiza, B. Mallavia, I. Lazaro, G. Ortiz-Munoz, O. Lopez-Franco, J. Egido, C. Gomez-Guerrero, Gene delivery of suppressors of cytokine signaling (SOCS) inhibits inflammation and atherosclerosis development in mice, Basic Res Cardiol, 110 (2015) 8.

[25] J. Wang, H. Zhou, Y. Han, X. Liu, M. Wang, X. Wang, G. Yin, X. Li, M. Xiang, SOCS3 methylation in synergy with Reg3A overexpression promotes cell growth in pancreatic cancer, J Mol Med (Berl), 92 (2014) 1257-1269.

[26] H. Yu, H. Lee, A. Herrmann, R. Buettner, R. Jove, Revisiting STAT3 signalling in cancer: new and unexpected biological functions, Nature reviews. Cancer, 14 (2014) 736-746.

[27] X. Liu, J. Wang, H. Wang, G. Yin, Y. Liu, X. Lei, M. Xiang, REG3A accelerates pancreatic cancer cell growth under IL-6-associated inflammatory condition: Involvement of a REG3A-JAK2/STAT3 positive feedback loop, Cancer letters, 362 (2015) 45-60.

[28] R. Jaster, G. Sparmann, J. Emmrich, S. Liebe, Extracellular signal regulated kinases are key mediators of mitogenic signals in rat pancreatic stellate cells, Gut, 51 (2002) 579-584.

[29] A. Masamune, K. Kikuta, M. Satoh, K. Kume, T. Shimosegawa, Differential roles of signaling pathways for proliferation and migration of rat pancreatic stellate cells, Tohoku J Exp Med, 199 (2003) 69-84.

[30] C.I. Schwer, P. Stoll, U. Goebel, H. Buerkle, A. Hoetzel, R. Schmidt, Effects of hydrogen sulfide on rat pancreatic stellate cells, Pancreas, 41 (2012) 74-83.

[31] R. Reinehr, S. Zoller, H. Klonowski-Stumpe, C. Kordes, D. Haussinger, Effects of angiotensin II on rat pancreatic stellate cells, Pancreas, 28 (2004) 129-137.

[32] A. Masamune, K. Kikuta, N. Suzuki, M. Satoh, K. Satoh, T. Shimosegawa, A c-Jun NH2-terminal kinase inhibitor SP600125 (anthra[1,9-cd]pyrazole-6 (2H)-one) blocks activation of pancreatic stellate cells, J Pharmacol Exp Ther, 310 (2004) 520-527.

[33] X. Gao, Y. Cao, D.A. Staloch, M.A. Gonzales, J.F. Aronson, C. Chao, M.R. Hellmich, T.C. Ko, Bone morphogenetic protein signaling protects against cerulein-induced pancreatic fibrosis, PLoS One, 9 (2014) e89114.

[34] Y. Nomiyama, M. Tashiro, T. Yamaguchi, S. Watanabe, M. Taguchi, H. Asaumi, H. Nakamura, M. Otsuki, High glucose activates rat pancreatic stellate cells through protein

kinase C and p38 mitogen-activated protein kinase pathway, Pancreas, 34 (2007) 364-372.

[35] N. Dhillon, B.B. Aggarwal, R.A. Newman, R.A. Wolff, A.B. Kunnumakkara, J.L. Abbruzzese, C.S. Ng, V. Badmaev, R. Kurzrock, Phase II trial of curcumin in patients with advanced pancreatic cancer, Clinical cancer research : an official journal of the American Association for Cancer Research, 14 (2008) 4491-4499.

[36] A. Arlt, S.S. Muerkoster, H. Schafer, Targeting apoptosis pathways in pancreatic cancer, Cancer letters, 332 (2013) 346-358.

[37] J. Niu, Z. Li, B. Peng, P.J. Chiao, Identification of an autoregulatory feedback pathway involving interleukin-1alpha in induction of constitutive NF-kappaB activation in pancreatic cancer cells, The Journal of biological chemistry, 279 (2004) 16452-16462.

[38] G.M. Sclabas, T. Uwagawa, C. Schmidt, K.R. Hess, D.B. Evans, J.L. Abbruzzese, P.J. Chiao, Nuclear factor kappa B activation is a potential target for preventing pancreatic carcinoma by aspirin, Cancer, 103 (2005) 2485-2490.

[39] H. Nakashima, M. Nakamura, H. Yamaguchi, N. Yamanaka, T. Akiyoshi, K. Koga, K. Yamaguchi, M. Tsuneyoshi, M. Tanaka, M. Katano, Nuclear factor-κB contributes to hedgehog signaling pathway activation through sonic hedgehog induction in pancreatic cancer, Cancer research, 66 (2006) 7041-7049.

[40] H. Chua, P. Bhat-Nakshatri, S. Clare, A. Morimiya, S. Badve, H. Nakshatri, NF-κ B represses E-cadherin expression and enhances epithelial to mesenchymal transition of mammary epithelial cells: potential involvement of ZEB-1 and ZEB-2, Oncogene, 26 (2007) 711-724.

[41] M.A. Huber, N. Azoitei, B. Baumann, S. Grünert, A. Sommer, H. Pehamberger, N. Kraut, H. Beug, T. Wirth, NF-κB is essential for epithelial-mesenchymal transition and metastasis in a model of breast cancer progression, The Journal of clinical investigation, 114 (2004) 569-581.

[42] D. Zhang, H. Lee, X. Wang, A. Rai, M. Groot, Y. Jin, Exosome-Mediated Small RNA Delivery: A Novel Therapeutic Approach for Inflammatory Lung Responses, Mol Ther, 26 (2018) 2119-2130.

[43] A. Ochi, C.S. Graffeo, C.P. Zambirinis, A. Rehman, M. Hackman, N. Fallon, R.M. Barilla, J.R. Henning, M. Jamal, R. Rao, S. Greco, M. Deutsch, M.V. Medina-Zea, U. Bin Saeed, M.O. Ego-Osuala, C. Hajdu, G. Miller, Toll-like receptor 7 regulates pancreatic carcinogenesis in mice and humans, J Clin Invest, 122 (2012) 4118-4129.

[44] A. Ochi, A.H. Nguyen, A.S. Bedrosian, H.M. Mushlin, S. Zarbakhsh, R. Barilla, C.P. Zambirinis, N.C. Fallon, A. Rehman, Y. Pylayeva-Gupta, S. Badar, C.H. Hajdu, A.B. Frey, D. Bar-Sagi, G. Miller, MyD88 inhibition amplifies dendritic cell capacity to promote pancreatic carcinogenesis via Th2 cells, The Journal of experimental medicine, 209 (2012) 1671-1687.

[45] M. Ikebe, Y. Kitaura, M. Nakamura, H. Tanaka, A. Yamasaki, S. Nagai, J. Wada, K. Yanai, K. Koga, N. Sato, Lipopolysaccharide (LPS) increases the invasive ability of pancreatic cancer cells through the TLR4/MyD88 signaling pathway, Journal of surgical oncology, 100 (2009) 725-731.

[46] T. Eigenbrod, A.H. Dalpke, TLR7 inhibition: A novel strategy for pancreatic cancer treatment?, JAKSTAT, 2 (2013) e23011.

[47] A. Li, N. Omura, S.M. Hong, A. Vincent, K. Walter, M. Griffith, M. Borges, M. Goggins, Pancreatic cancers epigenetically silence SIP1 and hypomethylate and overexpress miR-200a/200b in association with elevated circulating miR-200a and miR-200b levels, Cancer research, 70 (2010) 5226-5237.

[48] A. Li, J. Yu, H. Kim, C.L. Wolfgang, M.I. Canto, R.H. Hruban, M. Goggins, MicroRNA array analysis finds elevated serum miR-1290 accurately distinguishes patients with low-stage pancreatic cancer from healthy and disease controls, Clinical cancer research : an official journal of the American Association for Cancer Research, 19 (2013) 3600-3610.

[49] C.G. Ioannides, T.L. Whiteside, T cell recognition of human tumors: implications for molecular immunotherapy of cancer, Clin Immunol Immunopathol, 66 (1993) 91-106.

[50] Z. Zhu, A. Achreja, N. Meurs, O. Animasahun, S. Owen, A. Mittal, P. Parikh, T.W. Lo, J. Franco-Barraza, J. Shi, V. Gunchick, M.H. Sherman, E. Cukierman, A.M. Pickering, A. Maitra, V. Sahai, M.A. Morgan, S. Nagrath, T.S. Lawrence, D. Nagrath, Tumour-reprogrammed stromal BCAT1 fuels branched-chain ketoacid dependency in stromal-rich PDAC tumours, Nat Metab, 2 (2020) 775-792.

[51] M.G. Bachem, E. Schneider, H. Gross, H. Weidenbach, R.M. Schmid, A. Menke, M. Siech, H. Beger, A. Grunert, G. Adler, Identification, culture, and characterization of pancreatic stellate cells in rats and humans, Gastroenterology, 115 (1998) 421-432.

[52] M.G. Bachem, M. Schunemann, M. Ramadani, M. Siech, H. Beger, A. Buck, S. Zhou, A. Schmid-Kotsas, G. Adler, Pancreatic carcinoma cells induce fibrosis by stimulating proliferation and matrix synthesis of stellate cells, Gastroenterology, 128 (2005) 907-921.

[53] H.-x. Zhan, B. Zhou, Y.-g. Cheng, J.-w. Xu, L. Wang, G.-y. Zhang, S.-y. Hu, Crosstalk between stromal cells and cancer cells in pancreatic cancer: new insights into stromal biology, Cancer letters, 392 (2017) 83-93.

[54] K. Koikawa, K. Ohuchida, Y. Ando, S. Kibe, H. Nakayama, S. Takesue, S. Endo, T. Abe, T. Okumura, C. Iwamoto, T. Moriyama, K. Nakata, Y. Miyasaka, T. Ohtsuka, E. Nagai, K. Mizumoto, M. Hashizume, M. Nakamura, Basement membrane destruction by pancreatic stellate cells leads to local invasion in pancreatic ductal adenocarcinoma, Cancer letters, 425 (2018) 65-77.

[55] B. Garg, B. Giri, S. Modi, V. Sethi, I. Castro, O. Umland, Y. Ban, S. Lavania, R. Dawra, S. Banerjee, S. Vickers, N.B. Merchant, S.X. Chen, E. Gilboa, S. Ramakrishnan, A. Saluja, V. Dudeja, NFkappaB in Pancreatic Stellate Cells Reduces Infiltration of Tumors by Cytotoxic T Cells and Killing of Cancer Cells, via Up-regulation of CXCL12, Gastroenterology, 155 (2018) 880-891 e888.

[56] R.A. Hesler, J.J. Huang, M.D. Starr, V.M. Treboschi, A.G. Bernanke, A.B. Nixon, S.J. McCall, R.R. White, G.C. Blobe, TGF-β-induced stromal CYR61 promotes resistance to gemcitabine in pancreatic ductal adenocarcinoma through downregulation of the nucleoside transporters hENT1 and hCNT3, Carcinogenesis, 37 (2016) 1041-1051.

[57] C.K. Looi, F.F. Chung, C.O. Leong, S.F. Wong, R. Rosli, C.W. Mai, Therapeutic challenges and current immunomodulatory strategies in targeting the immunosuppressive pancreatic tumor microenvironment, J Exp Clin Cancer Res, 38 (2019) 162.

[58] M. Quante, S.P. Tu, H. Tomita, T. Gonda, S.S. Wang, S. Takashi, G.H. Baik, W. Shibata, B. Diprete, K.S. Betz, R. Friedman, A. Varro, B. Tycko, T.C. Wang, Bone marrow-derived myofibroblasts contribute to the mesenchymal stem cell niche and promote tumor growth, Cancer cell, 19 (2011) 257-272.

[59] N. Ishii, K. Araki, T. Yokobori, K. Hagiwara, D. Gantumur, T. Yamanaka, T. Handa, M. Tsukagoshi, T. Igarashi, A. Watanabe, N. Kubo, N. Harimoto, A. Masamune, K. Umezawa, H. Kuwano, K. Shirabe, Conophylline suppresses pancreatic cancer desmoplasia and cancer-promoting cytokines produced by cancer-associated fibroblasts, Cancer Sci, 110 (2019) 334-344.

[60] K.E. Richards, A.E. Zeleniak, M.L. Fishel, J. Wu, L.E. Littlepage, R. Hill, Cancer-associated fibroblast exosomes regulate survival and proliferation of pancreatic cancer cells, Oncogene, 36 (2017) 1770-1778.

[61] J. Gu, H. Saiyin, D. Fu, J. Li, Stroma—A double-edged sword in pancreatic cancer: A lesson from targeting stroma in pancreatic cancer with Hedgehog signaling inhibitors, Pancreas, 47 (2018) 382-389.

[62] C. Qu, Q. Wang, Z. Meng, P. Wang, Cancer-associated fibroblasts in pancreatic Cancer: should they be deleted or reeducated?, Integrative cancer therapies, 17 (2018) 1016-1019.

[63] X.B. Cheng, S. Kohi, A. Koga, K. Hirata, N. Sato, Hyaluronan stimulates pancreatic cancer cell motility, Oncotarget, 7 (2016) 4829-4840.

[64] E. Yoshida, D. Kudo, H. Nagase, A. Suto, H. Shimoda, S. Suto, I. Kakizaki, M. Endo, K. Hakamada, 4-Methylumbelliferone Decreases the Hyaluronan-rich Extracellular Matrix and Increases the Effectiveness of 5-Fluorouracil, Anticancer Res, 38 (2018) 5799-5804.

[65] G.J. Doherty, M. Tempero, P.G. Corrie, HALO-109-301: a Phase III trial of PEGPH20 (with gemcitabine and nab-paclitaxel) in hyaluronic acid-high stage IV pancreatic cancer, Future Oncol, 14 (2018) 13-22.

[66] A. Suto, D. Kudo, E. Yoshida, H. Nagase, S. Suto, J. Mimura, K. Itoh, K. Hakamada, Increase of Tumor Infiltrating γδ T-cells in Pancreatic Ductal Adenocarcinoma Through Remodeling of the Extracellular Matrix by a Hyaluronan Synthesis Suppressor, 4-Methylumbelliferone, Pancreas, 48 (2019) 292-298.

[67] A.D. Rhim, P.E. Oberstein, D.H. Thomas, E.T. Mirek, C.F. Palermo, S.A. Sastra, E.N. Dekleva, T. Saunders, C.P. Becerra, I.W. Tattersall, Stromal elements act to restrain, rather than support, pancreatic ductal adenocarcinoma, Cancer cell, 25 (2014) 735-747.

[68] N. Wang, H. Liang, K. Zen, Molecular mechanisms that influence the macrophage M1–M2 polarization balance, Frontiers in immunology, 5 (2014) 614.

[69] A. Schmieder, J. Michel, K. Schönhaar, S. Goerdt, K. Schledzewski, Differentiation and gene expression profile of tumor-associated macrophages, Seminars in cancer biology, Elsevier, 2012, pp. 289-297.

[70] K. Kuwada, S. Kagawa, R. Yoshida, S. Sakamoto, A. Ito, M. Watanabe, T. Ieda, S. Kuroda, S. Kikuchi, H. Tazawa, T. Fujiwara, The epithelial-to-mesenchymal transition induced by tumor-associated macrophages confers chemoresistance in peritoneally disseminated pancreatic cancer, J Exp Clin Cancer Res, 37 (2018) 307.

[71] J.B. Mitchem, D.J. Brennan, B.L. Knolhoff, B.A. Belt, Y. Zhu, D.E. Sanford, L. Belaygorod, D. Carpenter, L. Collins, D. Piwnica-Worms, S. Hewitt, G.M. Udupi, W.M. Gallagher, C. Wegner, B.L. West, A. Wang-Gillam, P. Goedegebuure, D.C. Linehan, D.G. DeNardo, Targeting tumor-infiltrating macrophages decreases tumor-initiating cells, relieves immunosuppression, and improves chemotherapeutic responses, Cancer research, 73 (2013) 1128-1141.

[72] L. Yao, M. Wang, Z. Niu, Q. Liu, X. Gao, L. Zhou, Q. Liao, Y. Zhao, Interleukin-27 inhibits malignant behaviors of pancreatic cancer cells by targeting M2 polarized tumor associated macrophages, Cytokine, 89 (2017) 194-200.

[73] T.A. Moo-Young, J.W. Larson, B.A. Belt, M.C. Tan, W.G. Hawkins, T.J. Eberlein, P.S. Goedegebuure, D.C. Linehan, Tumor-derived TGF-beta mediates conversion of CD4+Foxp3+ regulatory T cells in a murine model of pancreas cancer, J Immunother, 32 (2009) 12-21.

[74] C.M. Paluskievicz, X. Cao, R. Abdi, P. Zheng, Y. Liu, J.S. Bromberg, T Regulatory Cells and Priming the Suppressive Tumor Microenvironment, Frontiers in immunology, 10 (2019) 2453.

[75] X. Cao, S.F. Cai, T.A. Fehniger, J. Song, L.I. Collins, D.R. Piwnica-Worms, T.J. Ley, Granzyme B and perforin are important for regulatory T cell-mediated suppression of tumor clearance, Immunity, 27 (2007) 635-646.

[76] C.A. Bauer, E.Y. Kim, F. Marangoni, E. Carrizosa, N.M. Claudio, T.R. Mempel, Dynamic Treg interactions with intratumoral APCs promote local CTL dysfunction, J Clin Invest, 124 (2014) 2425-2440.

[77] L.C. Sandin, F. Eriksson, P. Ellmark, A.S. Loskog, T.H. Totterman, S.M. Mangsbo, Local CTLA4 blockade effectively restrains experimental pancreatic adenocarcinoma growth in vivo, Oncoimmunology, 3 (2014) e27614.

[78] D.I. Gabrilovich, Myeloid-Derived Suppressor Cells, Cancer Immunol Res, 5 (2017) 3-8.

[79] M. Karin, F.R. Greten, NF-kappaB: linking inflammation and immunity to cancer development and progression, Nat Rev Immunol, 5 (2005) 749-759.

[80] B. Huang, P.Y. Pan, Q. Li, A.I. Sato, D.E. Levy, J. Bromberg, C.M. Divino, S.H. Chen, Gr-1+CD115+ immature myeloid suppressor cells mediate the development of tumor-induced T regulatory cells and T-cell anergy in tumor-bearing host, Cancer research, 66 (2006) 1123-1131.

[81] M. Feng, G. Xiong, Z. Cao, G. Yang, S. Zheng, X. Song, L. You, L. Zheng, T. Zhang, Y. Zhao, PD-1/PD-L1 and immunotherapy for pancreatic cancer, Cancer letters, 407 (2017) 57-65.

[82] I.M. Stromnes, J.S. Brockenbrough, K. Izeradjene, M.A. Carlson, C. Cuevas, R.M. Simmons, P.D. Greenberg, S.R. Hingorani, Targeted depletion of an MDSC subset unmasks pancreatic ductal adenocarcinoma to adaptive immunity, Gut, 63 (2014) 1769-1781.

[83] S. Nagrath, L.V. Sequist, S. Maheswaran, D.W. Bell, D. Irimia, L. Ulkus, M.R. Smith, E.L. Kwak, S. Digumarthy, A. Muzikansky, P. Ryan, U.J. Balis, R.G. Tompkins, D.A. Haber, M. Toner, Isolation of rare circulating tumour cells in cancer patients by microchip technology, Nature, 450 (2007) 1235-1239.

[84] N. Aceto, A. Bardia, D.T. Miyamoto, M.C. Donaldson, B.S. Wittner, J.A. Spencer, M. Yu, A. Pely, A. Engstrom, H. Zhu, B.W. Brannigan, R. Kapur, S.L. Stott, T. Shioda, S. Ramaswamy, D.T. Ting, C.P. Lin, M. Toner, D.A. Haber, S. Maheswaran, Circulating tumor cell clusters are oligoclonal precursors of breast cancer metastasis, Cell, 158 (2014) 1110-1122.

[85] R. Harouaka, Z. Kang, S.Y. Zheng, L. Cao, Circulating tumor cells: advances in isolation and analysis, and challenges for clinical applications, Pharmacol Ther, 141 (2014) 209-221.

[86] S.C. Wong, C.M. Chan, B.B. Ma, E.P. Hui, S.S. Ng, P.B. Lai, M.T. Cheung, E.S. Lo, A.K. Chan, M.Y. Lam, T.C. Au, A.T. Chan, Clinical significance of cytokeratin 20-positive circulating tumor cells detected by a refined immunomagnetic enrichment assay in colorectal cancer patients, Clinical cancer research : an official journal of the American Association for Cancer Research, 15 (2009) 1005-1012.

[87] K. Pachmann, O. Camara, A. Kavallaris, S. Krauspe, N. Malarski, M. Gajda, T. Kroll, C. Jorke, U. Hammer, A. Altendorf-Hofmann, Monitoring the response of circulating epithelial tumor cells to adjuvant chemotherapy in breast cancer allows detection of patients at risk of early relapse, Journal of clinical oncology, 26 (2008) 1208-1215.

[88] T.M. Morgan, P.H. Lange, M.P. Porter, D.W. Lin, W.J. Ellis, I.S. Gallaher, R.L. Vessella, Disseminated tumor cells in prostate cancer patients after radical prostatectomy and without evidence of disease predicts biochemical recurrence, Clinical cancer research, 15 (2009) 677-683.

[89] N.M. Karabacak, P.S. Spuhler, F. Fachin, E.J. Lim, V. Pai, E. Ozkumur, J.M. Martel, N. Kojic, K. Smith, P.I. Chen, J. Yang, H. Hwang, B. Morgan, J. Trautwein, T.A. Barber, S.L. Stott, S. Maheswaran, R. Kapur, D.A. Haber, M. Toner, Microfluidic, marker-free isolation of circulating tumor cells from blood samples, Nature protocols, 9 (2014) 694-710.

[90] T.W. Lo, Z. Zhu, E. Purcell, D. Watza, J. Wang, Y.T. Kang, S. Jolly, D. Nagrath, S. Nagrath, Microfluidic device for high-throughput affinity-based isolation of extracellular vesicles, Lab Chip, 20 (2020) 1762-1770.

[91] R. Konigsberg, E. Obermayr, G. Bises, G. Pfeiler, M. Gneist, F. Wrba, M. de Santis, R. Zeillinger, M. Hudec, C. Dittrich, Detection of EpCAM positive and negative circulating tumor cells in metastatic breast cancer patients, Acta Oncol, 50 (2011) 700-710.

[92] M. Cegan, K. Kolostova, R. Matkowski, M. Broul, J. Schraml, M. Fiutowski, V. Bobek, In vitro culturing of viable circulating tumor cells of urinary bladder cancer, Int J Clin Exp Pathol, 7 (2014) 7164-7171.

[93] H.W. Hou, M.E. Warkiani, B.L. Khoo, Z.R. Li, R.A. Soo, D.S.-W. Tan, W.-T. Lim, J. Han, A.A.S. Bhagat, C.T. Lim, Isolation and retrieval of circulating tumor cells using centrifugal forces, Scientific reports, 3 (2013) 1259.

[94] T. Yeo, S.J. Tan, C.L. Lim, D.P. Lau, Y.W. Chua, S.S. Krisna, G. Iyer, G.S. Tan, T.K. Lim, D.S. Tan, W.T. Lim, C.T. Lim, Microfluidic enrichment for the single cell analysis of circulating tumor cells, Sci Rep, 6 (2016) 22076.

[95] T.L. Halo, K.M. McMahon, N.L. Angeloni, Y. Xu, W. Wang, A.B. Chinen, D. Malin, E. Strekalova, V.L. Cryns, C. Cheng, C.A. Mirkin, C.S. Thaxton, NanoFlares for the detection, isolation, and culture of live tumor cells from human blood, Proceedings of the National Academy of Sciences of the United States of America, 111 (2014) 17104-17109.

[96] J.T. Kaifi, M. Kunkel, A. Das, R.A. Harouaka, D.T. Dicker, G. Li, J. Zhu, G.A. Clawson, Z. Yang, M.F. Reed, N.J. Gusani, E.T. Kimchi, K.F. Staveley-O'Carroll, S.Y. Zheng, W.S. El-Deiry, Circulating tumor cell isolation during resection of colorectal

cancer lung and liver metastases: a prospective trial with different detection techniques, Cancer Biol Ther, 16 (2015) 699-708.

[97] A. Satelli, A. Mitra, Z. Brownlee, X. Xia, S. Bellister, M.J. Overman, S. Kopetz, L.M. Ellis, Q.H. Meng, S. Li, Epithelial-mesenchymal transitioned circulating tumor cells capture for detecting tumor progression, Clinical cancer research : an official journal of the American Association for Cancer Research, 21 (2015) 899-906.

[98] S. Lamouille, J. Xu, R. Derynck, Molecular mechanisms of epithelial-mesenchymal transition, Nature reviews. Molecular cell biology, 15 (2014) 178-196.

[99] M.A. Nieto, The ins and outs of the epithelial to mesenchymal transition in health and disease, Annu Rev Cell Dev Biol, 27 (2011) 347-376.

[100] J.W. Uhr, K. Pantel, Controversies in clinical cancer dormancy, Proceedings of the National Academy of Sciences of the United States of America, 108 (2011) 12396-12400.

[101] H. Liu, G. Ren, T. Wang, Y. Chen, C. Gong, Y. Bai, B. Wang, H. Qi, J. Shen, L. Zhu, Aberrantly expressed Fra-1 by IL-6/STAT3 transactivation promotes colorectal cancer aggressiveness through epithelial–mesenchymal transition, Carcinogenesis, 36 (2015) 459-468.

[102] H.J. Maier, U. Schmidt-Strassburger, M.A. Huber, E.M. Wiedemann, H. Beug, T. Wirth, NF-kappaB promotes epithelial-mesenchymal transition, migration and invasion of pancreatic carcinoma cells, Cancer letters, 295 (2010) 214-228.

[103] K. Gu, M.M. Li, J. Shen, F. Liu, J.Y. Cao, S. Jin, Y. Yu, Interleukin-17-induced EMT promotes lung cancer cell migration and invasion via NF-kappaB/ZEB1 signal pathway, Am J Cancer Res, 5 (2015) 1169-1179.

[104] M. Chanrion, I. Kuperstein, C. Barriere, F. El Marjou, D. Cohen, D. Vignjevic, L. Stimmer, P. Paul-Gilloteaux, I. Bieche, R. Tavares Sdos, G.F. Boccia, W. Cacheux, D. Meseure, S. Fre, L. Martignetti, P. Legoix-Ne, E. Girard, L. Fetler, E. Barillot, D. Louvard, A. Zinovyev, S. Robine, Concomitant Notch activation and p53 deletion trigger epithelial-to-mesenchymal transition and metastasis in mouse gut, Nat Commun, 5 (2014) 5005.

[105] X. Yang, S. Liu, Q. Yan, Role of fucosyltransferase IV in epithelial-mesenchymal transition in breast cancer cells, Cell Death Dis, 4 (2013) e735.

[106] A.V. Salnikov, L. Liu, M. Platen, J. Gladkich, O. Salnikova, E. Ryschich, J. Mattern, G. Moldenhauer, J. Werner, P. Schemmer, M.W. Buchler, I. Herr, Hypoxia induces EMT in low and highly aggressive pancreatic tumor cells but only cells with cancer stem cell characteristics acquire pronounced migratory potential, PLoS One, 7 (2012) e46391.

[107] X. Zheng, J.L. Carstens, J. Kim, M. Scheible, J. Kaye, H. Sugimoto, C.-C. Wu, V.S. LeBleu, R. Kalluri, Epithelial-to-mesenchymal transition is dispensable for metastasis but induces chemoresistance in pancreatic cancer, Nature, 527 (2015) 525-530.

[108] S. Zheng, Y. Liu, Y. Jiao, M. Wei, X. Zeng, Chemically modified heparins inhibit fibrinogen-bridged indirect adhesion between tumor cells and platelets, Oncology letters, 3 (2012) 497-502.

[109] S.B. Willingham, J.-P. Volkmer, A.J. Gentles, D. Sahoo, P. Dalerba, S.S. Mitra, J. Wang, H. Contreras-Trujillo, R. Martin, J.D. Cohen, The CD47-signal regulatory protein alpha (SIRPa) interaction is a therapeutic target for human solid tumors, Proceedings of the National Academy of Sciences, 109 (2012) 6662-6667.

[110] M. Mardani, A. AndishehTadbir, B. Khademi, M. Melekzadeh, L. Vaziri, Decreased Serum Monocyte Chemoattractant Protein1 in Salivary Gland Tumor Patients, Asian Pac J Cancer Prev, 17 (2016) 3601-3604.

[111] Y.S. Rocca, M.P. Roberti, E.P. Juliá, M.B. Pampena, L. Bruno, S. Rivero, E. Huertas, F. Sánchez Loria, A. Pairola, A. Caignard, Phenotypic and functional dysregulated blood NK cells in colorectal cancer patients can be activated by cetuximab plus IL-2 or IL-15, Frontiers in immunology, 7 (2016) 413.

[112] G.J. Villares, M. Zigler, A.S. Dobroff, H. Wang, R. Song, V.O. Melnikova, L. Huang, R.R. Braeuer, M. Bar-Eli, Protease activated receptor-1 inhibits the Maspin tumor-suppressor gene to determine the melanoma metastatic phenotype, Proceedings of the National Academy of Sciences of the United States of America, 108 (2011) 626-631.

[113] T.T. Li, H. Liu, F.P. Li, Y.F. Hu, T.Y. Mou, T. Lin, J. Yu, L. Zheng, G.X. Li, Evaluation of epithelial-mesenchymal transitioned circulating tumor cells in patients with resectable gastric cancer: Relevance to therapy response, World journal of gastroenterology, 21 (2015) 13259-13267.

[114] J.F. Chen, H. Ho, J. Lichterman, Y.T. Lu, Y. Zhang, M.A. Garcia, S.F. Chen, A.J. Liang, E. Hodara, H.E. Zhau, Subclassification of prostate cancer circulating tumor cells by nuclear size reveals very small nuclear circulating tumor cells in patients with visceral metastases, Cancer, 121 (2015) 3240-3251.

[115] R. Rostoker, S. Abelson, I. Genkin, S. Ben-Shmuel, R. Sachidanandam, E.J. Scheinman, K. Bitton-Worms, Z.S. Orr, A. Caspi, M. Tzukerman, D. LeRoith, CD24(+) cells fuel rapid tumor growth and display high metastatic capacity, Breast Cancer Res, 17 (2015) 78.

[116] J.M. Pavese, R.C. Bergan, Circulating tumor cells exhibit a biologically aggressive cancer phenotype accompanied by selective resistance to chemotherapy, Cancer letters, 352 (2014) 179-186.

[117] E. Pailler, N. Auger, C.R. Lindsay, P. Vielh, A. Islas-Morris-Hernandez, I. Borget, M. Ngo-Camus, D. Planchard, J.C. Soria, B. Besse, F. Farace, High level of chromosomal instability in circulating tumor cells of ROS1-rearranged non-small-cell lung cancer, Ann Oncol, 26 (2015) 1408-1415.

[118] Z. Krska, J. Svab, D. Hoskovec, J. Ulrych, Pancreatic Cancer Diagnostics and Treatment--Current State, Prague Med Rep, 116 (2015) 253-267.

[119] M.J. Duffy, C. Sturgeon, R. Lamerz, C. Haglund, V.L. Holubec, R. Klapdor, A. Nicolini, O. Topolcan, V. Heinemann, Tumor markers in pancreatic cancer: a European Group on Tumor Markers (EGTM) status report, Ann Oncol, 21 (2010) 441-447.

[120] W.J. Allard, J. Matera, M.C. Miller, M. Repollet, M.C. Connelly, C. Rao, A.G. Tibbe, J.W. Uhr, L.W. Terstappen, Tumor cells circulate in the peripheral blood of all major carcinomas but not in healthy subjects or patients with nonmalignant diseases, Clinical cancer research, 10 (2004) 6897-6904.

[121] T.M. Gall, A.E. Frampton, J. Krell, J. Jacob, J. Stebbing, L.R. Jiao, Is the detection of circulating tumor cells in locally advanced pancreatic cancer a useful prognostic marker?, Expert review of molecular diagnostics, 13 (2013) 793-796.

[122] B. Kulemann, M.B. Pitman, A.S. Liss, N. Valsangkar, C. Fernández-del Castillo, K.D. Lillemoe, J. Hoeppner, M. Mino-Kenudson, A.L. Warshaw, S.P. Thayer, Circulating tumor cells found in patients with localized and advanced pancreatic cancer, Pancreas, 44 (2015) 547-550.

[123] Y. Zhang, F. Wang, N. Ning, Q. Chen, Z. Yang, Y. Guo, D. Xu, D. Zhang, T. Zhan, W. Cui, Patterns of circulating tumor cells identified by CEP8, CK and CD45 in pancreatic cancer, Int J Cancer, 136 (2015) 1228-1233.

[124] J. Zhou, L. Hu, Z. Yu, J. Zheng, D. Yang, M. Bouvet, R.M. Hoffman, Marker expression in circulating cancer cells of pancreatic cancer patients, J Surg Res, 171 (2011) 631-636.

[125] J. Ankeny, C. Court, S. Hou, Q. Li, M. Song, D. Wu, J. Chen, T. Lee, M. Lin, S. Sho, Circulating tumour cells as a biomarker for diagnosis and staging in pancreatic cancer, British journal of cancer, 114 (2016) 1367-1375.

[126] O. Warburg, On the origin of cancer cells, Science (New York, N.Y.), 123 (1956) 309-314.

[127] O. Warburg, F. Wind, E. Negelein, The Metabolism of Tumors in the Body, J Gen Physiol, 8 (1927) 519-530.

[128] D. Hanahan, R.A. Weinberg, Hallmarks of cancer: the next generation, Cell, 144 (2011) 646-674.

[129] A. Kinnaird, E.D. Michelakis, Metabolic modulation of cancer: a new frontier with great translational potential, J Mol Med (Berl), 93 (2015) 127-142.

[130] J.M. Brown, W.R. Wilson, Exploiting tumour hypoxia in cancer treatment, Nature reviews. Cancer, 4 (2004) 437-447.

[131] A.L. Harris, Hypoxia--a key regulatory factor in tumour growth, Nature reviews. Cancer, 2 (2002) 38-47.

[132] W. Luo, H. Hu, R. Chang, J. Zhong, M. Knabel, R. O'Meally, R.N. Cole, A. Pandey, G.L. Semenza, Pyruvate kinase M2 is a PHD3-stimulated coactivator for hypoxia-inducible factor 1, Cell, 145 (2011) 732-744.

[133] N. Hay, Reprogramming glucose metabolism in cancer: can it be exploited for cancer therapy?, Nature Reviews Cancer, 16 (2016) 635.

[134] H. Zhang, P. Gao, R. Fukuda, G. Kumar, B. Krishnamachary, K.I. Zeller, C.V. Dang, G.L. Semenza, HIF-1 inhibits mitochondrial biogenesis and cellular respiration in VHL-deficient renal cell carcinoma by repression of C-MYC activity, Cancer cell, 11 (2007) 407-420.

[135] H. Zhang, M. Bosch-Marce, L.A. Shimoda, Y.S. Tan, J.H. Baek, J.B. Wesley, F.J. Gonzalez, G.L. Semenza, Mitochondrial autophagy is an HIF-1-dependent adaptive metabolic response to hypoxia, Journal of Biological Chemistry, 283 (2008) 10892-10903.

[136] C.V. Dang, J.-w. Kim, P. Gao, J. Yustein, The interplay between MYC and HIF in cancer, Nature Reviews Cancer, 8 (2008) 51-56.

[137] S. Hu, A. Balakrishnan, R.A. Bok, B. Anderton, P.E. Larson, S.J. Nelson, J. Kurhanewicz, D.B. Vigneron, A. Goga, 13C-pyruvate imaging reveals alterations in glycolysis that precede c-Myc-induced tumor formation and regression, Cell metabolism, 14 (2011) 131-142.

[138] R.A. Gatenby, R.J. Gillies, A microenvironmental model of carcinogenesis, Nature reviews. Cancer, 8 (2008) 56-61.

[139] S. Hui, J.M. Ghergurovich, R.J. Morscher, C. Jang, X. Teng, W. Lu, L.A. Esparza, T. Reya, Z. Le, J. Yanxiang Guo, E. White, J.D. Rabinowitz, Glucose feeds the TCA cycle via circulating lactate, Nature, 551 (2017) 115-118.

[140] H.R. Christofk, M.G. Vander Heiden, M.H. Harris, A. Ramanathan, R.E. Gerszten, R. Wei, M.D. Fleming, S.L. Schreiber, L.C. Cantley, The M2 splice isoform of pyruvate kinase is important for cancer metabolism and tumour growth, Nature, 452 (2008) 230-233.

[141] C.J. David, M. Chen, M. Assanah, P. Canoll, J.L. Manley, HnRNP proteins controlled by c-Myc deregulate pyruvate kinase mRNA splicing in cancer, Nature, 463 (2010) 364-368.

[142] R.A. Cairns, I.S. Harris, T.W. Mak, Regulation of cancer cell metabolism, Nature reviews. Cancer, 11 (2011) 85-95.

[143] J.A. Engelman, Targeting PI3K signalling in cancer: opportunities, challenges and limitations, Nature reviews. Cancer, 9 (2009) 550-562.

[144] K. Duvel, J.L. Yecies, S. Menon, P. Raman, A.I. Lipovsky, A.L. Souza, E. Triantafellow, Q. Ma, R. Gorski, S. Cleaver, M.G. Vander Heiden, J.P. MacKeigan, P.M. Finan, C.B. Clish, L.O. Murphy, B.D. Manning, Activation of a metabolic gene regulatory network downstream of mTOR complex 1, Mol Cell, 39 (2010) 171-183.

[145] S. Matoba, J.G. Kang, W.D. Patino, A. Wragg, M. Boehm, O. Gavrilova, P.J. Hurley, F. Bunz, P.M. Hwang, p53 regulates mitochondrial respiration, Science (New York, N.Y.), 312 (2006) 1650-1653.

[146] D.R. Green, J.E. Chipuk, p53 and metabolism: Inside the TIGAR, Cell, 126 (2006) 30-32.

[147] J.A. Smeitink, M. Zeviani, D.M. Turnbull, H.T. Jacobs, Mitochondrial medicine: a metabolic perspective on the pathology of oxidative phosphorylation disorders, Cell metabolism, 3 (2006) 9-13.

[148] H. Shi, M. Hayes, C. Kirana, R. Miller, J. Keating, D. Macartney-Coxson, R. Stubbs, TUFM is a potential new prognostic indicator for colorectal carcinoma, Pathology, 44 (2012) 506-512.

[149] S. Dasgupta, M.O. Hoque, S. Upadhyay, D. Sidransky, Mitochondrial cytochrome B gene mutation promotes tumor growth in bladder cancer, Cancer research, 68 (2008) 700-706.

[150] S.K. McBrayer, J.R. Mayers, G.J. DiNatale, D.D. Shi, J. Khanal, A.A. Chakraborty, K.A. Sarosiek, K.J. Briggs, A.K. Robbins, T. Sewastianik, S.J. Shareef, B.A. Olenchock, S.J. Parker, K. Tateishi, J.B. Spinelli, M. Islam, M.C. Haigis, R.E. Looper, K.L. Ligon, B.E. Bernstein, R.D. Carrasco, D.P. Cahill, J.M. Asara, C.M. Metallo, N.H. Yennawar, M.G. Vander Heiden, W.G. Kaelin, Jr., Transaminase Inhibition by 2-Hydroxyglutarate Impairs Glutamate Biosynthesis and Redox Homeostasis in Glioma, Cell, 175 (2018) 101-116 e125.

[151] K.E. Yen, M.A. Bittinger, S.M. Su, V.R. Fantin, Cancer-associated IDH mutations: biomarker and therapeutic opportunities, Oncogene, 29 (2010) 6409-6417.

[152] G. Kroemer, J. Pouyssegur, Tumor cell metabolism: cancer's Achilles' heel, Cancer cell, 13 (2008) 472-482.

[153] S. Jiang, L.F. Zhang, H.W. Zhang, S. Hu, M.H. Lu, S. Liang, B. Li, Y. Li, D. Li, E.D. Wang, M.F. Liu, A novel miR-155/miR-143 cascade controls glycolysis by regulating hexokinase 2 in breast cancer cells, EMBO J, 31 (2012) 1985-1998.

[154] X. Ma, C. Li, L. Sun, D. Huang, T. Li, X. He, G. Wu, Z. Yang, X. Zhong, L. Song, P. Gao, H. Zhang, Lin28/let-7 axis regulates aerobic glycolysis and cancer progression via PDK1, Nat Commun, 5 (2014) 5212.

[155] Z. Li, X. Li, S. Wu, M. Xue, W. Chen, Long non‐coding RNA UCA1 promotes glycolysis by upregulating hexokinase 2 through the mTOR–STAT3/microRNA143 pathway, Cancer science, 105 (2014) 951-955.

[156] J. Ou, H. Miao, Y. Ma, F. Guo, J. Deng, X. Wei, J. Zhou, G. Xie, H. Shi, B. Xue, H. Liang, L. Yu, Loss of abhd5 promotes colorectal tumor development and progression by inducing aerobic glycolysis and epithelial-mesenchymal transition, Cell Rep, 9 (2014) 1798-1811.

[157] K.T. Pate, C. Stringari, S. Sprowl-Tanio, K. Wang, T. TeSlaa, N.P. Hoverter, M.M. McQuade, C. Garner, M.A. Digman, M.A. Teitell, R.A. Edwards, E. Gratton, M.L. Waterman, Wnt signaling directs a metabolic program of glycolysis and angiogenesis in colon cancer, EMBO J, 33 (2014) 1454-1473.

[158] B. T Oronsky, N. Oronsky, G. R Fanger, C. W Parker, S. Z Caroen, M. Lybeck, J. J Scicinski, Follow the ATP: tumor energy production: a perspective, Anti-Cancer Agents in Medicinal Chemistry (Formerly Current Medicinal Chemistry-Anti-Cancer Agents), 14 (2014) 1187-1198.

[159] S.-C. Lin, D.G. Hardie, AMPK: sensing glucose as well as cellular energy status, Cell metabolism, 27 (2018) 299-313.

[160] A. Colell, J.E. Ricci, S. Tait, S. Milasta, U. Maurer, L. Bouchier-Hayes, P. Fitzgerald, A. Guio-Carrion, N.J. Waterhouse, C.W. Li, B. Mari, P. Barbry, D.D. Newmeyer, H.M. Beere, D.R. Green, GAPDH and autophagy preserve survival after apoptotic cytochrome c release in the absence of caspase activation, Cell, 129 (2007) 983-997.

[161] P.P. Hsu, D.M. Sabatini, Cancer cell metabolism: Warburg and beyond, Cell, 134 (2008) 703-707.

[162] N.N. Pavlova, C.B. Thompson, The Emerging Hallmarks of Cancer Metabolism, Cell metabolism, 23 (2016) 27-47.

[163] C.M. Metallo, P.A. Gameiro, E.L. Bell, K.R. Mattaini, J. Yang, K. Hiller, C.M. Jewell, Z.R. Johnson, D.J. Irvine, L. Guarente, Reductive glutamine metabolism by IDH1 mediates lipogenesis under hypoxia, Nature, 481 (2012) 380-384.

[164] L. Yang, T. Moss, L.S. Mangala, J. Marini, H. Zhao, S. Wahlig, G. Armaiz-Pena, D. Jiang, A. Achreja, J. Win, R. Roopaimoole, C. Rodriguez-Aguayo, I. Mercado-Uribe,

G. Lopez-Berestein, J. Liu, T. Tsukamoto, A.K. Sood, P.T. Ram, D. Nagrath, Metabolic shifts toward glutamine regulate tumor growth, invasion and bioenergetics in ovarian cancer, Mol Syst Biol, 10 (2014) 728.

[165] J. Son, C.A. Lyssiotis, H. Ying, X. Wang, S. Hua, M. Ligorio, R.M. Perera, C.R. Ferrone, E. Mullarky, N. Shyh-Chang, Glutamine supports pancreatic cancer growth through a KRAS-regulated metabolic pathway, Nature, 496 (2013) 101-105.

[166] J.R. Cantor, D.M. Sabatini, Cancer cell metabolism: one hallmark, many faces, Cancer discovery, 2 (2012) 881-898.

[167] M.J. Lukey, W.P. Katt, R.A. Cerione, Targeting amino acid metabolism for cancer therapy, Drug Discov Today, 22 (2017) 796-804.

[168] B.J. Dillon, V.G. Prieto, S.A. Curley, C.M. Ensor, F.W. Holtsberg, J.S. Bomalaski, M.A. Clark, Incidence and distribution of argininosuccinate synthetase deficiency in human cancers: a method for identifying cancers sensitive to arginine deprivation, Cancer, 100 (2004) 826-833.

[169] F. Qiu, J. Huang, M. Sui, Targeting arginine metabolism pathway to treat arginine-dependent cancers, Cancer letters, 364 (2015) 1-7.

[170] H. Takaku, M. Takase, S. Abe, H. Hayashi, K. Miyazaki, In vivo anti-tumor activity of arginine deiminase purified from Mycoplasma arginini, Int J Cancer, 51 (1992) 244-249.

[171] H. Takaku, M. Matsumoto, S. Misawa, K. Miyazaki, Anti‐tumor activity of arginine deiminase from Mycoplasma arginini and its growth‐inhibitory mechanism, Japanese journal of cancer research, 86 (1995) 840-846.

[172] D. Covini, S. Tardito, O. Bussolati, L.R. Chiarelli, M.V. Pasquetto, R. Digilio, G. Valentini, C. Scotti, Expanding targets for a metabolic therapy of cancer: L-asparaginase, Recent Pat Anticancer Drug Discov, 7 (2012) 4-13.

[173] A.S. Krall, S. Xu, T.G. Graeber, D. Braas, H.R. Christofk, Asparagine promotes cancer cell proliferation through use as an amino acid exchange factor, Nature communications, 7 (2016) 1-13.

[174] S.R. Knott, E. Wagenblast, S. Khan, S.Y. Kim, M. Soto, M. Wagner, M.-O. Turgeon, L. Fish, N. Erard, A.L. Gable, Asparagine bioavailability governs metastasis in a model of breast cancer, Nature, 554 (2018) 378-381.

[175] R.T. Williams, R. Guarecuco, L.A. Gates, D. Barrows, M.C. Passarelli, B. Carey, L. Baudrier, S. Jeewajee, K. La, B. Prizer, S. Malik, J. Garcia-Bermudez, X.G. Zhu, J. Cantor, H. Molina, T. Carroll, R.G. Roeder, O. Abdel-Wahab, C.D. Allis, K. Birsoy, ZBTB1 Regulates Asparagine Synthesis and Leukemia Cell Response to L-Asparaginase, Cell metabolism, 31 (2020) 852-861 e856.

[176] Y.D. Bhutia, E. Babu, S. Ramachandran, V. Ganapathy, Amino acid transporters in cancer and their relevance to “glutamine addiction”: novel targets for the design of a new class of anticancer drugs, Cancer research, 75 (2015) 1782-1788.

[177] V. Coothankandaswamy, S. Cao, Y. Xu, P. Prasad, P. Singh, C. Reynolds, S. Yang, J. Ogura, V. Ganapathy, Y. Bhutia, Amino acid transporter SLC6A14 is a novel and effective drug target for pancreatic cancer, British journal of pharmacology, 173 (2016) 3292-3306.

[178] P. Nicklin, P. Bergman, B. Zhang, E. Triantafellow, H. Wang, B. Nyfeler, H. Yang, M. Hild, C. Kung, C. Wilson, V.E. Myer, J.P. MacKeigan, J.A. Porter, Y.K. Wang, L.C. Cantley, P.M. Finan, L.O. Murphy, Bidirectional transport of amino acids regulates mTOR and autophagy, Cell, 136 (2009) 521-534.

[179] M.I. Gross, S.D. Demo, J.B. Dennison, L. Chen, T. Chernov-Rogan, B. Goyal, J.R. Janes, G.J. Laidig, E.R. Lewis, J. Li, A.L. Mackinnon, F. Parlati, M.L. Rodriguez, P.J. Shwonek, E.B. Sjogren, T.F. Stanton, T. Wang, J. Yang, F. Zhao, M.K. Bennett, Antitumor activity of the glutaminase inhibitor CB-839 in triple-negative breast cancer, Mol Cancer Ther, 13 (2014) 890-901.

[180] P. Gao, I. Tchernyshyov, T.C. Chang, Y.S. Lee, K. Kita, T. Ochi, K.I. Zeller, A.M. De Marzo, J.E. Van Eyk, J.T. Mendell, C.V. Dang, c-Myc suppression of miR-23a/b enhances mitochondrial glutaminase expression and glutamine metabolism, Nature, 458 (2009) 762-765.

[181] J.B. Wang, J.W. Erickson, R. Fuji, S. Ramachandran, P. Gao, R. Dinavahi, K.F. Wilson, A.L. Ambrosio, S.M. Dias, C.V. Dang, R.A. Cerione, Targeting mitochondrial glutaminase activity inhibits oncogenic transformation, Cancer cell, 18 (2010) 207-219.

[182] B.J. Altman, Z.E. Stine, C.V. Dang, From Krebs to clinic: glutamine metabolism to cancer therapy, Nature Reviews Cancer, 16 (2016) 619.

[183] L. Jin, D. Li, G.N. Alesi, J. Fan, H.-B. Kang, Z. Lu, T.J. Boggon, P. Jin, H. Yi, E.R. Wright, Glutamate dehydrogenase 1 signals through antioxidant glutathione peroxidase 1 to regulate redox homeostasis and tumor growth, Cancer cell, 27 (2015) 257-270.

[184] M. Pan, M.A. Reid, X.H. Lowman, R.P. Kulkarni, T.Q. Tran, X. Liu, Y. Yang, J.E. Hernandez-Davies, K.K. Rosales, H. Li, Regional glutamine deficiency in tumours promotes dedifferentiation through inhibition of histone demethylation, Nature cell biology, 18 (2016) 1090-1101.

[185] M.V. Recouvreux, M.R. Moldenhauer, K.M.O. Galenkamp, M. Jung, B. James, Y. Zhang, A. Lowy, A. Bagchi, C. Commisso, Glutamine depletion regulates Slug to promote EMT and metastasis in pancreatic cancer, The Journal of experimental medicine, 217 (2020).

[186] Y. Xiang, Z.E. Stine, J. Xia, Y. Lu, R.S. O'Connor, B.J. Altman, A.L. Hsieh, A.M. Gouw, A.G. Thomas, P. Gao, L. Sun, L. Song, B. Yan, B.S. Slusher, J. Zhuo, L.L. Ooi,

C.G. Lee, A. Mancuso, A.S. McCallion, A. Le, M.C. Milone, S. Rayport, D.W. Felsher, C.V. Dang, Targeted inhibition of tumor-specific glutaminase diminishes cell-autonomous tumorigenesis, J Clin Invest, 125 (2015) 2293-2306.

[187] J. Zhang, G. Wang, Q. Mao, S. Li, W. Xiong, Y. Lin, J. Ge, Glutamate dehydrogenase (GDH) regulates bioenergetics and redox homeostasis in human glioma, Oncotarget, 5 (2016).

[188] P. Korangath, W.W. Teo, H. Sadik, L. Han, N. Mori, C.M. Huijts, F. Wildes, S. Bharti, Z. Zhang, C.A. Santa-Maria, H. Tsai, C.V. Dang, V. Stearns, Z.M. Bhujwalla, S. Sukumar, Targeting Glutamine Metabolism in Breast Cancer with Aminooxyacetate, Clinical cancer research : an official journal of the American Association for Cancer Research, 21 (2015) 3263-3273.

[189] M.R. Sullivan, K.R. Mattaini, E.A. Dennstedt, A.A. Nguyen, S. Sivanand, M.F. Reilly, K. Meeth, A. Muir, A.M. Darnell, M.W. Bosenberg, C.A. Lewis, M.G. Vander Heiden, Increased Serine Synthesis Provides an Advantage for Tumors Arising in Tissues Where Serine Levels Are Limiting, Cell metabolism, 29 (2019) 1410-1421 e1414.

[190] R. Possemato, K.M. Marks, Y.D. Shaul, M.E. Pacold, D. Kim, K. Birsoy, S. Sethumadhavan, H.-K. Woo, H.G. Jang, A.K. Jha, Functional genomics reveal that the serine synthesis pathway is essential in breast cancer, Nature, 476 (2011) 346-350.

[191] G.M. DeNicola, P.H. Chen, E. Mullarky, J.A. Sudderth, Z. Hu, D. Wu, H. Tang, Y. Xie, J.M. Asara, K.E. Huffman, Wistuba, II, J.D. Minna, R.J. DeBerardinis, L.C. Cantley, NRF2 regulates serine biosynthesis in non-small cell lung cancer, Nat Genet, 47 (2015) 1475-1481.

[192] S. Pollari, S.M. Kakonen, H. Edgren, M. Wolf, P. Kohonen, H. Sara, T. Guise, M. Nees, O. Kallioniemi, Enhanced serine production by bone metastatic breast cancer cells stimulates osteoclastogenesis, Breast Cancer Res Treat, 125 (2011) 421-430.

[193] B. Ngo, E. Kim, V. Osorio-Vasquez, S. Doll, S. Bustraan, R.J. Liang, A. Luengo, S.M. Davidson, A. Ali, G.B. Ferraro, G.M. Fischer, R. Eskandari, D.S. Kang, J. Ni, A. Plasger, V.K. Rajasekhar, E.R. Kastenhuber, S. Bacha, R.K. Sriram, B.D. Stein, S.F. Bakhoum, M. Snuderl, P. Cotzia, J.H. Healey, N. Mainolfi, V. Suri, A. Friedman, M. Manfredi, D.M. Sabatini, D.R. Jones, M. Yu, J.J. Zhao, R.K. Jain, K.R. Keshari, M.A. Davies, M.G.V. Heiden, E. Hernando, M. Mann, L.C. Cantley, M.E. Pacold, Limited Environmental Serine and Glycine Confer Brain Metastasis Sensitivity to PHGDH Inhibition, Cancer discovery, 10 (2020) 1352-1373.

[194] O.D. Maddocks, C.R. Berkers, S.M. Mason, L. Zheng, K. Blyth, E. Gottlieb, K.H. Vousden, Serine starvation induces stress and p53-dependent metabolic remodelling in cancer cells, Nature, 493 (2013) 542-546.

[195] L.M. Nilsson, T.Z. Forshell, S. Rimpi, C. Kreutzer, W. Pretsch, G.W. Bornkamm, J.A. Nilsson, Mouse genetics suggests cell-context dependency for Myc-regulated metabolic enzymes during tumorigenesis, PLoS Genet, 8 (2012) e1002573.

[196] R. Nilsson, M. Jain, N. Madhusudhan, N.G. Sheppard, L. Strittmatter, C. Kampf, J. Huang, A. Asplund, V.K. Mootha, Metabolic enzyme expression highlights a key role for MTHFD2 and the mitochondrial folate pathway in cancer, Nat Commun, 5 (2014) 3128.

[197] W.C. Zhang, N. Shyh-Chang, H. Yang, A. Rai, S. Umashankar, S. Ma, B.S. Soh, L.L. Sun, B.C. Tai, M.E. Nga, K.K. Bhakoo, S.R. Jayapal, M. Nichane, Q. Yu, D.A. Ahmed, C. Tan, W.P. Sing, J. Tam, A. Thirugananam, M.S. Noghabi, Y.H. Pang, H.S. Ang, W. Mitchell, P. Robson, P. Kaldis, R.A. Soo, S. Swarup, E.H. Lim, B. Lim, Glycine decarboxylase activity drives non-small cell lung cancer tumor-initiating cells and tumorigenesis, Cell, 148 (2012) 259-272.

[198] E. Vacchelli, F. Aranda, A. Eggermont, C. Sautes-Fridman, E. Tartour, E.P. Kennedy, M. Platten, L. Zitvogel, G. Kroemer, L. Galluzzi, Trial watch: IDO inhibitors in cancer therapy, Oncoimmunology, 3 (2014) e957994.

[199] V.P. Balachandran, M.J. Cavnar, S. Zeng, Z.M. Bamboat, L.M. Ocuin, H. Obaid, E.C. Sorenson, R. Popow, C. Ariyan, F. Rossi, Imatinib potentiates antitumor T cell responses in gastrointestinal stromal tumor through the inhibition of Ido, Nature medicine, 17 (2011) 1094-1100.

[200] S. Löb, A. Königsrainer, D. Zieker, B.L. Brücher, H.-G. Rammensee, G. Opelz, P. Terness, IDO1 and IDO2 are expressed in human tumors: levo-but not dextro-1-methyl tryptophan inhibits tryptophan catabolism, Cancer immunology, immunotherapy, 58 (2009) 153-157.

[201] R.B. Sorensen, T. Kollgaard, R.S. Andersen, J.H. van den Berg, I.M. Svane, P. Straten, M.H. Andersen, Spontaneous cytotoxic T-Cell reactivity against indoleamine 2,3-dioxygenase-2, Cancer research, 71 (2011) 2038-2044.

[202] C.L. Miller, I.C. Llenos, J.R. Dulay, S. Weis, Upregulation of the initiating step of the kynurenine pathway in postmortem anterior cingulate cortex from individuals with schizophrenia and bipolar disorder, Brain Res, 1073-1074 (2006) 25-37.

[203] L. Pilotte, P. Larrieu, V. Stroobant, D. Colau, E. Dolusic, R. Frederick, E. De Plaen, C. Uyttenhove, J. Wouters, B. Masereel, B.J. Van den Eynde, Reversal of tumoral immune resistance by inhibition of tryptophan 2,3-dioxygenase, Proceedings of the National Academy of Sciences of the United States of America, 109 (2012) 2497-2502.

[204] C.J. Lynch, S.H. Adams, Branched-chain amino acids in metabolic signalling and insulin resistance, Nat Rev Endocrinol, 10 (2014) 723-736.

[205] X. Jiang, J.N. Buxbaum, J.W. Kelly, The V122I cardiomyopathy variant of transthyretin increases the velocity of rate-limiting tetramer dissociation, resulting in accelerated amyloidosis, Proceedings of the National Academy of Sciences of the United States of America, 98 (2001) 14943-14948.

[206] A.M. Paradis, B. Fontaine-Bisson, Y. Bosse, J. Robitaille, S. Lemieux, H. Jacques, B. Lamarche, A. Tchernof, P. Couture, M.C. Vohl, The peroxisome proliferator-activated

receptor alpha Leu162Val polymorphism influences the metabolic response to a dietary intervention altering fatty acid proportions in healthy men, Am J Clin Nutr, 81 (2005) 523-530.

[207] S. Zhang, X. Zeng, M. Ren, X. Mao, S. Qiao, Novel metabolic and physiological functions of branched chain amino acids: a review, J Anim Sci Biotechnol, 8 (2017) 10.

[208] R.A. Harris, M. Joshi, N.H. Jeoung, Mechanisms responsible for regulation of branched-chain amino acid catabolism, Biochem Biophys Res Commun, 313 (2004) 391-396.

[209] T. Li, Z. Zhang, S.C. Kolwicz, Jr., L. Abell, N.D. Roe, M. Kim, B. Zhou, Y. Cao, J. Ritterhoff, H. Gu, D. Raftery, H. Sun, R. Tian, Defective Branched-Chain Amino Acid Catabolism Disrupts Glucose Metabolism and Sensitizes the Heart to Ischemia-Reperfusion Injury, Cell metabolism, 25 (2017) 374-385.

[210] M.H. Stipanuk, Leucine and protein synthesis: mTOR and beyond, Nutr Rev, 65 (2007) 122-129.

[211] M.J. Rennie, J. Bohe, K. Smith, H. Wackerhage, P. Greenhaff, Branched-chain amino acids as fuels and anabolic signals in human muscle, The Journal of nutrition, 136 (2006) 264S-268S.

[212] M. Wallace, C.R. Green, L.S. Roberts, Y.M. Lee, J.L. McCarville, J. Sanchez-Gurmaches, N. Meurs, J.M. Gengatharan, J.D. Hover, S.A. Phillips, T.P. Ciaraldi, D.A. Guertin, P. Cabrales, J.S. Ayres, D.K. Nomura, R. Loomba, C.M. Metallo, Enzyme promiscuity drives branched-chain fatty acid synthesis in adipose tissues, Nature chemical biology, 14 (2018) 1021-1031.

[213] C. Jang, S.F. Oh, S. Wada, G.C. Rowe, L. Liu, M.C. Chan, J. Rhee, A. Hoshino, B. Kim, A. Ibrahim, L.G. Baca, E. Kim, C.C. Ghosh, S.M. Parikh, A. Jiang, Q. Chu, D.E. Forman, S.H. Lecker, S. Krishnaiah, J.D. Rabinowitz, A.M. Weljie, J.A. Baur, D.L. Kasper, Z. Arany, A branched-chain amino acid metabolite drives vascular fatty acid transport and causes insulin resistance, Nature medicine, 22 (2016) 421-426.

[214] M. Doi, I. Yamaoka, T. Fukunaga, M. Nakayama, Isoleucine, a potent plasma glucose-lowering amino acid, stimulates glucose uptake in C2C12 myotubes, Biochem Biophys Res Commun, 312 (2003) 1111-1117.

[215] J. Lei, D. Feng, Y. Zhang, S. Dahanayaka, X. Li, K. Yao, J. Wang, Z. Wu, Z. Dai, G. Wu, Regulation of leucine catabolism by metabolic fuels in mammary epithelial cells, Amino Acids, 43 (2012) 2179-2189.

[216] P. Li, D.A. Knabe, S.W. Kim, C.J. Lynch, S.M. Hutson, G. Wu, Lactating porcine mammary tissue catabolizes branched-chain amino acids for glutamine and aspartate synthesis, J Nutr, 139 (2009) 1502-1509.

[217] G.F.R. Teodoro, D. Vianna, F.L. Torres-Leal, L.C. Pantaleao, E.M. Matos-Neto, J. Donato Jr, J. Tirapegui, Leucine is essential for attenuating fetal growth restriction caused by a protein-restricted diet in rats, The Journal of nutrition, 142 (2012) 924-930.

[218] M. Negro, S. Giardina, B. Marzani, F. Marzatico, Branched-chain amino acid supplementation does not enhance athletic performance but affects muscle recovery and the immune system, Journal of Sports Medicine and Physical Fitness, 48 (2008) 347.

[219] Y. Huang, M. Zhou, H. Sun, Y. Wang, Branched-chain amino acid metabolism in heart disease: an epiphenomenon or a real culprit?, Cardiovasc Res, 90 (2011) 220-223.

[220] G. Bajotto, T. Murakami, M. Nagasaki, Y. Sato, Y. Shimomura, Decreased enzyme activity and contents of hepatic branched-chain alpha-keto acid dehydrogenase complex subunits in a rat model for type 2 diabetes mellitus, Metabolism, 58 (2009) 1489-1495.

[221] M. Doisaki, Y. Katano, I. Nakano, Y. Hirooka, A. Itoh, M. Ishigami, K. Hayashi, H. Goto, Y. Fujita, Y. Kadota, Regulation of hepatic branched-chain α-keto acid dehydrogenase kinase in a rat model for type 2 diabetes mellitus at different stages of the disease, Biochemical and biophysical research communications, 393 (2010) 303-307.

[222] G. Lu, H. Sun, P. She, J.Y. Youn, S. Warburton, P. Ping, T.M. Vondriska, H. Cai, C.J. Lynch, Y. Wang, Protein phosphatase 2Cm is a critical regulator of branched-chain amino acid catabolism in mice and cultured cells, J Clin Invest, 119 (2009) 1678-1687.

[223] M. Zhou, G. Lu, C. Gao, Y. Wang, H. Sun, Tissue-specific and nutrient regulation of the branched-chain alpha-keto acid dehydrogenase phosphatase, protein phosphatase 2Cm (PP2Cm), The Journal of biological chemistry, 287 (2012) 23397-23406.

[224] S. Nishitani, K. Takehana, Pharmacological activities of branched-chain amino acids: augmentation of albumin synthesis in liver and improvement of glucose metabolism in skeletal muscle, Hepatol Res, 30S (2004) 19-24.

[225] E. Blomstrand, B. Saltin, BCAA intake affects protein metabolism in muscle after but not during exercise in humans, American Journal of Physiology-Endocrinology And Metabolism, 281 (2001) E365-E374.

[226] M.M. Adeva-Andany, L. Lopez-Maside, C. Donapetry-Garcia, C. Fernandez-Fernandez, C. Sixto-Leal, Enzymes involved in branched-chain amino acid metabolism in humans, Amino Acids, 49 (2017) 1005-1028.

[227] N. Yang, L. Han, X. Gu, J. Ye, W. Qiu, H. Zhang, Z. Gong, Y. Zhang, Analysis of gene mutations in Chinese patients with maple syrup urine disease, Mol Genet Metab, 106 (2012) 412-418.

[228] F. Peinemann, D.J. Danner, Maple syrup urine disease 1954 to 1993, J Inherit Metab Dis, 17 (1994) 3-15.

[229] H.D. Park, D.H. Lee, Y.H. Hong, D.H. Kang, Y.K. Lee, J. Song, S.Y. Lee, J.W. Kim, C.S. Ki, Y.W. Lee, Three Korean patients with maple syrup urine disease: four novel mutations in the BCKDHA gene, Ann Clin Lab Sci, 41 (2011) 167-173.

[230] H. Sun, K.C. Olson, C. Gao, D.A. Prosdocimo, M. Zhou, Z. Wang, D. Jeyaraj, J.Y. Youn, S. Ren, Y. Liu, C.D. Rau, S. Shah, O. Ilkayeva, W.J. Gui, N.S. William, R.M. Wynn, C.B. Newgard, H. Cai, X. Xiao, D.T. Chuang, P.C. Schulze, C. Lynch, M.K. Jain, Y. Wang, Catabolic Defect of Branched-Chain Amino Acids Promotes Heart Failure, Circulation, 133 (2016) 2038-2049.

[231] X. Guo, C. Huang, K. Lian, S. Wang, H. Zhao, F. Yan, X. Zhang, J. Zhang, H. Xie, R. An, L. Tao, BCKA down-regulates mTORC2-Akt signal and enhances apoptosis susceptibility in cardiomyocytes, Biochem Biophys Res Commun, 480 (2016) 106-113.

[232] R. Kalluri, The biology and function of fibroblasts in cancer, Nature reviews. Cancer, 16 (2016) 582-598.

[233] A. Arina, C. Idel, E.M. Hyjek, M.L. Alegre, Y. Wang, V.P. Bindokas, R.R. Weichselbaum, H. Schreiber, Tumor-associated fibroblasts predominantly come from local and not circulating precursors, Proceedings of the National Academy of Sciences of the United States of America, 113 (2016) 7551-7556.

[234] P. Dey, J. Baddour, F. Muller, C.C. Wu, H. Wang, W.T. Liao, Z. Lan, A. Chen, T. Gutschner, Y. Kang, J. Fleming, N. Satani, D. Zhao, A. Achreja, L. Yang, J. Lee, E. Chang, G. Genovese, A. Viale, H. Ying, G. Draetta, A. Maitra, Y.A. Wang, D. Nagrath, R.A. DePinho, Genomic deletion of malic enzyme 2 confers collateral lethality in pancreatic cancer, Nature, 542 (2017) 119-123.

[235] J.T. Li, M. Yin, D. Wang, J. Wang, M.Z. Lei, Y. Zhang, Y. Liu, L. Zhang, S.W. Zou, L.P. Hu, Z.G. Zhang, Y.P. Wang, W.Y. Wen, H.J. Lu, Z.J. Chen, D. Su, Q.Y. Lei, BCAT2-mediated BCAA catabolism is critical for development of pancreatic ductal adenocarcinoma, Nature cell biology, 22 (2020) 167-174.

[236] M.Z. Lei, X.X. Li, Y. Zhang, J.T. Li, F. Zhang, Y.P. Wang, M. Yin, J. Qu, Q.Y. Lei, Acetylation promotes BCAT2 degradation to suppress BCAA catabolism and pancreatic cancer growth, Signal Transduct Target Ther, 5 (2020) 70.

[237] N. Li, C. Hwangbo, I.M. Jaba, J. Zhang, I. Papangeli, J. Han, N. Mikush, B. Larrivee, A. Eichmann, H.J. Chun, L.H. Young, D. Tirziu, miR-182 Modulates Myocardial Hypertrophic Response Induced by Angiogenesis in Heart, Sci Rep, 6 (2016) 21228.

[238] W.M. Wang, G. Lu, X.W. Su, H. Lyu, W.S. Poon, MicroRNA-182 Regulates Neurite Outgrowth Involving the PTEN/AKT Pathway, Front Cell Neurosci, 11 (2017) 96.

[239] Z.N. Dhanani, G. Mann, O.A.J. Adegoke, Depletion of branched-chain aminotransferase 2 (BCAT2) enzyme impairs myoblast survival and myotube formation, Physiol Rep, 7 (2019) e14299.

[240] Y. Hatazawa, M. Tadaishi, Y. Nagaike, A. Morita, Y. Ogawa, O. Ezaki, T. Takai-Igarashi, Y. Kitaura, Y. Shimomura, Y. Kamei, S. Miura, PGC-1alpha-mediated branched-chain amino acid metabolism in the skeletal muscle, PLoS One, 9 (2014) e91006.

[241] N. Shimizu, N. Yoshikawa, N. Ito, T. Maruyama, Y. Suzuki, S.-i. Takeda, J. Nakae, Y. Tagata, S. Nishitani, K. Takehana, Crosstalk between glucocorticoid receptor and nutritional sensor mTOR in skeletal muscle, Cell metabolism, 13 (2011) 170-182.

[242] C.M. Sousa, D.E. Biancur, X. Wang, C.J. Halbrook, M.H. Sherman, L. Zhang, D. Kremer, R.F. Hwang, A.K. Witkiewicz, H. Ying, J.M. Asara, R.M. Evans, L.C. Cantley, C.A. Lyssiotis, A.C. Kimmelman, Pancreatic stellate cells support tumour metabolism through autophagic alanine secretion, Nature, 536 (2016) 479-483.

[243] M. Tonjes, S. Barbus, Y.J. Park, W. Wang, M. Schlotter, A.M. Lindroth, S.V. Pleier, A.H.C. Bai, D. Karra, R.M. Piro, J. Felsberg, A. Addington, D. Lemke, I. Weibrecht, V. Hovestadt, C.G. Rolli, B. Campos, S. Turcan, D. Sturm, H. Witt, T.A. Chan, C. Herold-Mende, R. Kemkemer, R. Konig, K. Schmidt, W.E. Hull, S.M. Pfister, M. Jugold, S.M. Hutson, C. Plass, J.G. Okun, G. Reifenberger, P. Lichter, B. Radlwimmer, BCAT1 promotes cell proliferation through amino acid catabolism in gliomas carrying wild-type IDH1, Nature medicine, 19 (2013) 901-908.

[244] A. Hattori, M. Tsunoda, T. Konuma, M. Kobayashi, T. Nagy, J. Glushka, F. Tayyari, D. McSkimming, N. Kannan, A. Tojo, A.S. Edison, T. Ito, Cancer progression by reprogrammed BCAA metabolism in myeloid leukaemia, Nature, 545 (2017) 500-504.

[245] J.R. Mayers, C. Wu, C.B. Clish, P. Kraft, M.E. Torrence, B.P. Fiske, C. Yuan, Y. Bao, M.K. Townsend, S.S. Tworoger, S.M. Davidson, T. Papagiannakopoulos, A. Yang, T.L. Dayton, S. Ogino, M.J. Stampfer, E.L. Giovannucci, Z.R. Qian, D.A. Rubinson, J. Ma, H.D. Sesso, J.M. Gaziano, B.B. Cochrane, S. Liu, J. Wactawski-Wende, J.E. Manson, M.N. Pollak, A.C. Kimmelman, A. Souza, K. Pierce, T.J. Wang, R.E. Gerszten, C.S. Fuchs, M.G. Vander Heiden, B.M. Wolpin, Elevation of circulating branched-chain amino acids is an early event in human pancreatic adenocarcinoma development, Nature medicine, 20 (2014) 1193-1198.

[246] I. Knerr, N. Weinhold, J. Vockley, K.M. Gibson, Advances and challenges in the treatment of branched-chain amino/keto acid metabolic defects, J Inherit Metab Dis, 35 (2012) 29-40.

[247] J.H. Lee, Y.R. Cho, J.H. Kim, J. Kim, H.Y. Nam, S.W. Kim, J. Son, Branched-chain amino acids sustain pancreatic cancer growth by regulating lipid metabolism, Exp Mol Med, 51 (2019) 1-11.

[248] C.R. Green, M. Wallace, A.S. Divakaruni, S.A. Phillips, A.N. Murphy, T.P. Ciaraldi, C.M. Metallo, Branched-chain amino acid catabolism fuels adipocyte differentiation and lipogenesis, Nature chemical biology, 12 (2016) 15-21.

[249] P. Xue, F. Zeng, Q. Duan, J. Xiao, L. Liu, P. Yuan, L. Fan, H. Sun, O.S. Malyarenko, H. Lu, R. Xiu, S. Liu, C. Shao, J. Zhang, W. Yan, Z. Wang, J. Zheng, F. Zhu, BCKDK of BCAA Catabolism Cross-talking With the MAPK Pathway Promotes Tumorigenesis of Colorectal Cancer, EBioMedicine, 20 (2017) 50-60.

[250] P.J. White, R.W. McGarrah, P.A. Grimsrud, S.C. Tso, W.H. Yang, J.M. Haldeman, T. Grenier-Larouche, J. An, A.L. Lapworth, I. Astapova, S.A. Hannou, T. George, M. Arlotto, L.B. Olson, M. Lai, G.F. Zhang, O. Ilkayeva, M.A. Herman, R.M. Wynn, D.T. Chuang, C.B. Newgard, The BCKDH Kinase and Phosphatase Integrate BCAA and Lipid Metabolism via Regulation of ATP-Citrate Lyase, Cell metabolism, 27 (2018) 1281-1293 e1287.

[251] L.J. Reed, M.L. Hackert, Structure-function relationships in dihydrolipoamide acyltransferases, The Journal of biological chemistry, 265 (1990) 8971-8974.

[252] O. Niwa, T. Kumazaki, T. Tsukiyama, G. Soma, N. Miyajima, K. Yokoro, A cDNA clone overexpressed and amplified in a mouse teratocarcinoma line, Nucleic Acids Res, 18 (1990) 6709.

[253] J. Hull, M.E. Hindy, P.G. Kehoe, K. Chalmers, S. Love, M.E. Conway, Distribution of the branched chain aminotransferase proteins in the human brain and their role in glutamate regulation, Journal of neurochemistry, 123 (2012) 997-1009.

[254] J.R. Mayers, M.G. Vander Heiden, BCAT1 defines gliomas by IDH status, Nature medicine, 19 (2013) 816-817.

[255] O. Schuldiner, A. Eden, T. Ben-Yosef, O. YANuKA, G. Simchen, N. Benvenisty, ECA39, a conserved gene regulated by c-Myc in mice, is involved in G1/S cell cycle regulation in yeast, Proceedings of the National Academy of Sciences, 93 (1996) 7143-7148.

[256] A. Eden, G. Simchen, N. Benvenisty, Two yeast homologs of ECA39, a target for c-Myc regulation, code for cytosolic and mitochondrial branched-chain amino acid aminotransferases, The Journal of biological chemistry, 271 (1996) 20242-20245.

[257] K. Gupta, P. Salunke, Molecular markers of glioma: an update on recent progress and perspectives, J Cancer Res Clin Oncol, 138 (2012) 1971-1981.

[258] B. Zhang, Y. Chen, X. Shi, M. Zhou, L. Bao, K.J. Hatanpaa, T. Patel, R.J. DeBerardinis, Y. Wang, W. Luo, Regulation of branched-chain amino acid metabolism by hypoxia-inducible factor in glioblastoma, Cell Mol Life Sci, (2020) 1-12.

[259] P. Bertuccio, F. Turati, G. Carioli, T. Rodriguez, C. La Vecchia, M. Malvezzi, E. Negri, Global trends and predictions in hepatocellular carcinoma mortality, J Hepatol, 67 (2017) 302-309.

[260] H.G. Wang, R. Xie, P. Shen, X.D. Huang, G.Z. Ji, X.Z. Yang, BCAT1 expression in hepatocellular carcinoma, Clin Res Hepatol Gastroenterol, 40 (2016) e55-e56.

[261] M. Xu, Q. Liu, Y. Jia, K. Tu, Y. Yao, Q. Liu, C. Guo, BCAT1 promotes tumor cell migration and invasion in hepatocellular carcinoma, Oncol Lett, 12 (2016) 2648-2656.

[262] R.E. Ericksen, S.L. Lim, E. McDonnell, W.H. Shuen, M. Vadiveloo, P.J. White, Z. Ding, R. Kwok, P. Lee, G.K. Radda, H.C. Toh, M.D. Hirschey, W. Han, Loss of BCAA Catabolism during Carcinogenesis Enhances mTORC1 Activity and Promotes Tumor Development and Progression, Cell metabolism, 29 (2019) 1151-1165 e1156.

[263] Y.H. Zheng, W.J. Hu, B.C. Chen, T.H.M. Grahn, Y.R. Zhao, H.L. Bao, Y.F. Zhu, Q.Y. Zhang, BCAT 1, a key prognostic predictor of hepatocellular carcinoma, promotes cell proliferation and induces chemoresistance to cisplatin, Liver International, 36 (2016) 1836-1847.

[264] C. La Vecchia, Ovarian cancer: epidemiology and risk factors, Eur J Cancer Prev, 26 (2017) 55-62.

[265] Z.Q. Wang, A. Faddaoui, M. Bachvarova, M. Plante, J. Gregoire, M.C. Renaud, A. Sebastianelli, C. Guillemette, S. Gobeil, E. Macdonald, B. Vanderhyden, D. Bachvarov, BCAT1 expression associates with ovarian cancer progression: possible implications in altered disease metabolism, Oncotarget, 6 (2015) 31522-31543.

[266] S. Raffel, M. Falcone, N. Kneisel, J. Hansson, W. Wang, C. Lutz, L. Bullinger, G. Poschet, Y. Nonnenmacher, A. Barnert, BCAT1 restricts αKG levels in AML stem cells leading to IDH mut-like DNA hypermethylation, Nature, 551 (2017) 384.

[267] Z. Gu, Y. Liu, F. Cai, M. Patrick, J. Zmajkovic, H. Cao, Y. Zhang, A. Tasdogan, M. Chen, L. Qi, X. Liu, K. Li, J. Lyu, K.E. Dickerson, W. Chen, M. Ni, M.E. Merritt, S.J. Morrison, R.C. Skoda, R.J. DeBerardinis, J. Xu, Loss of EZH2 Reprograms BCAA Metabolism to Drive Leukemic Transformation, Cancer discovery, 9 (2019) 1228-1247.

[268] S.M. Talbot, A.I. Neugut, Epidemiological trends in colorectal cancer, Colorectal Cancer, Springer2002, pp. 23-46.

[269] R. Yoshikawa, H. Yanagi, C.-S. Shen, Y. Fujiwara, M. Noda, T. Yagyu, M. Gega, T. Oshima, T. Yamamura, H. Okamura, ECA39 is a novel distant metastasis-related biomarker in colorectal cancer, World journal of gastroenterology: WJG, 12 (2006) 5884.

[270] S.M. Mitchell, J.P. Ross, H.R. Drew, T. Ho, G.S. Brown, N.F. Saunders, K.R. Duesing, M.J. Buckley, R. Dunne, I. Beetson, K.N. Rand, A. McEvoy, M.L. Thomas, R.T. Baker, D.A. Wattchow, G.P. Young, T.J. Lockett, S.K. Pedersen, L.C. Lapointe,

P.L. Molloy, A panel of genes methylated with high frequency in colorectal cancer, BMC Cancer, 14 (2014) 54.

[271] S.K. Pedersen, E.L. Symonds, R.T. Baker, D.H. Murray, A. McEvoy, S.C. Van Doorn, M.W. Mundt, S.R. Cole, G. Gopalsamy, D. Mangira, L.C. LaPointe, E. Dekker, G.P. Young, Evaluation of an assay for methylated BCAT1 and IKZF1 in plasma for detection of colorectal neoplasia, BMC Cancer, 15 (2015) 654.

[272] G.P. Young, S.K. Pedersen, E. Dekker, S.R. Cole, J.M. Osborne, E.L. Symonds, R.C. Mallant-Hent, A. McEvoy, R. Baker, S. Gaur, Evaluation of a 2-gene (IKZF1 and BCAT1) DNA blood test for detection of colorectal cancer, Digestive Disease Week, Chicago, (2014).

[273] N. Grankvist, K.A. Lagerborg, M. Jain, R. Nilsson, Gabapentin Can Suppress Cell Proliferation Independent of the Cytosolic Branched-Chain Amino Acid Transferase 1 (BCAT1), Biochemistry, 57 (2018) 6762-6766.

[274] A.J. Valvezan, M. Turner, A. Belaid, H.C. Lam, S.K. Miller, M.C. McNamara, C. Baglini, B.E. Housden, N. Perrimon, D.J. Kwiatkowski, J.M. Asara, E.P. Henske, B.D. Manning, mTORC1 Couples Nucleotide Synthesis to Nucleotide Demand Resulting in a Targetable Metabolic Vulnerability, Cancer cell, 32 (2017) 624-638 e625.

[275] D. Shao, O. Villet, Z. Zhang, S.W. Choi, J. Yan, J. Ritterhoff, H. Gu, D. Djukovic, D. Christodoulou, S.C. Kolwicz, Jr., D. Raftery, R. Tian, Glucose promotes cell growth by suppressing branched-chain amino acid degradation, Nat Commun, 9 (2018) 2935.

[276] T. Armstrong, G. Packham, L.B. Murphy, A.C. Bateman, J.A. Conti, D.R. Fine, C.D. Johnson, R.C. Benyon, J.P. Iredale, Type I collagen promotes the malignant phenotype of pancreatic ductal adenocarcinoma, Clinical cancer research : an official journal of the American Association for Cancer Research, 10 (2004) 7427-7437.

[277] J. Franco-Barraza, R. Francescone, T. Luong, N. Shah, R. Madhani, G. Cukierman, E. Dulaimi, K. Devarajan, B.L. Egleston, E. Nicolas, R. Katherine Alpaugh, R. Malik, R.G. Uzzo, J.P. Hoffman, E.A. Golemis, E. Cukierman, Matrix-regulated integrin alphavbeta5 maintains alpha5beta1-dependent desmoplastic traits prognostic of neoplastic recurrence, eLife, 6 (2017).

[278] C. Bonnans, J. Chou, Z. Werb, Remodelling the extracellular matrix in development and disease, Nature reviews. Molecular cell biology, 15 (2014) 786-801.

[279] S. Linder, E. Castanos-Velez, A. von Rosen, P. Biberfeld, Immunohistochemical expression of extracellular matrix proteins and adhesion molecules in pancreatic carcinoma, Hepatogastroenterology, 48 (2001) 1321-1327.

[280] J.D. Humphrey, E.R. Dufresne, M.A. Schwartz, Mechanotransduction and extracellular matrix homeostasis, Nature reviews. Molecular cell biology, 15 (2014) 802-812.

[281] J. Kiefer, A. Alexander, M.C. Farach-Carson, Type I collagen-mediated changes in gene expression and function of prostate cancer cells, The Biology of Skeletal Metastases, Springer2004, pp. 101-124.

[282] J.A. Kiefer, M.C. Farach-Carson, Type I collagen-mediated proliferation of PC3 prostate carcinoma cell line: implications for enhanced growth in the bone microenvironment, Matrix Biol, 20 (2001) 429-437.

[283] T. Dahlman, E. Lammerts, D. Bergstrom, A. Franzen, K. Westermark, N.E. Heldin, K. Rubin, Collagen type I expression in experimental anaplastic thyroid carcinoma: regulation and relevance for tumorigenicity, Int J Cancer, 98 (2002) 186-192.

[284] P.K. Sengupta, E.M. Smith, K. Kim, M.J. Murnane, B.D. Smith, DNA hypermethylation near the transcription start site of collagen α2 (I) gene occurs in both cancer cell lines and primary colorectal cancers, Cancer research, 63 (2003) 1789-1797.

[285] R.S. Boyd, F.R. Balkwill, MMP-2 release and activation in ovarian carcinoma: the role of fibroblasts, Br J Cancer, 80 (1999) 315-321.

[286] B.F. Sloane, S. Yan, I. Podgorski, B.E. Linebaugh, M.L. Cher, J. Mai, D. Cavallo-Medved, M. Sameni, J. Dosescu, K. Moin, Cathepsin B and tumor proteolysis: contribution of the tumor microenvironment, Seminars in cancer biology, Elsevier, 2005, pp. 149-157.

[287] A.D. Theocharis, S.S. Skandalis, C. Gialeli, N.K. Karamanos, Extracellular matrix structure, Adv Drug Deliv Rev, 97 (2016) 4-27.

[288] H.X. Fan, H.X. Li, D. Chen, Z.X. Gao, J.H. Zheng, Changes in the expression of MMP2, MMP9, and ColIV in stromal cells in oral squamous tongue cell carcinoma: relationships and prognostic implications, J Exp Clin Cancer Res, 31 (2012) 90.

[289] M. Erkan, J. Kleeff, A. Gorbachevski, C. Reiser, T. Mitkus, I. Esposito, T. Giese, M.W. Buchler, N.A. Giese, H. Friess, Periostin creates a tumor-supportive microenvironment in the pancreas by sustaining fibrogenic stellate cell activity, Gastroenterology, 132 (2007) 1447-1464.

[290] E. Ozer, M.U. Mungan, B. Tuna, H. Kazimoglu, K. Yorukoglu, Z. Kirkali, Prognostic significance of angiogenesis and immunoreactivity of cathepsin D and type IV collagen in high-grade stage T1 primary bladder cancer, Urology, 54 (1999) 50-55.

[291] M.H. Sherman, R.T. Yu, D.D. Engle, N. Ding, A.R. Atkins, H. Tiriac, E.A. Collisson, F. Connor, T. Van Dyke, S. Kozlov, P. Martin, T.W. Tseng, D.W. Dawson, T.R. Donahue, A. Masamune, T. Shimosegawa, M.V. Apte, J.S. Wilson, B. Ng, S.L. Lau, J.E. Gunton, G.M. Wahl, T. Hunter, J.A. Drebin, P.J. O'Dwyer, C. Liddle, D.A. Tuveson, M. Downes, R.M. Evans, Vitamin D receptor-mediated stromal reprogramming suppresses pancreatitis and enhances pancreatic cancer therapy, Cell, 159 (2014) 80-93.

[292] M.H. Sherman, R.T. Yu, T.W. Tseng, C.M. Sousa, S. Liu, M.L. Truitt, N. He, N. Ding, C. Liddle, A.R. Atkins, M. Leblanc, E.A. Collisson, J.M. Asara, A.C. Kimmelman, M. Downes, R.M. Evans, Stromal cues regulate the pancreatic cancer epigenome and metabolome, Proceedings of the National Academy of Sciences of the United States of America, 114 (2017) 1129-1134.

[293] C. Commisso, S.M. Davidson, R.G. Soydaner-Azeloglu, S.J. Parker, J.J. Kamphorst, S. Hackett, E. Grabocka, M. Nofal, J.A. Drebin, C.B. Thompson, J.D. Rabinowitz, C.M. Metallo, M.G. Vander Heiden, D. Bar-Sagi, Macropinocytosis of protein is an amino acid supply route in Ras-transformed cells, Nature, 497 (2013) 633-637.

[294] D.H. Madsen, S. Ingvarsen, H.J. Jurgensen, M.C. Melander, L. Kjoller, A. Moyer, C. Honore, C.A. Madsen, P. Garred, S. Burgdorf, T.H. Bugge, N. Behrendt, L.H. Engelholm, The non-phagocytic route of collagen uptake: a distinct degradation pathway, The Journal of biological chemistry, 286 (2011) 26996-27010.

[295] H.J. Jurgensen, K.S. Norregaard, M.M. Sibree, E. Santoni-Rugiu, D.H. Madsen, K. Wassilew, D. Krustrup, P. Garred, T.H. Bugge, L.H. Engelholm, N. Behrendt, Immune regulation by fibroblasts in tissue injury depends on uPARAP-mediated uptake of collectins, The Journal of cell biology, 218 (2019) 333-349.

[296] L. Yang, Y. Pang, H.L. Moses, TGF-beta and immune cells: an important regulatory axis in the tumor microenvironment and progression, Trends Immunol, 31 (2010) 220-227.

[297] D.G. Stover, B. Bierie, H.L. Moses, A delicate balance: TGF-beta and the tumor microenvironment, J Cell Biochem, 101 (2007) 851-861.

[298] A.C. Correia, J.-R.A. Moonen, M.G. Brinker, G. Krenning, FGF2 inhibits endothelial–mesenchymal transition through microRNA-20a-mediated repression of canonical TGF-β signaling, Journal of cell science, 129 (2016) 569-579.

[299] R. Derynck, Y.E. Zhang, Smad-dependent and Smad-independent pathways in TGF-beta family signalling, Nature, 425 (2003) 577-584.

[300] Y. Zhang, P.B. Alexander, X.F. Wang, TGF-beta Family Signaling in the Control of Cell Proliferation and Survival, Cold Spring Harb Perspect Biol, 9 (2017) a022145.

[301] L.H. Katz, Y. Li, J.S. Chen, N.M. Munoz, A. Majumdar, J. Chen, L. Mishra, Targeting TGF-beta signaling in cancer, Expert Opin Ther Targets, 17 (2013) 743-760.

[302] I. Reynisdottir, K. Polyak, A. Iavarone, J. Massague, Kip/Cip and Ink4 Cdk inhibitors cooperate to induce cell cycle arrest in response to TGF-beta, Genes Dev, 9 (1995) 1831-1845.

[303] F.J. Kohlhapp, A.K. Mitra, E. Lengyel, M.E. Peter, MicroRNAs as mediators and communicators between cancer cells and the tumor microenvironment, Oncogene, 34 (2015) 5857-5868.

[304] J. Liu, N. Akanuma, C. Liu, A. Naji, G.A. Halff, W.K. Washburn, L. Sun, P. Wang, TGF-beta1 promotes acinar to ductal metaplasia of human pancreatic acinar cells, Sci Rep, 6 (2016) 30904.

[305] S. Ottaviani, J. Stebbing, A.E. Frampton, S. Zagorac, J. Krell, A. de Giorgio, S.M. Trabulo, V.T. Nguyen, L. Magnani, H. Feng, TGF-β induces miR-100 and miR-125b but blocks let-7a through LIN28B controlling PDAC progression, Nature communications, 9 (2018) 1-18.

[306] D.S. Micalizzi, C.A. Wang, S.M. Farabaugh, W.P. Schiemann, H.L. Ford, Homeoprotein Six1 increases TGF-beta type I receptor and converts TGF-beta signaling from suppressive to supportive for tumor growth, Cancer research, 70 (2010) 10371-10380.

[307] S. Thuault, E.J. Tan, H. Peinado, A. Cano, C.H. Heldin, A. Moustakas, HMGA2 and Smads co-regulate SNAIL1 expression during induction of epithelial-to-mesenchymal transition, The Journal of biological chemistry, 283 (2008) 33437-33446.

[308] Y.H. Huang, J. Hu, F. Chen, N. Lecomte, H. Basnet, C.J. David, M.D. Witkin, P.J. Allen, S.D. Leach, T.J. Hollmann, C.A. Iacobuzio-Donahue, J. Massague, ID1 Mediates Escape from TGFbeta Tumor Suppression in Pancreatic Cancer, Cancer discovery, 10 (2020) 142-157.

[309] O. Elaskalani, N.B.A. Razak, M. Falasca, P. Metharom, Epithelial-mesenchymal transition as a therapeutic target for overcoming chemoresistance in pancreatic cancer, World journal of gastrointestinal oncology, 9 (2017) 37.

[310] P.J. Mishra, P.J. Mishra, R. Humeniuk, D.J. Medina, G. Alexe, J.P. Mesirov, S. Ganesan, J.W. Glod, D. Banerjee, Carcinoma-associated fibroblast-like differentiation of human mesenchymal stem cells, Cancer research, 68 (2008) 4331-4339.

[311] T.L. Yeung, C.S. Leung, K.K. Wong, G. Samimi, M.S. Thompson, J. Liu, T.M. Zaid, S. Ghosh, M.J. Birrer, S.C. Mok, TGF-beta modulates ovarian cancer invasion by upregulating CAF-derived versican in the tumor microenvironment, Cancer research, 73 (2013) 5016-5028.

[312] S.G. Zheng, J. Wang, P. Wang, J.D. Gray, D.A. Horwitz, IL-2 is essential for TGF-β to convert naive CD4+ CD25− cells to CD25+ Foxp3+ regulatory T cells and for expansion of these cells, The Journal of Immunology, 178 (2007) 2018-2027.

[313] A.A. Delvig, J.J. Lee, Z.M. Chrzanowska-Lightowlers, J.H. Robinson, TGF-beta1 and IFN-gamma cross-regulate antigen presentation to CD4 T cells by macrophages, Journal of leukocyte biology, 72 (2002) 163-166.

[314] D.A. Thomas, J. Massague, TGF-beta directly targets cytotoxic T cell functions during tumor evasion of immune surveillance, Cancer cell, 8 (2005) 369-380.

[315] Y. Xia, Q. Zhang, Q. Zhen, Y. Zhao, N. Liu, T. Li, Y. Hao, Y. Zhang, C. Luo, X. Wu, Negative regulation of tumor-infiltrating NK cell in clear cell renal cell carcinoma patients through the exosomal pathway, Oncotarget, 8 (2017) 37783.

[316] M. Yu, A. Bardia, N. Aceto, F. Bersani, M.W. Madden, M.C. Donaldson, R. Desai, H. Zhu, V. Comaills, Z. Zheng, B.S. Wittner, P. Stojanov, E. Brachtel, D. Sgroi, R. Kapur, T. Shioda, D.T. Ting, S. Ramaswamy, G. Getz, A.J. Iafrate, C. Benes, M. Toner, S. Maheswaran, D.A. Haber, Cancer therapy. Ex vivo culture of circulating breast tumor cells for individualized testing of drug susceptibility, Science (New York, N.Y.), 345 (2014) 216-220.

[317] L. Cayrefourcq, T. Mazard, S. Joosse, J. Solassol, J. Ramos, E. Assenat, U. Schumacher, V. Costes, T. Maudelonde, K. Pantel, C. Alix-Panabieres, Establishment and characterization of a cell line from human circulating colon cancer cells, Cancer research, 75 (2015) 892-901.

[318] D. Gao, I. Vela, A. Sboner, P.J. Iaquinta, W.R. Karthaus, A. Gopalan, C. Dowling, J.N. Wanjala, E.A. Undvall, V.K. Arora, J. Wongvipat, M. Kossai, S. Ramazanoglu, L.P. Barboza, W. Di, Z. Cao, Q.F. Zhang, I. Sirota, L. Ran, T.Y. MacDonald, H. Beltran, J.M. Mosquera, K.A. Touijer, P.T. Scardino, V.P. Laudone, K.R. Curtis, D.E. Rathkopf, M.J. Morris, D.C. Danila, S.F. Slovin, S.B. Solomon, J.A. Eastham, P. Chi, B. Carver, M.A. Rubin, H.I. Scher, H. Clevers, C.L. Sawyers, Y. Chen, Organoid cultures derived from patients with advanced prostate cancer, Cell, 159 (2014) 176-187.

[319] Z. Zhang, H. Shiratsuchi, J. Lin, G. Chen, R.M. Reddy, E. Azizi, S. Fouladdel, A.C. Chang, L. Lin, H. Jiang, Expansion of CTCs from early stage lung cancer patients using a microfluidic co-culture model, Oncotarget, 5 (2014) 12383.

[320] L. Rivera-Baez, I. Lohse, E. Lin, S. Raghavan, S. Owen, R. Harouaka, K. Herman, G. Mehta, T.S. Lawrence, M.A. Morgan, K.C. Cuneo, S. Nagrath, Expansion of Circulating Tumor Cells from Patients with Locally Advanced Pancreatic Cancer Enable Patient Derived Xenografts and Functional Studies for Personalized Medicine, Cancers (Basel), 12 (2020).

[321] T. Ashworth, A case of cancer in which cells similar to those in the tumours were seen in the blood after death, Aust Med J, 14 (1869) 146-149.

[322] W.J. Allard, J. Matera, M.C. Miller, M. Repollet, M.C. Connelly, C. Rao, A.G. Tibbe, J.W. Uhr, L.W. Terstappen, Tumor cells circulate in the peripheral blood of all major carcinomas but not in healthy subjects or patients with nonmalignant diseases, Clin Cancer Res, 10 (2004) 6897-6904.

[323] S. Nagrath, R.M. Jack, V. Sahai, D.M. Simeone, Opportunities and Challenges for Pancreatic Circulating Tumor Cells, Gastroenterology, 151 (2016) 412-426.

[324] E. Lin, L. Rivera-Baez, S. Fouladdel, H.J. Yoon, S. Guthrie, J. Wieger, Y. Deol, E. Keller, V. Sahai, D.M. Simeone, M.L. Burness, E. Azizi, M.S. Wicha, S. Nagrath, High-Throughput Microfluidic Labyrinth for the Label-free Isolation of Circulating Tumor Cells, Cell systems, 5 (2017) 295-304 e294.

[325] S.F. Boj, C.I. Hwang, L.A. Baker, Chio, II, D.D. Engle, V. Corbo, M. Jager, M. Ponz-Sarvise, H. Tiriac, M.S. Spector, A. Gracanin, T. Oni, K.H. Yu, R. van Boxtel, M. Huch, K.D. Rivera, J.P. Wilson, M.E. Feigin, D. Ohlund, A. Handly-Santana, C.M. Ardito-Abraham, M. Ludwig, E. Elyada, B. Alagesan, G. Biffi, G.N. Yordanov, B. Delcuze, B. Creighton, K. Wright, Y. Park, F.H. Morsink, I.Q. Molenaar, I.H. Borel Rinkes, E. Cuppen, Y. Hao, Y. Jin, I.J. Nijman, C. Iacobuzio-Donahue, S.D. Leach, D.J. Pappin, M. Hammell, D.S. Klimstra, O. Basturk, R.H. Hruban, G.J. Offerhaus, R.G. Vries, H. Clevers, D.A. Tuveson, Organoid models of human and mouse ductal pancreatic cancer, Cell, 160 (2015) 324-338.

[326] P.P. Praharaj, S.K. Bhutia, S. Nagrath, R.L. Bitting, G. Deep, Circulating tumor cell-derived organoids: Current challenges and promises in medical research and precision medicine, Biochim Biophys Acta Rev Cancer, 1869 (2018) 117-127.

[327] D. Roife, B. Dai, Y. Kang, M.V.R. Perez, M. Pratt, X. Li, J.B. Fleming, Ex Vivo Testing of Patient-Derived Xenografts Mirrors the Clinical Outcome of Patients with Pancreatic Ductal Adenocarcinoma, Clinical cancer research : an official journal of the American Association for Cancer Research, 22 (2016) 6021-6030.

[328] X. Jiang, Y.D. Seo, J.H. Chang, A. Coveler, E.N. Nigjeh, S. Pan, F. Jalikis, R.S. Yeung, I.N. Crispe, V.G. Pillarisetty, Long-lived pancreatic ductal adenocarcinoma slice cultures enable precise study of the immune microenvironment, Oncoimmunology, 6 (2017) e1333210.

[329] M.A. van Geer, K.F. Kuhlmann, C.T. Bakker, F.J. ten Kate, R.P. Oude Elferink, P.J. Bosma, Ex-vivo evaluation of gene therapy vectors in human pancreatic (cancer) tissue slices, World journal of gastroenterology, 15 (2009) 1359-1366.

[330] K. Sellers, M.P. Fox, M. Bousamra, 2nd, S.P. Slone, R.M. Higashi, D.M. Miller, Y. Wang, J. Yan, M.O. Yuneva, R. Deshpande, A.N. Lane, T.W. Fan, Pyruvate carboxylase is critical for non-small-cell lung cancer proliferation, J Clin Invest, 125 (2015) 687-698.

[331] J.J. Kamphorst, M. Nofal, C. Commisso, S.R. Hackett, W. Lu, E. Grabocka, M.G. Vander Heiden, G. Miller, J.A. Drebin, D. Bar-Sagi, C.B. Thompson, J.D. Rabinowitz, Human pancreatic cancer tumors are nutrient poor and tumor cells actively scavenge extracellular protein, Cancer research, 75 (2015) 544-553.

[332] C.J. Halbrook, C. Pontious, I. Kovalenko, L. Lapienyte, S. Dreyer, H.J. Lee, G. Thurston, Y. Zhang, J. Lazarus, P. Sajjakulnukit, H.S. Hong, D.M. Kremer, B.S. Nelson, S. Kemp, L. Zhang, D. Chang, A. Biankin, J. Shi, T.L. Frankel, H.C. Crawford, J.P. Morton, M. Pasca di Magliano, C.A. Lyssiotis, Macrophage-Released Pyrimidines Inhibit Gemcitabine Therapy in Pancreatic Cancer, Cell metabolism, 29 (2019) 1390-1399 e1396.

[333] S. Dalin, M.R. Sullivan, A.N. Lau, B. Grauman-Boss, H.S. Mueller, E. Kreidl, S. Fenoglio, A. Luengo, J.A. Lees, M.G. Vander Heiden, D.A. Lauffenburger, M.T. Hemann, Deoxycytidine Release from Pancreatic Stellate Cells Promotes Gemcitabine Resistance, Cancer research, 79 (2019) 5723-5733.

[334] M.D. Neinast, C. Jang, S. Hui, D.S. Murashige, Q. Chu, R.J. Morscher, X. Li, L. Zhan, E. White, T.G. Anthony, J.D. Rabinowitz, Z. Arany, Quantitative Analysis of the Whole-Body Metabolic Fate of Branched-Chain Amino Acids, Cell metabolism, 29 (2019) 417-429 e414.

[335] O. Olivares, J.R. Mayers, V. Gouirand, M.E. Torrence, T. Gicquel, L. Borge, S. Lac, J. Roques, M.N. Lavaut, P. Berthezene, M. Rubis, V. Secq, S. Garcia, V. Moutardier, D. Lombardo, J.L. Iovanna, R. Tomasini, F. Guillaumond, M.G. Vander Heiden, S. Vasseur, Collagen-derived proline promotes pancreatic ductal adenocarcinoma cell survival under nutrient limited conditions, Nat Commun, 8 (2017) 16031.

[336] S. Sprangers, N. Behrendt, L. Engelholm, Y. Cao, V. Everts, Phagocytosis of Collagen Fibrils by Fibroblasts In Vivo Is Independent of the uPARAP/Endo180 Receptor, J Cell Biochem, 118 (2017) 1590-1595.

[337] D. Ohlund, A. Handly-Santana, G. Biffi, E. Elyada, A.S. Almeida, M. Ponz-Sarvise, V. Corbo, T.E. Oni, S.A. Hearn, E.J. Lee, Chio, II, C.I. Hwang, H. Tiriac, L.A. Baker, D.D. Engle, C. Feig, A. Kultti, M. Egeblad, D.T. Fearon, J.M. Crawford, H. Clevers, Y. Park, D.A. Tuveson, Distinct populations of inflammatory fibroblasts and myofibroblasts in pancreatic cancer, The Journal of experimental medicine, 214 (2017) 579-596.

[338] G. Biffi, T.E. Oni, B. Spielman, Y. Hao, E. Elyada, Y. Park, J. Preall, D.A. Tuveson, IL1-Induced JAK/STAT Signaling Is Antagonized by TGFbeta to Shape CAF Heterogeneity in Pancreatic Ductal Adenocarcinoma, Cancer discovery, 9 (2019) 282-301.

[339] E. Elyada, M. Bolisetty, P. Laise, W.F. Flynn, E.T. Courtois, R.A. Burkhart, J.A. Teinor, P. Belleau, G. Biffi, M.S. Lucito, S. Sivajothi, T.D. Armstrong, D.D. Engle, K.H. Yu, Y. Hao, C.L. Wolfgang, Y. Park, J. Preall, E.M. Jaffee, A. Califano, P. Robson, D.A. Tuveson, Cross-Species Single-Cell Analysis of Pancreatic Ductal Adenocarcinoma Reveals Antigen-Presenting Cancer-Associated Fibroblasts, Cancer discovery, 9 (2019) 1102-1123.

[340] J. Baddour, Therapeutic targeting of pancreatic cancer through stromal reprogramming and malic enzyme depletion, 2016.

[341] P. Louis, H.J. Flint, Formation of propionate and butyrate by the human colonic microbiota, Environ Microbiol, 19 (2017) 29-41.

[342] M. Gao, J. Skolnick, A comprehensive survey of small-molecule binding pockets in proteins, PLoS Comput Biol, 9 (2013) e1003302.

[343] A.C. West, R.W. Johnstone, New and emerging HDAC inhibitors for cancer treatment, J Clin Invest, 124 (2014) 30-39.

[344] C.Y. Lin, J.A. Gustafsson, Targeting liver X receptors in cancer therapeutics, Nature reviews. Cancer, 15 (2015) 216-224.

[345] N.R. Candelaria, S. Addanki, J. Zheng, T. Nguyen-Vu, H. Karaboga, P. Dey, C. Gabbi, L.L. Vedin, K. Liu, W. Wu, P.K. Jonsson, J.Z. Lin, F. Su, L.R. Bollu, S.E. Hodges, A.L. McElhany, M.A. Issazadeh, W.E. Fisher, M.M. Ittmann, K.R. Steffensen, J.A. Gustafsson, C.Y. Lin, Antiproliferative effects and mechanisms of liver X receptor ligands in pancreatic ductal adenocarcinoma cells, PLoS One, 9 (2014) e106289.

[346] G. Cui, X. Qin, L. Wu, Y. Zhang, X. Sheng, Q. Yu, H. Sheng, B. Xi, J.Z. Zhang, Y.Q. Zang, Liver X receptor (LXR) mediates negative regulation of mouse and human Th17 differentiation, J Clin Invest, 121 (2011) 658-670.

[347] C. Hong, P. Tontonoz, Liver X receptors in lipid metabolism: opportunities for drug discovery, Nat Rev Drug Discov, 13 (2014) 433-444.

[348] A.J. Fowler, M.Y. Sheu, M. Schmuth, J. Kao, J.W. Fluhr, L. Rhein, J.L. Collins, T.M. Willson, D.J. Mangelsdorf, P.M. Elias, K.R. Feingold, Liver X receptor activators display anti-inflammatory activity in irritant and allergic contact dermatitis models: liver-X-receptor-specific inhibition of inflammation and primary cytokine production, J Invest Dermatol, 120 (2003) 246-255.

[349] P.S. Minhas, L. Liu, P.K. Moon, A.U. Joshi, C. Dove, S. Mhatre, K. Contrepois, Q. Wang, B.A. Lee, M. Coronado, D. Bernstein, M.P. Snyder, M. Migaud, R. Majeti, D. Mochly-Rosen, J.D. Rabinowitz, K.I. Andreasson, Macrophage de novo NAD(+) synthesis specifies immune function in aging and inflammation, Nat Immunol, 20 (2019) 50-63.

[350] Y. Yang, A.A. Sauve, NAD(+) metabolism: Bioenergetics, signaling and manipulation for therapy, Biochimica et biophysica acta, 1864 (2016) 1787-1800.

[351] L. Liu, X. Su, W.J. Quinn, 3rd, S. Hui, K. Krukenberg, D.W. Frederick, P. Redpath, L. Zhan, K. Chellappa, E. White, M. Migaud, T.J. Mitchison, J.A. Baur, J.D. Rabinowitz, Quantitative Analysis of NAD Synthesis-Breakdown Fluxes, Cell metabolism, 27 (2018) 1067-1080 e1065.

[352] P. Bieganowski, C. Brenner, Discoveries of nicotinamide riboside as a nutrient and conserved NRK genes establish a Preiss-Handler independent route to NAD+ in fungi and humans, Cell, 117 (2004) 495-502.

[353] A. Grozio, K.F. Mills, J. Yoshino, S. Bruzzone, G. Sociali, K. Tokizane, H.C. Lei, R. Cunningham, Y. Sasaki, M.E. Migaud, Slc12a8 is a nicotinamide mononucleotide transporter, Nature metabolism, 1 (2019) 47-57.

[354] J. Ratajczak, M. Joffraud, S.A. Trammell, R. Ras, N. Canela, M. Boutant, S.S. Kulkarni, M. Rodrigues, P. Redpath, M.E. Migaud, J. Auwerx, O. Yanes, C. Brenner, C. Canto, NRK1 controls nicotinamide mononucleotide and nicotinamide riboside metabolism in mammalian cells, Nat Commun, 7 (2016) 13103.

[355] P. Belenky, K.C. Christensen, F. Gazzaniga, A.A. Pletnev, C. Brenner, Nicotinamide riboside and nicotinic acid riboside salvage in fungi and mammals. Quantitative basis for Urh1 and purine nucleoside phosphorylase function in NAD+ metabolism, The Journal of biological chemistry, 284 (2009) 158-164.

[356] S.M. Hutson, T. Hall, Identification of the mitochondrial branched chain aminotransferase as a branched chain alpha-keto acid transport protein, Journal of Biological Chemistry, 268 (1993) 3084-3091.

[357] K. Birsoy, T. Wang, W.W. Chen, E. Freinkman, M. Abu-Remaileh, D.M. Sabatini, An essential role of the mitochondrial electron transport chain in cell proliferation is to enable aspartate synthesis, Cell, 162 (2015) 540-551.

[358] J. Berger, D. Moller, The mechanisms of action of ppars. Annu Rev Med, (2002).

[359] F.J. Gonzalez, Y.M. Shah, PPARalpha: mechanism of species differences and hepatocarcinogenesis of peroxisome proliferators, Toxicology, 246 (2008) 2-8.

[360] F. Filip-Ciubotaru, L. Foia, C. Manciuc, C. Grigore, [PPARs: structure, mechanisms of action and control. Note I], Rev Med Chir Soc Med Nat Iasi, 115 (2011) 477-484.

[361] R.C. Reddy, Immunomodulatory role of PPAR-gamma in alveolar macrophages, J Investig Med, 56 (2008) 522-527.

[362] W.S. Yang, B.R. Stockwell, Ferroptosis: Death by Lipid Peroxidation, Trends in cell biology, 26 (2016) 165-176.

[363] E.K. Schmidt, G. Clavarino, M. Ceppi, P. Pierre, SUnSET, a nonradioactive method to monitor protein synthesis, Nature methods, 6 (2009) 275-277.

[364] D.S. Bilan, M.E. Matlashov, A.Y. Gorokhovatsky, C. Schultz, G. Enikolopov, V.V. Belousov, Genetically encoded fluorescent indicator for imaging NAD(+)/NADH ratio changes in different cellular compartments, Biochimica et biophysica acta, 1840 (2014) 951-957.

[365] A.J. Cooper, M. Conway, S.M. Hutson, A continuous 96-well plate spectrophotometric assay for branched-chain amino acid aminotransferases, Anal Biochem, 308 (2002) 100-105.